Water

Ethiopian Journal of Water Science and Technology

Special Issue

Proceeding of the 18th International Symposium on Sustainable Water Resources Development Arba Minch University from June 08-09, 2018

Tel: 0961011095/0910959874/0911560105

SYMPOSIUM ORGANIZING COMMITTEE MEMBERS

Dr. Samuel Dagalo (Chairperson of Symposium Organizing Committee)
Dr. Abdella Kemal
Dr. Besha Mogesse
Dr. Simon Shibru
Mr. Ayalkibet Mekonnen
Mr. Behailu Hussien
Mr. Mekuanent Muluneh

Proceeding Editors Committee

Dr. Samuel Dagalo
Mr. Ayalkibet Mekonnen
Mr. Mekuanent Muluneh
Mr. Behailu Hussien

Forwarding

Welcome Speech and Introduction

Y.E. Dr. Engineer Sileshi Bekele, Minister, Ministry of Water, Irrigation and Electricity,
Y.E. Dr. NegashWagesho, State Minister for Water Supply and Sanitation Sector, Ministry of Water, Irrigation and Electricity and the Chairman of the Board of Arba Minch University,
Y.E. Dr. Abreha Adugna, State Minister Irrigation and Drainage Sector, Ministry of Water, Irrigation and Electricity,
H.E. Dr. Engineer Habtamu Itefa, Director General of Oromia Regional State Roads Authority,
Y.E. Dr. Damtew Darza, the President of Arba Minch University,
Honorable AMU higher management bodes, Distinguished guests and esteemed paper presents and the entire symposium participants: -

We warmly welcome you to this 18th international Symposium on Sustainable Water Resources Development, here in Arba Minch. Thank you, thank you so much for your time and commitment to make this event happen.

As it can be recalled, Arba Minch University organizes a symposium on "Sustainable Water Resources Development" since the last eighteen years. The objective of the symposium is to create a platform where professionals, researchers, practitioners, decision-makers and concerned stalk holders come together to share ideas, communicate research results, good practices and innovations in the area of water resources development, use and management that can enhance knowledge and understanding for the sustainable water resources development. This year's symposium marks the 18th in the series. The symposium organizing committee has received over 100 papers in six thematic areas. The papers have been thoroughly reviewed and 24 papers were selected for oral presentation and 6 papers were selected for poster presentation. In this two days Symposium, these papers will be presented as per the program schedule. The oral presentations will be made in this and the other auditorium next door. Poster presentations will be conducted at the outside during the tea break-times.

In this first day, we will have a common session here in the main auditorium and tomorrow we will have parallel sessions. In the morning session, we will have presentation by His H.E. and then we leave the session for break. Technical sessions will follow then after and that is the go.

Now, may I call Dr. Ing. Abdella Kemal, the Scientific Director of AWTI to deliver a welcome speech.

Thank you.
Samuel Dagalo (Ph.D.)
Director, Water Resources Research Center, Arba Minch University

Welcome address

Y.E. Dr. Engineer Sileshi Bekele, Minister, Ministry of Water, Irrigation and Electricity,
Y.E. Dr. Negash Wagesho, State Minister for Water Supply and Sanitation sector, Ministry of Water, Irrigation and Electricity and the Chairman of the Board of Arba Minch University,
Y.E. Dr. Abreha Adugna, State Minister Irrigation and drainage sector, Ministry of Water, Irrigation and Electricity,
Y.E. Dr. Engineer Habtamu Itefa, Director General of Oromia Regional State Roads Authority,

Dear Symposium Participants, Ladies and Gentlemen,

It gives me great pleasure to be here today and open the 18th international symposium on symposium on Sustainable Water Resources Development which has been organized by Arba Minch University.

Water is one of the most important resources that sustain life on earth. However, this resource is becoming scarce in many parts of the world. Not only is the physical scarcity of water is of concern but also the deterioration of water quality. Scarcity and quality of water poses serious treats to socio-economic development and ecosystems functions. Fortunately, Ethiopia has immense physical water resources potentials. However, the erratic nature of its availability and other capacity limitations has been hindering the country to utilize this resource for its socio-economic development.

The world population is increasing and this needs increased production of food supply. The food supply of human kind mainly comes from agricultural production. Agriculture is the largest consumer of water for producing crops. This means that we need to have more water in a given space and time to satisfy these escalating demands. However, the availability of water is limited and needs due attention. Agricultural production with less supply of water is then mandatory for sustainable use of the water resources. Good quality of water and sanitation systems is also important which could safeguard the health of the citizens. This is why the government of Ethiopia has been giving due emphasis to water based development projects.

Long year effects of socio economic activities have resulted in serious environmental degradation and global climate change. Therefore, the issue of sustainability becomes a priority of concern. “Sustainability” here emphasizes the utilization and management of available water resources without compromising the ability of the next generation to use the resource. One of the general water resources management policy objectives of Ethiopia is conserving, protecting and enhancing water resources on sustainable basis. This shows that the subject of sustainable management of water resources should be given due attention in all of the water resources development programs.

The government of Ethiopia, in its plan of climate resilient Green Economy, promotes and tries to implement projects that enhance economic development of the country in an environmentally friendly way. As we know, there are several Mega water resources development projects have been implemented and under construction throughout the country including the Great Ethiopian Renaissance Dam.

Ladies and Gentlemen,

Implementation of physical infrastructure without due attention to sustainable management cannot guarantee the achievement of the project objectives. These efforts need to be supported by scientific methods and approaches. The contribution of research and extension to the water sector development has been low which calls for attention.

Arba Minch University commits itself to capacity building and research which play a central role in developing skills, generating knowledge, and transferring technology useful for sustainable development of our water resources. I believe that forums like this symposium could be an effective media for exchange of research results and good practices in the water sector.

I thank Arba Minch Water Technology Institute and the organizing committee for creating and sustaining this event. I do hope that the institute will continue and do more in this regard in the future.

Ladies and Gentlemen, with this few remarks, I wish you success and fruitful deliberations on this symposium.

I wish you fruitful deliberations and hereby declare that the workshop is officially open.

Thank you!

Damtew Darza (Ph.D.)

President, Arba Minch University

Contents

Keynote speech

Overview of the Ministry of Water, Irrigation and Electricity, its sectors role and future partnership directions with Arba Minch University

MWRIE visional concept is to see Ethiopia achieve clean drinking water supply, irrigation and renewable energy development and supply, and join middle income countries by 2025. The mission of the ministry is to contribute to the economic and social development of the country by implementing integrated and sustainable water and renewable energy resources development and administration in an environmentally sustainable and integrated manner. Innovation and creativity, fairness and equity, quality, endurance and aspiration, environment and sustainable development, continuous learning and teamwork and detest corruption are the fundamental values of the ministry. The minister administers the state ministers of Electricity, Irrigation, Water supply and sanitation and planning and development sectors.

Both surface and ground water resources potential are managed by different sectors under MWRIE. With estimated surface water and groundwater potential of 123 Billion m^3 and 36-40 Billion m^3, respectively during the past 100 years, per capital water availability reduced from 6000 m^3 to 1000 m^3. This puts the country under economic water scarcity. Another important point the ministry understood that rainfall distribution of the country is uneven and considerable parts of Ethiopia are rainfall scarce. The ministry believes that if water resources management & infrastructure improves, there are possibilities to combat economic scarcity with available water resources.

It is learnt that most of the rivers are transboundary, and management aspects needs collateral agreement with neighboring countries. Ethiopia planned to join middle income countries by 2025 and developed different policies, strategies and programs. One of the bases for such plan is SDGs, which is targeted at 2030. Five elements underpin the agenda of SDGs, namely people, planet, prosperity, peace and partnership. SDGs are 17 and universal in its nature with 169 targets. Goal 6 which targets water issues stated as “Ensure availability and sustainable management of water and sanitation for all.” This goal has 6 targets i.e. 6.1. Drinking water for all, 6.2. sanitation and hygiene for all, 6.3. improve water quality, 6.4. increase water use efficiency, 6.5. IWRM and transboundary cooperation, and 6.6. restore water-related ecosystems. Target 6.1 is addressed by GTP-I and GTP-II where the rural and urban water supply coverage is improved. Improvements in WASH projects are observed when targeting to meet MDG, and Ethiopia is one of 147 countries who have met MDG drinking water supply target. The country played important role when 424 million people from Sub-Saharan Africa had access to improved water source and access coverage increased on Average from 33% to 52% (19% point increase). During the MDG period, 48 million people from Ethiopia (57.2%) had access to improved water source and Water Supply access coverage increased from 14% to 57% (43% point increase).

New flagship program namely climate resilient, CR-WASH, has started under Single Integrated One WaSH National Program with objectives of providing adequate, safe, resilient and sustainable WaSH

services to the people in arid and semi-arid areas of Ethiopia and Satisfying water supply requirements for livestock, agro- industries and other users. Major challenges to initiate the program is the countries vulnerability towards climate change. According to 2015/16 El Nino drought response, 382 districts fall in vulnerable areas, with most of them are in Arid and Semi- arid lowlands. The framework of CR-WASH includes DTM, RS and GIS based analysis platform, water sources, quality settlement, administration information, planning and design, construction of infrastructure, resource mobilization and capacity development for operation and maintenance.

According to studies, irrigation potential of Ethiopia is estimated to be 5.3 million hectares. To manage the agricultural water on potential irrigation areas field conservation practices, supplemental irrigation, water harvesting, ground water irrigation and large-scale irrigation has been practiced within a range of pure rainfed up to Fully irrigated areas. These practices are targeted to Insure food security at household and national levels, to produce of raw materials for agro industries and produce crops for export earnings.

GTP-I irrigation study and design achieved more than 100%, but construction coverage is only 43.05%. Rehabilitation and expansion coverage are also met surpassing 100%. The GTP-II is now targeted 915,881-hectare to land to study and design irrigation systems and perform construction of 954,000 hectare of land by 2020. One of the future programs to meet GTP-II irrigation target is the flagship youth irrigation program. This program can enable 30,000 young graduates aimed to develop 124,000 hectares of land.

The electricity coverage and future plans of the country is also another development issue with Goal 7 of SDGs addressing access to affordable, reliable, sustainable, and modern energy for all. Installed hydropower potential of Africa up to 2014 was estimated 27 GW, and it is the least compared to other continents. The country, currently producing 4300 MW of Energy, planned to produce 3,000MW of Energy by 2035 (year in Ethiopian Calendar). This forecast integrates transport (1564 MW), agriculture (5219 MW), industrial (7002 MW) and service (2624 MW) sectors. Ethiopia's renewable energy resources potential estimated as Hydropower (~ 45,000 MW), Geothermal potential (~ 10,000 MW), Solar energy potential (~ 5.5kWh /m^2 /day), Wind energy potential (>1000 GW with average wind speed of ≥7 m/s @50 m above ground level), Wood (~ 1,120 million t/year), Agricultural waste (~ 15 to 20 million t/year), Natural gas (~ 113 Bm^3), Coal (~ 300 Million tons) and Oil shale (~ 253 Million tons). To tap the hydropower potential, there are currently 15 existing and 24 proposed dam sites and construction steps are on the way. The generation capacity of the country is now 4,284 MW that is accumulated from Hydropower (3810 MW), wind (324 MW), Geothermal (7 MW) and Diesel (143M MW). 8910 MW of Hydropower, 100MW of Solar and 1000 MW of geothermal energies are under construction. About 13 wind energy sites are under study.

The country's energy policy framework aimed to Ensure a reliable supply of energy at the right time and at affordable prices, particularly to support the country 's agricultural and industrial development. It is predicted that by 2030, the world will need to produce around 50% more food and energy, together with 30% more freshwater, whilst mitigating and adapting to climate change.

To address the above-mentioned issues, fulfilling the professional capacity with groundwater Resource exploration, Sanitary Engineering, Solid and liquid waste management and Renewable energy (solar, wind & geothermal) are necessary. This identify research areas with Groundwater exploration and mapping, Surface and subsurface resources mapping and modelling using GIS and RS, Water quality analysis, Irrigation and drainage: appropriate water harvesting technology, Lake eco-hydrology management for sustainable use, Watershed modelling, Reservoir behavior analysis; Dam safety analysis and Assessing off-grid electric solutions for rural areas. These research areas can be addressed by collaboration with AMU though university-industry linkage, joint research, capacity building, by establishing advisory group and joint appointment.

Compiled by: Mekuanent Muluneh

Oral presentation

Theme One: Hydrology and Integrated Water Resources Development

Linear spectral unmixing algorithm for modeling suspended sediment concentration of flash flood, upper Tekeze River, Ethiopia

Hagos Gebreslassie.[1,4*], Assefa M. Melesse[2], Kevin Bishop[3] and Azage Gebreyohanse[4]

[1]Adigrat University, Ethiopia, [2] Department of Earth and Environment, Florida International Universities, USA, [3] University of Uppsala, Swedish Universities of Agriculture, Sweden, [4] Ethiopian institute of water resources, Addis Ababa University, Ethiopia

* Corresponding Author: hagmeb@gmail.com

Abstract

Sedimentation is the outermost challenge for design and operation of energy and water resource infrastructures. Remote sensing modeling of suspended sediment concentrations (SSCs), the cost effective compared to the traditional on-field sampling technique, has been commonly relied on less accurate and non-universal empirical approaches. A laboratory and field experiments were conducted to determine effect of selected factors and generate a linear spectral unmixing (LSU) model for improving application of remote sensing on monitoring suspended sediment concentration. River bed deposited sediments and upper 20cm layer of flash floods occurred on Tekeze River and its tributary, Tsirare, were used as samples for laboratory and on-site spectral signature measurement using a high-resolution remote sensing spectro-radiometer. The coefficient of determination (R^2) and root mean square of error (RMSE) were used to evaluate the performance of the generated linear spectral unmixing model and to compare it with the empirical remote sensing model in simulating suspended sediment concentrations of the reaches in upper Tekeze. The results have depicted that the Pearson non-parametric correlation coefficient between SSCs and reflectance were varied based on the level of sediment concentrations, geological colors and grain sizes. The LSU remote sensing approach was found more accurate (R^2= 0.91, RMSE=±0.66g/l in Tsirare and R^2=0.99, RMSE=±0.73 in the main river) than the empirical non-linear remote sensing (R^2=0.76, RMSE=±10.87g/l in Tsirare and R^2=0.81, RMSE=±2.65g/l in the main river) approach of simulating SSCs. The linear spectral unmixing approach of remote sensing was found relatively accurate and universal in monitoring and modeling the variability of SSCs that could be applied to upper Tekeze basin.

Key words*: empirical remote sensing, linear spectral unmixing, flash flood, suspended sediment concentration Tekeze River*

1. Introduction

Sediment transport, the outermost challenge for operation and design of hydraulic infrastructures, is among the environmental processes that vary spatiotemporally. The variability (as in Ethiopia) is related to the driving forces including climatevariability (Gebremichael et al., 2013; Alemseged and Rientjes, 2015), land use change (Hurni et al., 2005; Amsalu et al., 2007) and geomorphologies (Tamene et al., 2006). Thus, there is a need of an area and time specific characterization of the sediment transportation and deposition rate in river systems. Even though most Ethiopian river basins are amongthe international rivers with higher and variable sediment concentration, the monitoringtechnique in the basinshad beenrelied on limited and cost infeasible traditional sampling technique.It is hardly possible to get adequate and continuous sediment data for most rivers.

Hence, researchers in the area are in searching easily applicable and cost feasible technique of monitoring sediment yield. Some researchers have proposed an empirical sediment rating curves developed by relating the sediment concentrations with water discharge (Haregeweyn et al., 2006; Tamene et al., 2006; Haregeweyn et al., 2008). Others also proposed process based models including Hydrologic Engineering Center River Analysis System, (HEC-RAS; HEC, 1995), Water Erosion Prediction Technology (WEPP, Nearing et al., 1989) tested by Zeleke (2000), Deferesha et al. (2012), Maalim et al.(2013),Agricultural Non-Point Source Pollution (AGNPS; Young et al., 1989) tested by Haregeweyn and Yohannes (2003) and Mohammed et al. (2004), Soil and Water Assessment Tool (SWAT; Arnold et al., 1998) tested by Setegn et al. (2011, 2008), Mohammad et al. (2015), and the artificial neural network (ANN; Masoumeh and Mehdi, 2012; Melesse et al., 2011).But, applying the process based models ischallenging that most of them were originally developed for areas that have large amounts of data and in regions with temperate climate where the runoff mechanisms are governed by infiltration excess unlikemost Ethiopian basins relied on saturation excess runoff (Steenhuis et al., 2009; Bayabil et al., 2010; Tilahun et al., 2013).In this case there are some efforts (eg. Easton et al., 2010; White et al., 2010) done to improve SWAT to Ethiopian casesby replacing infiltration excess runoff processes with the saturation excess.

Recently, remote sensing technology has been found cost effective in its potential in providing synoptic, continuous and long-term observation and monitoring sediment transportation.The principle working to apply this technology in monitoring sediment transport is using the fact that suspended sediments increase the radiance emergent from surface waters in the visible and NIR of the electromagnetic spectrum (Ritchie and Schiebe, 2000). Accordingly, remote sensing has been tested and found effective

in detecting suspended sediment concentration of coastal (Islam et al., 2003; Doxaran et al., 2003; Wang et al., 2010; Fang et al., 2010; Wang et al., 2012), lake environments (Ritchie and Cooper, 1991; Ma and Dai, 2005; Ayana et al., 2015).

Though not developed like in oceans and costal water systems, remote sensing has been applied to monitor sediment concentration in river systems (Chu et al., 2009; Wang and Lu., 2010). The coarsertemporal, spatial, spectral and radiometric resolutions of sensors, atmospheric conditions interventions and its limited capability tothe upper surface only are among the problems facing it. Moreover, the relationship between sediment concentration and reflectance could be affected by multiple factors including inherent optical properties of the suspended sediment (texture, colour and organic matter) and characteristic of the flowing water including depth and turbulence (Nina et al., 2012). Despite the above variability at finer resolution, remote sensing technology has been used mixed designation approach that single representations of multiple objects or processes having distinct spectral signature (Keshava & Mustard, 2002; Quintano, et al., 2012). The mixed representation of objects by remote sensing has been treated poorly thatmost previous remote sensing applications to rivers' sediment monitoring havebeen relied upon the empirical relationships between sediment concentrations and the reflectance which are limited in their universal application and may not extend to the full ranges of conditions present in river systems.Accordingly, different types of relationship between SSCs and reflectance have been reported. Linear relationship between SSCs in the range of below 50g/l and reflectance was reported (eg. Ritchie et al., 2003a; Kilham et al., 2012) and a non-linear relationship was found at higher concentrations (Ritchie et al., 2003b; Pavelsky and Smith, 2009). Moreover sediment varies in type (colour and grain size) across rivers and in time; the relationship between level of sediment concentration and reflectance also varies accordingly (Navo et al., 2007; Volpe et al., 2010).This all implies that the need for sediment type and even concentration specific calibration of models for application which is difficult and costly.

Consequently, establishing a physical basis remote sensing for modelling the SSCscould prove to a more reliable assessment of SSC which present a general approach that can be appliedacross a range of rivers, conditions, and over periods of time. To achieve this, a detail analysis of the components and their spectral mixing property in the turbid water is important. Therefore linearspectral unmixing approach, process of decomposing the spectral signature of a mixed reflectance into a set of constituents and their corresponding abundances (Somers et al.,2011; Shi and Wanga, 2014),was proposed in this study. Flood (especially the flash flood types), outermost sediment transporting agent and inaccessible for in-situ

sampling but scarcely introduced to the remote sensing technology, was targeted in this research. This study was significant to provide critical physical basis and instructional assistance for simulating SSC directly from remote sensing in highly turbid rivers in terms of band selection, equation determination, as well as error analysis and reduction.The specific objectives of this study were to (1)identify wave length range effective for monitoring sediment concentrationof Tekeze river(2) determine effect of grain size and color variability on the relationship between spectral signature and sediment concentrations, and (3)generate and compare the performance of empirical and LSU remote sensing models in simulating SSCs.

2. Material and methods

2.1. Study area description

Tekeze River basin (called Atbara in Sudan) is situated to north-western Ethiopia, Southern of Eritrea and eastern part of Sudan and forms the northern most part of the Nile Basin of East Africa. Its headwaters starts at an altitude of 3,500m.a.s.l from Meket mountain near Lalibela, Ethiopia and flows northward until it turns westward along the Ethio-Eritrean border covering a distance of 600km until it crosses the Ethio-Sudan border near Humera at an altitude of 550m.a.s.l., Ethiopia. It is the second largest tributary of the Nile from Ethiopia and covers about a quarter of Nile drainage area. The total mean annual flow from the Tekeze river basin is estimated to be 8.2 BMC covering 13% and 22% of the main Nile flow at dry and wet seasons respectively (Zaghloul et al., 2007). The ground water resource is not promising except in a few areas that its flow is determined by the immediate surface runoff after the torrential and seasonal rainfall. Euric Vertisol with soil depth of more than 50cm is dominant on the level lands while Leptosols are the most common soils on the steeply sloping lands. Moderately deep soils cover less than 5% of the area. The major land use classes on the basin include cultivated land, woodland, open grass land and sparsely vegetated land. Most of the climax vegetation of the basin has disappeared and the Afro-alpine and sub-afro-alpine heath vegetation lies between 3700 and 3900m.a.s.l around semen mountains.

2.2 Experimental setup

Both on-site and laboratory experiments were carried to characterize the signals from different sediment types in the Upper Tekze basin. The upper part of Tekeze basin on which Tekeze hydroelectric dam dependent was selected purposely to propose an alternative sediment monitoring technique to support the scarce sediment monitoring practice in the basin.

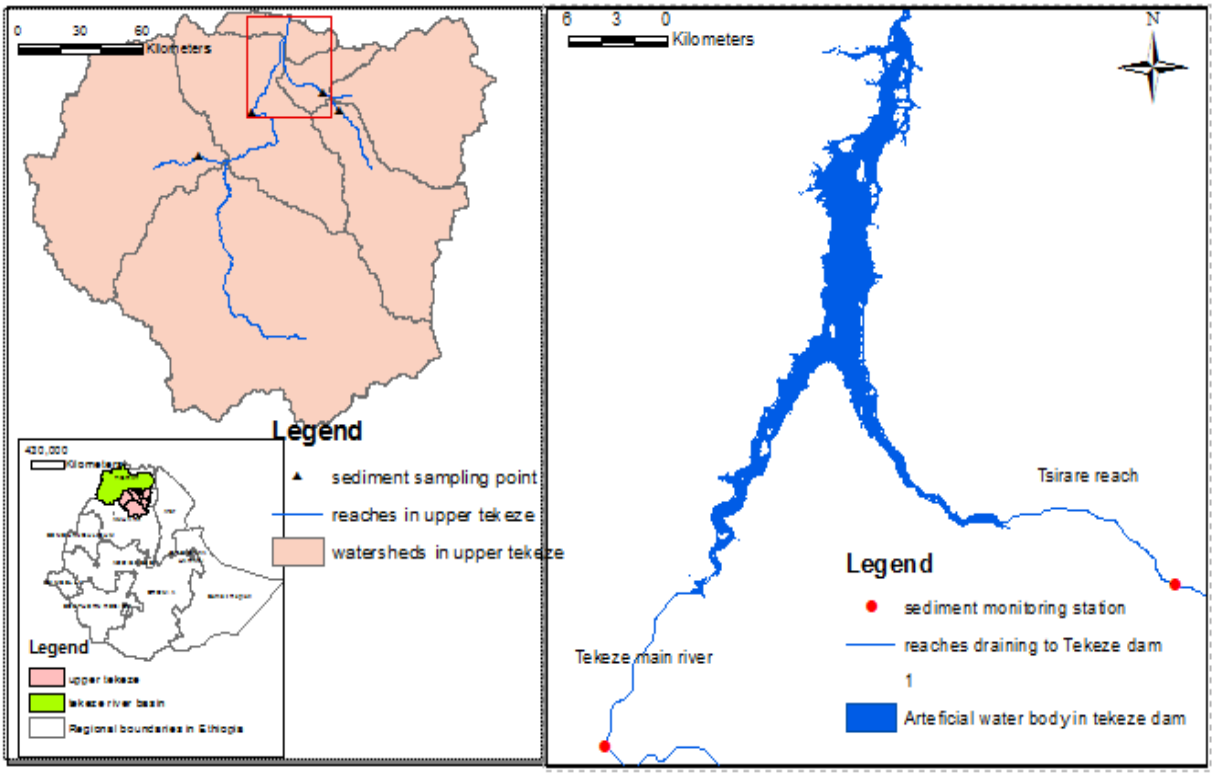

Figure 1: Location of study area

The two main rivers in the upper Tekeze basin including Tsirare and Tekeze Main River wereselected for this purpose. Bed deposited sediment samples from different locations of the selected rivers by considering the color variation that is two of them were taken from the sediments supposed to be relatively black and red and the other two were also taken from the immediate inlets of the Tekeze hydroelectric dam at Tsirare and Tekeze main River.The sediments' color was separated to be 5YR6/1, 5YR7/5, 5YR7/5 and5YR7/1 respectively.

Table 1: Physical properties of the sampled sediment

Sediment type	**Color**	**Grain size composition (%)**		
		Clay (<0:002mm)	Silt (0:002 -0:05mm)	Sand (>0:05mm)
Black sediment	5YR6/1	61.58	14.67	23.75
Red sediment	5YR7/5	56.89	19.01	24.1
Tsirare's sediment	5YR8/1	59.56	15.32	25.13
Main river's sediment	5YR7/1	58.55	18.03	23.42

Continuous sampling of sediment laden watersfrom the upper 20cm depth and spectral reflectance of the flood occurred in Tsirare and in the main river during the 2017 summer (July 2, 2017 –September 3, 2017) had been collected simultaneously. These sediment samples together with the sediment laden water were processed and their spectral signature had been characterized in the soil laboratory at Mekelle University, Ethiopia. The sediments were pre-processed following four steps: (1) drying in air and pulverization; (2) filtration by passing through 2mm mesh sieves to remove gravels; (3) mixing with water to filter the tiny residues floating up on the surface of the water, and (4) drying in an oven at $105^{o}_{C}$for 12 hours. Portions of the pre-possessed sediments were further separated into clay, silt and sand by using the sieving method to enable the investigation of the effect of particle size on the spectral properties of sediment-laden water. Sixteen sediment types were generated (natural, clay, silt, and sand sediment types for each of the black, red and bed soils from Tsirare and the main river. The "natural" represents the original sediment with natural grain size distribution. From each sediment type a 2g, 5g, 10g, 15g, 20g, 25g, 30g, 40g, 50g and 60g were prepared and therefore 160 sediment samples were used in this study.

Each of the above sediment samples were added in to one liter distilled water then was shacked with electrical shaker. The reflectance of each sediments solution was detected using high resolution spectro-radiometer organized as follow. Two 500w halogen lamps organized at 45^{o} to the sample in the two directions, the spectro-radiometer was arranged at 90^{o} to the sample, 1 litter volume cylinder painted with black colour and laptop were connected using USB cable with the spectro-radiometer were organized. The FieldSpec ®HandHeld2^{TM} Spectro-radiometer (ASD Inc. Boulder, Colorado, USA) which acquires data at 1nm intervals, ranging from 325 to 1075nm with resolution of plus and minus 1nm and accuracy less than 3nm at 700nm were used. 5”x5” spectral reflectance panel which reflects all incoming energies was used as the calibration standard to know incoming energy from solar system and from the artificial source of light. The panel was checked for diffusely reflectance nearly 100% of the incident light throughout the spectral range. The wavelength specific reflectance $R_s(\lambda)$ was computed using the following equation.

$$R_s(\lambda) = \frac{R_{rad}(\lambda)}{R_p(\lambda)} C_{al}(\lambda) \quad (1)$$

Where Rs(λ) is the wavelength specific reflectance, $R_{rad}(\lambda)$ is the wavelength-specific radiance from the sediment solution surface, for each sample, which is measured by the spectroradiometer three times. $R_p(\lambda)$) is white reference that is collected by putting the reference panel above the water surface. The White reference was updated before each measurement of water sample. C_{al} (λ) is the calibration factor

for reflectance panel that come out with the product. The measurements were repeated three times and the averages were used in the calculation. All laboratory measurements were carried at night to avoid external light.

The on-site reflectance measurement and sampling of sediment laden water were done on carefully selected section of the flood. The Visible (VIS) which is photo-synthetically active radiations including the Blue (400 - 525nm, B_1), Green (526 - 605nm, B_2), Yellow (606 - 655nm, B_3), Red (656 – 750, B_4), as well as the Short Wave Near Infrared (SW-NIR, 750 - 1075nm) categorized in to 750-950nm (B_5) and 951 – 1075nm (B_6) ranges were applied to determine the spectral signature of sediment laden water both at laboratory and at field to each flood occurred during 2017 summer. Parallel to each of the field reflectance measurements and sampling to laboratory, the speed as well as the depth of the flow had been measured.

2.3 Spectral Unmixing Algorithm

The spectral unmixing algorithm proposed in this study was the linear spectral unmixing algorithm. In this case, it was supposed that the mixed reflectance of sediment laden water at a specific wavelength is the sum of linearly combined reflectance from each primary component. The spectral reflectance of a volume of turbid water can be conceptualized into a composite signal by using the weighted sum of the primary constituents of the water such as clean water, suspended sediments, phytoplankton and others. Therefore, LSUs in this study was to mean estimating the change of reflectance of the mixture due to the change in abundance of the constituentson the turbid flood water. Some researchers called it linear spectral mixing opposing to the activity (Chu et al., 2009;Oyama et al.,2007; Oyama et al., 2009).
Distilled water and dry sediments were the only constituents of the water sample in this experiment as it was for flash flood water. Based on this, the water reflectance at each SSC level was translated to the spectral mixing index of primary water constituents (Equation 2).

$$R(\lambda) = SMCwRw(\lambda) + SMCsRs(\lambda) \quad (2)$$

Where SMCw and SMCs are for spectral mixing coefficients of water and sediment, respectively. Rw (λ) and Rs (λ) represented the distinctive spectral patterns of clean water and dry sediment. The spectral mixing coefficient for sediment (SMCs) and water (SMCw) in each band and each concentration (SSCs from 2 - 60g/l) were estimated by solving the following equation.

$$R(B_i) = SMCwRw(B_i) + SMCsRs(B_i) \quad (3)$$

Where $R(B_i)$, $Rw(B_i)$, $Rs(B_i)$ (i = 1; 2; 3; 4;5;6) were stood for the reflectance sediment laden water, standard reflectance for clean water, and standard reflectance of dry sediment at the i^{th} band,

respectively. The standard clean water and dry sediment reflectance (figure 2) in this study were considered the spectro-radiometer based measurement in laboratory for the distilled water and pre processed sediment samples for each colours.

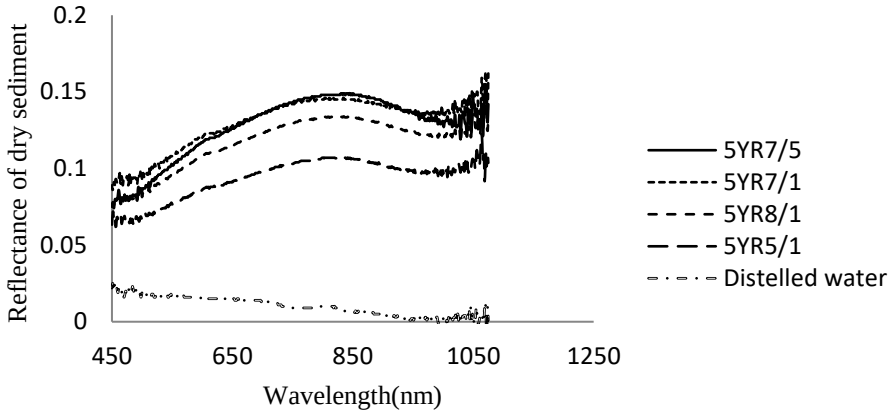

Figure 2: Average reflectance of dry sediments (5YR7/5 (Red sediment), 5YR7/1 (main river bed soil), 5YR8/1 (Tsirare river bed soil) and 5YR6/1(black sediment)) and distilled water

2.5 Data Analysis

The Pearson correlation coefficient (C) in R software, a nonparametric measure of statistical dependence between the two variables (between SSC and reflectance in our case) was applied. The correlation was tested between the reflectance of soil colours (black, red and intermediates) in 10 SSC levels (2-60g/l) and the six simulated bands including band one (B_1, 400 - 525 nm), band two (B_2, 526 - 605 nm), band three (B_3, 606 - 655 nm), band four (B_4, 656 – 750), as well as the Short Wave Near Infrared (SW-NIR, 750 - 1075 nm) categorized in to band five (B_5, 750-950nm) and band six (B_6, 951 – 1075nm). The performance of the generated models in simulating the SSCs in the upper Tekeze River reaches were evaluated using the coefficient of determination (R) and root mean square error (RMSE) that is a model with higher R but lower RMSE were considered as well performing model.

$$R = \frac{\sum_{i=1}^{n}(X_i - X)(Y_i - Y)}{\sqrt{\sum_{i=1}^{n}(X_i - X)^2}\sqrt{\sum_{i}^{n}(Y_i - Y)^2}} \quad (4)$$

$$RMSE = \sqrt{\frac{\sum_{i=1}^{n}(X_i - Y_i)^2}{n}} \quad (5)$$

Where R and RMSE are for coefficient of determination and root mean square error respectively, X_i is observed value and Y_i is simulated values and X and Y are the means for the observed and simulated value, respectively.

3. Results

3.1 Spectral reflectance signatures

The spectral reflectance curves along the entire measured bandwidth (325 nm to 1075 nm) were generated to determine the spectral characteristics of the sediment-laden water for sediment in upper Tekeze basin. The spectral signatures of the sediment types varied in color (5YR7/5, 5YR6/1, 5YR7/1 and 5YR8/1), ingrain size (natural, clay,silt and sand) and in concentrations (2g, 5g, 10g, 15g, 20g, 25g, 30g, 40g, 50g and 60g) were not consistent. This variability was not only from the sediment types; there was also variability based on the wave length range changing. The reflectance showed an increasing trend from coarser to finer grain size almost in the whole wave length range (325-1075nm) and relatively highest reflectance magnitude was found in the natural composition of grain size (fig 3). Moreover, the reflectance was increasing as the SSCs increased.In most of the sediment types considered an overlapping reflectance values were observed in the wave length ranging 325-450nm and 950-1075nm but were clearly separated in the wave length ranging from 450-950nm. This indicates that the possible wave length range for separating level of SSC in upper Tekeze basin is 450-950nm. But, the peak reflectance and clear variability due to sediment type were observed at SW-NIR wavelength ranging from 750-950nm in all levels of SSCs (fig 3).

3.2 Correlation between reflectance and SSC in simulated bands

The Pearson correlation coefficient (R_s) was used to test the association between reflectance and level of SSCs for all sediment types over the bandwidth (450 nm to 1075 nm). The $R_s$value was exceeded from 0.55 in the whole wavelengths ranging from 450 to 950nm. Relatively higher correlations (Rs>0.7) were found in the wave lengths ranging 750-950nm. The strength of the correlation between sediment concentrations and reflectance was varied due to grain size. Stronger correlations (average Rs= 0.82) were found between reflectance and level of SSCs in fine grain size (clay) than in the coarser (sand) sediment types (average Rs=0.75) and the intermediate (silt) grain size (average Rs=0.78). The reflectance from the natural grain sizes were loosely associated with its level of concentration (average Rs=0.68).Comparatively higher correlation between SSCs and reflectance was found in the sediment type sampled from Tsirare colored as 5YR8/1 (average Rs=0.75) than the sediment type from the main river (5YR7/1), the black (5YR6/1) and the red (5YR7/5).

3.3 Empirical and LSU Remote Sensing models

3.3.1 Empirical Remote Sensing Modeling

The spectral profiles in Figure 3 is developed from the relationship between the SSCs (2, 5, 10, 15, 20, 25, 30, 40, 50, 60g/l) under clay, silt, sand and natural grain sizes and their respective reflectance measured using high resolution spectro-radiometer in the wave length 750-950nm (B_5).

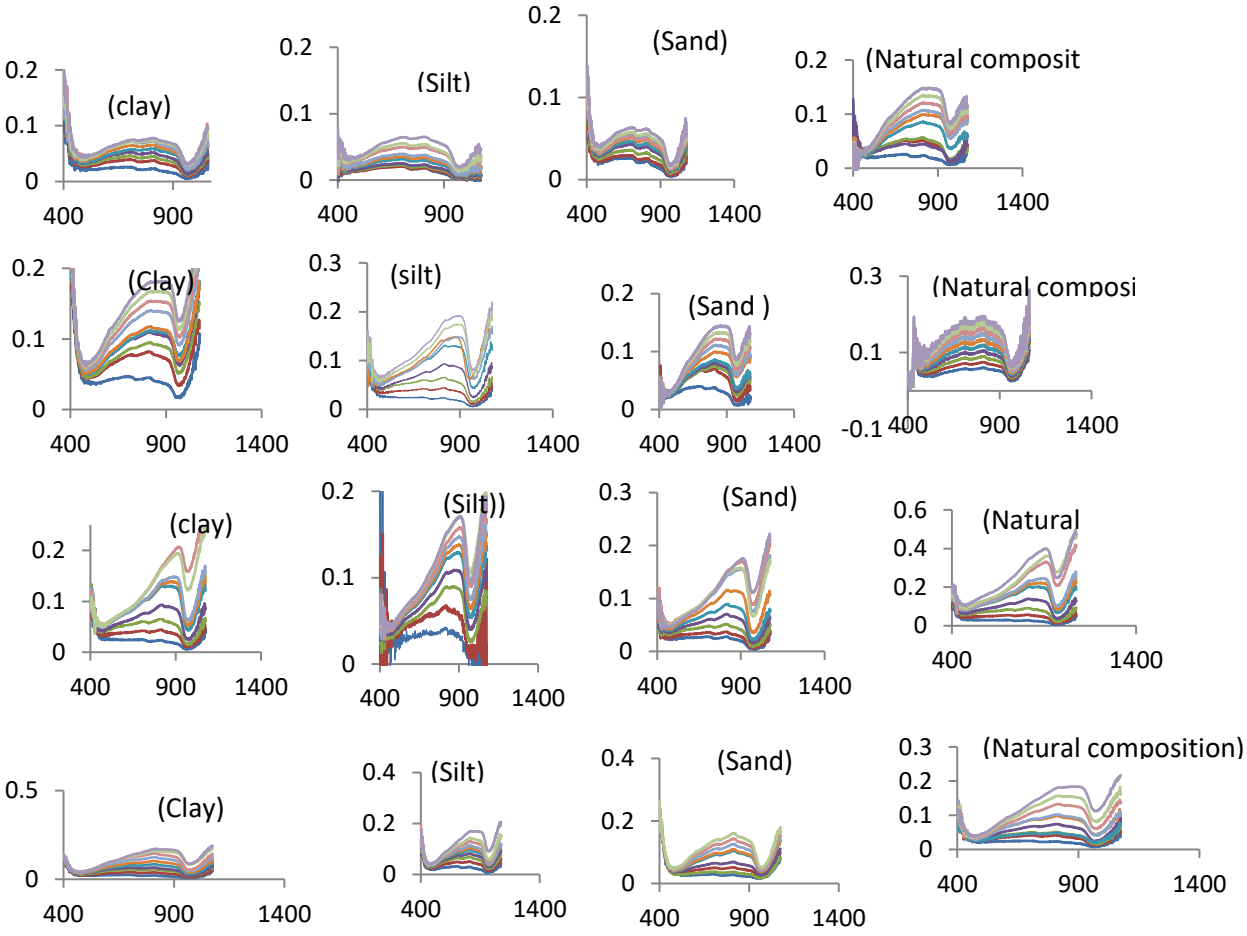

Figure 3: Reflectance profiles of sediment-laden water from upper Tekeze basin. The colored curves represent the SSC changing from 2to 60 g/l for sediment types. The y axis represents reflectance and the x axis represents the wave length range (nm) at which the reflectance was detected using hand held spectro-radiometer. The figures in the first, second, third and fourth row refers to the sample taken from the main river, Tsirare, extremely black and red sediment in the upper Tekeze basin respectively.

The scatter plots in Figure 3 were from reflectance measured using spectro-radiometer and SSCsunder different sediment colorsand grain sizes (clay, silt, sand and natural). The scattering was not uniform among the sediment colors and grain sizesindicating sediment typeswasimportant factor that affected the reflectance. Greater scattering was found in the sediment type from the main river than the sediments from others. Higher reflectance curve values were also presented from the natural grain size compared to

the other grain sizes in all sediment types. An empirical remote sensing exponential equationgiven below (Equation 6) was found well fitted to the relationship between SSCs and reflectance.

$$R = ae^{(SSC/b)} \quad (6)$$

Where SSC and R refers to the suspended sediment concentration (g/l) and the reflectance at 750-950nm (B_5) respectively, aand b were coefficients. More than 0.8coefficient of determinations (R) and non random estimates (a, and b) were resulted from non linear regression analysis under a significance level of 99%.

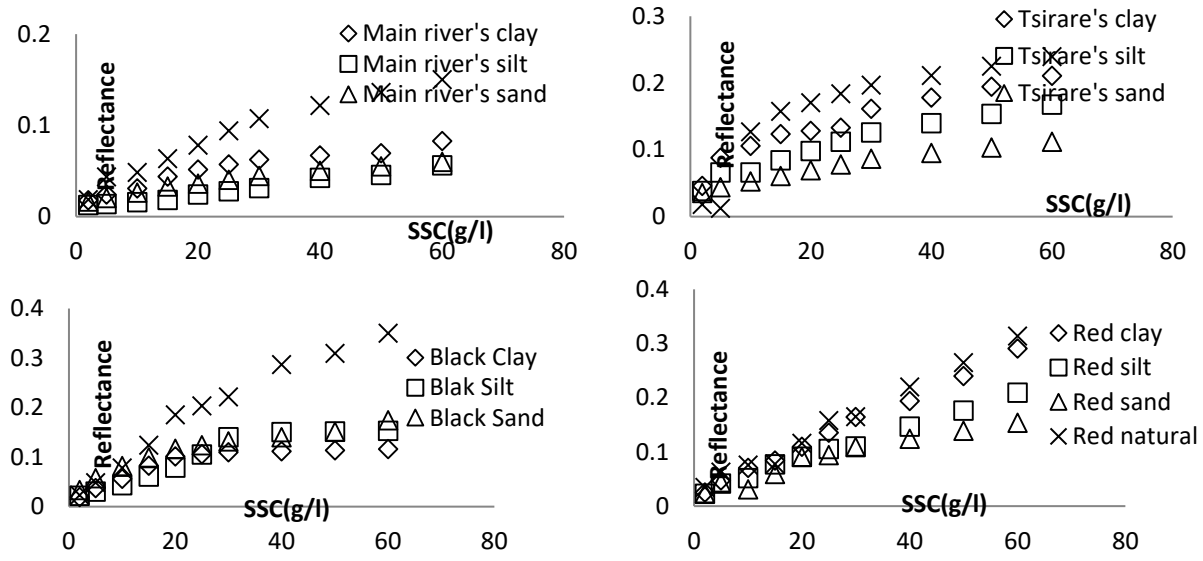

Figure 4: Reflectance profiles of SSCs with different grain size in the wave length range of band 5 (B5, 750-950nm). The sediments were sampled from the bed of Tekeze main river colored 5YR7/), Bed of Tsirare river colored 5YR8/1 and from the relatively black (5YR6/1) and red (5YR7/5) sediments in the basin.

3.3.2. LSU modeling of SSC

The linear spectral unmixing algorithm was introduced to maximize the accuracy of simulating SSC using remote sensing. The reflectance variability in 750-950nm (B_5) from the considered levels of SSCs were translated to spectral mixing coefficients (SMCs) variability using equation3. The relationship between the SSCs and their respective SMC values from the different sediment types were presented in figure 4.

The scatter plots from LSU and SSCs (figure 4) were not well Figure 5: SMCs profiles of sediment laden water in the wave length range 750-950nm (B_5) from the main river bed (5YR7/1, a), Tsirare river bed (5YR8/1, b) and from the relatively black (5YR6/1,c) and red (5YR7/5, d) sediments in basin.

separated like in the scatter plots from reflectance and SSCs (figure 3). Consistent trend scattering was not observed among the sediment color and grain size deviations. The valid exponential regression equationrepresenting the relationship between SSCs and the SMC was determined to be as in equasion7.

$$SSC = ae^{b(SMC)} \quad (7)$$

Where SSC and SMC refer to the suspended sediment concentration (g/l) and the linear spectral mixing coefficients values respectively, a and b are coefficients, was found more fitted to the relationship between SSCs and respective LSUs. The coefficients of determination (R^2) were above 0.89 in all sediment types.

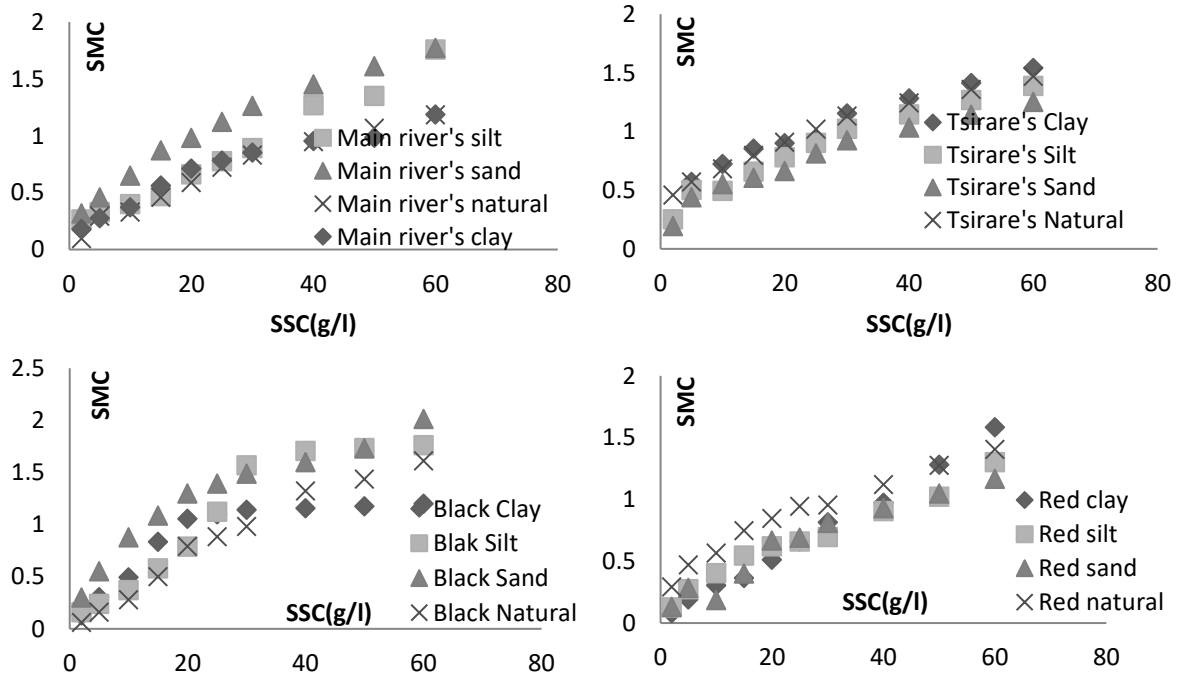

Fihure 5: Reflectance profiles of SSCs

4. Discussion

4.1 Spectral profiles and correlation

The relationship between SSC and reflectance was varied as the level of concentration, grain size and color types as well as due to the wave length variations. In general, reflectance was increased as the grain size of the suspended sediment dropped from sand to clay sediment type and comparatively higher reflectance was presented in the natural grain size sediment concentrations indicating the particle mixture among different types enhanced reflectance. The reflectance at the wavelength ranging from 750nm to 950nm (B_5) was strongly correlated with Pearson correlation coefficient and this was

consistent with Wang's studies on Yangtze River Wang et al. (2009b); Wang and Lu (2010), in which near-infrared (NIR) was reported best indicator of water turbidity. Despite of the higher reflectance valuesfrom the natural grain size distribution, the Pearson correlation between their level of concentrations and the reflectance were found comparatively very loose. This evidenced that higher reflectance values may not mean higher concentration of sediment. Non linear relationship between reflectance and sediment concentrations was found in this study and this finding was in line with Ritchie et al. (2003b), and Pavelsky and Smith, (2009) that they found a non linear relationship when sediment concentration increased. The daily SSCsoccurred on summer, 2017 in the upper portion of the Tekeze River specifically at the immediate inlets to Tekeze hydroelectric dam were varied from the lower concentration 2g/l to higher concentration 68g/l. Therefore the correlation between SSC and reflectance must be validated before building a reliable model for the remote sensing of SSC.

4.2 Comparing Empirical and LSU Remote Sensing Performances

More scattered curves were found between the SSCs and respective reflectance than the SSCs with LSUs. This indicated that the relationship between SSCs and LSUs was less sensitive to sediment variability from grain size and geological colors. The empirical and LSU remote sensing models developed for the natural grain size from the Tekeze main river and Tsirare river(figure 5) were further tested their performance to simulate the SSCs occurred in 2017 summer against the SSCs measured using the traditional sampling technique. The exponential equationsfrom empirical remote sensing (1) and from the LSUs (2) were first transformed to logarithm for convenienceof linear regression analysis and simulated the SSCs using theestimates for the natural grain size of sediment sampled from the tributary Tsirare (figure5 a, a') and Tekeze Main River beds (figure5b, b') developed from the laboratory analysis.

The SSCs simulated from the empirical remote sensing models for both rivers were deviated from the measured SSCs. Especially, when the level of SSCs increased, the deviations from the measured SSCs were also increased (Figure 5a, a'). This can evidence that empirical remote sensing models developed from some measurements were less accurate and non universal in simulating SSCs. This indicated that empirical remote sensing model was capable of site and time specific predictions of SSCs with reasonable accuracy but are limited in their universal application and may not extend to the full range of conditions present in river systems (Ritchie et al., 2003a).

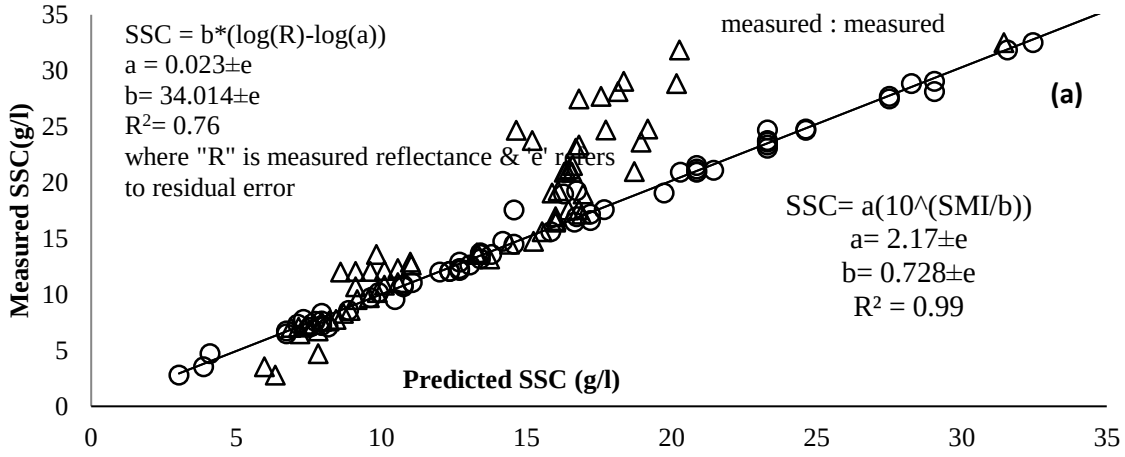
SSC = b*(log(R)-log(a))
a = 0.023±e
b= 34.014±e
R²= 0.76
where "R" is measured reflectance & 'e' refers to residual error
measured : measured
(a)
SSC= a(10^(SMI/b))
a= 2.17±e
b= 0.728±e
R² = 0.99
Measured SSC(g/l)
Predicted SSC (g/l)
0
5
10
15
20
25
30
35

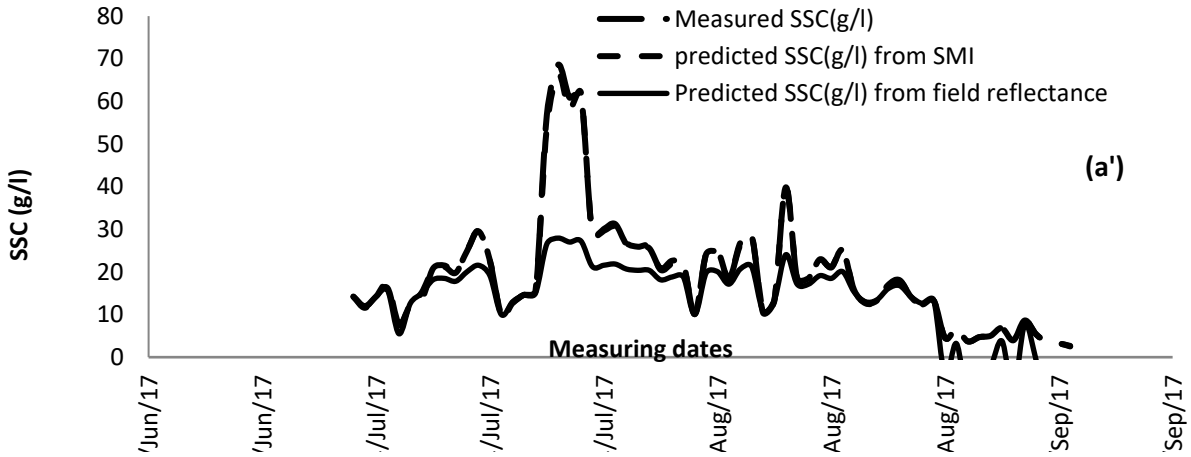
Measured SSC(g/l)
predicted SSC(g/l) from SMI
Predicted SSC(g/l) from field reflectance
(a')
SSC (g/l)
Measuring dates
0
10
20
30
40
50
60
70
80
'Jun/17
'Jun/17
/Jul/17
/Jul/17
/Jul/17
Aug/17
Aug/17
Aug/17
Sep/17
Sep/17

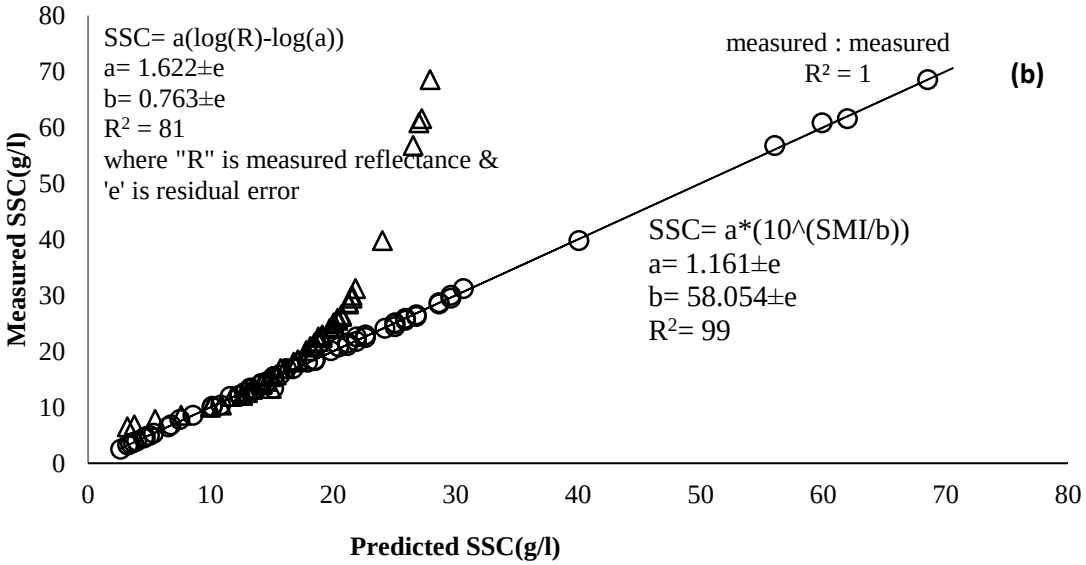
SSC= a(log(R)-log(a))
a= 1.622±e
b= 0.763±e
R² = 81
where "R" is measured reflectance & 'e' is residual error
measured : measured
R² = 1
(b)
SSC= a*(10^(SMI/b))
a= 1.161±e
b= 58.054±e
R²= 99
Measured SSC(g/l)
Predicted SSC(g/l)
0
10
20
30
40
50
60
70
80

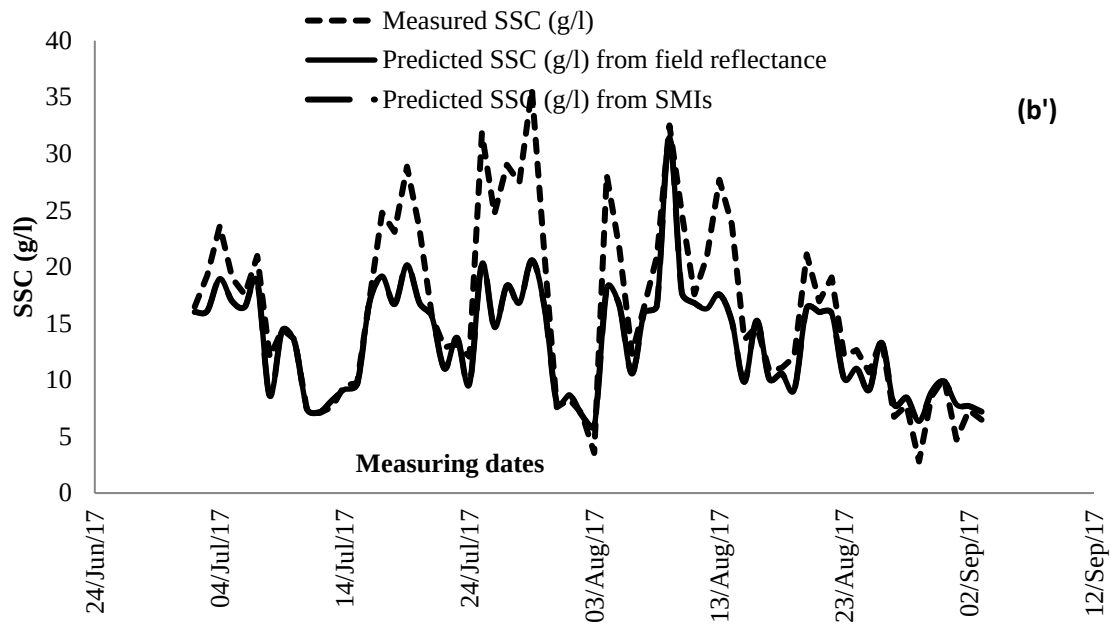

Figure 6: Evaluating simulating potential of LSU and empirical Models for natural SSC at the Tekeze main river (a , a') and Tsirare river (b,b') starting from on 2July 2017 to 3 September 2017. The curves represented by triangles, circles and smooth line were representing the predicted SSCs using the empirical, LSU exponential equations and using the field measurements respectively.

Unlike the empirical remote sensing models, the LSU remote sensing based simulations of SSCs were well fitted to the measured SSCs showing the method is accurate and less sensitive to the variability of grain size and colors. Oyama et al. (2007,2009)'s research on the remote sensing of non-phytoplankton suspended sediments demonstrated that the spectral mixing modeling approach (R^2 = 0.96) estimated non-phytoplankton suspended sediments (1mg/l to 100 mg/l) more accurately than the traditional empirical model for the same sediment concentrations. Chu,et al.(2009)also foundenhanced relationshipof reflectance and SSC using spectral mixing algorithm.

5. Conclusion

The effect of grain size distribution and geological colors variations in the upper Tekeze reaches evidently affects the relationship between SSC and reflectance. The spectral signatures of the suspended sediment concentrations in Tekeze Riverswerenot consistent across the 325-1075nm wave length ranges.These variations together with the extreme variability of suspended sediment concentrations in the reaches of upper Tekeze kept empirical remote sensing less accurate and non-universal in simulating the daily sediment concentrations. Unlike the empirical remote sensing model, the linear spectral

unmixing (LSU) remote sensing model was found less sensitive to sediment type and concentration variability in the basin. The LSU remote sensing model wasfound relatively accurate and universal in the river system to simulate the SSCs over the extensive stream reaches of the upper Tekeze basin. In general, this research has come with a conclusion that application of remote sensing for monitoring and modeling SSCs in river systems need identifying wavelength range and modeling approach working at dynamic sediment transportation.

References

Alemseged, T.H. and Rientjesb, T. (2015). Evaluation of regional climate model simulations of rainfall over the Upper Blue Nile basin.*Atmospheric Research, 161(162),*57–64.

Amsalu, A.L., Stroosnijder, L., Graaf J. (2007). Long-term dynamics in land resource use and the driving forces in the Beressa watershed, highlands of Ethiopia.*Journal of Environmental Management, 83 (4),*448–459.

Arnold, J. G., Srinivasan, R., Muttiah, R. S. and Williams, J. R..(1998). Large area hydrologic modelling and assessment part I. Model development, *JAWRA, 34,* 73–89.

Assegahegn, M.A., and Zemadim, B. (2013). Erosion modelling in the upper Blue Nile basin: The case of Mizewa watershed in Ethiopia. In: Wolde Mekuria. (ed). 2013. Rainwater management for resilient livelihoods in Ethiopia: Proceedings of the Nile Basin Development Challenge science meeting, Addis Ababa, 9–10 July 2013. NBDC Technical Report 5. Nairobi, Kenya: International Livestock Research Institute.

Ayana, E.K., Worqlul, A.W., Steenhuis, T.S.(2015). Evaluation of stream water quality data generated from MODIS images in modeling total suspended solid emission to a freshwater lake, *Sci. Total Environ, 523,*170–177.

Balthazar, V., Vanacker V, Girma A, Poesen J, Golla G. (2013). Human impact on sediment fluxes within the Blue Nile and Atbara River basins, *Geomorphology 180(181),*231–241.

Bayabil, H. K., Tilahun, S. A., Collick, A. S., Yitaferu, B., and Steenhuis, T. S.(2010). Are runoff processes ecologically or topographically driven in the (sub) humid Ethiopian highlands? The case of the Maybar watershed.*Ecohydrology, 3,* 457–466.

Belete, K. (2007).Sedimentation and Sediment Handling at dams in Tekeze River Basin, Ethiopia. PhD thesis, Norwegian University of Science and Technology, Faculty of Engineering Science and Technology, Department of hydraulic and Environmental Engineering, Trondheim, Norway.

Choubey, V.K., and Subramanian, V.(1991). Spectral response of suspended sediments in water under controlled conditions.*Journal of hydrology, 122,*301-308.

Chu, V., Laurence,W., Smith, C., Rennermalm, K., Richard, R., Forster, Jason, E., and Niels, R. (2009). Sediment plume response to surface melting and supraglacial lake drainages on the Greenland ice sheet.*Journal of Glaciology, 55(194),*1072-1082.

Cohen, H., and Jonathan, L.(2005). High rates of sediment transport by flash floods in the Southern Judean Desert, Israel.*Hydrological processes, 19(8),*1687–1702.

Defersha, M.B., Melesse, A.M., and McClain, M. (2012). Watershed scale application of WEPP and EROSION 3D models for assessment of potential sediment source areas and runoff flux in the Mara River Basin, Kenya, *CATENA, 95*, 63–72.

Doxaran, D., Jean-Marie, F., and Patrice, C. (2003). Remote-sensing reflectance of turbid sediment-dominated waters, reduction of sediment type variations and changing illumination conditions effects by use of reflectance ratios. *Applied Optics, 42(15),*2623-2634.

Easton, Z. M., Fuka, D. R., White, E. D., Collick, A. S., Biruk, A. B., McCartney, M., Awulachew, S. B., Ahmed, A. A., and Steenhuis, T. S. (2010). A multi basin SWAT model analysis of runoff and sedimentation in the Blue Nile, Ethiopia, *Hydrol. Earth Syst. Sci., 14*, 1827–1841.

Fang, G., Chen, S., Wang, H., Qian, J., and Zhang, L. (2010). Detecting marine intrusion into rivers using EO-1 ALI satellite imagery: Modaomen Waterway, Pearl River Estuary, China. *International Journal of Remote Sensing, 31(15),*4125-4146.

Guzman, C. D., Tilahun, S. A., Zegeye, A. D., and Steenhuis, T. S.(2013). Suspended sediment concentration–discharge relationships in the (sub-) humid Ethiopian highlands. *Hydrol. Earth Syst. Sci., 17*, 1067–1077.

Haregeweyn, N., Poesen, J., Nyssen, J., Govers, G., Verstraeten, G., De Vente, J., Deckers, J., Moeyersons, J., and Haile, M. (2008). Sediment yield variability Northern Ethiopia: a quantitative analysis of its controlling factors. *Catena, 75*, 65–76.

Haregeweyn, N., Poesen, J., Nyssen, J., De Wit, J., Haile, H., Govers, G., and Deckers, J. (2006). Reservoirs in Tigray: characteristics and sediment deposition problems. *Land Degrad Dev, 17*,211–230.

Haregeweyn, N., Poesen, J., Nyssen, J., Verstraeten, G., de Vente, J., Govers, G., Deckers, J., and Moeyersons, J. (2005). Specific sediment yield in Tigray-Northern Ethiopia: assessment and semi-quantitative modelling. *Geomorphology, 69*,315–331.

Haregeweyn, N. and Yohannes, F. (2003). Testing and evaluation of the agricultural non-point source pollution model (AGNPS) on Augucho catchment,Western Hararghe, Ethiopia.*Agr. Ecosyst. Environ., 99*, 201–212.

Hurni, H., Kebede,T., and Gete, Z.(2005). The implications of changes inpopulation, land use, and land management for surface runoff inthe upper Nile basin area of Ethiopia. *Mt. Res. Dev., 25*,147–154.

Hydrologic Engineering Centre, HEC.(1995). Flow Transitions in Bridge Backwater Analysis, US Army Corps of Engineers, Davis, CA, pp.71.

Islam, A., Gao,J., Ahmad, W., Neil, D., and Bell, P. (2003). Image calibration to like-values in mapping shallow water quality from multi temporal data. *Photogrammetric Engineering and Remote Sensing, 69(5),*567-575.

Keshava, N. and Mustard, J. F. (2002). "Spectral unmixing," IEEE Signal Process. *Mag., 19(1),*44–57.

Kilham, E., Roberts, D., and Singer, M. B. (2012). Remote sensing of suspended sediment concentration during turbid flood conditions on the Feather River, California a modelling approach, *Water Resources 48,* doi:10.1029/2011WR010391.

Kindiye, E., Atsushi, T., Nigussie, H., Enyew, A., Derege, T., Dagnachew, A., Tsugiyuki, M., Mitsuru, T., Dagnenet, S., Ayele, A., Mesenbet, Y. (2018). Analyzing the variability of sediment yield: A case study from paired watersheds in the Upper Blue Nile basin, Ethiopia. *Geomorphology, 303,*446–455.

Ma, R.,and Dai, J. (2005). Investigation of chlorophyll-a and total suspended matter concentrations using land sat ETM and field spectral measurement in Taihu Lake, China. *International Journal of Remote Sensing, 26(13),*2779-2795.

Maalim, F. K., Melesse, A.M., Belmont, P., and Gran, K. (2013). Modeling the impact of land use changes on runoff and sediment yield in the Le Sueur Watershed, Minnesota using GeoWEPP, *Catena, 107,* 35–45.

Masoumeh, R. and Mehdi, F. (2012). Estimating Suspended sediment concentration by a neural differential evolution (NDE) and comparison to ANFIS and three ANN Models. *Disaster Adv., 5,*346–359.

Melesse, A.M., Ahmad, S., McClain, M., Wang, X., and Lim, H. (2011). Sediment Load prediction in Large Rivers: ANN Approach.*Agricultural Water Management, 98,* 855–866.

Moges, A., Fasikaw, A., Muluken, L., Getaneh, K., Dessalegn, C., Seifu, A., and Tammo, S. (2016). Sediment concentration rating curves for a monsoonal climate: upper Blue Nile.*SOIL, 2,* 337–349.

Mohammed, A., Yohannes, F., and Zeleke, G. (2004). Validation of agricultural non-point source (AGNPS) pollution model in Kori watershed, South Wollo, Ethiopia, *Int. J. Appl. Earth Obs.,* 6, 97–109.

Mohammed, H., Alamirew, T., Assen, M., and Melesse, A.M.(2015). Modeling of sediment yield in Maybar gauged watershed using SWAT, northeast Ethiopia, *CATENA, 127,* 191–205.

Nearing, M., Foster, G., Lane, L., and Finkner, S. (1989). A process-based soil erosion model for USDA-Water Erosion Prediction Projecttechnology, T. Am. *Soc. Agr. Biol. Eng., 32,*1587–1593.

Nina, E. K., Dar, R.., and Michael, B. S. (2012). Remote sensing of suspended sediment concentration during turbid flood conditions on the Feather River, California, A modeling approach.*Water resources research,*48, doi:10.1029/2011WR010391.

Novo, E. M., Hansom, J. D., Curran, P. J. (2007). The effect of sediment type on the relationship between reflectance and suspended sediment concentration. *International Journal of Remote Sensing, 10(7),* 1283-1289.

Oyama, Y., Matsushita, B., Fukushima, T., Matsushige, K., and Imai, A. (2009). Application of spectral decomposition algorithm for mapping water quality in a turbid lake (Lake Kasumigaura, Japan) from Landsat TM data. ISPRS.*Journal of Photogrammetry and Remote Sensing, 64(1*),73-85.

Oyama, Y., Matsushita, B., Fukushima, T., Nagai, T., and Imai, A. (2007). A new algorithm for estimating chlorophyll a concentration from multispectral satellite data in case II waters: a simulation based on a controlled laboratory experiment. *International Journal of Remote Sensing, 28(7).*1437-1453.

Quintano, C., Fernandez-Manso, A., Shimabukuro, Y. E., and Pereira, G. (2012). Spectral unmixing. *International Journal of Remote Sensing*, 33: 5307–5340.

Ritchie J. C. and Cooper C. M.(1991). Algorithm for estimating surface suspended sediment concentrations with Landsat MSS digital data. *Water Resources Bulletin, 27(3),* 373-379.

Ritchie, J. C., Zimba., P. V. and Everitt J. H. (2003a). Remote sensing techniques to assess water quality, *Photogram. Eng. Remote Sens., 69(6),*695–704.

Ritchie, J C Zimba, P V and Everitt. J H.(2003b). Remote sensing techniques to assess water quality. *Photogrammetric Engineering and Remote Sensing, 69(6),*695-704.

Ritchie, J.C. and Schiebe F.R. (2000). Remote Sensing in Hydrology and Water Management, Water Quality, In: G.A. Schultz and E.T. Engman (eds.) Springer-Verlag, Berlin, Germany, 351-352.

Setegn, S. G., Ragahavan, S., and Bijan, D. (2008). Hydrological modeling in the Lake Tana Basin, Ethiopia using SWAT model, *Open Hydrol. J., 2*, 49–62.

Setegn, S. G., Rayner, D., Melesse, A. M., Dargahi, B., and Srinivasan,R. (2011). Impact of climate change on the hydroclimatology of Lake Tana Basin, Ethiopia, Water Resour. Res., 47, W04511, doi:10.1029/2010WR009248.

Shi C. and Wanga L. (2014). Incorporating spatial information in spectral unmixing (review). *Remote Sensing of Environment, 149,* 70–87.

Somers B., Asner G P., Tits L., Pol C. (2011). Endmember variability in Spectral Mixture Analysis (review), *remote sensing of environment, 115*,1603-1616.

Steenhuis, T., Collick, A., Easton, Z., Leggesse, E., Bayabil, H., White, E., Awulachew, S., Adgo, E., and Ahmed, A. (2009). Predicting discharge and sediment for the Abay (Blue Nile) with a simple model, *Hydrological Processes*, *23*, 3728–3737.

Tamene L., Park S.J., Dikau R., and Vlek P.L.G. (2006). Reservoir siltation in the semi-arid highlands of northern Ethiopia: sediment yield–catchment area relationship and a semi-quantitative approach for predicting sediment yield. *Earth surface processes and landforms, 31(11). 1364-1383.*

Tilahun, S. A., Mukundan, R., Demisse, B. A., Engda, T. A., Guzman, C. D., Tarakegn, B. C., Easton, Z. M., Collick, A. S., Zegeye, A. D., Schneiderman, E. M., Parlange J. Y., and Steenhuis, T. S. (2013). A Saturation Excess Erosion Model, T. Am. *Soc. Agr. Biol. Eng., 56*, 681–695.

Tilahun, S.A., Guzman, C. D., Zegeye,A. D., Sime,A., Collick, A. c., Rimmer, A. and Steenhuis, T. S. (2013). An efficient semi-distributed hillslope erosion model for the sub-humid Ethiopian Highlands. *Hydrological Earth System Sciences, 9*, 2121-2155.

Vanmaercke, M., Amanuel, Z., Poesen, J., Nyssen, J., Verstraeten, U., and Deckers, J. (2010). Sediment dynamics and the role of flash floods in sediment export from medium-sized catchments: a case study from the semi-arid tropical highlands in northern Ethiopia. *Journal of soils and sediments, 10(4),*611-627.

Volpe, V., Silvestri, S., Marani, M . (2011). Remote sensing retrieval of suspended sediment concentration in shallow waters, *remote sensing of environment, 115*, 44–54.

Wang, F, B., Zhou, J., Xu, L., Song, and Wang, X.(2009). Application of neural network and MODIS 250 m imagery for estimating suspended sediments concentration in Hangzhou Bay, China. *Environmentalgeology*, 56(6), 1093-1101.

Wang, F., Bin, Z., Xingmei, L., Gendi Z., and Keli Z. (2012). Remote-sensing inversion model of surface water suspended sediment concentration based on in situ measured spectrum in Hangzhou Bay, China. *Environmental Earth Sciences, 67(6),* 1669-1677.

Wang, J J., Lu, X.X., Liew, S. C. and Zhou,Y. (2010). Remote sensing of suspended sediment concentrations of large rivers using multi-temporal MODIS images: an example in the Middle and Lower Yangtze River, China. *International Journal of Remote Sensing, 31(4).*

Wang, J. J., Lu, X. X., Soo, C. L., and Yue. Z. (2009). Retrieval of suspended sediment concentrations in large turbid rivers using Landsat ETM+: an example from the Yangtze River, China. *Earth surfaceprocess landforms, 34(8),*1082-1092.

White, E. D., Easton, Z. M., Fuka, D. R., Collick, A. S., Adgo, E., McCartney, M., Awulachew, S. B., Selassie, Y., and Steenhuis, T.S. (2010). Development and application of a physically based landscape water balance in the SWAT model.*Hydrological process, 23,* 3728–3737.

Yatheendradas, S., Thorsten, W., Hoshin, G., Carl, U., David, G., Mike, S.,and Anne, S. (2008). Understanding uncertainty in distributed flash flood forecasting for semiarid regions. *Water resources research,*44(5).

Young, R. A., Onstad, C., Bosch, D., and Anderson, W. P., AG-NPS. (1989). A non point source pollution model for evaluating agricultural watersheds.*journal of soil and water conservation, 44,* 168–173.

Zaghloul, S.S., El-Moattassem, M., Rady, A.A. (2007). The hydrological interactions between Atbara River and the main Nile at the confluence area. International congress on river basin management. Antalya, Turkey, 787-799. Retrieved from http://www.dsi.gov.tr/english/congress2007/.

Trends and abrupt changes in hydro-climatic variables in a Kulfo catchment, Ethiopia

Santosh Murlidhar Pingale[1*], AyalkibetMekonnen[2], Samuel DagaloHatiye[1&2],

[1]Faculty of Water Resources and Irrigation Engineering, Arba Minch Water Technology Institute (AWTI), Arba Minch University, Arba Minch, Ethiopia, P.O. Box 21, [2] Water Resources Research Centre, AWTI, Arba Minch University, Arba Minch, Ethiopia

*Corresponding author: pingalesm@gmail.com

Abstract

The availability of freshwater has been identified as a prime global problem. The reliable evaluation and quantification of natural water resources within the catchment is required to boost the sustainable development and management of water resources properly. Therefore, the trends and abrupt changes in hydro-climatic variables (i.e., rainfall, temperature (maximum, minimum& average), evapotranspiration, natural springs and river flow) at seasonal and annual timescales have been carried out using statistical methods (Mann-Kendall test and Pettitt–Mann–Whitney (PMW) test) in the Kulfo catchment, Ethiopia. It has been found a significant change and shifts in the Forty springs flow, which is the lifeline of the Arba Minch for different uses of water especially drinking purpose. The results indicate the significant increase in Kulfo river flow while a decrease in forty spring flow. The predominant changes and shift were also observed in climatic variables at seasonal and annual scale within the Kulfo catchment. This implies that there is a significant reduction in the recharge zone of the forty spring catchment. This change can be attributed to both anthropogenic activities and natural causes. This is a very useful study for city administration and community to manage and plan water resources properly in the future under a scarcity of water and in view of alarming effects of climate change.

Keywords Trends analysis, Mann-Kendall test, PMW test, Rift Valley Lakes basin, Ethiopia

1. Introduction

Catchments are dynamic and complex systems involving a range of physical processes (natural or anthropogenic) which may operate simultaneously and have different spatial and temporal influences. The natural hydrological systems are characterized by tremendous variability in space, time and process (Kirnbauer et al., 2005) and the hydrological response of a catchment to land use/land cover (LULC) change and rainfall on different timescales is the result of this complex system. Understanding those processes is essential for managing the quality and quantity of runoff, especially when environmental conditions (climate or land use) are changing (Naef et al., 2002;Negley and Eshleman, 2006; Stewart and Fahey, 2010).The IPCC projected the global precipitation to increase but, at the same time, both increases and decreases are projected at the regional scale (IPCC, 2007). It has been seen that the

average earth's temperature increased 0.6ºC to 5.4ºC by the end of the 21st century as per the projections made by the various climate prediction models (IPCC 2001). Micro-scale studies are required to assess climate change and to identify the real cause of climate change for the proper planning and management of water resources (Saadat et al., 2011; Halbe et al., 2013).

After the establishment of Arba Minch town in 1955, forty springs are the potential water source of the town and it is tourism potential for the area.Effective utilization and management of thefortyspring water resources require detecting and simulating impacts of LULC changes and management practices on its hydrological regimes and its effect on water availability for downstream NechSar national park and source of water supply for Arba Minch town. It requires optimizing the allocation of these potential resources of water among Arba Minch town with increasing population growth, the water demand will increase or decrease in the past and exist, and the effect for downstream ecological purposes. Therefore, to understand the impact of LULC and climate variability on Forty spring flow is necessary for making future water resources management strategy. The statistical analysis should be extended to analyze additionalhydro-climatic parameters and their relationships with water resources, LULC, urbanization etc.

No studies have been reported in the literature which investigated climate in terms of inter-seasonal and inter-annual variation in hydro-climatic time series along with annual and seasonal shifts at Kulfo catchment in Ethiopia. Therefore,the present study was undertakento assess the trends and abrupt changes in the hydro-climatic variables, and its implications on Kulfo River flow and Forty springs flow on the annual and seasonal scale within the Kulfo catchmentin Ethiopia.This studywas carried out by using the Mann-Kendall (MK) test and Pettitt–Mann–Whitney (PMW) testat annual and seasonal time scale. The comparative assessment of the trends and abrupt changesin the climatic variables were also carried out within the Kulfo catchment. Further, the significant impacts of climatic variability on forty spring flow and Kulfo river streamflow were investigated.This study can help different stakeholders for sustainable management of water resourcesand meet the increased water demand in the future under water scarcity and adverse climatic conditions.

2. Materials and Methodology

2.1. Study area

The study area (i.e. Kulfo and Forty spring's catchment) is located in theAbaya-Chamo sub-basin of the southern Ethiopian Rift Valley Lake basin. Forty springsare the ultimate source of Arba Minch town water supply system and it drains into Lake Chamo. The catchment is situated at 37° Eastern longitude and 6° Northern latitude and has a land area of 127.09 km^2. The geographic location of the study area is shown in Fig.1. Precipitation is generally dependent on altitude in the Lake Abaya-Chamobasin (Bekele, 2001; Thiemann, 2006). Thiemann and Foerch (2005) identified the dependence of precipitation on altitude is more pronounced in the rainy season than in the dry season. Thepattern of monthly precipitation of Kulfo catchmentis found to bea bimodal distribution withprecipitation peak in April/May and September/October (Fig. 2). Average maximum anda minimum temperature of Kulfo catchment vary between 32.19°C and 9.28°C. Theaverage maximum temperature of Arba Minch ranges between 28ºC to 33.51ºC, while the minimum ranges between 15ºC to 18ºC.The predominant soil associations of the watershed include orthicacrisols, dystricnitosols, and eutricfluvisols etc. Bushes and Grassland mostly cover the upstream catchment of the area. Some parts are highly eroded and no fertile soil has left. Along the River, vegetation included a strip of the forest only in the lower part of theKulfo River near Lake Abaya-Chamo and NechSar National Park. The natural forest left in the higher mountain region on the land is used for cultivation, grazing, fuelwood,and housing. The most crops grow in the catchment area are a banana, cotton, maize,sugarcane, sweet potatoes, and barley, wheat,

enset, peas, beans, onion and apple in the middle and upper sub-catchment(Wayand et al. 1999; Mengistu, 2009).

2.2. Data used

For this study, daily hydro-meteorological datawere obtained from the Ethiopian National Meteorological Agency, Ministry of Water, Irrigation,and Energy for the different periods.The meteorological data (i.e., rainfall, maximum and minimum temperature, relative humidity, sunshine hour, wind speed and evaporation) was collected from the Arba Minch meteorological stations for the period of 1987 to 2016. The rainfall and temperature (minimum and maximum) data were also collected for the period 1987 to 2011 from other meteorological stations in and around the Kulfo catchment (i.e. Chencha, Dorze, Daramalo, Kemba, andZigiti) (Fig. 1). The potential evapotranspiration was estimated for the Arba Minch station using the FAO Penman-Monteith equation on the annual and seasonal scale. The Forty springs flow and Kulfo River flow data were obtained for the period 1981 to 2005 and 1980 to 2013, respectively. The catchment has three distinctive seasons based on rainfall regime namely Kiremt (main rainy season during June to September), Belg (short rainy season during February to May) and Bega (a dry season which lasts from October to January) (Gebere et al. 2015).The datasets were subjected toinitial quality checks including filling of the missing and inconsistencies in the data. For this study, normal ratio and station averaged method wasused to fill the missed rainfall datawhen normal annual rainfall at the nearby station differs from the missed station by more than 10% and less than 10% from the missing data stations, respectively (Subramanya 2008). The consistency of rainfall data was tested by

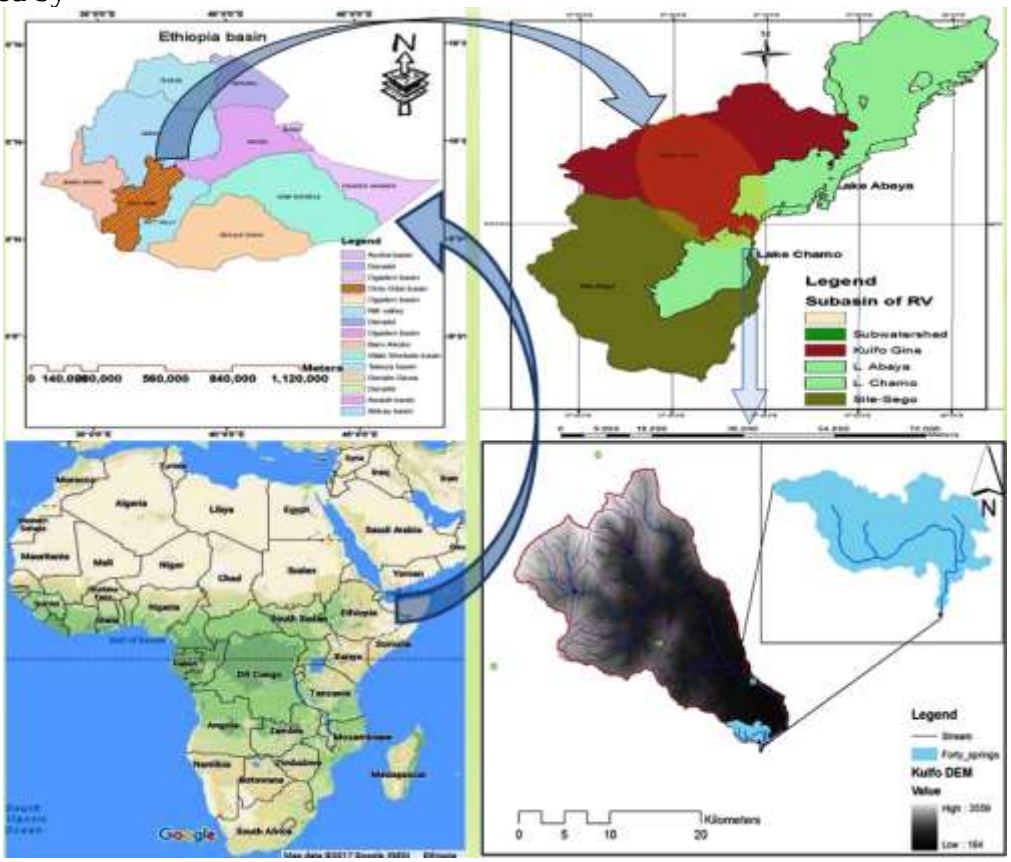

Fig. 1 Location of the study area

double mass curve analysis. The selected stations in this study have not undergone any significant change during the study period. The homogeneity test was evaluated using RAINBOW software for rainfall and streamflow data separately and confirms the presence of homogeneity among them.

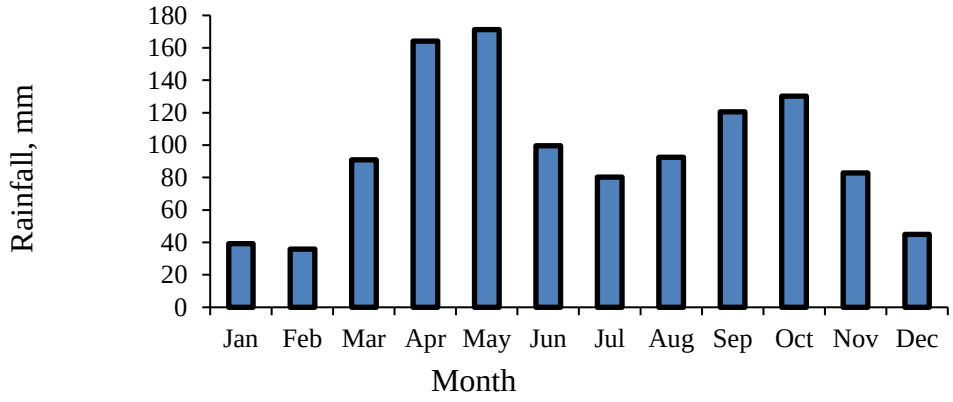

Fig. 2. Monthly average daily rainfall at the Kulfo catchment

2.3. Methodology

2.3.1 Estimation of potential evapotranspiration

The daily potential evapotranspiration (ET_o) at Arba Minch station was estimated using the FAO Penman-Monteith (PM) method (Allen et al., 1998). The data used for the estimation of ET_oincluderelative humidity, wind speed, sunshine hours, maximum and minimum temperature. The FAO PM equation was used in this study as follow:

$$ET_o = \frac{0.408\Delta(R_n - G) + \gamma \frac{900}{T+273} u_2 (e_s - e_a)}{\Delta + \gamma(1 + 0.34u_2)} \quad (1)$$

Where, ET_o is reference evapotranspiration (mm/day), Δ is slope of saturation vapour pressure curve (kPa/^{o}C), $R_n$is net radiation (MJ m^{-2} day^{-1}), G is a soil heat flux density (MJ m^{-2} day^{-1}), γ is a psychometric constant (kPa/^{o}C), T is the mean daily air temperature (^{o}C),$e_s$is saturation vapour pressure (kPa),e_a is actual vapour pressure (kPa), and $u_2$is average daily wind speed at 2 m height (m/s).

2.3.2 Mann-Kendall test

The MK test isa non-parametric test used for identifying trends in a time series (Mann 1945). The non-linear trend and the turning point can be derived from Kendall test statistics (Kendall 1975). This method searches for a trend in a time series without specifying whether the trend is linear or nonlinear. It has been found to be an excellent tool for trend detection and many researchers have used this test to assess the significance of trends in hydro-climatic time series such as water quality, streamflow, temperature and precipitation (e.g. Ludwig et al. 2004; McBean and Motiee 2008;Basistha et al. 2009; Rai et al. 2010; Nalley et al. 2013; Pingale et al. 2016). The MK test can be applied to a time series x_i ranked from $i = 1, 2... n-1$ and x_j ranked from $j = i+1, 2...n$. Each data point x_i is used as a reference point and is compared with all other data points x_j such that:

$$\operatorname{sgn}(x_j - x_i) = \begin{cases} 1 & if\ (x_j - x_i) > 0 \\ 0 & if\ (x_j - x_i) = 0 \\ -1 & if\ (x_j - x_i) < 0 \end{cases} \quad (2)$$

The Kendall test statistic (S) is given below:

$$S = \sum_{k=1}^{n-1} \operatorname{sgn}(x_j - x_k) \quad (3)$$

Where $\operatorname{sgn}(x_j - x_k)$ is the signumfunction. The test statistic (S) has been assumed to be asymptotically normal, with $E(S) = 0$ for sample size $n \geq 8$ and variance as follows:

$$V(S) = \frac{[n(n-1)(2n+5) - \sum_t t(t-1)(2t+5)]}{18} \quad (4)$$

Where t_i denotes the number of ties to sample i

The standardized MK test statistics (Z_{mk}) can be estimated as follows:

$$Z_{mk} = \begin{cases} \frac{S-1}{\sqrt{V(S)}} & if\ S > 0 \\ 0 & if\ S = 0 \\ \frac{S+1}{\sqrt{V(S)}} & if\ S < 0 \end{cases} \quad (5)$$

The standardized MK test statistics (Z_{mk}) follows the standard normal distribution with a mean of zero and variance of one. If $\pm Z_{mk} \leq Z_{\alpha/2}$ (here $\alpha = 0.05$), then the null hypothesis for no trend was accepted in a two-sided test for trend and the null hypothesis for no trend was rejected, if $\pm Z_{mk} \geq Z_{\alpha/2}$. Failing to reject H_o (i.e.null hypothesis) does not mean that there is no trend. Rather, it is a statement that the evidence available is not sufficient to conclude that there is a trend (Helselet al. 2002).A positive and negative value of Z_{mk} indicates an increasing and decreasing trend. The significance levels (p-values) for each trend test can be obtained from the following equation (Coulibalyand Shi, 2005):

$$p = 0.5 - \phi(|Z_{mk}|) \quad (6)$$

where $\phi(\,)$ denotes the cumulative distribution function (CDF) of a standard normal variate. At a significance level of 0.05, if $p \leq 0.05$ then the existing trend is considered to be statistically significant.

2.2.5 Sen's estimator and percentage change

The Sen'sslope estimator was used to estimate the change per unit time of the observed trends in the hydro-climatic time series.If a linear trend is present in a time series, then the true slope of trend can be determined by using a simple non-parametric procedure (Theil 1950; Sen 1968). The slope estimates were computed from:

$$Q_i = Median\left(\frac{x_j - x_k}{j-k}\right) \forall k \leq j \quad (7)$$

Where x_j and x_k are data values at times *j* and *k* (*j* > *k*), respectively. The median of N values of Q_i is a Sen's estimator of the slope. If *N* is odd, then the Sen's estimator is computed by $Q_{med} = Q_{(N+1)}/2$ and if N is even, then the Sen's estimator is computed by $Q_{med} = \lfloor Q_N/2 + Q_{(N+2)}/2 \rfloor / 2$. Finally, Q_{med} is

tested by a two-sided test at $100(1-\alpha)\%$ the confidence interval and, the true slope may be estimated from the non-parametric test.The negative and positive sign of the values indicates a downward slope and upward slope, respectively.

The percentage change (%) was estimated assuming the linear trend in which magnitude by Theil and Sen's median slope, and mean were used (Yue and Hashino 2003; Basisthaet al. 2009). The % changes over a period were expressed as follows:

$$\%\ change = \left(\frac{Median\ Slope \times length\ of\ \ period}{mean} \right) \tag{8}$$

2.2.5Pettitt–Mann–Whitney (PMW) test

The PMW test can be used to identify the shift in the time series data (Pettitt 1979). This test was applied to the hydro-climatic time series data using the Xlstat 2018 software (evaluation version). This test can be briefly described as follows using PMW statistics (Kielyet al. 1998; Basisthaet al. 2009; Pingale et al. 2016). Let, T be the length of the time series and τ be the year of the most likely change point. Considering the time series as two samples represented by $X_1 \ldots X_\tau$ and $X_{\tau+1} \ldots X_T$, the index V_τ is defined as:

$$V_\tau = \sum_{j=1}^{T} \mathrm{sgn}(X_\tau - X_j) \text{ for any } \tau \tag{9}$$

Let a further index U_τ be defined as:

$$U_\tau = \sum_{i=1}^{\tau} \sum_{j=1}^{T} \mathrm{sgn}(X_i - X_j) \tag{10}$$

A plot of U_τ against τ for a time series with no change point would result in a continually increasing value of $|U_\tau|$. However, if there is a change point, then $|U_\tau|$ would increase up to the change point and then begin to decrease. The most significant change point τ can be identified as the point where the value of $|U_\tau|$ is a maximum, as follows:

$$K_T = \max_{1 \le \tau \le T} |U_\tau| \tag{11}$$

The probability of a change point year, where $|U_\tau|$ is the maximumestimated by:

$$p = 1 - \exp\left[\frac{-6K_T^2}{T^3 + T^2} \right] \tag{12}$$

Further for $1 \le \tau \le T$, the series

$$\hat{U}(\tau) = |U_\tau| \tag{13}$$

is introduced, and defined as:

$$p(\tau) = 1 - \exp\left[\frac{-6\hat{U}(\tau)^2}{T^3 + T^2} \right] \tag{14}$$

Using the equations 8 to 13, the hydro-climatic time series consisting of probabilities of the change points were determinedto identify abrupt changesin the series at annual and seasonal (Kiremt, Belg,andBega) scale over a period of timeinthe Kulfo catchment.

3. Results and Discussion

The trends and abrupt changesin hydro-climatic variables were carried out using MK and PMW test on the annual and seasonal scale (Kiremt, Bega, and Belg) at 5% level of significance. The results were

derived for each variable at different temporal scales and compared with each other and among the different stations within the Kulfo catchment. The MK test statistics (S) and $Z_{mk}$are presented for both the significant and non-significant trends of hydro-climatic variablesfor Arba Minch station (Table 1)(other stations are not mentioned for brevity).The corresponding Sen's slope estimator, mean, percentage changesand shifts in the hydro-climatic variables were determined at annual and seasonal time scale for the Kulfo catchment.This represents the annual and seasonal changes and variability in all the hydro-climatic variables over the period of time in the Kulfocatchment.

3.1 Trend analysis

Trend test results indicated that the significant increasing trend in total rainfall at Zigiti (annual @ 12.56 mm) and Daramalo station (annual @ 17.67mm and short rainy season @ 9.53mm) at 5% level of significance. Similarly, the significant increasing trend was observed in annual maximum daily rainfall at Arba Minch (main season @ 0.67mm), Zigiti (main season and annual @ 1.5mm, respectively) (Table 1 and Fig. 3) and Daramalo station (annual@ 0.87 mm). The significant increasing trend was found in annualmaximum daily temperature at Arba Minch during seasonal (except short rainy season) and annual scales (Fig. 4a-c). Except for Zigiti station, other stations do not show any significant trend in case of annual and seasonal temperature by using MK test at 5% levelofsignificance.

Parameter/Season	Main rainy season				Short rainy season				Dry season				Annual			
	S statistics	Kendall t	Sen slope	P value	S statistics	Kendall t	Sen slope	P value	S statistics	Kendall t	Sen slope	P value	S statistics	Kendall t	Sen slope	P value
Total rainfall, mm	17	0.04	1.01	0.78	7	0.02	0.23	0.92	55	0.13	1.99	0.34	61	0.14	3.89	0.284
Annual max daily rainfall, mm	113	0.26	0.67	**0.046**	-27	-0.06	-0.12	0.64	70	0.16	0.29	0.22	63	0.15	0.46	0.269
Annual max daily temperature, ^{o}C	161	0.38	0.05	**0**	34	0.02	0.02	0.56	135	0.32	0.05	**0.02**	183	0.43	0.06	**0.001**
Annual minimum daily temperature, ^{o}C	15	0.04	0.01	0.8	27	0.06	0	0.64	98	0.23	0.06	0.08	91	0.21	0.06	0.107
Minimum temperature,^{o}C	3	0.01	0.01	0.97	18	0.04	0.01	0.76	14	0.03	0	0.82	5	0.01	0	0.943
Average temperature, ^{o}C	65	0.15	0.04	0.25	45	0.1	0.04	0.43	37	0.09	0.02	0.52	55	0.13	0.02	0.335
Maximum temperature, ^{o}C	91	0.21	0.03	0.11	27	0.06	0.01	0.64	-11	-0.03	0	0.86	97	0.22	0.02	0.087
Relative humidity, %	-51	-0.12	-0.1	0.37	-9	-0.02	-0.05	0.89	-9	-0.02	-0.03	0.89	-31	-0.07	-0.08	0.592
Wind speed, m/s	-142	-0.38	-0.02	**0.01**	-182	-0.48	-0.03	**0**	-160	-0.42	-0.02	**0**	-168	-0.44	-0.02	**0.001**
Sunshine hours	40	0.11	0.01	0.44	-90	-0.24	-0.03	0.08	-24	-0.06	-0.01	0.65	-58	-0.15	-0.01	0.26
Average annual ET_o, mm	86	0.29	0.77	**0.05**	-14	-0.05	-0.03	0.76	42	0.14	0.23	0.34	68	0.23	0.84	0.118
Annual maximum dailyET_o, mm	72	0.24	0.81	0.1	-14	-0.05	-0.03	0.76	31	0.1	0.17	0.48	50	0.17	0.47	0.252

Table 1: Trend analysis (bold values indicate significant trend)

However, it was found that average and annual maximum daily temperature (annual and seasonal) shows the non-significant increasing trend at Arba Minch station (Table 1). The null hypothesis of no trends reveals that the evidence of trend was not enough on the annual and seasonal scale at 5% level of significance. The significant decreasing trendwas observed in annual and seasonal average wind speed at Arba Minch (Table 1). The relativehumidity and sunshine hours did not indicateany significant trend at annual and seasonal scale (Table 1).

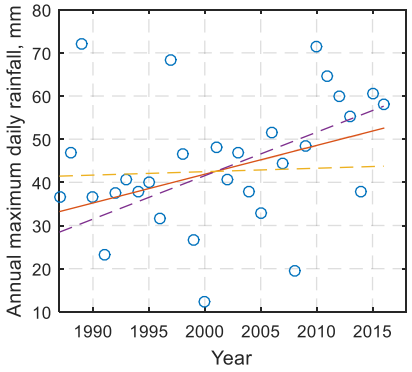

Fig. 3. The significant trend in main season maximum daily rainfall at the Arba Minch station

The average annual ETo showssignificant increasingtrend during the main season at 5% level of significance (Fig. 5). It is revealed that the trend for temperature is significantly increasing in specific months, which indicated higher evapotranspiration at both 5% significant and non-significant level. Along with temperature, other climatic variables such as wind speed, solar radiation, and humidity have also influence on evaporation.

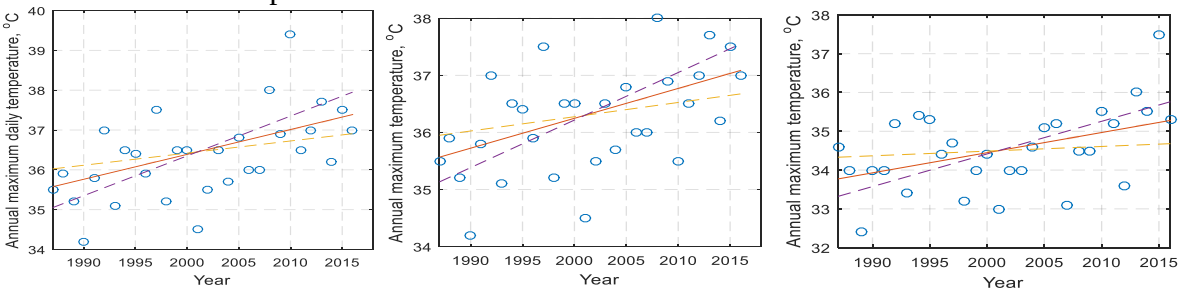

Fig. 4 The significant trend in (Left) annual and (Middle) main rainy season, (Right) dry rainy season average annual maximum daily temperature of the Arba Minch station

Similar observation of higher evapotranspiration was also reported by several researchers (e.g. Wang et al. 2012; Kumar et al. 2018). The Sen's slope and % changes in average rainfall (total & annual maximum daily rainfall) and temperature show the predominant changes in the Kulfo catchment during annual & seasonal time scale (Table 2).

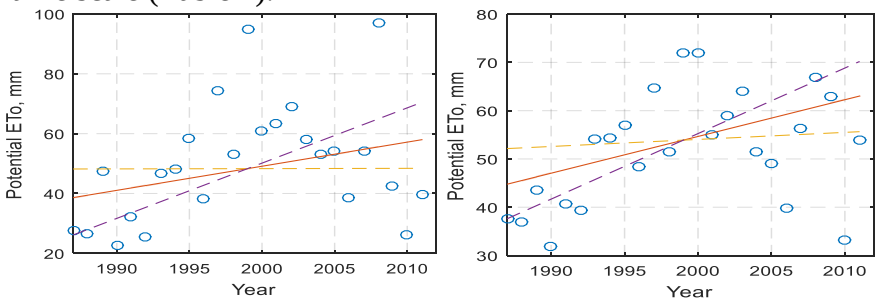

Fig. 5. The significant trends in (Left) annual maximum daily potential $ET_o$and (Left) average potential ET_oduring the main season at the Arba Minch station

Forty spring is the lifeline of the Arba Minch especially for drinking purpose. The average annual and seasonal scale forty spring's flow shows the significant decreasing trend at 5% level of significance (Table 3). Similarly, average daily streamflow during annual and seasonal scale shows a significant

decreasing trend (Table 3 and Fig. 6). This implies that there is a significant reduction in the recharge zone of the forty-spring catchment. While the significant increasing trend was found in average annual and daily Kulfo river flow during the annual and seasonal time scale at 5% significance level (Table 3 and Fig. 7). The increase in Kulfo river flow indicates that there are significant LULC changes occurring in the catchment, which results in a decrease in infiltration and groundwater recharge with an increase in runoff within the Kulfo catchment. This may result increase in Kulfo River flow. The Sen's slope and % changes in both Kulfo River flow and Forty springs flow also indicates predominant changes during the annual and seasonal time scale (Table 3 and 4).The study results of significant or insignificant (increase, decrease or no trend) trends in hydro-climatic variables were in agreement with earlier studies in different regions of the World and in particular in Ethiopia (e.g. Wagesho et al. 2012; 2013;Pingale et al. 2016).

3.2 Abrupt change detection analysis

The abrupt change detection is very important for identifying evidence of climate change (Matalas 1997; Pingale et al. 2016) and also provides valuable information for planning the adaptation measures (Fischer et al. 2012). Therefore, the abrupt change detection analyses for the hydro-climatic variables were performed at seasonal and annual time scale using PMW test at 5% level of significance. The abrupt changes were observed in statistically significant hydro-climatic time series in the Kulfo catchment over a period of time (Table 2&4). No shift was observed in total annual rainfall and annual maximum daily rainfall at Arba Minch, Dorze, Chencha, Kemba (Table 2&4). Only annual maximum daily rainfall shows a significant shift during annual (2000) and main rainy season (2001) at Zigiti. While annual and short-season total and annual maximum daily rainfall at Daramaloindicatea significant shift in the year 1995 and 1994, respectively (Table 2). No significant shift was found in average and annual maximum and minimum daily temperature (^{o}C) during seasonal scale at Arba Minch and Dorze. The average temperature also reveals a significant shift at Arba Minch station. However, the relative humidity and sunshine hours did not show any significant shift at annual and seasonal scale (Table 2). The average annual ET_o during mainrainy season and annual average ET_o shows significant except short and dry season in the years 1992. Annual maximum daily ET_o also indicates a significant shift during the annual and seasonal scale in the years 1992&1993 (Table 2).Average maximum and minimum temperature show a significant shift during the annual and seasonal scale at Zigiti (Table 4).The shifts in climatic variables may be caused due to the global climate changes or localized climatic effects, changes in forest cover and anthropogenic activities (e.g., Basistha et al. 2009).

A significant increase and decrease in the shiftwere found in average daily Kulfo river flow and forty spring's streamflow during the study period (Table 4). The significant shift was found in an annual and seasonal mean daily Kulfo river flow at 5% level of significance at Arba Minch gauging station (Fig. 8). The significant shift was found in an annual maximum mean daily Kulfo river flow during annual and seasonal scale, except during main rainy season no significant shift was found at Arba Minch gauging station (Fig. 8). Similarly, a significant shift was observed in an annual minimum mean daily Kulfo river flow during the annual and seasonal scale (Table 4). The significant shift was found in an annual and seasonal mean daily forty springs flow at 5% level of significance (Fig. 9). Also, a significant shift was found in average daily spring flow (Table 4). The significant shift was found in a total annual maximum and minimum mean daily spring flow during annual and seasonal scale. Also, the significant shift was found in total seasonal and annual average streamflow during the years 1981 to 2005 (Table 4).

Table 2. The mean, percentage changes and a shift in climatic variables on the annual and seasonal scale at Arba Minch station (Y= Yes, N=No)

Parameter/Season	Main rainy season			Short rainy season			Dry season			Annual		
	Mean	%change	Shift(Y/N)	Mean	%change	Shift(Y/N)	Mean	% change	Shift(Y/N)	Mean	% change	Shift(Y/N)
Total rainfall, mm	346.03	8.77	N	302.48	2.31	N	289.35	20.59	N	937.86	12.45	N
Annual max daily rainfall, mm	44.84	44.62	N	44.14	-8.36	N	41.27	21.3	N	56.47	24.33	N
Annual max daily temperature, ^oC	36.22	4.31	N	32.98	1.36	N	34.52	4.35	N	36.35	5.2	Y (2007)
Annual minimum daily temperature, ^oC	12.91	1.39	N	13.9	0	N	10.94	17.54	N	10.75	17.86	Y (2008)
Minimum temperature,^oC	17.97	0.83	N	17.95	1	N	16.26	0.74	N	17.39	0.17	N
Average temperature, ^oC	31.38	4.21	Y (1993)	29.05	4.34	Y (1993)	29.61	2.43	N	30.01	2.1	Y (1993)
Maximum temperature, ^oC	31.8	3.21	N	28.9	1.45	N	31	-0.29	N	30.57	1.77	N
Relative humidity, %	55.43	-5.25	N	59.65	-2.56	N	55.55	-1.62	N	56.88	-4.01	N
Wind speed, m/s	0.67	-67.26	Y (1992)	0.74	-87.6	Y (1993)	0.51	-78.43	Y (1992)	0.64	-78	Y (1992)
Sunshine hours	8.06	2.79	N	5.79	-14.24	N	8.4	-2.08	N	7.4	-3.38	N
Average annual ET_o, mm	51.79	36.93	Y (1992)	26.26	-2.48	N	55.73	10.27	N	133.78	15.68	Y (1992)
Annual maximum daily ET_o, mm	50.1	40.17	Y (1992)	20.92	-3.82	Y (1992)	42.58	10.16	Y (1993)	53.63	21.91	Y (1993)

Table 3. Summary of trend statistics of hydrologic variables on an annual and seasonal scale (bold values indicate significant trends)

Parameter/Season	Main rainy season				Short rainy season				Dry season				Annual			
	S statistics	Kendall t	Sen slope	P value	S statistics	Kendall t	Sen slope	P value	S statistics	Kendall t	Sen slope	P value	S statistics	Kendall t	Sen slope	P value
Average annual & seasonal monthly spring flow, m^3/s	-138	-0.46	-0.01	**0.001**	-164	-0.55	-0.02	**0**	-140	-0.47	-0.02	**0.001**	-164	-0.55	-0.05	**0**
Maximum spring flow, m^3/s	-137	-0.46	-0.01	**0.001**	-172	-0.57	-0.02	**0**	-150	-0.5	-0.02	**0.001**	-168	-0.57	-0.01	**0.0001**
Minimum spring flow, m^3/s	-111	-0.37	-0.01	**0.01**	-138	-0.46	-0.01	**0.001**	-139	-0.46	-0.01	**0.001**	-146	-0.49	-0.04	**0.001**
Annual and seasonal average daily spring flow, m^3/s	-138	-0.46	-0.39	**0.001**	-164	-0.55	-0.5	**0**	-142	-0.47	-0.48	**0.001**	-164	-0.55	-1.37	**0**
Average annual & seasonal river flow, m^3/s	243	0.43	0.22	**0**	201	0.36	0.27	**0.003**	247	0.44	0.21	**0**	265	0.47	0.25	**0.0001**
Annual maximum daily river flow, m^3/s	138	0.25	0.35	**0.042**	204	0.37	0.81	**0.003**	181	0.32	0.5	**0.008**	177	0.32	0.83	**0.009**
Annual minimum daily river flow, m^3/s	158	0.28	0.11	**0.02**	134	0.24	0.13	**0.048**	91	0.16	0.05	0.182	65	0.12	0.04	0.342
Annual and seasonal average daily river flow, m^3/s	218759	0.39	0.01	**0**	193849	0.35	0.01	**0**	214698	0.39	0.01	**0**	238051	0.43	0.01	**0.0001**

Table 4. The mean, percentage changes and a shift in hydrologic variables on an annual and seasonal scale (: Y= Yes, N=No)

Parameter/Season	Main rainy season			Short rainy season			Dry season			Annual		
	Mean	% change	Shift (Y/N), Year	Mean	% change	Shift (Y/N), Year	Mean	% change	Shift (Y/N), Year	Mean	% change	Shift (Y/N), Year
Average annual & seasonal monthly spring flow, m^3/s	0.58	-56.23	Y(1987)	0.6	-66.78	Y(1998)	0.64	-62.11	Y(1987)	1.82	-61.78	Y(1997)
Maximum spring flow, m^3/s	0.63	-56	Y(1987)	0.65	-85.27	Y(1998)	0.69	-69.34	Y(1987)	0.19	-77.32	Y(1987)
Minimum spring flow, m^3/s	0.54	-50.74	Y(1998)	0.56	-53.86	Y(1998)	0.6	-54.08	Y(1997)	1.7	-51.44	Y(1997)
Annual and seasonal average daily spring flow, m^3/s	17.36	-55.59	Y(1987)	18.25	-68.49	Y(1998)	19.8	-60.36	Y(1987)	55.41	-61.95	Y(1997)
Average annual & seasonal river flow, m^3/s	8.71	87.04	Y(1999)	10.86	84.5	Y(1999)	9.52	74.98	Y(1996)	9.7	87.99	Y(1999)
Annual maximum daily river flow, m^3/s	28.54	41.1	N	30.01	91.44	Y(1995)	27.63	61.42	Y(1996)	37.76	74.92	Y(1993)
Annual minimum daily river flow, m^3/s	3.15	116.72	Y(1994)	4.68	93.07	Y(1994)	2.59	60.43	Y(1994)	2.19	58.94	Y(1994)
Annual and seasonal average daily river flow, m^3/s	8.73	2.72	Y	10.88	2.81	Y	9.51	2.5	Y	9.7	2.8	Y

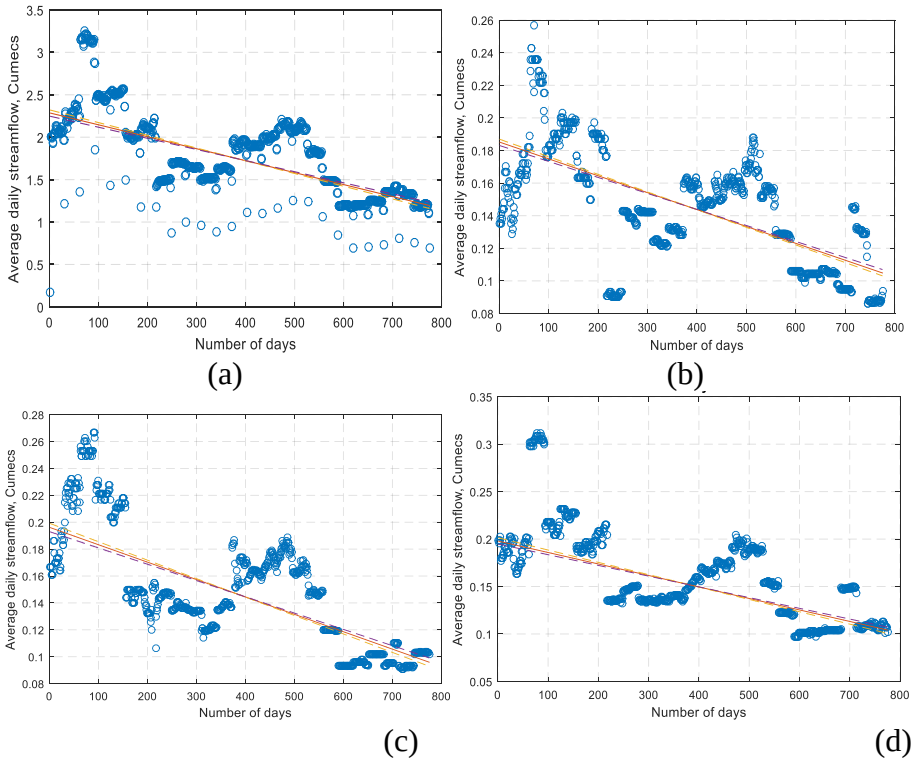

Fig. 6. The significant trends in average daily streamflow duringa) annual b) main season, c) short rainy season, and d) dry season of the forty springs

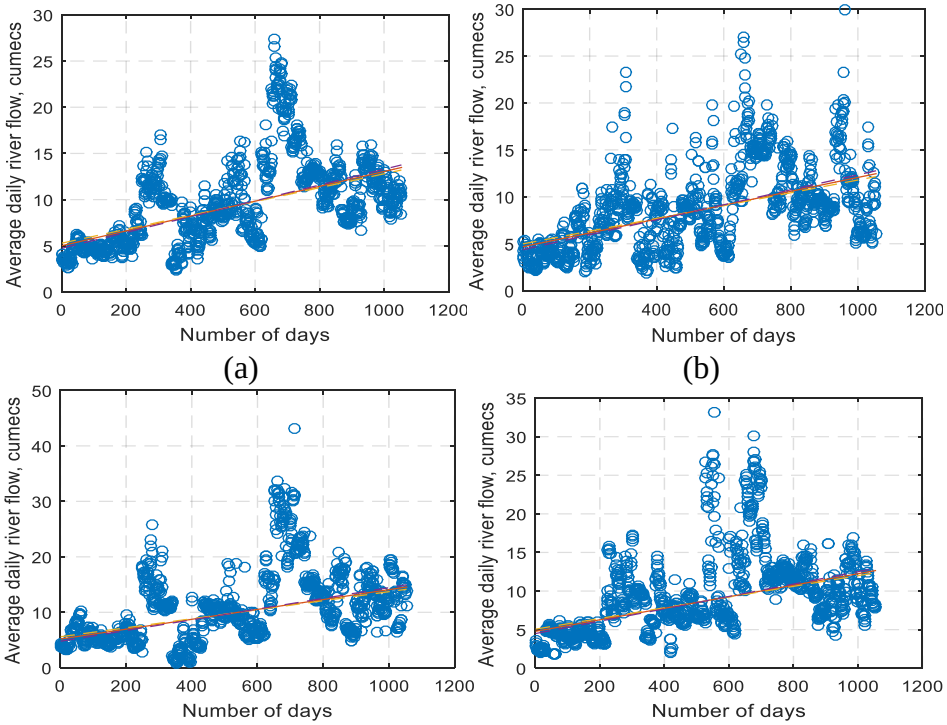

Fig. 7. The significant trends in average daily Kulfo river flow duringa) annual b) main season, c) short season and d) dry season

A significant increase and decrease in the shiftwere found in average daily Kulfo river flow and forty spring's streamflow during the study period (Table 4). The significant shift was found in an annual and seasonal mean daily Kulfo river flow at 5% level of significance at Arba Minch gauging station (Fig. 8). The significant shift was found in an annual maximum mean daily Kulfo river flow during annual and seasonal scale, except during main rainy season no significant shift was found at Arba Minch gauging station (Fig. 8). Similarly, a significant shift was observed in an annual minimum mean daily Kulfo river flow during the annual and seasonal scale (Table 4). The significant shift was found in an annual and seasonal mean daily forty springs flow at 5% level of significance (Fig. 9). Also, a significant shift was found in average daily spring flow (Table 4). The significant shift was found in a total annual maximum and minimum mean daily spring flow during annual and seasonal scale. Also, the significant shift was found in total seasonal and annual average streamflow during the years 1981 to 2005 (Table 4).

The assessment of trends and shifts in different hydro-climatic variables on the annual and seasonal scale is crucial for adaptation planning in the developing country like Ethiopia and in particular Kulfo catchment, where the Arba Minch city mainly depends upon forty springs flow for drinking water and serving as a lifeline for Arba Minch. Pingale et al. 2014 were also revealed that assessing trends on the annual and seasonal scalesare important for adaptation and planning measures at the different spatial and temporal scales.

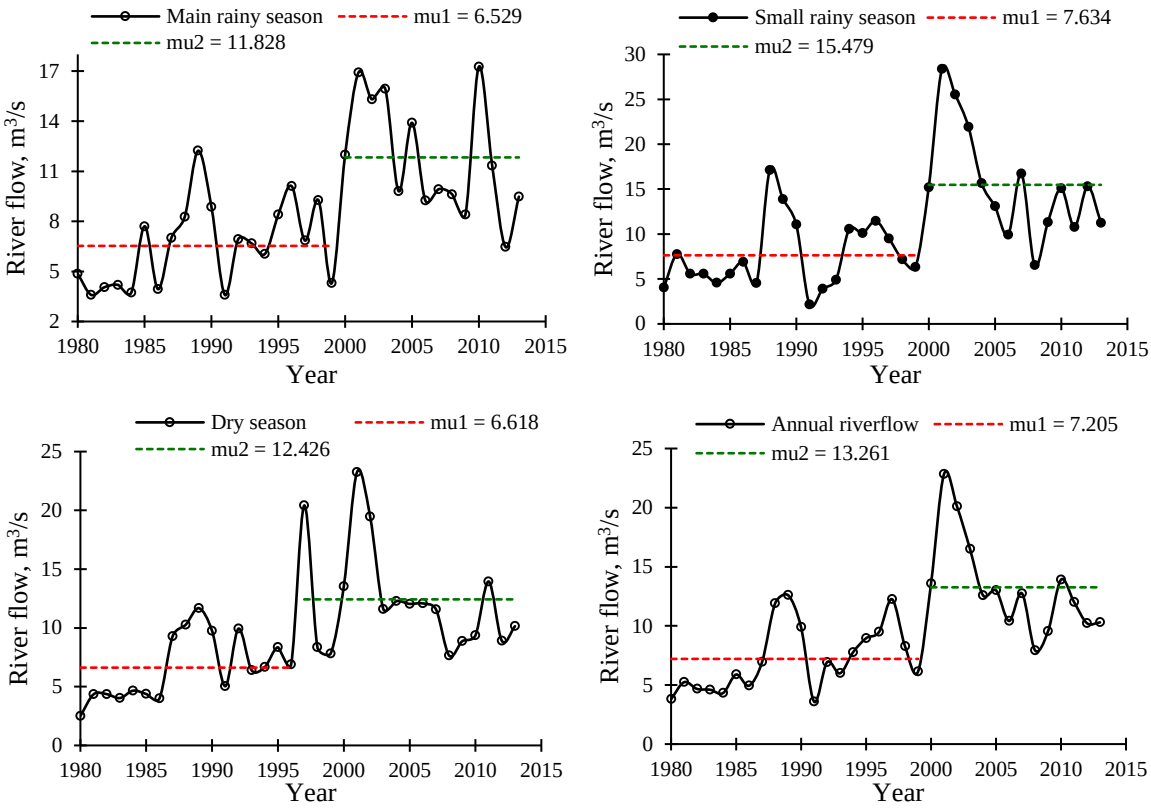

Fig. 8. Annual and seasonal average Kulfo river flow from 1980 to 2013

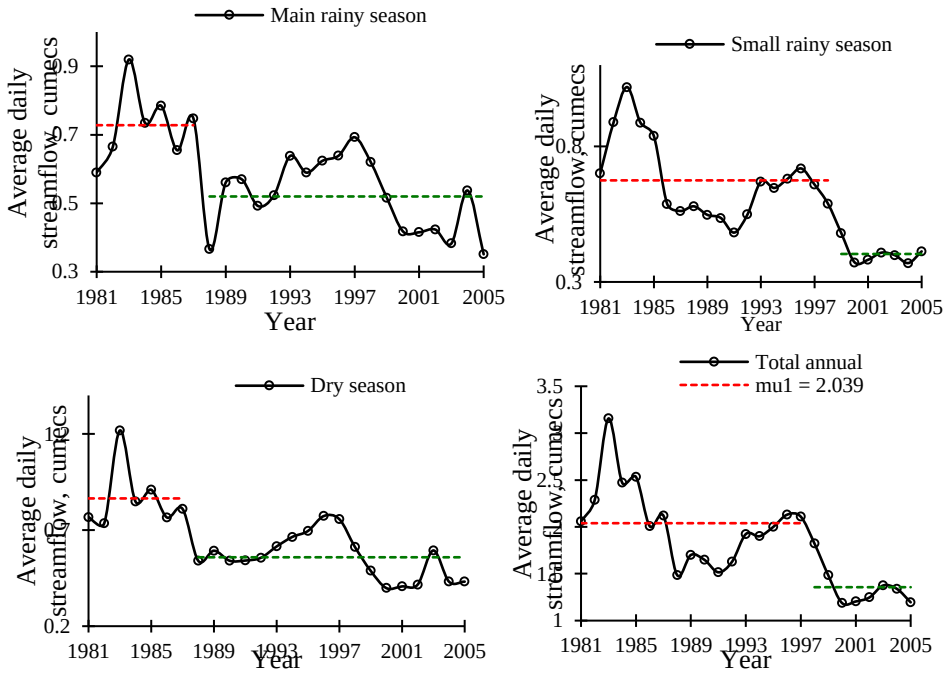

Fig. 9. Annual and seasonal average daily forty springsflow from 1981 to 2005

4. Conclusions

In this study, trend and abrupt change detection analysis of hydro-climatic variables onannual and seasonal scales (i.e., Kiremt, Belg, andthe Bega) werecarried out for the different timeperiods inKulfocatchment of Rift Valley lake basin in Ethiopia. This analysis is carried out using the MK test and PMW test at5% level of significance. The Sen's slope and % changesin hydro-climatic variables were also estimatedin the Kulfo catchment. The trend test results indicated that the significant increasing trend in total rainfall at Zigiti and Daramalo station at 5% level of significance. Similarly, the significant increasing trend was observed in annual maximum daily rainfall at Arba Minch, Zigiti and Daramalo station. The significant increasing trend was found in annual maximum daily temperature at Arba Minch and Zigiti. Other stations do not show any significant trend in case of temperature. The relative humidity, sunshine hours and potential ET_o does not show any significant trend except average annual ET_o during the main season which indicatesthe significant increasingtrend at 5% level of significance. The Sen's slope, % changes and shift (by using PMW test) in average rainfall (total & annual maximum daily rainfall), temperature (average, minimum & maximum), Wind speed and potential ET_o during annual and seasonal scale show the predominant changes in the Kulfo catchment during annual and seasonal time scale.

Forty springs showa significant decrease in average daily, annual and seasonal scale.While the significant increasing trend was found in Kulfo river flow during the annual and seasonal time scale at a 5% significance level. The Sen's slope and % changes in both Kulfo River and Forty springs flow also indicates predominant changes during the annual and seasonal time scale. This implies that there is a significant reduction in the recharge zone of the forty spring catchment. The PMW test also indicates significant shifts in KulfoRiver and forty springs flow at 5% level of significance. This change can be attributed to both anthropogenic activities and natural causes in the catchment. Being abundant natural water resources (Forty springs, Kulfo river, Abaya lake and Chamo lake), this study can be helpful for different stakeholdersin sustainable water resources planning and management andmaintain the ecosystem services within Kulfo catchment.Eventually, this study will help for city administrators in Arba Minch city, researchers and communities to focus on planning and adaptation measures at a catchmentscale by considering thehydro-climatic variability and land use/land cover changes within the catchmentin the future. Further, this study recommends assessing the realistic water demand for Arba Minch city and water supply from Forty springs flow for future planning of water resources.

Acknowledgments

The financial assistance providedby the Water Resources Centre, Arba Minch University is duly acknowledged. Dr. Abdella Kemal, Scientific Director, Arba Minch Water Technology Instituteis also acknowledged for his support.We would like to acknowledge the Ethiopian Ministry of Water, Irrigation and Energy and National Meteorological Agency for providing the necessary data for this study.

References

Allen RG, Pereira LS, Raes, Smith DM. (1998)Crop evapotranspiration: Guidelines for computing crop water requirements. FAO Irrigation and drainage paper 56, Rome, Italy.

Basistha A, Arya DS, Goel NK.(2009) Analysis of historical changes in rainfall in the Indian Himalayas.Int J of Climatol 29:555–572.

Bekele S. (2001) Investigation of water resources aimed at multi-objective development with respect to limited data situation: The case of Abaya-Chamo basin, Ethiopia. InstitutfürWasserbau und TechnischeHydromechanik, WasserbaulicheMitteilungen, 19.

Coulibaly P., Shi, X., (2005)Identification of the effect of climate change on future design standards of drainage infrastructure in Ontario, final report, McMaster University, Department of Civil Engineering, Ontario.

Gebere SB, Alamirew T, Merkel BJ, Melesse AM. (2015) Performance of high-resolution satellite rainfall products over data scarce parts of eastern Ethiopia. Remote Sens 7:11639–11663. doi: 10.3390/rs70911639.

Halbe J, Pahl-Wostl C, Sendzimir J, Adamowski J. (2013) Towards adaptive and integrated management paradigms to meet the challenges of water governance. Water Science and Technology: Water Supply, 67, 2651-2660.

Helsel DR, Hirsch RM. (2002) Statistical methods in water resources techniques of water resources investigations, Book 4, chapter A3. U.S. Geological Survey.522 pages.

IPCC (2001) Third Assessment Report, Vol. 1 The Scientific Basis, Cambridge Univ. Press.

IPCC.(2007) AR4 Working group I report, The physical science basis.Cambridge Univ. Press.

Kendall MG (1975) Rank Correlation Methods.4th ed., Charles Griffin, London.

Kiely G, Albertson JD, Parlange MB (1998)Recent trends in diurnal variation of precipitation at valentina on the West Coast of Ireland. Journal of Hydrology207(3–4): 270–279.

Kirnbauer R., Bloschl G., Haas P., Muller G., Merz B. (2005) Identifying space-time patterns of runoff generation – A case study from the Lohnersbach catchment, Austrian Alps, in: Global ¨ change and mountain regions – a state of knowledge overview, edited by: Huber, U., Bugmann, H., and Reasoner, M., Springer Verlag, 309–320.

Kumar N, Tischbein B, Beg MK (2018) Multiple trend analysis of rainfall and temperature for a monsoon‐dominated catchment in India. Meteorology and Atmospheric Physics https://doi.org/10.1007/s00703-018-0617-2.

Ludwig W, Serrat P, Cesmat L, Esteves JG. (2004) Evaluating the impact of the recent temperature increase on the hydrology of the Tˆet River (Southern France).J of Hydrol 289: 204–221.

Mann HB. (1945) Non-parametric test against trend.Econometrica 13:245–259.

Matalas NC. (1997) Stochastic hydrology in the context of climate change. Climatic Change 37: 89–101.

McBean E, Motiee H. (2008) Assessment of impacts of climate change on water resources: a long term analysis of the Great Lakes of North America. Hydrology and Earth System Sciences12: 239-255.

Mengistu KT. (2009) Watershed hydrological responses to changes in land use and land cover, 415 and management practices at Hare watershed, Ethiopia [dissertation]. [Siegen 416 (Germany)]: Universität Siegen.

Naef F., Scherrer S., Weiler M. (2002) A process based assessment of the potential to reduce flood runoff by land use change. Journal of Hydrology264(1): 74–79.

Nalley D, Adamowski J, Khalil B, Ozga-Zielinski B. (2013) Trend detection in surface air temperature in Ontario and Quebec, Canada during 1967-2006 using the discrete wavelet transform. Journal of Atmospheric Research, 132/133, 375-398.

Negley T.L., EshlemanK.N. (2006) Comparison of stormflow responses of surface-mined and forested watersheds in the Appalachian Mountains, USA, Hydrol. Processes, 20, 3467 – 3483, doi:10.1002/ hyp.6148.

Pettitt AN. (1979) A non-parametric approach to the change-point problem. Appl. Statist., 28(2): 126-135.

Pingale S, Khare D, Jat M,Adamowski J. (2014)Spatial and temporal trends of mean and extreme rainfall and temperature for the 33 urban centres of the arid and semi-arid state of Rajasthan, India. Journal of Atmospheric Research, 138, 73-90.

Pingale S.M., Khare D., Jat M.K., Adamowski J. (2016) Trend analysis of climatic variables in an arid and semi-arid region of the Ajmer District, Rajasthan, India. Journal of Water and Land Development 28(1): 3–18.

Rai, R.K., Upadhyay, A., Ojha,C.S.P., (2010)Temporal variability of climatic parameters of yamuna river basin: spatial analysis of persistence, trend and periodicity. The Open Hydrology Journal4, 184-210.

Saadat H, AdamowskiJ, Bonnell R, Sharifi F, Namdar M, Ale-Ebrahim S. (2011) Land use and land cover classification over a large area in Iran based on single date analysis of satellite imagery. Journal of Photogrammetry and Remote Sensing, 66, 608-619.

Sen PK. (1968) Estimates of the regression coefficient based on Kendall's tau. J of the American Statistical Association 39:1379–1389.

Stewart M.K., Fahey B.D. (2010) Runoff generating processes in adjacent tussock grassland and pine plantation catchments as indicated by mean transit time estimation using tritium. Hydrol. Earth Syst. Sci., 14, 1021-1032.

Subramanya K.(1998) Engineering Hydrology, Tata McGraw-Hill 2nd Edition.

Theil H. (1950) A rank-invariant method of linear and polynomial regression analysis.I, II, III.Nedal.Akad.Wetensch. Proc. 53:386-392.

Thiemann S., Foerch (2005) Water resources assessment in the Bilate River catchment- Precipitation variability. Proceeding of Lake Abay Research Symposium

Thiemann S.D. (2006) Detection and assessment of erosion and soil erosion risk in the wetland of the Bilate River, South Ethiopian Rift Valley, PhD Thesis, FreieUnivesität Berlin, pp 236.

Wagesho N, Goel NK, Jain MK. (2012)Investigation of non-stationarity in hydro-climatic variables at Rift Valley lakes basin of Ethiopia. Journal of Hydrology 444-445:113-133.

Wagesho N, Goel NK, Jain MK. (2013) Temporal and spatial variability of annual and seasonal rainfall over Ethiopia. Hydrological Sciences Journal 58(2), 354-373.

Wang K, Dickinson RE, Liang S (2012) Global atmospheric evaporative demand over land from 1973 to 2008. J Clim 25:8353–8361.

Wayand, A. (1999) Description of Kulfo and Hare River Watershed Characteristics in the Abaya Chamo Basin in South Ethiopia with Support of GIS. Siegen, Germany

Yue S, Hashino M. (2003)Long term trends of annual and monthly precipitation in Japan. J of the American Water Resources Association39(3):587–596.

Development of Rainfall Intensity-Duration-Frequency (IDF) curve for Lower Omo-Gibe River Basin under changing climate

WozaderWoldeKachama *[1]; Mamuye Busier Yesuf[2] ; Fiseha Behulu Muluneh[3]

*[1] Aksum University, School of Water Technology, E-mail: wozwolde@gmail.com, Aksum, Ethiopia, [2]Jimma University (JiT), School of Civil and Environmental Engineering, E-mail: mamuyebusier@yahoo.com, Jimma, Ethiopia, [3]Addis Ababa University (AAiT), School of Civil and Environmental Engineering, E-mail: fiseha.behulu@aait.edu.et, Addis Ababa, Ethiopia

* Corresponding Author Email: wozwolde@gmail.com Cell Phone: +251916070386

Abstract

Rainfall Intensities-Duration- Frequency (IDF) curves have got important role in planning and designs of storm water projects and other water related infrastructures. The reliability of IDF is highly associated with the appropriate choice of rainfall data. However, high emissions of greenhouse gasses exert pressure on atmospheric processes and now a day affects rainfall characteristics. In different water resources development activities, one means of adaptation to climate change is through updating (IDF) curves developed from historical datasets with respect to possible future climate change scenarios. This study is aimed to assess the impact of climate change on IDF curves of selected cities namely, Bulki (Mindre), Jinka and Arba Minch in lower Omo-Gibe River basin. Observed historical rainfall data of 34 years (1980-2013) were used as an input. In order to evaluate the climate change impact, the most recent data from Coordinated Regional Climate Downscaling Experiment (CORDEX) data scenarios were used as additional source. The CORDEX data were thoroughly evaluated and appropriate bias correction using power transformation method was undertaken. Daily based data were disaggregated to 5, 10, 20,30,60,90,120 minutes to define IDF curve appropriately. Projected data period (2040-2069) of three scenarios were examined for evaluations of potential impact of climate change. IDF curve from comparative evaluation of all scenarios showed that there will be likely increase in intensities in the future for all cites. Therefore future water infrastructure development of the selected cities can be designed by utilizing the approaches developed in this study.

Key Words: *Climate Change, CORDEX, IDF Curve, Lower Omo-Gibe River Basin, Rainfall*

1. Introduction

Degradation of water quality, property damage and potential loss of life due to flooding is caused by extreme rainfall events (De Paola et al., 2014).Historic rainfall event statistics (in terms of intensity, duration, and frequency) are used to design storm water management facilities, erosion and sediment control structures, flood protection structures, and many other civil engineering structures involving hydrologic flows (Prodanovic and Simonovic, 2007).

The reliability of IDF curve is highly associated with the appropriate choice of rainfall data.However, during the last century the concentration of carbon dioxide (CO_2) and other greenhouse gases (GHGs) in the earth's atmosphere has risen due to increased industrial activities (Prodanovic and Simonovic, 2007). This increment in GHG concentrations now a day exerts pressure on atmospheric processes so that affects rainfall characteristics and other meteorological parameters. As long as rainfall characteristics are used to design water infrastructures, reviewing and updating rainfall characteristics (i.e., Intensity–Duration–Frequency (IDF) curves) for future climate scenarios is necessary (Mirhosseini et al., 2013). The need for considering the potential effect of changing climate when working with IDF curve has been suggested by many scholars in many parts of the world(Mirhosseini et al., 2012 ; De Paola et al., 2014; Shrestha et al., 2017). The need for such understanding comes from the fact that the existingdrainage systems are designed to cope with past records of rainfall events and as such they may be insufficient to accommodate future rainfall characteristics. Hence, development of appropriate present and future Intensity–Duration–Frequency (IDF) curves assist in hydrological study for the urban drainage system performance analysis, design and operation (Shrestha et al., 2017).Therefore, the objective of this study isto assess the impact of climate change on IDF curves of selected cites namely, Bulki (Mindre), Jinka and Arba Minch in lower Omo-Gibe River basin.

2. Study area and data Sources

The analysis has been performed on two cities locate with in lower valley of Omo-Gibe river basin and Arba Minch city outside's ridge of the basin which are characterized by different rainfall pattern.

Table 1 Characteristics of meteorological stations and corresponding RCM grid point of cities

S. N	Stations	Grid Code	Latitude	Longitude	Elev. (m)
1	Bulki (Mindre)	GP[1]109208	6.16	36.52	1196.30
2	Jinka	GP109207	5.72	36.52	1017.39
3	Arbaminch	GP111208	6.16	37.40	1637.79

Observed daily time series rainfall of a period (1980-2013) for the three stations were collected from National Meteorological Agency (NMA). On the other hand, climate data model for future climate projection isfrom Coordinated Regional Climate Downscaling Experiment (CORDEX) data set. For this study, dynamically downscaled outputs by the recent version of the Rossby Centre Regional Climate Model—RCA4 were used. The model is developed in Swidish Meteorological and Hydrological Institute (SMHI). Spatially, the RCA4 simulations cover the CORDEX-Africa domain at resolution of 0.44° × 0.44° (~50 km × 50 km) for the 1951–2100 time period which is divided into two: historical (1951–2005) and scenario (2006–2100) periods. Data sets of three climate model scenarios namely RCP 2.6, RCP 4.5 and RCP 8.5 were considered which is a cumulative measure of all anthropogenic emissions of GHG's from all source expressed in Watts per square meter, by 2100(Van Vuuren *et al.*, 2011).RCP 2.6 scenario is characterized by low emissions consistence with ambition of GHG emission reduction over time and become zero at 2100(Van Vuuren *et al.*, 2011).RCP 4.5 is intermediate scenario

which is a stabilization without overshoot pathway to 4.5 W/m^2 at stabilization after 2100 through the use of various policies and technologies to minimize greenhouse gas emissions (Thomson *et al.*, 2011). Whereas RCP 8.5 is characterized by comparatively high greenhouse gas emissions and absence of climate change policies resulting to a radiative forcing of 8.5 W/m^2 in 2100(Riahi *et al.*, 2011).

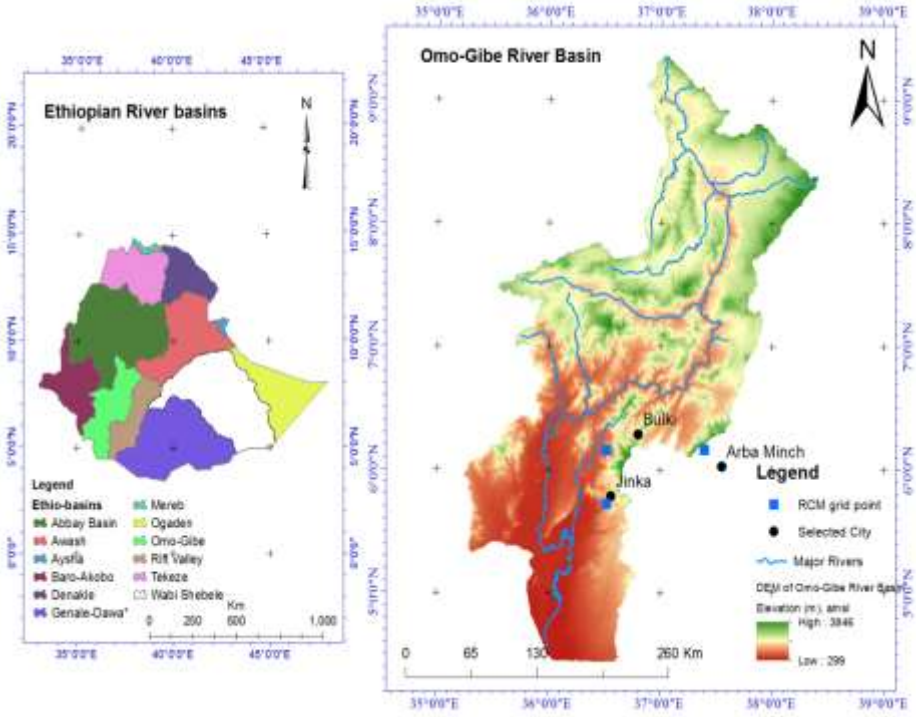

Figure1, Geographical location of the study area

3. Methodology

3.1 Observed rainfall Data

Observed raw data collected from NMA passed through quality control techniques.Nearest neighbormethod was adopted for data gap filling, given that aspecial attention for rainy season (Jun to September) as well as (March to May). Data period of (1980-2013) were used for developing IDF curves of baseline period. For validating raw RCM data with observed data, data series of a reference period (1980-2005) were used.

3.2 Bias correction

Data from RCM were not directly used for the analysis as it may have systematic error introduced from considered boundary condition and downscaling steps. In order to match quantiles of simulated RCM rainfall data withrespect to point scalerainfall data series, bias correction was applied. In this study, power transformation method was employedwhich could adjust the mean as well as the variance statistics of a precipitation time series(Lenderink *et al.*, 2007; Teutschbein and Seibert, 2012). The method also adopted on Hare watershed, southern rift valley of Ethiopia (Biniyam and Kemal, 2017).

$$p^{*} = a\, p^{b} \tag{1}$$

Where; P^{*} is corrected daily data in the projection period; a & b are parameters obtained from calibration in the baseline period and then subsequently applied to the projection period; whereas, p is daily precipitation amount of scenario data. TheFuture projection was made for mid-21st century by using data of a time slice ranges (2040-2069).

3.3 Outlier test

Outliers are data points which depart significantly from the trends of remaining data. The test was carried for both lower and higher outliers and the threshold was determined according to Water Resources Council technique. Because, outliers significantly affect the magnitude of statistical parameters computed from the data series(Water Resources Council, 1981). Graphical approach‘s was adopted for easy detection of both outliers in the data series of baseline and projected period.

3.4 Probability distribution function

The annual maximum rainfalls were fitted into Gumbel’s distribution, Log Pearson type III distribution and lognormal distribution. The goodness of fit (GOF) testwere carried byusing Kolgomorov-Smirnov (K-S), Anderson–Darling and Chi-Squared.

Log Pearson type III probability distribution was found to be best fit for all stations based on overall rank of GOF tests earned from computed parameters.Basically, this distribution is the standard distribution for frequency analysis of annual maximum floods in the United States (Benson, 1968).

Its probability density function is given as;

$$f(x) = \frac{\alpha^{\beta}(y-\gamma)^{\beta-1} e^{-\alpha(1-\gamma)}}{x\Gamma(\beta)}; \log x \geq \gamma \tag{2}$$

$$\alpha = \frac{\delta_y}{\sqrt{\beta}}$$

Where, $\beta = \left[\frac{2}{C_s(y)}\right]^2$ (3)

$$\gamma = \overline{Y} - \delta_y \sqrt{\beta}$$

$y = \log x$ and assuming $C_s(y)$ is positive

Where α, β and γ are the scale, shape and location parameters of the distribution and y= log(x), assuming the skewness$C_s(y)$ is positive.

The methodology used in this study to estimate events for varies return period was based on Hershfield technique, (Chow *et al.*, 1987)

$$X_T = \chi_{avg} + \Delta \chi_T \tag{4}$$

Where, $\Delta \chi_T = K_T \delta$ is departure of the variate from the mean. δ is standard deviation and $K_T$referrers to frequency factor commuted as; (Kite, 1977)

$$K_T = z + \left(z^2 - 1\right)k + \frac{1}{3}\left(z^3 - 6z\right)k^2 - \left(z^2 - 1\right)k^3 + zk^4 + \frac{1}{3}k^5 \tag{5}$$

Where, $k = \frac{C_s}{6}$ Where $C_s \neq 0$, (Kite, 1977)

The intensity is time rate of rainfall which is rainfall depth (d) per unit time (t). The average intensity is commonly expressed as;

$$i = d/t \tag{6}$$

*Disaggregation:*Short duration rainfall data in sub hourly time series is required to define IDF curves appropriately.So that,it is necessary to disaggregate precipitation data collected on highertimescale (e.g., daily) to a different, shorter timescale (Fadhel *et al.*, 2017)**.**Disaggregation in this study followed technique adopted in Ethiopian Road Authority's drainage design manual (ERA, 2013).

3.5 Creating IDF Curve

The process of creating IDF curves consists of the following steps.

i. Extract annual maximum daily time series of rainfall depth form the quality controlled raw data;
ii. Fit the data to the commonly available theoretical probability distributions;
iii. Extrapolate precipitation magnitude for different return periods by using the best fit distribution (Log- Pearson Type III in our case);
iv. Repeat the thirdsteps for different return periods (2, 5, 10, 25, 50 and 100) years
v. Disaggregate output of the fourthstep data series in to (5, 10, 20, 30, 60, 90, and 120) minutes time series;
vi. Compute corresponding time rate of rainfall
vii. Plot the IDF curve

However, for creating future IDF curve, the above steps must be adopted after bias correction techniques are applied to RCMrainfall data series of a period 2040-2069.

4. Results and Discussions

4.1 Rainfall frequency analysis

Events for different return periods were extrapolated from annual maximum of baseline period as well as projected data for a period (2040-2069) by using best fit frequency distribution. Simple comparison was made between baseline period and projected period. The comparison was made on rainfall depthof base period and three scenarios (RCP 2.6, RCP 4.5 and RCP 8.5) of different return period.

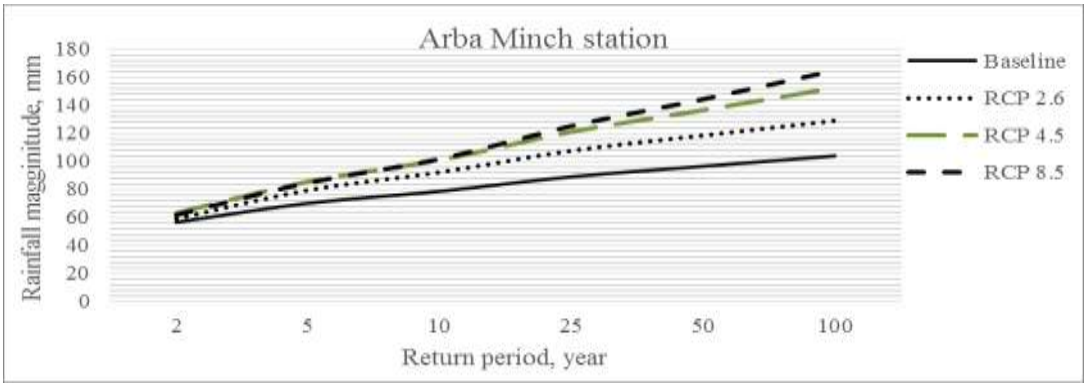

Figure 2, Extrapolated rainfall magnitude ofArba Minch for different return period

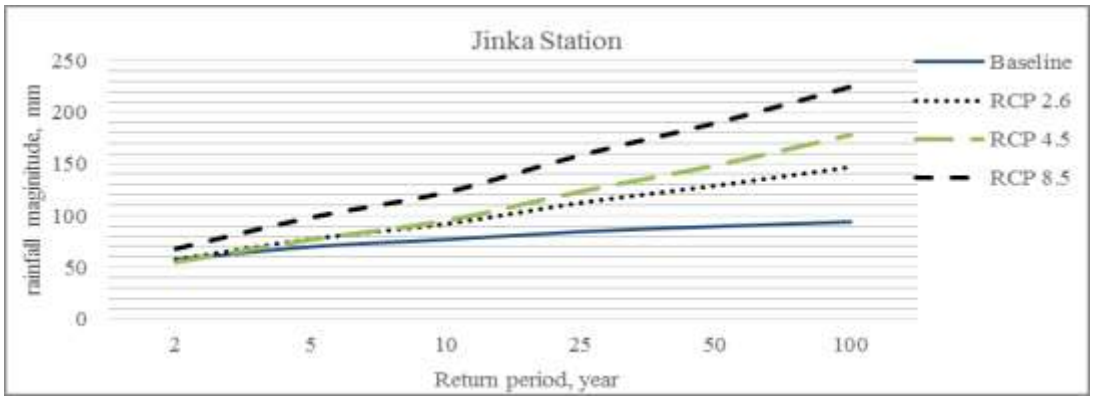

Figure 3, Extrapolated rainfall magnitude ofJinka for different return period

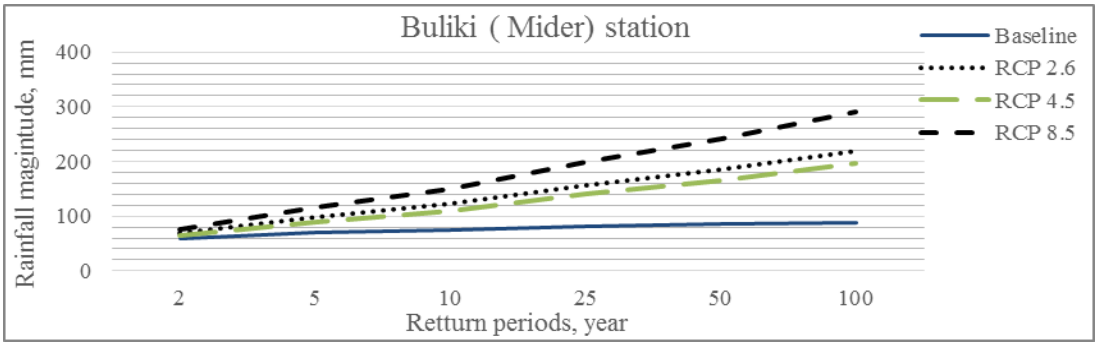

Figure 4, Extrapolated rainfall magnitude of Bulki for different return period

Figure 1-4, shows comparison between rainfall magnitudes of historical and future period of different recurrence intervals projected under changing climate scenarios. Accordingly, the three scenarios projected increased rainfall magnitude above baseline period for the three cities depending on the return periods. RCP 8.5 scenario predicted more high value than projection under RCP 2.6 and RCP 4.5 scenarios for all cities. The projection under RCP 8.5 scenario for Arba Minch match with study conducted on Hare watershed which indicates future severe rainfall is subjected to increasing under changing climate condition(Biniyam and Kemal, 2017).

4.2 IDF curves

For developing IDF curve, durations up to 120 minutes were considered as short duration maycause flash flood events (De Paola *et al.*, 2014).However, for simple demonstration of impact of changing climate on future IDF curve, rainfall intensity with 25 and 50 years recurrence interval is plotted for Arba Minch, Bulki andJinka.

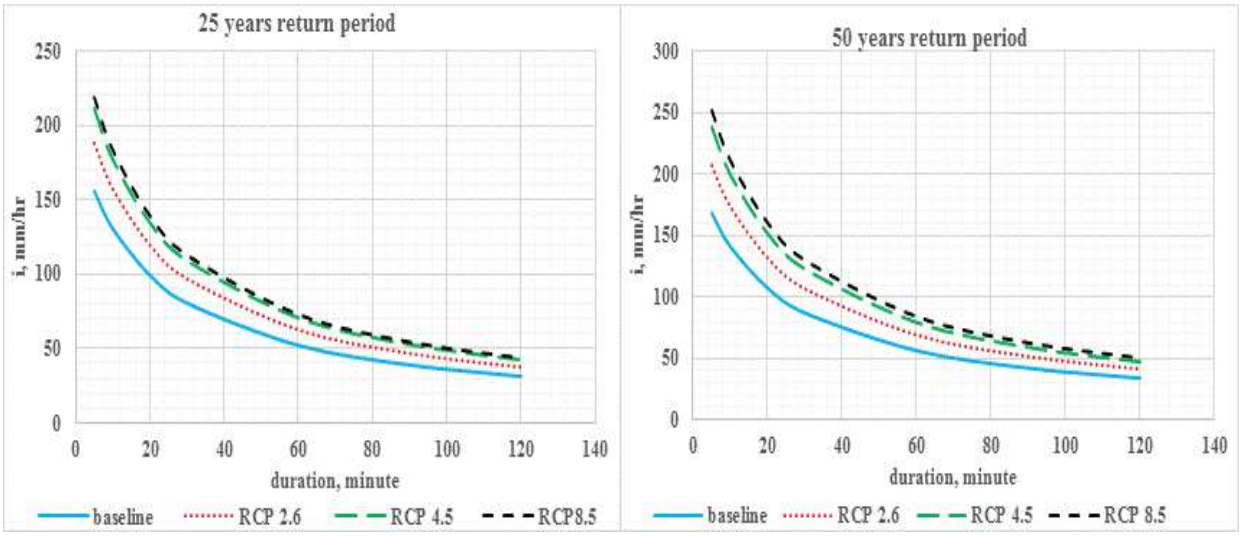

Figure 5, IDF curvesunder baseline and projected period forArba Minchcity

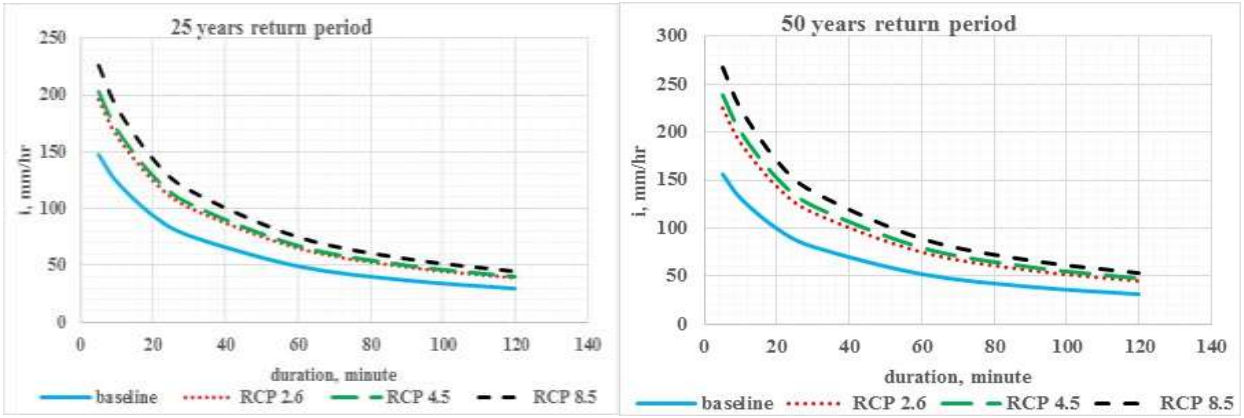

Figure 6, IDF curvesunder baseline and projected period forJinkacity

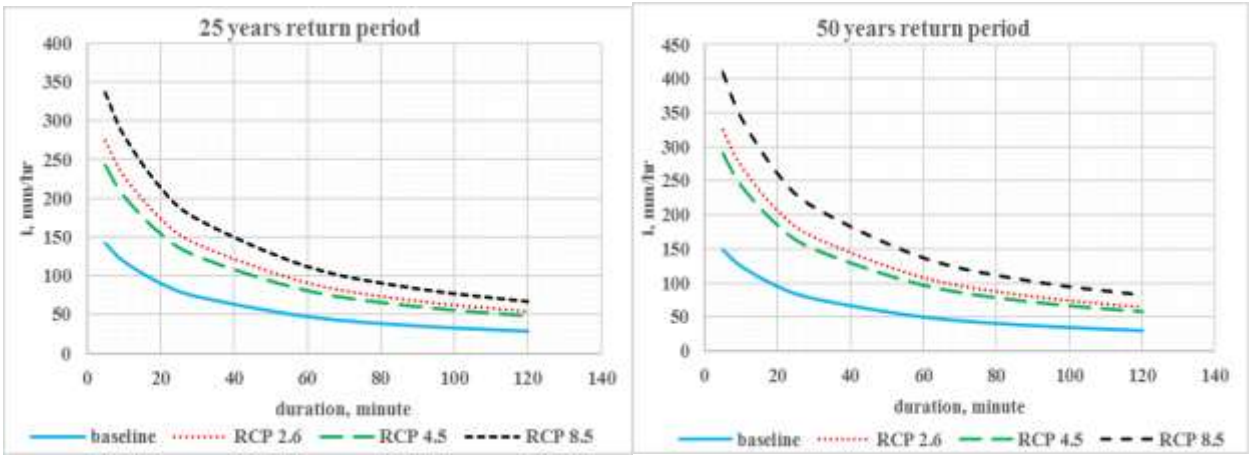

Figure 7, IDF curvesunder baseline and projected period forBulkicity

Figure 5-7illustrates thata possible potential increment of rainfall intensities for all citiesunder different changing climate scenarios. For Arba Minch, RCP 4.5 and RCP 8.5scenarios projected somewhat similar and a little bit higher than projection under RCP 2.6 scenario. On the other hand, RCP 2.6 and RCP 4.5 scenarios have shown almost similar projection for Jinka relative to RCP 8.5 scenario. However, RCP 8.5 projection has shown substantial deviation when compared to projection under RCP 2.6 and RCP 4.5 for Jinka and Bulki.Other important thing demonstrated from the analysis is RCP 8.5 scenarioprojected higher value for all cites which clearly showssignificant consequencesassociated to no policy changes to reduce GHG emissions.Accordingly, the potential over estimation under RCP 2.6 scenario ranges in percent (20.8-23); (36-41) under RCP 4.5 scenario and (40-49) under RCP 8.5 scenario for Arba Minch. For Jinka, the percentage increment ranges (33-44) under RCP 2.6 scenario; (37-52.8) for RCP 4.5 scenario and (52-81.2) under RCP 8.5 scenario. However, for Bulki the increment goes above 70 percent under RCP 2.6 and RCP 4.5 scenarios; and extends as high as beyond its double value under high emission scenario. Generally, overall outcome of the study indicates that, future IDF curve has shown significant deviation from that of baseline period for all citiesregardless of the realizations under consideration. Therefore, it can be certainly taken from this investigation that changing climate condition could likelyexert stress on future IDF curve and may tend to increasing in magnitude depends on the return period.

In forth coming manuscript under preparation, evaluations were carried to see spatial variability of IDF curve as well asthe effect of changing climate on future IDF curve for the entire Omo-Gibe river basins.

5. Conclusion

This study comparatively evaluates IDF curves developed under climate changing scenarios with the IDF curves of baseline climatefor three cities. To investigate the potential effect of changing climate on future IDF curves, bias corrected rainfall data projected for a period (2040-2069) were used from three RCP's scenarios. The analysis result from climate model projection shows that future severe rainfall intensities could be subjected to increasing depending on the return period. This could affect

Engineering infrastructures and poses problem on existing municipal storm water management system. In line with the outcome of this study, it can be concluded that future water infrastructure development of the selected cities can be designed by utilizing the approaches developed in this study. However, to draw strong conclusion, additional climate model should be incorporated to get more realistic information about potential effect of climate change on future IDF curve. Therefore, appropriate recommendation could be drawn as adaptation mechanism for the selected cities.

References

BENSON, M. A. (1968) Uniform flood-frequency estimating methods for federal agencies, *WaterResour. Res.*, vol. 4, no. 5, pp. . 891-908, [Cross reff).

BINIYAM, Y. & KEMAL, A. (2017) The Impacts of Climate Change on Rainfall and Flood Frequency: The Case of Hare Watershed, Southern Rift Valley of Ethiopia. *J Earth Sci Clim Change*, 8.

CHOW, V. T., MAIDMENT, D. R. & MAYS, L. W. (1987) *Applied Hydrology*, New york, St. Louis San Francisco Auckland Bogota, Mc Graw-Hill International Edition: Civil Engineering Series.

DE PAOLA, F., GIUGNI, M., TOPA, M. E. & BUCCHIGNANI, E. (2014) Intensity-Duration-Frequency (IDF) rainfall curves, for data series and climate projection in African cities *SpringerPlus*, 3/133; Doi 10.1186/2193-1801-3-133.

ERA (2013) Ethiopian Road Authority: Drainage Design Manual federal democratic republic of Ethiopia. Addis Ababa, Ethiopia.

FADHEL, S., RICO-RAMIREZ, M. A.&HAN, D. (2017) Uncertainty of Intensity–Duration–Frequency (IDF) curves due to varied climate baseline periods. *Journal of Hydrology*, 547**,** 600–612: http://dx.doi.org/10.1016/j.jhydrol.2017.02.013.

KITE, G. W. (1977) *Frequency and Risk Analysis in Hydrology*. *Water Resources Publications, Fort Collins, Colo. [CrossRef]*.

LENDERINK, G., A. BUISHAND & DEURSEN, W. V. (2007) Estimates of future discharges of the river Rhine using two scenario methodologies: direct versus delta approach. . *Hydrology and Earth System Sciences Discussions, European Geosciences Union,*, 11**,** 1145-1159, [Cross ref].

MIRHOSSEINI, G., SRIVASTAVA, P. & STEFANOVA, L. (2012) The impact of climate change on rainfall Intensity-Duration-Frequency (IDF) curves in Alabama: ; USA. . *Reg Environ Change***,** 1-9; DOI 10.1007/s10113-012-0375-5.

MIRHOSSEINI, G., SRIVASTAVA, P. & STEFANOVA, L. (2013) The impact of climate change on rainfall Intensity-Duration-Frequency (IDF) curves in Alabama. *Reg Environ Change*, 13**,** 25-33.

PRODANOVIC, P. & SIMONOVIC, S. P. (2007) Development of rainfall intensity duration frequency curves for the City of London under the changing climate. Department of Civil and Environmental Engineering, . *Report 058* London, Ontario, Canada,, The University of Western Ontario.

RIAHI, K., RAO, S., KREY, V., CHO, C., CHIRKOV, V., FISCHER, G., KINDERMANN, G., NAKICENOVIC, N. & RAFAJ, P. (2011) RCP 8.5—A scenario of comparatively high greenhousegas emissions. *Springer: International Institute for Applied Systems Analysis (IIASA), 2361 Laxenburg, Austria*

SHRESTHA, A., BABEL, M. S., WEESAKUL, S. & VOJINOVIC, Z. (2017) Developing Intensity-Duration-Frequency (IDF) Curves under Climate Change Uncertainty: The Case of Bangkok, Thailand:. *water, MDPI,* 9**,** 1-22

TEUTSCHBEIN, C. & SEIBERT, J. (2012) Bias correction of regional climate model simulations for hydrological climate-change impact studies: Review and evaluation of different methods. *Journal of Hydrology*, 456–457 12-29.

THOMSON, A. M., CALVIN, K. V., SMITH, S. J., KYLE, G. P., VOLKE, A., PATEL, P., DELGADO-ARIAS, S., BOND-LAMBERTY, B., WISE, M. A., CLARKE, L. E. & EDMONDS, J. A. (2011) RCP4.5: A Pathway for Stabilization of Radiative Forcing by 2100. *Climatic Change*.

VAN VUUREN, D. P., EDMONDS, J., KAINUMA, M., RIAHI, K., THOMSON, A., HIBBARD, K., HURTT, G. C., KRAM, T., KREY, V., LAMARQUE, J.-F., MASUI, T., MEINSHAUSEN, M., NAKICENOVIC, N., SMITH, S. J. & ROSE, S. K. (2011) The representative concentration pathways: an overview. *Clamatic change*, 109**,** 5−31: DOI 10.1007/s10584-011-0148-z.

WATER RESOURCES COUNCIL (1981) now called Interagency Advisory Committee on Water Data), Guidelines for determining flood flow frequency, . *bulletin 17B, available from Office of Water Data Coordination,*, U.S. Geological Survey, Reston, VA 22092.

Experimental study on hydraulics of gabion weirs

Dessalew Tadesse[1], Z. Ahmad[2], Muhammed Hashid[2]

[1]School of Civil and Hydraulic Engineering, University of Gondar, P.O.Box 196, Ethiopia,Cell Phone: -+251912377780, Email: -dessalew2005@gmail.com, [2] Department of Civil Engineering, Indian Institute of Roorkee, Roorkee, 247667, Uttarakhand, India, Email: - zulfifce@iitr.ac.in, mhashid@gmail.com

Abstract

In recent years gabion weirs, which are constructed using stones filled on a wire mesh attract attention; because these structures are environmental friendly unlike impermeable weirs. In the present study, laboratory experiments were conducted to investigate the discharge characteristics of gabion weirs at submerged and free surfaceflow conditions. To achieve this, nine different gabion weir models were tested in a horizontal laboratory concrete flume of 9.47 m length, 0.65m depth and 0.5 m width for various range of discharge, depth of flow upstream and downstream of weir, weir height and filling material of gabion. Based on dimensional analysis theory multilinear regression equations were developed to compute the discharge passing over the permeable weirs at submerged and free surface flow regimes.The computed discharges using proposed equations in the present study are within $\pm$ 10 % of the observed ones for both flow conditions.Checking the accuracy of existing relationship between pressure gradient and seepage velocity were conducted. The Ergun equation predicts accurately the observed data of water flow through permeable weir by blocking the over flow when compare to Modified Stephenson equation.

Key Words: - Gabion weir, Solid weir, free surface flow, Submerged flow, Pressure Gradient

1. Introduction

A weir is a hydraulic structure constructed across a river to change the flow characteristics of it. The common uses of weirs are to measure discharge, to alter the rivers flow to prevent flooding, and help render rivers navigable. Gabion Weirs are structures made by loose stones filled on a wire net basket. Gabion weirs allow the easy pass of materials which exist with flowing water and movement of aquatic life. This structure has less negative impact on environment of water and is accepted as environmental familiar compare to solid weirs. In gabion weirs, the water flow through the permeable weir is an important characteristic, one which also makes conditions of flow more complex. Flow occurs only

through the permeable weir, when the discharge supplied is low.In order to estimate discharge through gabion weir, it is important to use a reliable non-Darcy relationship, since the flow within permeable weir is usually turbulent. Figure 1(a) and (b) shows the definition sketch of models used in the present study to determine the pressure gradient and profiles of water surface over gabion weir respectively. Various studies have been conducted by (Forchheimer, 1901, Ergun, 1952, and Stephenson, 1979) to determine the pressure gradient of water flow through porous media and empirical relations were also proposed in each of these studies. Forchheimer (1901) developed a model to estimate fluid pressure drop which passes through permeable body of the structure. He described the hydraulic gradient and seepage velocity relation as shown below by incorporating Darcy and non-Darcy flow.

$$i = aV + bV^2 \tag{1}$$

Where i is the hydraulic gradient in the flow direction, V isthe seepage velocity, and a, and b are Forchheimer coefficients.

Ergun (1952) developed the most widely applied resistance model for Newtonian fluid flow through packed beds. The equation is as follows.

$$\frac{\Delta P}{L} = 150\mu \frac{(1-\varepsilon)^2}{d_m^2 \varepsilon^3} V + 1.75\rho \frac{(1-\varepsilon)}{d_m^2 \varepsilon^3} V^2 \tag{2}$$

Stephenson (1979) proposed a relation to determine the pressure gradient through the porous media.

$$i = \frac{K_t}{g\varepsilon^3 d_m} V^2 \tag{3a}$$

Modified Stephenson equation could be written as

$$i = 800\nu \frac{V}{g\varepsilon d_m} + 4\frac{V^2}{g\varepsilon d_m} \tag{3b}$$

Michioku*et al.* (2005) evaluated discharge which passes through permeable rubble mound weir by conducting 1D analysis and laboratory experiment. After analysing discharge experimentally and theoretically, they showed that the theoretical and experimental discharge is satisfactory for a various range of flow conditions. Various investigators made experimental studies on gabion weirs for flow of water through the weir. Chanson (2009) in his study concluded that the interaction of seepage and over

flow cannot be ignored, so further study is needed. The present study investigated discharge characteristics of gabion weirs for free surface and submerged flow conditions.

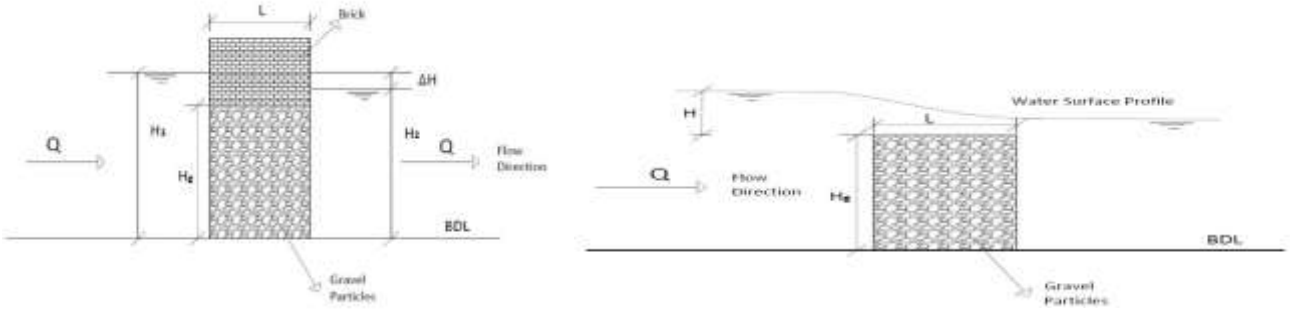

Figure: -1(Left) and (Right) show the definition sketches of the models used in the present study.

2. Experimental Programme

Laboratory experimentswere conducted at the Hydraulic laboratory of Civil Engineering Department, Indian Institute of Technology Roorkee, Roorkee, India. A concrete flume 0.5m wide, 9.47m in length, and 0.65 m in height was used for the experimentation as shown in Figure 2.

Water was pumped from sump to an overhead tank and supplied to the channel through a supply pipe, which was fitted with a valve for the regulation of discharge. The splitter plates and wave suppressors were provided at the entrance of the flume to ensure the alignment of the flow and to minimize disturbances of the surface respectively. Experimental works were performed for three different height of gabion weirs (i.e. H_g=20cm, 30cm and 40cm) filled with d_m = 41.25mm, 47.5mm and 57.5mm. Each model was filled up with different gravel material sizes. The top of the weir was blocked by brick to prevent the flow over the weir (Figure 1a). As well by removing the bricks experiments have been performed for free surface and submerged flow conditions. A sharp crested weir was used at the downstream end of the flume to measure the discharge. Two point gauges operated manually were used upstream and downstream of the model to obtain elevations of the flume,weir elevations, and water levels. All measurements were taken at the centre line of flume.

2.1 Checking the accuracy of existing relationships of pressure gradient versus seepage velocity

Pressure gradient of water flow through gabion weir filled with different mean size of material is shown in Figure 3. Comparisons between the Modified Stephenson equation of Eq. (3b), the Ergun equation of

Eq. (2), and the observed data were conducted. As shown in Figure (3a) the observed data and the values obtained by proposed equation of Ergun agree more for the three mean diameter of gravel. So Ergun equation can predict the experimental data well. However, the modified Stephenson equation deviates more from the experimental data.

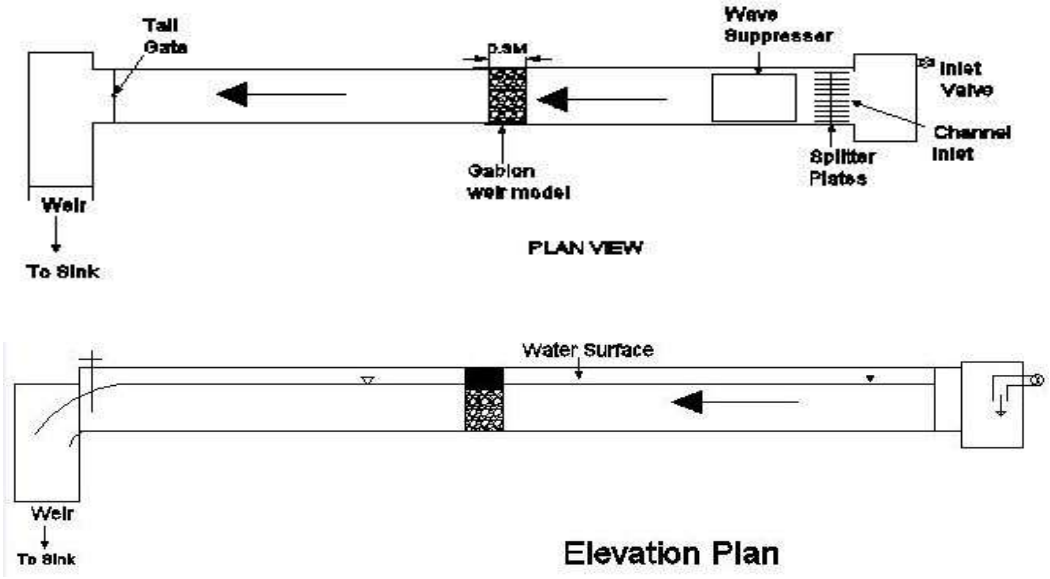

Figure 2: - Experimental setup

Table 1: - Range of data collected in the present study

Parameter	Symbol	Value	Range			Units
			From		To	
Weir height	H_g	40, 30, 20	-----			Cm
Weir length	L	30	-----			Cm
Discharge	Q	Various	7.622	-----	35.21	L/s
Upstream water depth	H_1	Various	26.3	-----	54.83	cm
Downstream water Depth	H_2	Various	14.73	-----	47.78	cm
Gravel Mean size	d_m	4.125, 4.75, 5.75	-----			cm
Porosity	ε	0.41, 0.44, 0.48	-----			----

3. Results and Discussion

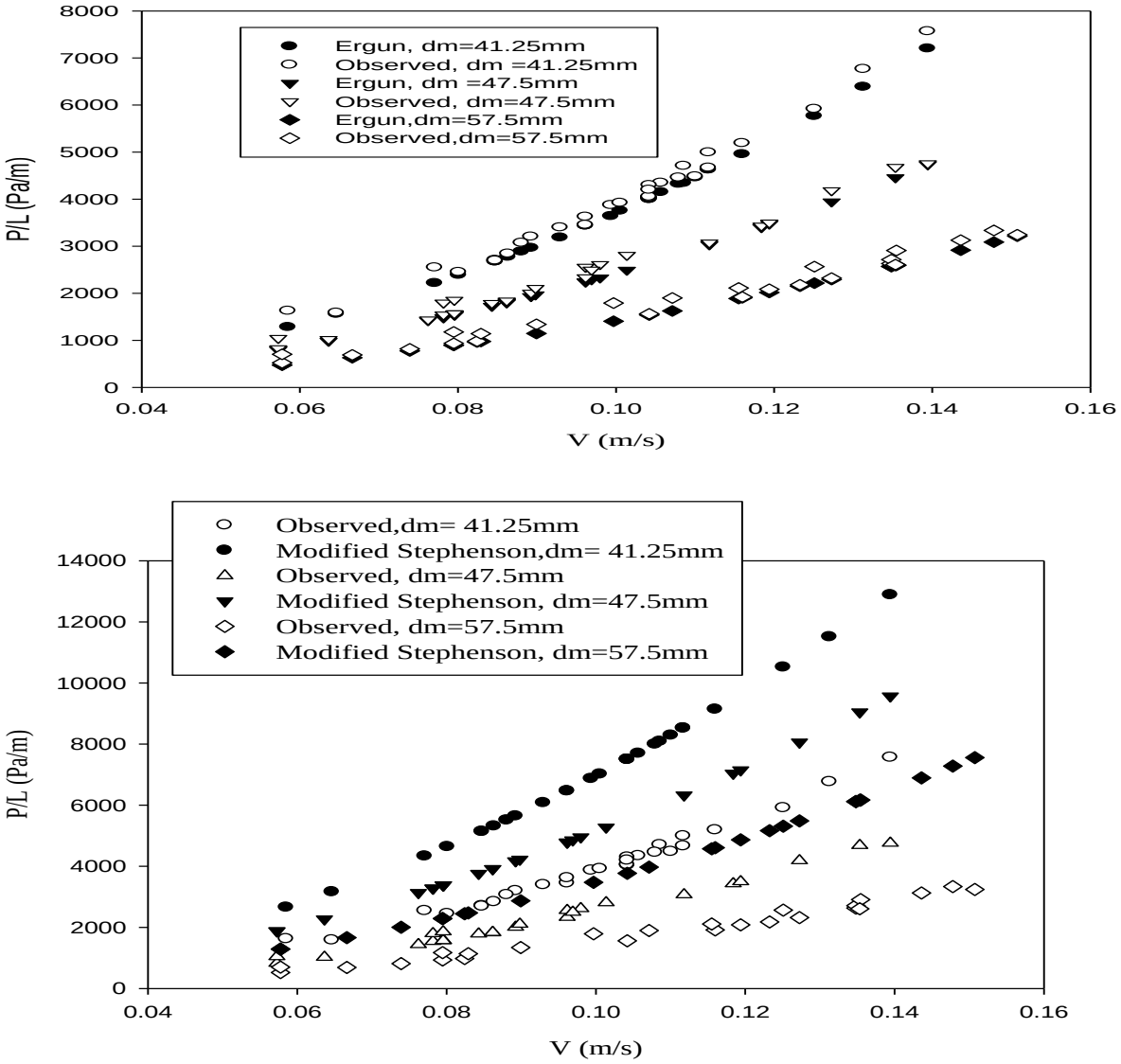

Figure 3:- Pressure gradient of water flow in gabion weirs filled with three different mean diameters of gravels (Top). Using Ergun equation of Eq. (2) (Bottom). Modified Stephenson equation of Eq. (3b)

3.1.Dimensional Analysis

A physical pertinent relation of the typical rating curve i.e discharge and upstream water depth and other parameters may be obtained by dimensional analysis.

The discharge Q relation with other parameters can be described as follows

$$Q = f\left(H_1, H_2, B, H, H_g, L, d_m, g, \mu, \rho\right) \quad (4)$$

Where H_1 and H_2 = upstream and downstream water depths respectively; H = water head above the weir;H_g = height of gabion weir; L = weir length; d_m =average size of filling material; ρ = density of fluid; and g = gravity of acceleration.

The non-dimensional expression is given below

$$\frac{Q}{BH_1^{1.5}\sqrt{g}} = \varphi\left(\frac{Q\rho}{B\mu}, \frac{H}{L}, \frac{d_m}{H_g}, \frac{H_1 - H_2}{H}\right) \quad (5)$$

With $F_r = \frac{Q}{BH_1^{1.5}\sqrt{g}}$, $R_e = \frac{Q\rho}{B\mu}$, and $S_r = \frac{H_1 - H_2}{H}$

3.2.Free Surface Flow

Figure 4 shows the surface profiles of water over the gabion weir different filling material sizes and the impermeable weir having similar flow rate at condition of free surface flow.The crest head increases as the mean size of gravel decreases.

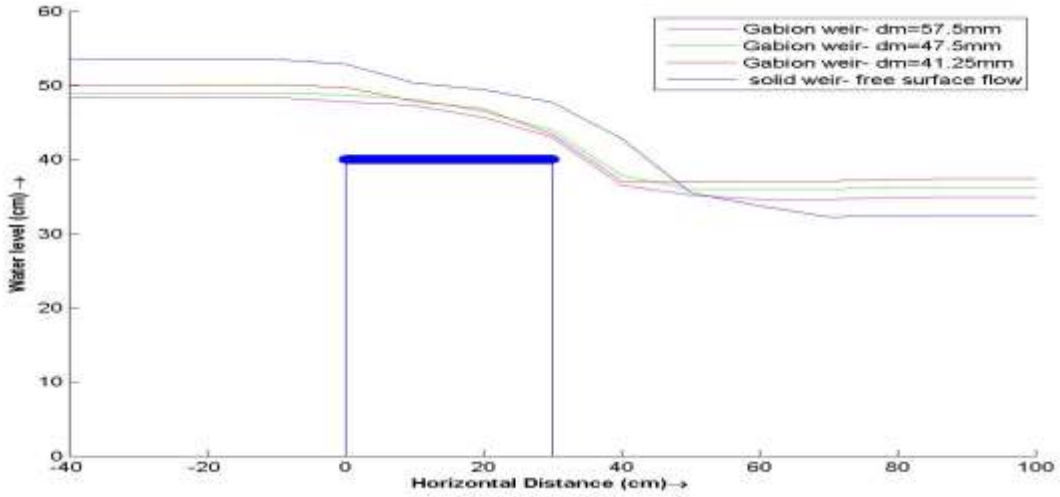

Figure 4: -Water surface profiles over gabion weir at free surface flow condition filled with different sizes of material.

3.3.Proposed Equation for Dimensionless discharge for free surface flow condition

Parameters which are shown in Eq. (5) have been correlated using regression analysis. The equation developed for free surface flow condition for computation of discharge over weir is as follow.

$$\frac{Q}{BH_1^{1.5}\sqrt{g}} = -0.253 + 0.22\left(\frac{d_m}{H_g}\right) + 0.061\left(\frac{H}{L}\right) + 0.055\log R_e, R^2 = 0.797 \quad (6)$$

Where correlation coefficient, R^2, is 0.797 and the standard error is 0.0055

Figure 5 shows the values of the discharge computed by using Eq. (6) against the observed discharge. This shows that there is a good agreement between the computed discharge and the observed one.

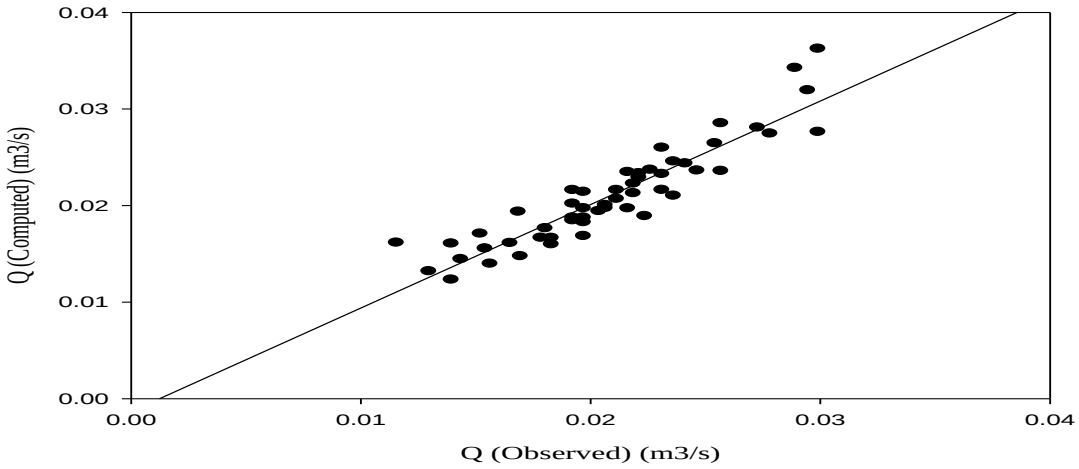

Figure 5: -Discharge computed by using Eq. (6) against measured value at free surface flow condition.

3.4.Submerged flow

Figure 6 shows submerged flow condition water profiles over the gabion weir filled with three different mean sizes of gravels and the impermeable weir having similar discharge. When compare to free surface condition of flow, the head decrease is less.

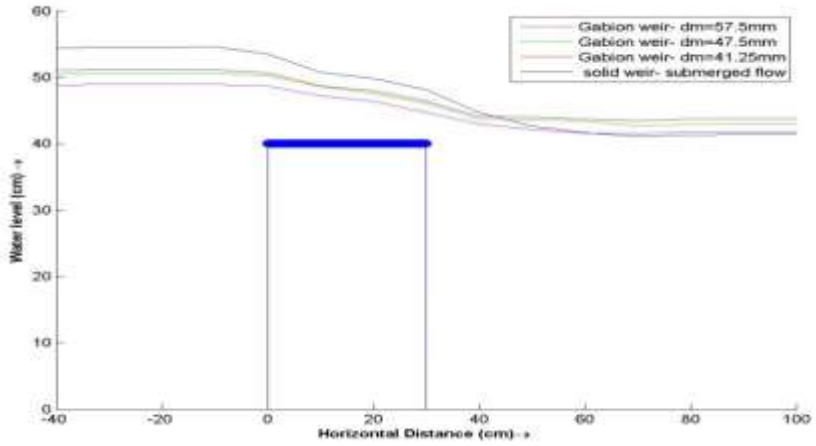

Figure 6:-Water surface profiles over gabion weir at submerged flow condition filled with different sizes of material

3.5.Proposed Equation for Dimensionless discharge for submerged flow condition

Parameters which are shown in Eq. (5) have been correlated using regression analysis. The equation developed for submerged flow condition for computation of discharge over weir is as follow.

$$\frac{Q}{BH_1^{1.5}\sqrt{g}} = -0.602 + 0.253\left(\frac{d_m}{H_g}\right) - 0.0053\left(\frac{H}{L}\right) + 0.131\log R_e + 0.0124S_r, \quad R^2=0.915 \tag{7}$$

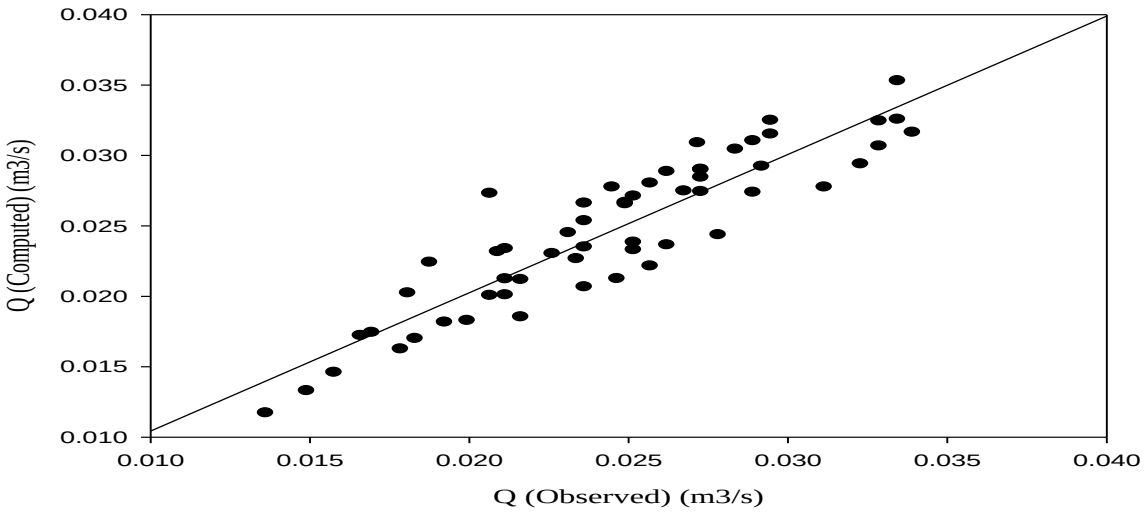

Figure 7:- Discharge computed by using Eq. (7) against measured value at submerged flow condition

As shown above in Figure 7 the values of the discharge computed by using Eq. (7) against the observed discharge. It is shown in the Figure 7 that the computed discharge is within $\pm 10\,\%$ of the observed ones. This shows that there is a good agreement between the computed discharge and the observed one.

4. Conclusions

In present study flow of water through and over the gabion weir have been investigated experimentally. Based on the experimental work done on the present programme the following conclusions are drawn.

- The Ergun equation of Eq. (2) predicts accurately the observed data of water flow through permeable weir by blocking the over flow when compare to Modified Stephenson equation of Eq. (3b).
- By maintain the similar flow rate; it is impossible to get the same head over solid weir and gabion weir. It is less in gabion weir. The head over the crest decreases as material size increases
- Dimensional analysis concept has been used to develop regression analysis equations which enable to compute discharge passing over the gabion weir at submerged and free surface flow conditions.

References

1. Chanson, H.(2009). Embankment Overtopping Protections System and Earth Dam Spillways, in "Dams: Impact, Stability and Design". Hayes, W.P., Barnes, M.C., Nova Science Publishers, Hauppauge NY, USAS, 101-132
2. Ergun, S., (1952). Fluid flow through packed columns. Chem. Eng. Prog. 48, 89-94
3. Forchheimer, P.H., (1901). WasserbewegundurchBoden. Z. Ver. Dtsch. Ing. 45, 1782- 1788
4. Michioku, K., Maeno, S., Furusawa, T., and Haneda, M. (2005). Discharge through a permeable rubble mound weir. J. Hydraul. Eng., 131(1), 1-10
5. Stephenson, D., (1979). Rockfill in hydraulic engineering. Elsevier Science Publishers By (North Holland), Amsterdam, The Netherlands, 19-24

Theme: Two: Renewable Energy

Dynamic Analysis of Middle Awash Multi-Purpose Dam

Yared Mulat Tassew

Ethiopian Construction Works Design and Supervision Corporation (Addis Ababa, Ethiopia) Address: Email: yaredthequestion@gmail.com, Phone number: +251911900766/+251965651887, P.o.box: 25668, Addis Ababa, Ethiopia)

Abstract:

In this dynamic analysis research, Middle Awash high dam which is located in Ethiopian rift valley seismic zone is analyzed for pre and post-earthquake stability and permanent deformations due to earthquake loads. The dynamic analysis is done adopting three elsewhere recorded earthquake time histories, which have different period and duration. Applying these seismic shocks and using the Newmark deformation method, it was found that the induced deformations do not require additional extension of dam or cumber height. The upstream and downstream slopes showed sufficient performance against sliding. The upstream section steepening is found to be more economical, yet achieving the minimum required factors of safety for static and post-earthquake sliding failure. The thick alluvium foundation of the dam is found to liquefy immediately after the design base earthquake started. The pseudo-static seismic analysis recommends uneconomical dam section modification. The Finite Element and Limit Equilibrium Methods shown to be conservative in calculating sliding factor of safety for downstream and upstream slopes, respectively.

Key words: Maximum credible earthquake, Design base earthquake, Finite element method, Limit equilibrium method, Permanent deformation and Liquefaction.

1. Introduction

Improper seismic analysis of high dams in earthquake zone could lead to a disastrous collapse and limited serviceability. On the other end, if the analysis ended up with amplified results, the project will end being uneconomical. Pseudo-static seismic analysis of a dam could not capture all events, in addition to its' conservative results. (Fantahun Getachew, unknown)

In Ethiopia, there is a record of loss of millions of dollar and priceless lives by earthquake occurred between 1900 to 2013 A.D. (Siân Herbert, 2013) From the three earthquake origins of East Africa including the Gulf of Aden and the Red sea, 90% of seismicity is attributed to the East African Rift System in Ethiopia. Dam located in such areas, with an active fault radius of 10km and having 45m or more height is categorized as dam located under hazardous. The previously dominant pseudo-static dam

seismic analysis is now replaced by dynamic type as the advancement of numeric based computer applications is developing in an amazing rate.

In this paper, the Middle Awash Multi-purpose high dam located at the rift axis of the Main Ethiopian Rift (MER) of Afar Depression will be evaluated for its serviceability and safety performance during and post-earthquake event with its foundation. The multi-purposed dam will not face loss of project benefits if not well modeled for seismic load effects, but also loss of priceless lives of people living downstream of the project. (WWDSE, 2015) The next method part of this paper begins with a need for dynamic analysis for the project. Result, discussion and summary will follow preceding recommendation.

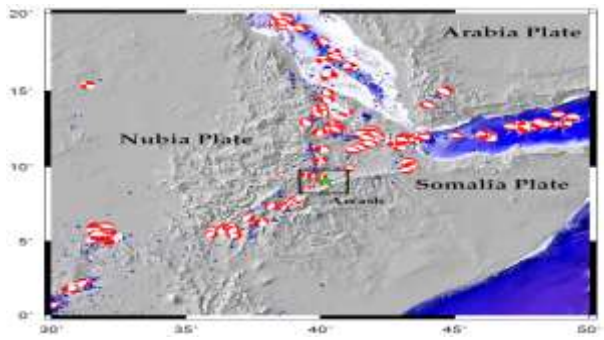

Blue and red circles represent earthquakes that occurred for the last 110 years in the region .The green star shows the location of the Middle Awash Dam Project site.

Figure 3: Seismicity data for the Horn of Africa (WWDSE, 2016)

2. Method

The dam is 120m high zoned embankment dam with a crest length of 453m across Awash River. The feasibility design before proceeding to the detail was assessed for the dynamic stability.

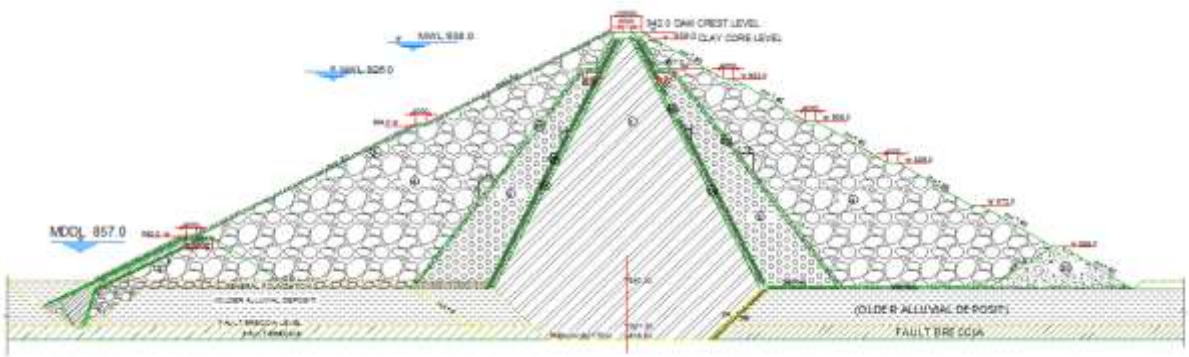

Figure 4: Middle Awash Multi-Purpose Dam zoning at critical section (WWDSE,2016)

The dam site has an expected maximum credible earthquake acceleration which is greater than 0.25g. In addition, the dam is planned to rest on a foundation which is about 15m thick alluvium deposit, which should be assessed for liquefaction.

Table 2: Dam salient features (WWDSE,2016)

Dam height above river bed: 124.75 meter	Crest length: 453 meter
Crest level: 942 m.a.s.l	Upstream berms: 2 with a width of 4m
Normal water level: 926 m.a.s.l	Upstream slope: 1.9
Maximum water level: 938 m.a.s.l	Downstream berms: 5 with a width of 4m
Minimum drawdown level: 857 m.a.s.l	Downstream slope: 1.65
Crest width: 12 meter	Clay cored/ shell and rock fill shoulder

2.1. Seepage analysis and liquefaction potential assessment

In the seepage analysis material model conductivity is related to matric suction. Liquefaction potential for granular material is assessed based on Tsuchida chart. Fine particles could also liquefy if these three criteria's meet; Clay content less than or equal to 15% by weight (particles smaller than0.005), the liquid limit is less than or equal to 35% and the natural moisture content is greater than or equal to 0.9 times the liquid limit. (Seed and Idris,1982)

2.2 Earthquake characterization

Due to unavailability, considering resemblance factors, elsewhere recorded time history data was compared and adopted. Modification to the design base (DBE) and maximum credible earthquake (MCE) amplitude of the dam site was done to make it fit to the site condition.MCE and DBE were taken to consider 1000 and 144 years of return periods, respectively. The Ambrasey equation for determination of period was used to determine the dam’s period ranging between 0.2-2sec.The vertical ground acceleration was taken to be half of the horizontal. (J. E. Ahlberg,1972)

2.3 Initial static stress and slope stability before earthquake

The dynamic analysis gives the shear stresses due to the self-weight, pore-water pressure, hydrostatic pressure and the cyclic shear stress. To determine the specific dynamic shear stress, responsible for deformations and slope instability, the stress determined by the initial static stress is subtracted from the dynamic analysis stress. The constitutive material model selected for initial static stress analysis is elastic-plastic. A limit equilibrium technique of numerical analysis with a Mohr-Coulumb constitutive material model is used to evaluate slope safety.

2.4 Finite Element and dynamic analysis modeling

The finite element model is done with both structured and unstructured mesh, having 4960 nodes where equations are checked, and 5702 elements, at which material properties are extracted. The quads and triangular element geometry is selected for their compatibility in unstructured mesh. For the dynamic analysis, starting with a specified value, stiffness was modified by the computed strain for the subsequent analysis using Equivalent- Linear model. Shear modulus reduction function and damping ratio function relates main dynamic parameters to the strain occurred. As the confining stress increases the cyclic shear stress required to trigger liquefaction will also increase. A correction function is attached to the cyclic number function to account for this effect. Depending on the density of the soil, the initial static stress also influences the cyclic stress required to trigger liquefaction. The shear modulus is also a function of overburden stress.

2.5 The slope stability after earthquake, permanent deformation and response spectrum

Slope stability analysis is done in every earthquake motion time steps. (0.02 sec) In the limit equilibrium method the earthquake acceleration is changed to inertial force for every slice. For the Finite equilibrium analysis, the additional dynamic shear stress in each element at the base of the slice is averaged and added to the static finite element slope stability analysis for each time step. The 1965 developed Newmark model is used to determine deformation. Amplitude amplification at the crest of the dam is expected and should be checked.

3. Result and discussion

3.1 Steady state seepage and liquefaction potential assessment

Safe seepage is determined and pore-water pressure contour is generated. The thick alluvium deposits' 70% and 53 % of the material are in potentially liquefiable and most liquefiable region in the Tsuchida chart, respectively. For the clay core, the three criteria's do not meet simultaneously. This indicates the necessity of liquefaction analysis on the alluvium deposit.

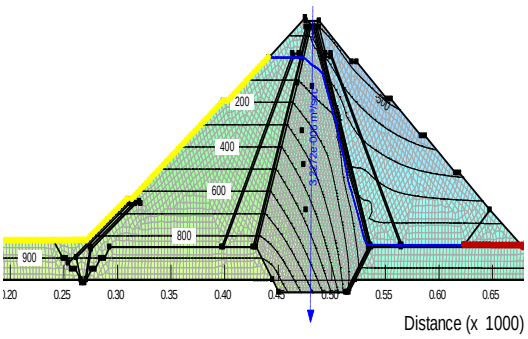

Figure 3: Seepage analysis result; the blue line is zero pressure line, while the white background numbers are pore pressure contours in kpa.

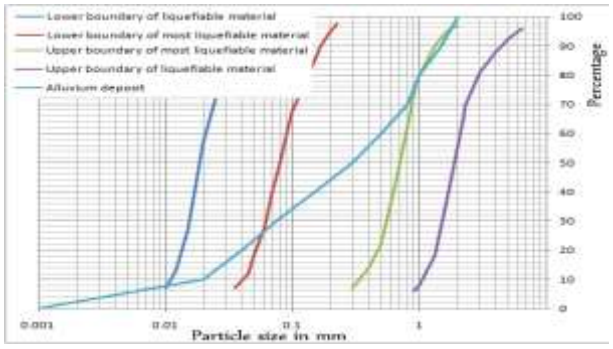

Figure 4: Liquefaction potential assessment result for thick alluvium foundation using Tsuchida chart

3.2 Earthquake characterization

The dam period is determined to be 0.33 sec considering the highest shell material shear modulus and 0.2 sec period amplitude is selected as being sufficiently conservative. From the site specific hazard assessed the selected peak ground acceleration corresponding to MCE and DBE are 0.4107g and 0.212g, respectively. The three elsewhere recorded data different in frequency and duration are; Elcentro, Kobe and Hachinohe. (USA and Japan records)

3.3 Initial Static Stress and Slope stability analysis before the earthquake shaking

The minimum required slope stability factors of safety for static conditions are satisfied.

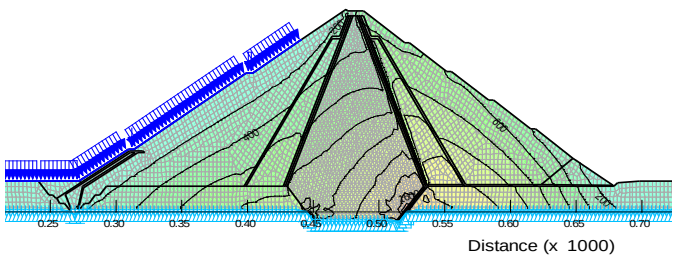

Figure 5: Effective stress distribution; the white background numbers are stress values in kpa and the maximum recorded at clay core bottom.

Table 2: LEM and FEM calculated slope stability result summary

	Downstream	Upstream
FEM	1.484	1.639
LEM	1.66	1.772

In the LEM method stresses are calculated using slice geometry and character. But in the FEM the stresses are calculated by the FEM

3.4 Dynamic analysis

Amplification distribution along zoned dam depicts that amplification in the upper part (approximately 80% of the dam height) is highest. (Pelin O.,2014) The above fact is revealed at 0.84height of the dam where the highest amplification (1.76-3.01times) is determined.

3.5 Slope stability analysis after earthquake shaking (post-earthquake)

The minimum factor of safety for downstream face occurred during Hachinhoe is a result of longer duration, where amplitudes are peak in most of the cycles. The duration and the cycle's peak amplitude are more strong factors than peak amplitude acceleration in lowering stability.

Table 3 Slope stability factor of safety (during earthquake)

Earthquake type	Earthquake considered	FEM		LEM	
		Up stream	Down stream	Up stream	Down stream
DBE	Elcentro	1.615	1.373	1.745	1.523
	Hachinhoe	1.215	0.976	1.336	1.033
	Kobe	1.609	1.421	1.745	1.523
MCE	Elcentro	1.718	1.331	1.745	1.52
	Hachinhoe	1.273	0.925	1.335	1.028
	Kobe	1.605	1.414	1.745	1.523

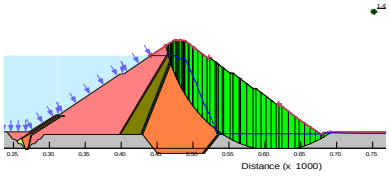

Figure 6: Kobe DBE slope failure surface determined using FEM stress; Factor of safety: 1.421

3.6 Newmark Deformation

The only deformation of 0.4m occurred in Hachinhoe MCE indicates duration of earthquake reaching uniform peak acceleration is the crucial factor of deformation.

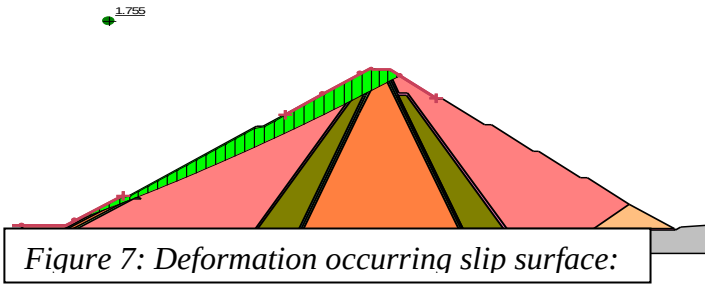

Figure 7: Deformation occurring slip surface:

The direction of the deformation (resultant) is assumed to be in the direction of chord of the slip surface. (Messele, 2006)

3.7 Liquefaction result

In all cases of earthquake liquefaction will occur in all parts of the alluvium foundation except a small region at the toe of the dam.

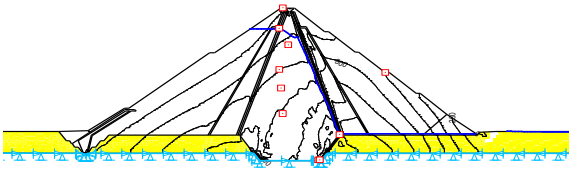

Figure 5: Liquefaction occurrence; liquefaction starts after few seconds in all the yellow region.

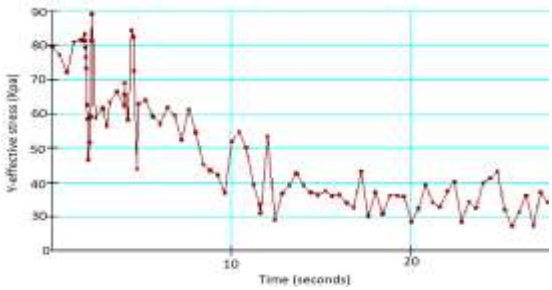

Figure 9: Effective stress at the dam toe during DBE of Elcentro

In Pseudo-static approach, during DBE, upstream and downstream factor of safety are determined to be 0.921 and 1.113, respectively. The economical and safe slope reduction for upstream slope results a slope modification of 1:1.9 to 1:1.75. The new deformation becomes 0.48m in the modified slope and condition of rapid draw down providing a minimum 30 days of drawdown. The whole volume of fill to be decreased is 99,660 cubic meters.

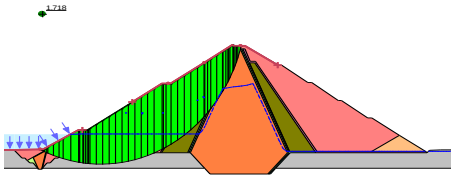

Figure 6: Reduced slope upstream sliding face and critical slip surface at 100th day of drain;

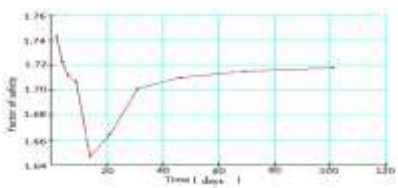

Figure 11: Factor of safety versus time for rapid drawdown;

4. Conclusion

The post-earthquake slope stability analysis ensures stability of upstream and downstream after the earthquake shaking. Post-earthquake slope stability is highly affected by shaking duration reaching peak acceleration in most of the cycles. In evaluating the post earthquake case, results method of Finite Element showed conservative results related to stress determination approach. The finite element method also presented conservative results for the upstream slopes which is attributed to the impounded water mechanics. The permanent deformations of 0.4m can be entertained in cumber height of 1.25m provided. In creating a permanent deformation ground acceleration, shaking duration and uniformity of peak accelerations in cycles are influential factors. The determined occurrence of liquefaction in the alluvium foundation after a few seconds of earthquake including the short duration and minimum peak amplitude of Kobe earthquake showed foundations' weak performance. A trial of steepening upstream slope from 1:1.9 to 1:1.75 result a safe performance indicating required optimization of slope considering economics. The slopes DBE and MCE post-earthquake performance are very similar in the amount of factor of safety against sliding. If the analysis was done in pseudo-static approach comparably, the result difference would be very wide. Thus, dynamic analysis considers the cyclic effect well and is not improperly influenced by earthquake inertial effect.

5 Recommendation

(I) It is necessary to replace the alluvium foundation with a well compacted shell and gravel dominant sandy material. Parts of the downstream foundation which have a relative density lower than 55% should be removed and replaced by gravel dominant sandy material. (II) By steepening upstream slope from 1:1.9 to 1:1.75, an economical upstream section can be adopted which satisfies minimum critical value of factor of safety. (III) Further increase of dam height and cumber must be avoided. (IV) In a dam seismic stability analysis, a dynamic analysis type must be picked over pseudo-static analysis to overcome problem of conservative results which leads to uneconomical dam geometry and insufficient capturing of events.

References

1. Fantahun Getachew. Comparison of pseudo-static and dynamic response analysis of Sibilu dam[Journal] // Addis Ababa,unnown.

2. Fell Robin [et al.] Geotechnical engineering of dams [Book Section]. - London : Taylor and Francis group plc, 2005.

3. ICOLD, 1983. International Commission for Large Dams, Seismic and dam design, Bulletin 46. ICOLD, Paris, France.
4. J. E. Ahlberg, J. Fowler, L W. Heller. Earthquake resistance of earth and rock fill dams U.S. Amy Engineer Waterways Experiment Station Soils and Pavements Laboratory, Vicksburg, Mississippi,1972.
5. Kenji Ishihara. Soil Behaviuor in Earthquake Geotechnics [Book]. - New York : Oxford University, Anthony Rowe Ltd., Eastbourne, 2003.

6. Kramer Steven L. Geotechnical Earthquake Engineering [Book]. - New Jersy : Prentice- Hall ,Upper Saddle River, 1996.

7. Messele Haile, Hadush Seged Earthquake induced liquifaction analysis of Tendaho earth-fill dam[Journal] // Addis Ababa,2006.

8. Newmark N. M. Effects of earthquakes on dams and embankments, Rankine Lecture [Journal] // Geotechnique. - 1965. - 2 : Vol. 15.

9. PelinÖzener and BurakKayhanBeşli. Investigation of Effects on Seismic Response characterstics of earthfill and rockfill dams. Proceedings 10th conference on earthquake engineering,Alaska. Yildiz Technical University, Istanbul.2014.
10. Seed, H.B. Earthquake-resistant design of earth dams. Proc., Symp. Seismic Design. Of Earth Dams and Caverns, ASCE, New York,1983, pp. 41–64
11. Siân Herbert. Assessing seismic risk in Ethiopia. Government social development humanitarian conflict[Journal] // Addis Ababa,2013.
12. US Corps of Engineers. Engineering and design –Time-History Dynamic Analysis of Concrete Hydraulic Structures, Engr. Manual EM1110-2-6051, Dept. of the Army, Corp of Engineers., Office of the Chief of Engineers 2003.

13. WWDSE, Water Works Design and Supervision Enterprise, MIDDLE AWASH FEASIBILITY STUDY AND DETAIL DESIGN OF MULTIPURPOSE DAM PROJECT VOLUME-V, PART-I DAM AND APPERTENANT STRUCTURE DRAFT FEASIBILITY DESIGN REPORT, Addis Ababa, Ethiopia, 2015.

Investigating Reservoir Sedimentation and its Implication to Watershed Sediment Yield: The Case of two Small Dams in Data Scarce Upper Blue Nile Basin, Ethiopia

Michael M. Moges[1]

[1]Faculty of Civil and Water Resources Engineering, Bahir Dar Institute of Technology, Bahir Dar University, Ethiopia; E-mail: **micky_mehari@yahoo.com** ; Tel: +251-9-24148568

Abstract

Bathymetric and sedimentation surveys were conducted using a sonar based depth gauge system in two small reservoirs (Selamko and Shina) in the data scarce Upper Blue Nile Basin, Ethiopia. Pre-impoundment topographic information was obtained from dam owners and designers. Bathymetric differencing was then used to investigate and quantify, distribution, and volume estimates of deposited sediment, long term average annual sediment flux, and remaining water storage capacity. Calculated long term average sediment accumulation rates were used to estimate remaining lifetimes of each reservoir. Results from the depth sonar surveys and GIS analyses suggest that the Shina Reservoir has a projected lifetime of approximately 7 years compared to a projected lifetime for Selamko Reservoir of approximately 22 years. Moreover, it indicated that annual average sedimentation rate of both reservoirs is beyond the global average of 1% (1.67% for Shina and 2.295% for Selamko). Specific sediment yield is relatively bigger for both watersheds (2499 and 4333.6 t km $^{-2}$ year^{-1} for Shina and Selamko respectively) indicating that the watersheds are degraded by any world standard. The revised universal soil loss equation (RUSLE) model generated erosion magnitude only slightly larger from the watersheds of both reservoirs compared to the bathymetric estimates. These data and analyses also provide a baseline relevant to understanding sedimentation processes and are necessary for development of long term management plans for these reservoirs and their watersheds.

Key words: Blue Nile Basin, reservoir; sedimentation; bathymetry; depth sonar; GIS

1. Introduction

Sustainable land management and water resource development are threatened by soil erosion and sediment-related problems especially in most developing countries(Morris and Fan, 1998). In Ethiopia, accelerated sedimentation of reservoirs that are intended to provide irrigation water has resulted in the loss of both the intended services from the dams and considerable investments made for their construction. Although it is true that all reservoirs will be filled with sediment eventually, several factors contribute for a rapid and unprecedented loss in storage. Xiaoqing(2003) mentioned the rate of sedimentation and how well the problem is addressed both during the planning stage and while reservoir sedimentation is occurring as major factors. Sediment yield estimates are important parameters in the dam design process especially for appropriate sizing of planned constructions(Verstraeten and Poesen,

2001). However, this data is lacking both in quantity and quality for most Ethiopian watersheds, although recently some improvements have been made in the Northern Ethiopia(Haregeweyn et al., 2006, Tamene et al., 2006a). Consequently, dam designers opted on data for the country as a whole, whose value ranging between 800 and 1200 tkm^{-2} $year^{-1}$(Haregeweyn et al., 2006) or sometimes apply a regional approach and construct a composite rating curve as has been adopted in the Ribb and Megech high dam projects (SMEC, 2008).

The overall objective of this study was therefore to investigate reservoir sedimentation in the data-scarce upper Blue Nile basin and its implication to understand watershed sediment yield. The specific objectives were to: (A) estimate capacity loss and useful life of Selamko and Shina reservoirs; (B) estimate sediment yield of Selamko and Shina watersheds based on bathymetric information; (C) compare bathymetric survey results with preliminary estimates of watershed sediment yield derived from RUSLE to better understand sediment delivery to reservoirs in the basin.

2. Materials and Methods

2.1 Description of the Study Area

The study was conducted at Selamko and Shina Irrigation Dams in the Upper Blue Nile Basin, Tana Sub-BasinEthiopia (Figure 1).

Selamko Reservoir was created in 2005 by construction of an earthen dam across the Selamko River approximately 5 km northeast of Debre Tabor City. At its normal pool elevation of 2498 m above mean sea level, Selamko Reservoir has a surface area of 0.129 km^2 and total storage of 1.03 Mm^3. The watershed occupies a total area of 7.39 km^2.

Shina Reservoir was created in 2007 by construction of an earthen dam across the Shina River approximately 8 km northeast of Hamusit town. At its normal pool elevation of 1801 m above mean sea level, Shina Reservoir has a surface area of 0.185 km^2 and total storage of 1.264 Mm^3. The watershed occupies a total area of 10.87 km^2.The specific sediment yield used by the designers of Selamko and Shina dams is 1,100 tkm^{-2} $year^{-1}$and 1152 t km^{-2} $year^{-1}$ respectively. However, it is not clearly stated in the design document how these valuesare chosen. Both watersheds are part of the Nile Basin and more particularly part of Lake Tana sub-basin which is situated on the South Eastern side of Lake Tana, the biggest lake in Ethiopia.The reservoirs have never been flushed since their construction. Methods

2.2 Bathymetry Survey

For both reservoirs, we used two sets of reservoir topographic maps; one produced for the construction of Shina and Selamko Dams (pre-impoundment topography) and the other collected in July 2015 bathymetric survey. The HawkEye H22PX Digital Sonar system and GARMIN GPS on a small local boat was used to collect bathymetric information. A total of 1100 points for Shina and 1057 points for Selamko are collected in an approximate regular grid. The data density was such that there was approximately 60 data points for Shina and 82 data points for Selamko for every hector of reservoir

surface area. Then the DEM difference approach was used to calculate the areal average annual sediment contribution rate of the two reservoirs.

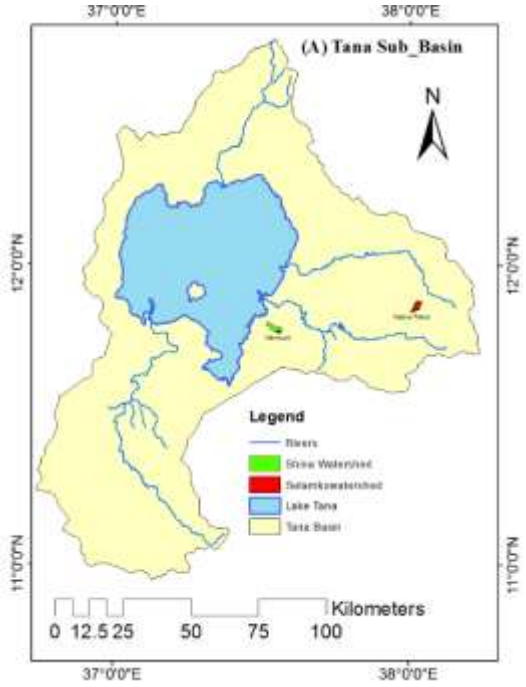

Figure 1: Location map of the study area.

The total capacity loss (TCL, %) of Shina reservoir for the study period, 2007–2015, and Selmako reservoir 2005–2015, and actual life of both reservoirs weredetermined by using the following relationshiprespectively (Haregeweyn et al., 2012):

$$TCL\ (year)\ =\ \frac{(C-C'')}{(CxN)}x100 \quad (1)$$

$$LE = \frac{DSV}{SR} \quad (2)$$

Where, TCL, C, C" and N are the sedimentation rate in percent, original capacity (at the time of construction), current capacity (at time of most recent sedimentation level survey) and Age of the dam (Year of last survey – Year of construction) respectively.LE is the life expectancy of the reservoir (in years), DSV is the dead storage volume of the reservoir, calculated as the capacity loss at the dead storage level and SR is the sediment deposition rate (m^3yr^{-1}). For comparing reservoirs of different sizes, it is convenient to express the rate of sedimentation as the percent of the original storage volume lost per year, and calculated by:

$$SR = \frac{SV}{\Delta T} \quad (3)$$

Where, SV is the sediment volume (m^3) that is accumulated between the year of construction and year of bathymetry survey (ΔT). Sediment yield (SY; $m^3\ y^{-1}$) or specific sediment yield (SSY; $t\ km^{-2}\ y^{-1}$), was then calculated as follows:

$$SY = \frac{SV\ x\ dBD}{STE\ x\ \Delta T} \tag{4}$$

$$SSY = \frac{SY}{A} \tag{5}$$

Where, SV is the measured volumetric sediment input into the reservoir (m^3), STE is the sediment trap efficiency (%), ΔT is the time interval (years) between two successive bathymetric reservoir surveys, dBD is the average dry bulk density of the sediment (tm^{-3}), and A is the watershed area (km^2).Volumetric sediment input was obtained by subtracting DEM of the reservoir bottom obtained by bathymetric survey in 2015 from the reservoir topography before impoundment.

2.3 Linking reservoir sedimentation with watershed erosion

Coupling GIS and RUSLE has been shown in many cases to be an effective approach for estimating soil loss and identifying spatial locations vulnerable to soil erosion. The RUSLE provides an estimate of soil erosion (expressed as tons/ha/year) based on improved computation of watershed parameters including rainfall index, topographical slopes, soil characteristics, and land use as expressed in the soil loss equation

$$A = R * K * LS * C * P \tag{6}$$

where A is the soil loss (tons/ha/y), R is the rainfall index (dimensionless), K is the soil erodibility factor (tons/ha/y), LS is the slope and slope length factor (dimensionless), C is the cropping and management factor or the land cover factor (dimensionless), and P is the support practice (dimensionless) (Mitra et al., 1998).

3. Result and discussion

3.1 Rate and Distribution of Reservoir Sediment

Selamko and Shina reservoirs were relatively shallow; with approximately half of the reservoir less than 6 m. The average depth of the reservoirs was also around 6 m in Selamko and 5 m in Shina, with a maximum of approximately 15.3 m for Selamko and 12 m for Shina near the dam on the north western and north-eastern part of the reservoirs respectively. The bathymetric maps (Figures 2 A, B and Figure 3 A, B) and a longitudinal profile down the long axis of the reservoirs (Figure 4 A and B) indicated a generally smooth, steep reservoir floor sloping from the headwater to the dam. Longitudinal profiles were established using two raster maps of reservoir topography before dam construction and overlying the river bank by Arc-GIS (3D analyst tool of surface interpolation)(Issa, 2015). In both cases uniform sediment thickness immediately after the delta with maximum deposition depth of approximately 4 to 5

m occurred close to the dam. The bottom of both reservoirs indicated that the deposited sediment is more of fine deposit i.e. clay, silt and fine sand particles (on average 46% clay and 30% silt and 24% fine sand in Selamko and 29% clay, 28% silt and 43% fine sand in Shina). In either case, results suggested that severe sedimentation occurred during the last 7 to 10 years.

For Selamko Reservoir analysis of the maps showed that the dead storage capacities at 2,486 masl were 0.0562 and 0.0142 Mm^3 during construction (2005) and 2015, respectively, losing approximately 75% of its capacity. The total storage capacities at 2,498 masl were 1.034 and 0.797 Mm^3, in 2005 and 2015 respectively. The estimated live storage capacities, calculated as the difference between the total and dead storage capacities, were 0.978 and 0.782 Mm^3 in 2005 and 2015, respectively.

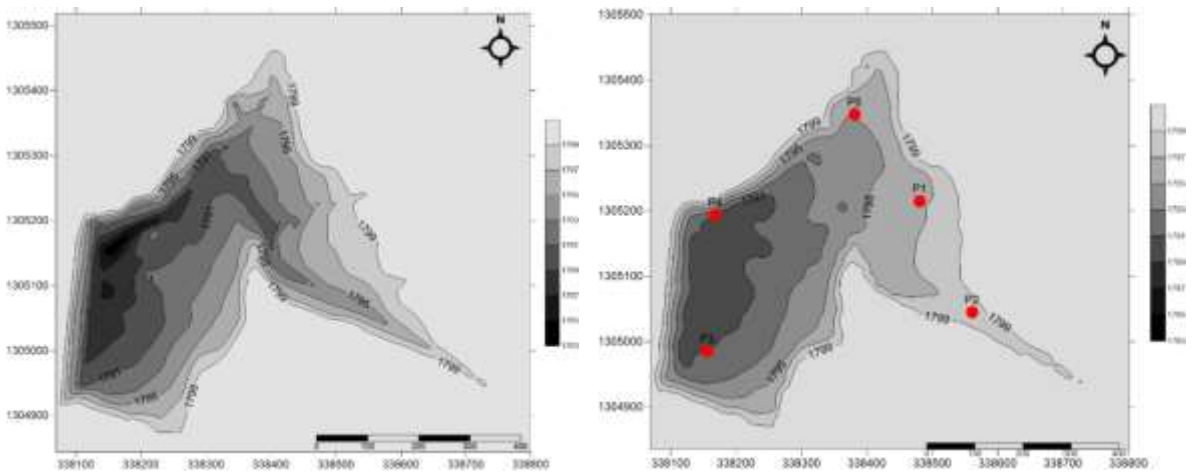

Figure 2: Bathymetric Maps of Shina Reservoir. Contour Interval is 2 m. (A) Pre-impoundment topography derived by digitizing an existing topographic map used during dam construction. (B) Present-day (year 2015) bathymetry derived from Sonar Depth Survey. Dots indicates soil sampling points.

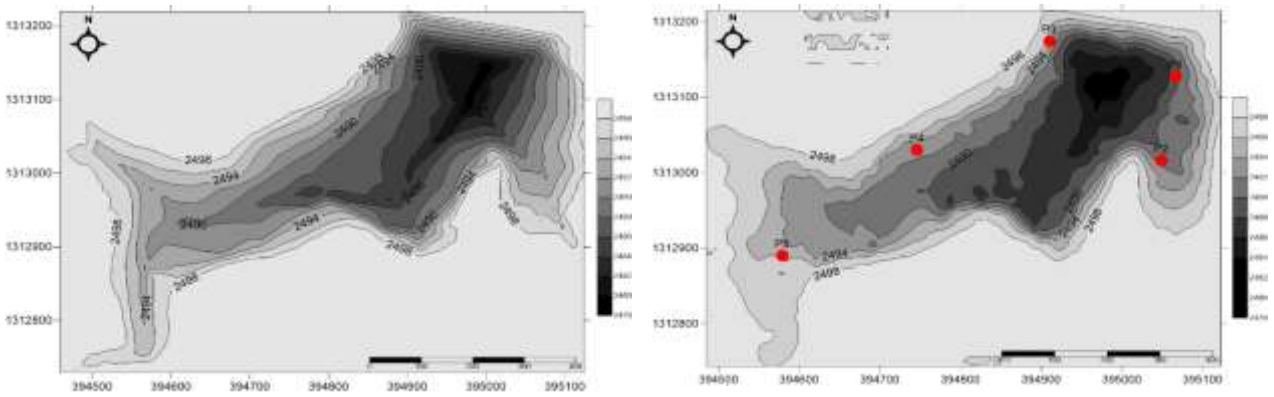

Figure 3: Bathymetric Maps of Selamko Reservoir. Contour Interval is 2 m. (A) Pre-impoundment topography derived by digitizing an existing topographic map used during dam construction (B) Present-day (year 2015) bathymetry derived from Sonar Depth Survey. Dots indicates soil sampling points.

For Shina Reservoir analysis of the maps confirmed that the dead storage capacities at 1,788 masl were 0.01118 and 0 Mm^3 during construction (2007) and 2015, respectively, losing 100% of its capacity. The

total storage capacities at 1,801 masl were 1.26 and 1.09 Mm^3, in 2007 and 2015 respectively. The estimated live storage capacities, calculated as the difference between the total and dead storage capacities, were 1.2488 and 1.09 Mm^3 in 2007 and 2015, respectively.

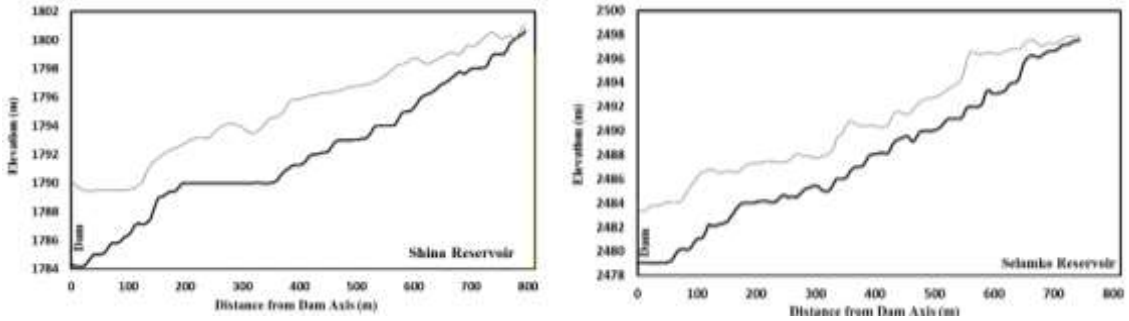

Figure 4: Topographic Profiles along (A) the axis of Shina Reservoir upstream of the dam (B) the axis of Selamko Reservoir upstream of the dam showing profiles of Pre-Impoundment topography in black line and profiles of Post-Impoundment topography in gray line.

The long-term average annual sediment accumulation rate was calculated by dividing observed accumulated sediment volume values by the age of the Reservoirs (eight years for Shina and ten years for Selamko). This yielded long term annual sedimentation rate of 21130 m^3/year for Shina and 23740 m^3/year for Selamko reservoirs respectively. This implied an average annual storage loss due to sedimentation of 1.67 percent for Shina and 2.295 percent for Selamko Reservoir. This rate is relatively high as compared to losses experienced elsewhere and greater than the average annual worldwide rate of 1% that was proposed by Mahmood (1987). Although quantitative study of reservoir siltation is not available in abundant quantity in Ethiopia, storage losses of up to 4% were observed in the northern parts of the country(Haregeweyn et al., 2006, Haregeweyn et al., 2011).However, it is evident that in many cases rates of sedimentation calculated are dependent up on the accuracy not only of the current bathymetry but also of the original bathymetry. For instance, Interview with elders and local residents who participated in the construction of Selamko dam indicated that material for construction were excavated from the reservoir bottom after surveying for pre-impoundment topography was completed. Data on the actual quantity of excavated material could not be obtained. However, it is evident that average annual storage loss could have been even more than what it is at the present.

The life of Selamko and Shina reservoirs were projected by linear interpolation to be 8 and 7 years respectively. This projection is done by dividing the reservoirs' capacity at intake level by their respective siltation rate. This is done assuming that although water might still be available within the reservoir, it may not be accessible as minimum reservoir water level is above the water intake level. Thus, the remaining storage volume at intake level will be completely used up by the end of 2023 and 2022 for Selamko and Shina respectively.

The findings of this study also showed that the sedimentation problem is still severe as compared with the findings of most studies of similar reservoirs in other parts of Ethiopia and eastern Africa. Haregeweyn et al.(2012) reported capacity loss of 4%, 3% and 3% for the periods 1997-2005, 2005-

2007 and 1997-2007 for Angereb Reservoir in the same Lake Tana Basin. Annual capacity loss values ranging between 0.18 – 4% have also been reported for 13 reservoirs in northern Ethiopia(Haregeweyn et al., 2006). This study also confirmed that although there are efforts in soil and water conservation for the past few years mainly focusing in the uplands (Hurni, 1988), sedimentation in rivers and reservoirs didn't reduce (Steenhuis et al., 2014).

3.2. Specific Sediment Yield from Shina and Selamko Watersheds

The specific sediment yield (SSY) of Shina and Selamko reservoirs is 2499 and 4333.6 t km $^{-2}$ year^{-1}. The SSY values are significantly higher than the global and African averages, about 1500 and 1000 t km^{-2} year^{-1}, respectively (Lawrence and Dickinson, 1995). They are also higher than the tolerable soil loss rate for sustainable crop productivity and soil generation rate, which is 2 to 18 t ha^{-1} year^{-1}(Hurni 1985) and 3 to 7 t ha^{-1} year^{-1}(Hurni, 1983) for Ethiopia respectively. However, SSY values in the order of 30 t ha^{-1} year^{-1} and 75 t ha^{-1} year^{-1} have been recorded at the gully dominated Anjeni and EneChilala watersheds respectively (Ayele et al., 2016).The high SSY of both watersheds in this study and specifically Selamko watershed can generally be attributed to several factors. Among them are dominance of fine soil fractions, moderately steep topography, and very limited soil and water conservation in recent years only may be mentioned. Moreover, presence of many active gullieswith significant depth and width and disturbance of watershed for production of excessive road construction materials in unmanaged way are becoming very common in Selamko. Consequently, it is not surprising that the SSY values are very high by any standard. The presence of dense networks of gullies increases slope collapse and catchment connectivity and facilities sediment delivery (e.g.(Owens and Slaymaker, 1993, Wasson, 1994, Poesen et al., 2003).

3.3. Linking catchment erosion to reservoir sedimentation

The total annual sediment load derived from the RUSLE for Selamko watershed was estimated to be 1.3 times (39,493 tons) the calculated annual sediment deposition measured for Selamko Reservoir based on the bathymetric survey result (32,025 tons) giving a sediment delivery ration of around 81%. This value from bathymetric survey is obtained using average dry sediment bulk density of 1244 kg/m^3 and trap efficiency of 92.3% based on the Brown's method and derived from dividing observed sediment volume by reservoir age. In the Shina watershed, however, the total annual sediment load derived from the RUSLE was 46,834 tons. This value was approximately 1.72 times the annual sediment deposition measured for the reservoir using the bathymetric survey (27,164 tons, using average dry sediment bulk density of 1178 kg/m^3 and trap efficiency of 91.6% based on the Brown's method), dividing observed sediment volume by reservoir age. This will make the sediment delivery ration for Shina to be in the order of 58%, a value much less than Selamko.

The obtained results of the RUSLE model suggest that rill erosion may not be the dominant process of sediment erosion and transport within both watersheds (Tables 1). This is true as based on texture the largest portion of both watersheds soil is classified as clay and clay loam with a minimum coverage of sandy loam. Coarser texture sediment and sediment from sheet and rill erosion have more chances to be

deposited or to be trapped, compared to fine sediment and sediment from channel erosion. This means the delivery ratios of fine sediment or sediment from channel erosion is relatively higher. Moreover, both watersheds are small in size. Consequently, there is more chance for eroded sediments to arrive to downstream reservoirs relatively quickly.

Table 1: RUSLE Model results for Shina watershed

	Shina					**Selamko**				
Slope Interval (Percent)	0-2	2-10	10-15	15-30	30-44	0-2	2-10	10-15	15-30	30-50
LS Factor	0.84	1.2	2.06	2.77	2.57	0.36	2.61	2.83	5.98	11.83
Area (Ha)	73.89	842.04	129.08	38.99	3.29	67.49	396.39	189.89	79.27	6.25
Average Sediment Generated (t/Ha/yr)	29.9	38.51	62.78	97.56	88.78	23.5	44.47	68.11	85.18	95.10
Annual Load (Tons)	2207.8	32427	8103.6	3803.9	292.1	1586	17627.5	12933.4	6752.2	594.4

4. Conclusion

This paper demonstrates the application of bathymetric survey to estimate reservoir sedimentation and predict its lifespan. Also, an attempt has been made to compare erosion estimates using RUSLE integrated with GIS and bathymetric surveys.

The two small reservoirs (Shina and Selamko) are suffering from an extreme sedimentation problem that will start reducing the irrigation water supply and consequently social conflicts among the users. The designers used a SSY value of 1152 tkm^{-2} $year^{-1}$ and 1,100 tkm^{-2} $year^{-1}$ in the design of Shina and Selamkoreservoirs respectively, whereas the actual SSY, measured in this study, is approximately 2499 and 4333 tkm^{-2} $year^{-1}$ for Shina and Selamko respectively. This finding indicates that the watershed is highly degraded by world standards.

GIS-based RUSLE was used to estimate soil loss from the entire watershed. This attempt to relate watershed scale erosion and reservoir sedimentation might help in translating the role of rill and related erosion processes to reservoir sedimentation in Selamko and Shina watersheds. The outcome would help to take suitable erosion control measures in the severely affected areas. The results obtained from the study can assist in developing management scenarios and provide options to policy makers for managing soil erosion hazards in the most efficient manner for prioritization of different regions of the basin for treatment.

References

Ayele, G. K., Gessess, A. A., Addisie, M. B., Tilahun, S. A., Tebebu, T. Y., Tenessa, D. B., Langendoen, E. J., Nicholson, C. F. & Steenhuis, T. S. 2016. A Biophysical and Economic Assessment of a Community-based Rehabilitated Gully in the Ethiopian Highlands. Land Degradation & Development, 27, 270-280

The Viability of Investment in Solar Irrigation: Evidence from Experimental data in Ethiopia

Gebrehaweria Gebregziabher[1] Amare Haileselassie[1], Nicole Lefore[1]

International Water Management Institute (IWMI)

Corresponding author: g.gebregziabher@cgiar.org, Mobile: +251 (0)92175373

Abstract

Data used in this study came from a pilot study of solar irrigation in part of the Rift-valley that can be applied in other part of the country. Overall result shows that investment in solar irrigation is profitable given that the minimum required land is available. As solar is clean (zero-carbon) energy, the technology is very much consistent with the Ethiopian Climate Resilient Green Economy (CRGE) strategy. However, the profitability of the technology depends on crop type and water delivery system where drip system was found superior than furrow and overhead water application system. Our result also shows that land size matters implying that a minimum land size is required for a viable investment in solar irrigation where the minimum required land size itself depends on different factors including type of water application system, crop type, discount rate and location. Because access to affordable financing is crucial for smallholder farmers, the microfinance institutions can server as a reliable source of finance than the formal banking system. Moreover, although high initial investment cost is potentially a barrier for smallholder farmers to adopt the technology, cost sharing can be a solution, especially if additional investment is made on drip system because it can increase irrigable land size to about half a hectare. Additionally, partnerships between key actors, such as the private sector and rural financial institutions is essential for a positive outcome and sustainability of investment in solar irrigation. While one can argue that commercialization is essential for sustainable market growth, targeted subsidies are needed at early stage till competitive prices are reached. In conclusion, the piloted type of solar pumping system has been analyzed with its scope and limitations

1. Introduction

The agricultural sector accounts for 0.2% of Ethiopia's energy consumption (Teferra, 1986) and 89% of total water withdrawals among which irrigation accounts for 85% of total water withdrawal (FAO, 2016). Solar powered irrigation as a source of renewable energy resources and increased efficiency in water application offers the potential to reduce the energy and water consumption. Costly diesel pumping systems pose an economic risk to farmers. The ever-increasing mismatch between demand and supply of energy is posing challenges, especially to farmers in remote areas where supply of fuel is a

problem and are forced to look at alternate sources of energy for running irrigation pumps. The high operational cost of diesel pumps may also force farmers to practice deficit irrigation of crops, considerably reducing their yield and income. Therefore, solar pump can be an alternative to the diesel pumps for irrigated crop production. Throughout Ethiopia, the annual distribution of mean daily radiation allows the most efficient use of solar systems (Tefera, 1986). Shakti (2014)has assessed the benefits of solar water pumping in India and has highlighted the crop yield improvements due to timely and adequate water availability for irrigation.Contrasting to diesel pumps that have proven to be expensive and environmentally unsustainable, solar pump provides an environment friendly and low maintenance cost option for pumping irrigation water.Likewise, water pumping systems powered by solar energy are clean, decentralized and economical alternative for the irrigation of crops. It is also in line with the Ethiopian Government's Climate Resilient Green Economy (CRGE) strategy.

Since Ethiopia is located in the tropical zone near to the equator, it has huge solar energy potential. According to HYDROCHINA CORPORATION (2012), for example, the annual total solar radiation in any region of Ethiopia reaches class "very rich. Teferra (1986) also indicated that the total primary solar radiation reaching the ground is estimated at about 1,953 million Tcals/year. Although the day time sunshine suitable for solar energy production reaches 10 to 12 hours in the south east, northern and north east lowlands; most parts of the country receive over 7 hours of bright sunshine daily.

The aim of this paper is to contribute to the development of business model for solar pump by assessingthe profitability of investment in the technology for smallholder irrigation. Data used for this analysis comes from pilot experiments that was done with eight farmers in Oromia and SNNPR of Ethiopia. Three different water application (i.e. drip, furrow and overhead) systems and four crops (pepper, head-cabbage, carrot and fodder) where considered in the analysis.Different water application methods and crops can have different profitability effects, hence this paper is assumed to contribute totheknowledge aboutsolar powered pumping and its agricultural use.To this end a methodology that capture the technical and economic performance of three major systems ofthe technology (i.e. the pumping, the irrigation and the crop systems) was considered. This approach leads to the development and analysis of scenario based comparative analysis of profitability and viability of investment in solar pump for irrigation purposes.

2. Description of the demonstrated solar pump technology and pilot study

The International Water Management Institute (IWMI), through the Livestock and Irrigation Value Chain (LIVES) and AfricaRISINGprojects has piloted eightsolar pumps, for smallholder irrigation with selected farm households in Oromia and the Southern Nations, Nationalities and Peoples' (SNNP) regions.

The aim of the pilot was to demonstrate and test whether solar pump can provide smallholder farmers with an affordable and sustainable irrigation water pumping. Solar pump panel captures the sunlight and convert it into electricity which drives the pump (Figure 1).

Figure 1: Piloted solar water pumps

Although there are different versions of solar pumps, we demonstrated a suction version (see Table 1 for detail specification). On a clear day, the upper limit capacity of the pump that we have demonstrated is $13M^3$/day when water is lifted from 4 meters depth https://www.practica.org/projects/introduction-solar-irrigation-pumps/). Besides the pump, we also have field tested three water application methods including drip, furrow and overhead (Figure 2).

As the amount of water supplied and other costs (such as, labor, agronomic practices and related costs) differ by irrigation method, it helped us to do a comparative analysis between the different water application methods. For example, the drip system would provide precision in water application leading to a decreased water loss from wind and evaporation, hence the long-term advantages would be lower energy, operating costs and water saving.

Figure 2: Demonstrated water application methods (overhead, furrow and drip, respectively)

Each solar pump was purchased at a cost of 650 USD, approximately equivalent to 13000 Birr at the time of investment excluding tax, transport and related costs. Each pump has a discharge capacity of 0.5 liter per second from a maximum of seven-meter depth shallow well to fully irrigate 0.20 hectare using furrowwater application system. The size of irrigable land can increase to a quarter (0.25ha) of a hectare if the depth of water table is reduced to about 4 meters. Six of the eight solar pumps weredemonstrated in Gamo-Gofa and Hosaena zones of the SNNPR, while the rest four pumps were demonstrated in Duguda and Bora woredas, both in the central Rift-Valley of the Oromia region. The farm households who demonstrated the solar pump were selected based on their access to shallow groundwater, willingness to adopt and demonstrate the technology and to collaborate with the projects allowing usto collect data. The central Rift-Valley is one of the hubs of vegetable production for Addis-Ababa and surrounding major markets, while Gamo-Gofa is relatively remote. Both sites are among the high radiation potential sites in Ethiopia fertile to produce solar energy on big scale.

Table 1: Descriptionof the field-tested solar pump

Farmer	Hola	Jambo	Goda	Gum	Abayneh	Ewunetu	Tefera	Berhanu
Site (	Rift-	Rift-	Gam	Gam	Lemo	Lemo	Lemo	Lemo
Size of demonstration plot (M^2) and implementing project name								
Drip	200	150	200	200	--	--	--	--
Furrow	200	200	200	200	--	--	--	--
Overhe	100	100	100	100	50	50	50	50
Crop	Pepper	Pepper	Pepper	Pepper	Cabbage/Carrot/fodder	Carrot	Cabbage/Carrot/fodder	Cabbage/Carrot/fodder
Project	LIVE	LIVE	LIVE	LIVE	AfricaRISING	Africa	AfricaRISING	AfricaRISING
Depth of well and technical specifications of pump								
Depth (meter)	4	3.5	4	2.5	7.5	3.55	6.15	5.7
Water table	1.8	2	1	1.5	6	2	4.8	3.7
Yield (liter)	20.4	25	15	15	15	15	15	20
Time (sec)	72	62	30	30	48	47	74	91
Capacit (l/min)	17	24.19	30	30	18.8	19.1	12.2	13.2
Capacity (lit/hour	1020	1451.4	1800	1800	1128	1146	732	792
Capacity and characteristics of solar pump technology								
Yield l/hr@ 1 meter	2500	2500	2500	2500	2500	2500	2500	2500
Yield l/hr @ 6 meter	1500	1500	1500	1500	1500	1500	1500	1500
Maximum depth (m)	7	7	7	7	7	7	7	7
Expected life span	20 years	20 years	20 yrs	20 years	20 years	20 years	20 years	20 years

Unlike in the Africa RISING sites where we have demonstrated only overhead irrigation system, in each LIVES site, an additional investment of 3500 Birr[2] and 3000 Birr was made in tanker and drip systems, respectively. On top of that, an installation cost of 21000 Birr per site was incurred.

2.1 Validating the feasibility of investment in solar pump irrigation

We used the UNIDO (1972) approach to estimate NPV and IRR as a measure of financial viability of investment in solar pump-based smallholder irrigation as specified below (Eq. 1).

$$NPV = \sum_{t=1}^{n} \frac{(B_t - C_t)}{(1+r)^t} \quad (1)$$

Where NPV stands for net present value; n is the time period, $B_t$stands forbenefits at time t; C_t *is* cost at time t; and r is the real discount rate. The NPV is the present value of net cash flows generated by smallholder farmers who irrigate and produce using solar pump. It is a reliable measure used in capital budgeting, because it accounts for temporal changes in the value of money by using discounted annual cash flows.

The internal rate of return (IRR) presented in Eq. 2 is defined as the rate of return of an investment that equates the net present value of benefits and costs so that the net present value of the investment becomes zero.

$$IRR = \sum_{t=1}^{n} \frac{B_t}{(1+r)^t} - \sum_{t}^{n} \frac{C_t}{(1+r)^t} = 0 \quad (2)$$

The IRR is equivalent to the discount rate (r) that satisfies equation (Eq. 2). For convenience, Birr (Ethiopian currency) was used as the common unit for the financial feasibility analysis.

Data on production, cost of investment (cost of solar pump, drip kit, tanker and installation cost) and variable costs including labor, fertilizer, chemicals, seed, etc. were collected. The size of demonstration plot varybetween 50m^2 to 200 m^2. All costs were estimated equivalent to the maximum (potential) and minimum requirement of irrigable land size (see Table 2). Data presented in Table 2 shows that the size of land that can be irrigated using a drip system is twofold of the size of land that can be irrigated using furrow and overhead system indicating that a significant amount of water is saved to irrigated larger size of land leading to positive gains from economics of scale. Although the manufacturer's description (see

Table 1) indicate that the use-life of a solar pump is 20 years, we consider 10 years of life span for our purpose, because we assumed that this positioned us in a safe side not to overestimate the value of NPVs and IRRs.

Table 2: Estimating the capacity of the solar pump by water application method

Variables	Drip	Furrow	Overhead-LIVES	Overhead-AR
Crop type	Pepper	Pepper	Pepper	Cabbage, carrot, fodder
Demonstration plot (m2)	200	200	100	68
Amount of water used (m3)	52	105.3	41.2	27.4
Per ha equivalent (m3)	2600	5266.1	4118.5	4028.1
Pumping capacity l/second	0.5	0.5	0.5	0.24
Total discharge l/hr.	1800	1800	1800	864
Total discharge m3/day	14.4	14.4	14.4	6.9
Cropping season (days)	80	80	80	131
Total discharge m3/season	1152	1152	1152	905.5
Potential irrigable land (m2)	4431	2188	2797	2248

In Ethiopia,the formal (commercial) banking system could not address the financialneeds of the rural poor households for the very fact that they are not their ultimatetarget clients and the transaction costs and risks involved inserving the rural poor households are perceived to be too high.The Development Bank of Ethiopia's (DBE) main focus area is on relatively big and long term investment projects, it is less likely for the smallholder farmers to access such strategically designed credit sources. Hence, we considered that the rural micro finance institutions (MFIs) are the main credit sources for smallholder farm households.

Moreover, on account of the non-suitability of commercial banking system, different Micro Finance Institutions (MFIs) were established, joined the financial market mainly to provide financial services to the rural poor household as their primary objective is to enhance the living conditions of the rural poor households.

Likewise, most of MFIs' loans fall into different loan categories among which agricultural loans (irrigation and modern agricultural inputs) are among the major loan categories constitute the rural loan

package. Despite the appropriateness of MFIs as a source of credit for the smallholder, their lendinginterest rate that range between 15% to a 24% (see Table 3) is higher than the lending interest rates of commercial banks, but still lower than other sub-Saharan countries (Wiedmaier-Pfister et al. 2008).

Table 3: Description of Micro Finance Institutions' credit procedure

Name of MFI	Loan size (Birr)	Grace period (year)	Interest rate (%)	Region
Dedebit Credit and Saving Institution (DECSI)	5000	2	15	Tigray
Amhara Credit and Saving Institution (ACSI)	5000	3	18	Amhara
Omo Micro Finance Institution S.C.	5000	1	18	SNNPR
Oromia Credit & Saving Institution S.C.	5000	1	14.5	Oromia
Bussa Gonofa Micro Finance S.C.	5000	2	24	Oromia

Source: Wiedmaier-Pfister et al. 2008

In this analysis, we considered the highest lending interest rate as discount (r). Moreover, since our demonstration sites are in Oromia and SNNPR where Oromia credit and saving institution and Omo micro finance institution are operating (Table 3), we adopt 18% and 15% discount rates for SNNPR and Oromia regions, respectively to check the sensitivity of investment in solar pump for smallholder irrigation. On top of the discount rate (r), because variability in production costs including wage rates and prices may affect the viability of investment in solar pump for smallholder irrigation, we estimate NPVs and IRRs based on different site and crop-based scenarios. This gave us an indication on how investment in solar pump for smallholder irrigation might be sensitive to variability in site and crop type.

2.2 Dual benefits of solar pump: Reduced drudgery and increased production

Based on data generated from the experiment and description of the technology (Table 1), the pumping capacity of piloted solar pump is between 1800 and 2500 liter/hour (depending on the depth of water). It can irrigate about 2000 m^2 of land using furrowirrigation method, but the size of land can be increased to about 2797 $m^2$and 4431 $m^2$with overhead and drip irrigation systems, respectively (see Table 2).With the exception of the Africa RISING (AR) sites where supplementary irrigation with relatively longer rainy season was practiced, the amount of labor use per hectare was significantly lower when the technology is supplemented with drip system than with furrow and overhead systems (Figure 3). This indicates the labor/drudgery reducing effect of drip system and its suitability for labor constrained, usually female headed households.

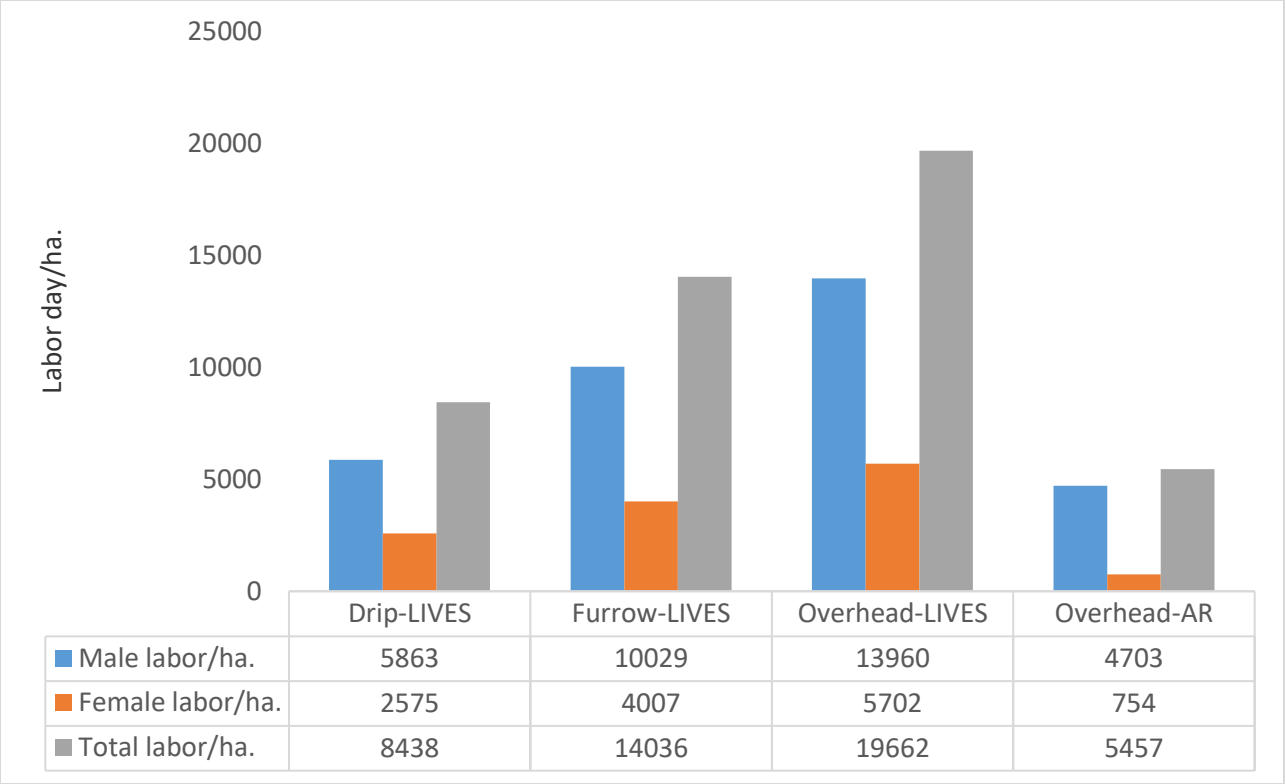

	Drip-LIVES	Furrow-LIVES	Overhead-LIVES	Overhead-AR
Male labor/ha.	5863	10029	13960	4703
Female labor/ha.	2575	4007	5702	754
Total labor/ha.	8438	14036	19662	5457

Figure 3: Amount of male and female labor use/hectare.

Figure 4 presents the cost and production per hectare. Unlike to the amount of labor use, the cost of labor per hectare is higher in the AR sites, probably due to higher wage rate in the area. On the other hand, as compared to furrow and overhead systems, the value of production per hectare is significantly higher when drip water application system is used suggesting that investment in solar pump is more productive and cost effective when supplemented with drip system possibly due to the water and labor-saving effects of drip system.

2.3 The Crop-Water Application Systems and Discount Rate effect

The feasibility of investment depends on a multidimensional factor, including the combination of discount rate, crop type and water application methods. Table 4 present and compare a multi scenariofeasibility (NPV) analysis. Three discount rates (15%, 18% and 24%) with a different combination of crop and water application methods were used to compare and check the sensitivity of the viability of investment in solar pump. Subsequently, the estimated NPVs revealed that the feasibility of investment in solar pump more feasible when additional investment is made in drip system.

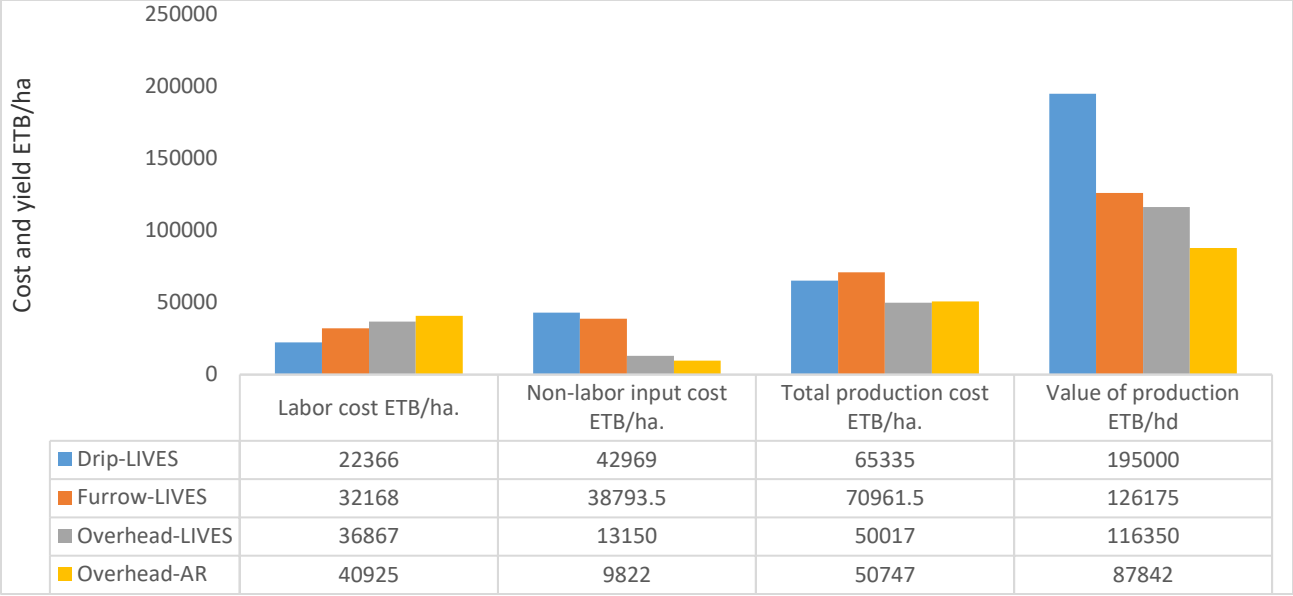

	Labor cost ETB/ha.	Non-labor input cost ETB/ha.	Total production cost ETB/ha.	Value of production ETB/hd
Drip-LIVES	22366	42969	65335	195000
Furrow-LIVES	32168	38793.5	70961.5	126175
Overhead-LIVES	36867	13150	50017	116350
Overhead-AR	40925	9822	50747	87842

Figure 4: Cost and production per hectare

2.4 The Crop-Water Application Systems and Discount Rate effect

The feasibility of investment depends on a multidimensional factor, including the combination of discount rate, crop type and water application methods. Table 4 present and compare a multi scenariofeasibility (NPV) analysis. Three discount rates (15%, 18% and 24%) with a different combination of crop and water application methods were used to compare and check the sensitivity of the viability of investment in solar pump. Subsequently, the estimated NPVs revealed that the feasibility of investment in solar pump more feasible when additional investment is made in drip system.

Table 4: NPV by crop type and water application method

Crop type by water application method	Discount rate (15%)	Discount rate (18%)	Discount rate (24%)
Drip-pepper	221294	191100	145670
Furrow-pepper	30323	25532	18375
Overhead -Pepper	27061	22464	15619
Overhead-Cabbage	16889	13587	8698
Overhead-Carrot	25817	21378	14772
Overhead-fodder	4626	2885	354

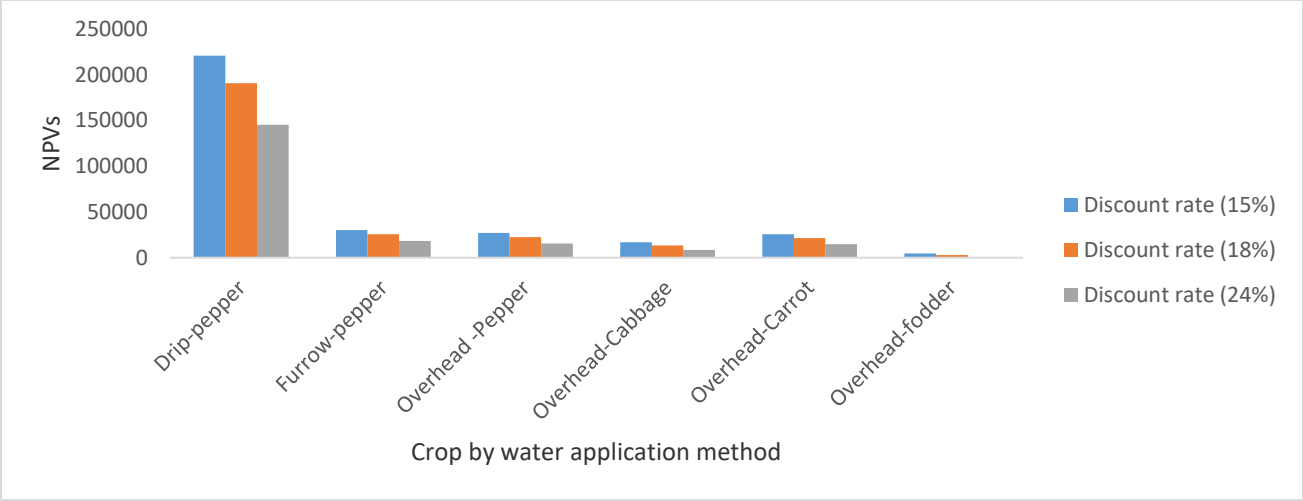

Figure 5: Comparative feasibility analysis by crop type and water application method

On top of the discount rate and water application method, availability of land is an important factor. As presented in Table 2, the potential (maximum) irrigable land size varyby the type of water application and location, because the when drip system is used, the amount of water required to irrigated a certain size of plot is less than the amount of water required when furrow and overhead systems are used. Equally, difference in location/site captures the bio-physical factors that affects the ground water table and a recharging capacity of the solar pump which in turn affect the size of irrigable land.

On the other hand, the minimum land size required for a feasible outcome of investment on solar pump vary by the level of discount rate (Table 5 and Figure 6). When the discount rate increases, the minimum size of land required for feasible outcome of an investment also increases. As expected, for furrow system to yield a feasible result, it requires larger land size than drip and overhead systems.

Table 5: Minimum required land size by discount rate

Crop type and water application system	Minimum required plot size (m2)		
	15%	18%	24%
Pepper-Drip	710	790	950
Pepper-Furrow	1510	1690	2070
Pepper-Overhead	830	930	1125
Cabbage-Overhead	175	195	240
Carrot-Overhead	365	410	500
Fodder-Overhead	265	295	360

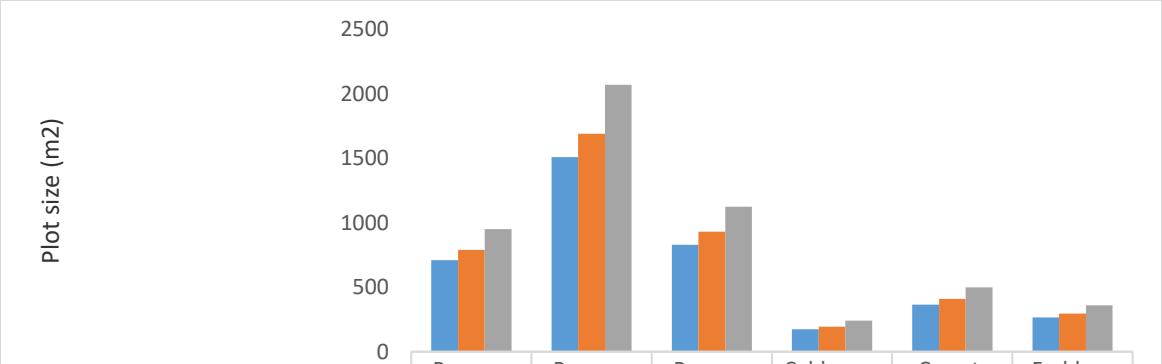

	Pepper-Drip	Pepper-Furrow	Pepper-Overhead	Cabbage-Overhead	Carrot-Overhead	Fodder-Overhead
Minimum required plot size (15%)	710	1510	830	175	365	265
Minimum required plot size (18%)	790	1690	930	195	410	295
Minimum required plot size (24%)	950	2070	1125	240	500	360

Figure 6: Minimum required plot size at different discount rates

3. Conclusion

The overall result shows that investment in solar pump is profitable, given that the minimum land size is available. As solar energy is a clean (zero-carbon) energy, the technology is very much consistent with the Ethiopian Government Climate Resilient Green Economy (CRGE) strategy (FDRE, 2012). The profitability of the technology depends on crop type and water delivery system where drip system was found superior than furrow and overhead system. Our data also shows that land size matters implying that a minimum land size is required for a viable investment in solar pump irrigation, but the minimum required land size itself depends on different factors, including type of water application system, crop type, discount rate and location. Because access to affordable financing is crucial for smallholder farmers, the microfinance institutions can server as a reliable source of finance than the formal banking system.

Although high initial investment cost is a potential barrier for smallholder farmers to adopt the technology, cost sharing can be a solution, especially if additional investment is made on drip system where land size can increase to about half a hectare. Moreover, partnerships between key actors including rural financial institutions are essential for a positive outcome of investment in solar pump. While, one can argue that commercialization is essential for sustainable market growth, yet targeted subsidies are needed at early stage till competitive prices are reached.

In general, solar pumping system has many advantages including, its negligible operating cost. Because there is no fuel required for the pump like electricity or diesel, the operating cost is minimal. A well-

designed solar pump requires little maintenance beyond cleaning of the panels once a week (Maurya et al. 2015). Solar energy is clean and harmonious with nature. Flexibility is another advantage of solar pump, because the panels need not be right beside the water source. They can be used anywhere up to 20 meters away from the water source.

Besides, the technology has some limitations including: i) the technology that we have piloted is not suitable for large scale commercial irrigated farms unless the capacity is augmented by adding more panels which in turn increased the investment cost to make it more expensive, ii) The water yield of the solar pump changes according to the sunlight. It is highest around noon and least in the early morning and evening. However, for countries like Ethiopia where it locates in the equator and has longer (about 10) hours of sunlight per day, this problem is less likely to be a limiting factor.

In conclusion, the piloted type of solar pumping system has been analyzed with its scope and limitations. Finally, we recommend that attention should be given to the system of irrigation water distribution and application to the crops. For example, our pilot experiment shows that when solar pump is supplemented with a drip system, the size of irrigable land is almost doubled as compared to furrow and overhead irrigation and minimizes water loss. Equally important is its effect of reduced labor use per hectare.

Reference

Federal Democratic Republic of Ethiopia (FDRE), 2012. Ethiopia's Green Economy Strategy

FAO (2016), Ethiopia: Geology, Climate and Population.at:http://www.fao.org/nr/water/aquastat/countries_regions/eth/index.stm, accessec on December 13, 2016.

Gebregziabher, G., Hagos, F., Haileslassie, A., Getnet, K., Hoekstra, D., Gebremedhin, B., Bogale, A. and Getahun, G. 2016. Does investment in solar pump-based smallholder irrigation lead to financially viable input intensification and production? An economic assessment. LIVES Working Paper 13. Nairobi, Kenya: International Livestock Research Institute (ILRI).

Hydrochina corporation (2012). Master Plan Report of Wind and Solar Energy in the Federal Democratic Republic of Ethiopia (Final Version)

Shakti (2014). Feasibility analysis for solar agricultural water pumps in India. At: http://shaktifoundation.in/wp-content/uploads/2014/02/feasibility-analysis-for-solar-High-Res-1.pdf accessed on November 9, 2016

Teferra (1986). Energy and economic growth in Ethiopia: The Ethiopian Economy: Structure, Problems and Policy Issues. at: http://www.eeaecon.org/sites/default/files/publications/Mengistu%20Teferra_Energy%20and%20Economic%20Growth%20in%20Ethiopia.pdf accessed on December 13, 2016

DBE's Priority Areas Interest Rate on Hold: http://addisfortune.net/articles/dbes-priority-areas-interest-rate-on-hold/

Ethiopian Business Development Services Network (EBDSN), 2004. Loan Conditions of Commercial Banks and Micro Finance Institutions. Addis Ababa, Ethiopia

Wiedmaier-Pfister, M.; Gesesse, D.; Amha, W.; Mommartz, R.; Eric Duflos, E.; and Steel, W., 2008. Access to finance in Ethiopia: Sector assessment study: Volume 2

Maurya, V.N.; Ogubazghi, G.; Misra, B. P.; Maurya, A. K.; Arora, D. K., 2015. Scope and Review of Photovoltaic Solar Water Pumping System as a Sustainable Solution Enhancing Water Use Efficiency in Irrigation. American Journal of Biological and Environmental Statistics

Theme Three: Irrigation and Drainage

Promoting biological and mechanical techniquesfor enhancing rainwater infiltration and crop productivity in the Ethiopian highlands

Habtamu Muche*[1], Misba Abdela[1], Petra Schmitter[2], Prossie Nakawuka[2], SeifuAdmasu Tilahun[1], Tammo Steenhuis[1, 3], Jennie Barron[2], Abera Adie[4], Michael Blummel[4]

[1]Faculty of Civil and Water Resource Engineering, Bahir Dar Institute of Technology, Bahir Dar University, Ethiopia (habtamu.100@gmail.com); [2]International Water Management Institute (IWMI), Addis Abeba, Ethiopia; [3]Biological and Environmental Engineering, Cornell University, Ithaca, USA; [4]International Livestock Research Institute (ILRI)

Abstract

Many years of cultivation using the conventional *Maresha* plow, pulled by oxen, has resulted in the formation of hardpan to a depth below 20cm. The hardpanrestrictsinfiltration and aeration as well as plantroot development. Several studies have shown that breaking of hardpan can be achieved either mechanically (e.g. *Berken* plow, *mattock*) or using strong rooted covered crops (e.g. *Pigeonpea and Radish*). However, limited studies are available in Ethiopia that assesses the opportunities and challenges between the mechanical and biological treatments within rainfed agricultural system. Five plots with subplots of five different tillage treatments were setup in Robit watershed were monitored from 2015 to 2017. The treatments were (i) no-till (NT), no plowing; (ii) conventional (CT), plots tilled three times using oxen driven *Maresha*, (iii) deep (DT), manual digging up to 60 cm using a *mattock*; (iv) *Berken* tillage (BT), plots tilled three times using an oxen driven *Berken* plough and (vi) Biological (Bi-T), tap rooted *pigeon pea* grown on plots tilled similar to CT. Soil physical parameters (e.g. penetration resistance, bulk density) where measured before tillage treatment and after the cropping season. Additionally, crop performance (plant height, yield, residual biomass and root depth) and measurements on infiltration, soil moisture, sediment yield and runoff were collected for two consecutive years. Results showed that mean tillage depth was significantly higher in DT (60 cm) followed by BT (27.58 cm) and CT & Bi-T (18.13 cm).Infiltration capacity increased from 115.2 mm hr^{-1} (NT), and 120 mm hr^{-1} (CT) to 187.2 mm hr^{-1}(Bi-T), 242.4 mm hr^{-1} (BT), and 261.6 mm hr^{-1} (DT) ($p<0.01$). The sub-plot treated by improved tillage system (mechanical and biological) had significantly higher moisture than other tested treatments; conventional and no-till treatments.Likewise,root penetration resistance,runoff depth and sediment concentrations were significantly ($p<0.05$) reduced by the mechanical breakage of the hardpan (BT&DT) compared to other tillage treatment.The grain yield responses nearly were the same on BTand Bi-T treatments, and increased by 5 % and 18 %as compared to the remained sub-plots in 2016 and 2017, respectively.Improved tillage practices such as biological anddeep tillage or *Berken* plow could increase rainwater penetration and therefore root penetration and agricultural productivity whilst decreasing erosion and runoff in the Ethiopian highlands. The adoption of these techniques in the Ethiopian highlands could improve the sustainability of rainfed agriculture and water availability in shallow groundwater.

***Key words**:* Tillage systems, Hardpan, Infiltration and Grain yield

1. Introduction

The Upper Blue Nile catchments are considered to be the water towers to many of the tributary rivers. In this area repeated tillage is made by the local *Mareshaf*or loosen surface soil before planting. Repeated tillage is carried out through cross ploughing, and during cross ploughing, farmers are forced to run over the already tilled soil in an attempt to access the unplowed part. Consequently, they spend almost 50% of the time passing across already plowed land in search of missed strips, which is even more during the third tillage that is aimed at reaching spots of unplowed land left after the second ploughing. Such a repeated action also imparts a high amount of energy on some ofthe soil particles leading to localized excessive pulverization resulting in poor soil structure (Rockström and Valentin, 1997; Temesgen, 2012).Continuous use of this implement for years has led to the development of restrictive soil layers commonly known as hardpans in the soil profile of < 20cm (Tibebeu et al., 2015). The presence of a hardpan which hinders the movement of water, root penetration and inhibits growth and yield of crops has been reviewed by many researchers' (Chen et al., 2005; Estienne et al., 2009; Temesgen et al., 2012; Tibebeu et al., 2015). It is believed that the presence of a pan will lead to temporary perching of soil water during periods of rainfall, thereby reducing soil permeability. This will eventually give rise to increased runoff and consequently leading to more soil erosion compared with a free draining soil. It is generally agreed that the presence of a hardpan will lead to accelerated soil erosion and sediment associated nutrients exported from plant root zones. The present study area, Robit-Bata watershed is an area whose soils' textures range from sandy clay loam to heavy clay, and due to repeated ploughing at the same depth using the local *Maresha* season after season, hardpans have developed over the years (Abidela et al., 2015). Presence of the hardpans where confirmed using cone penetrometer instrument, a study conducted by Abidela et al. (2015).

Therefore, the need to break the prevailing hardpan is unquestionable so as to increase permeability of water in the sub-soils and crop productivity as well. Therefore, this study initiated totest biological and mechanical techniques to break hardpan, improve infiltration and crop productivity.

2. Methods and materials

2.1 Description of study area

An experimental watershed, called Robit-Bata watershed (Fig. 1) is located at the south-eastern edge of Lake Tana, Amhara Region, BahirdarZuriaWoreda, Robit-Bata Kebele administration. The watershed is located around 10km North of Bahirdar city, along the Bahirdar to Gondar main road. The watershed area has about 40.56ha. More than 60% of the land is covered by cultivated farm land.

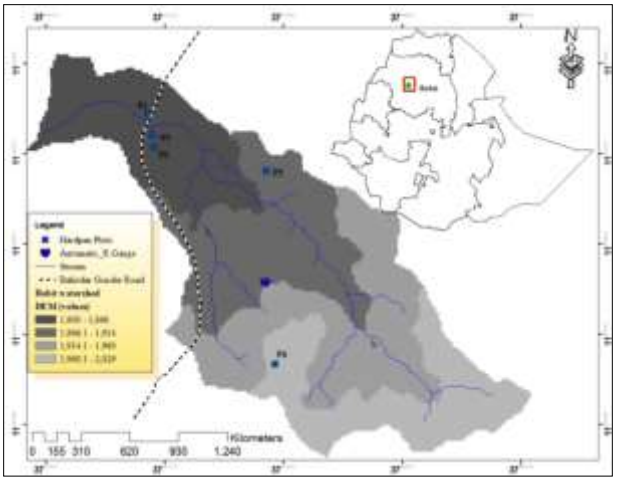

Figure 7. Map of Robit watershed and study experimental plots

2.2 Site selection

Penetration resistance and bulk density values are highly indicative of the status of soil quality and greatly affects the infiltration capacity of the soil, nutrient availability and other physical and chemical processes that take place in the soil system. Higher penetration resistance (>2Mpa) and bulk density (>1.6g/cm^3) values indicate higher degree of soil compaction (Temesgen et al., 2012; Tibebu et al., 2016) which further affects the infiltration capacity of the soil, and plant root penetrations. Before application of tillage treatments, a pre-field study was performed to assess the presence of the hard pan and the results were present in the table below.

Table 1. Physical characteristics of experimental plots at pre-study

Plot code	Topographic location	Soil depth (m)	BD (g/cm^3)	SPR (Mpa)	Hardpan existence depth (cm)	IC (mm/hr)	Slope (%)	Elevation (m.a.s.l)
P1	Down stream	0.6	1.62	3.01	< 20	194.4	6	1850
P2	Down stream	>3.5	1.62	2.39	< 20	175.2	9.4	1863
P3	Down stream	>3.5	1.56	2.99	< 20	220.8	10	1873
P4	Upstream	0.8	1.45	2.23	< 20	141.6	8	1976
P5	Upstream	>3.5	1.59	2.96	< 20	194.4	8.3	1930

BD; bulk density, SPR; soil penetration resistance, IC; infiltration capacity

2.3 Experimental plots setup

The study was carried out under monsoon season todetermine the effect of different tillage techniques on some hydrological variables and crop productivity. The experiment was arandomized complete block design with 30 m by 16 m plots andfive replicates in the Robit-Bata watershed.Each plot was divided into five sub-plots with dimension of 4*30m. The following treatments listed in Table 2 were applied at selected subplots in each plot before planting:

Table 3. Description of tillage treatments performed at experimental plots

Treatments	Descriptions
No tillage (NT)	▪ No ploughing for two consecutive years opening the soil particularly for placing seed without use of farming implement
Conventional tillage (CT)	▪ Plots cross ploughed using ox driven *Maresha* three times ▪ Tillage was done twice before sowing (before the onset of rain, and after firstrain shower) ▪ One superficial tillage operation afterthe seeds row planted to cover it with soil easily
Deep tillage (DT)	▪ Manually digging up to a depth of 60 cm using a *mattock* for two consecutive years.
Berken tillage (BT)	▪ Plots contour ploughed (i.e. Perpendicular to slope of plots) ▪ Three times using an ox driven *Berken*Maresha. ▪ Tillage was done twice before sowing ▪ Similar to CT, one superficial tillage operation after the seeds row planted to cover it with soil easily
Biological tillage (Bi-T)	▪ The ploughing system was similar to CT with the same implement ▪ All other things also been the same with CT subplot, the only difference was hard rooted *pigeonpea* are intercropped with maize crop

2.4 Measurements

Soil penetration resistance: Weekly based soil penetration resistance measurement was performed using a cone penetrometer (Duiker, 2002). All the measurements were taken 24 hour after an intensive rainfall had occurred, when the subplots were assumed at field capacity.

Infiltration: Infiltration measurements were taken before tillage treatments assigned across subplots and also after post-harvest using double ring infiltrometer.

Runoff and suspended sediment: Daily runoff and suspended sediment were carried out at experimental subplots. Two collection troughs (barrels) were installed downstream part of each subplot so as to collect the runoff and sediment leaving the subplot.

Figure 2. Layout of single replication on one farmer's farm plot

Ten outlets (pipes) were attached close to the top of the first barrel. One of these pipes was connected to the second barrel. The second barrel was thus taking 10% of the volume from the first barrel. Therefore, total daily runoff has been weighted and summation of the volumes of the two barrels, B1 and B2 was done, using the equation below:

$$V = \frac{\pi D^2}{4} * (H1 + 10H2)$$

Where; V is the daily runoff volume from the plot; D and H refers to the barrel diameter and depth of barrel engaged by runoff, respectively, in the two barrels.

A liter of runoff water samples was taken after stirring for 30 seconds from runoff barrels and the sampled water was then filtered using filter paper.

Crop yield: Three rows of maize crops were taken located from two rows from the upper and lower sides of subplots, while the third row was located at the center of the plot. Therefore, total weight of maize yield was measured using a stationary balance of 50 kg capacity in the field.

Statistical analysis: The statistical analysis performed using SAS statistical package.The GLMwas used for the analysis of variance and multiple-comparison post hocTukey's honest significance difference (HSD) test was also used for separating group of means in the ANOVA setting when the analysis of variance showed statistically significant differences ($p<0.05$).

3. Result and discussion

3.1Tillage depth

The schematic representation of the field test results are shown in Figure 3 the mean tillage depth was significantly higher in BT (27.58 cm) followed by CT & Bi-T (18.13 cm). Tillage depth variation among the treatments emanated from the difference in the design of the implements.

Figure 3. Schematic representation of biological and Berken tillage system

3.2 Infiltration capacity

There was great difference in infiltration capacity among tillage treatments after two cropping seasons. Tillagetreatment, DT (261 mm hr^{-1}) sub-plot brought better infiltration capacity followed by BT (242 $mmhr^{-1}$). In before and after comparison, significance improvement was observed under DT (45%) and BT (41%) subplot followed by Bi-T (30%), while CT subplot deceased by 15%. The three treatments (BT,DT and Bi-T) were producing above the median infiltration value 180mm hr^{-1}. The lower soil bulk density and penetration resistances values might be the possible reasons for the treatments difference ininfiltration rates.

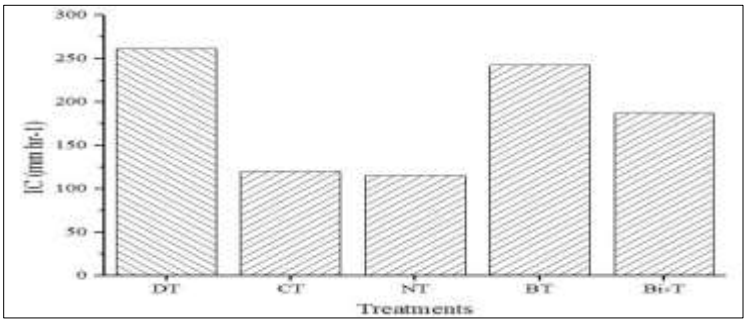

Figure 4. Infiltration capacity values under different tillage treatments (mean ±SE) after the cropping season.

3.3 Penetration resistance

The penetration resistance of the sub-plots after the tillage treatments, showed significant difference ($p<0.01$) as indicated in Fig 5. No-till and conventional tillage treatments responses were beyond recommended penetration resistance value (>2Mpa) at 20-40cm depth. However, treatments positive effect on PR has not been continued below 40cm after the cropping season.

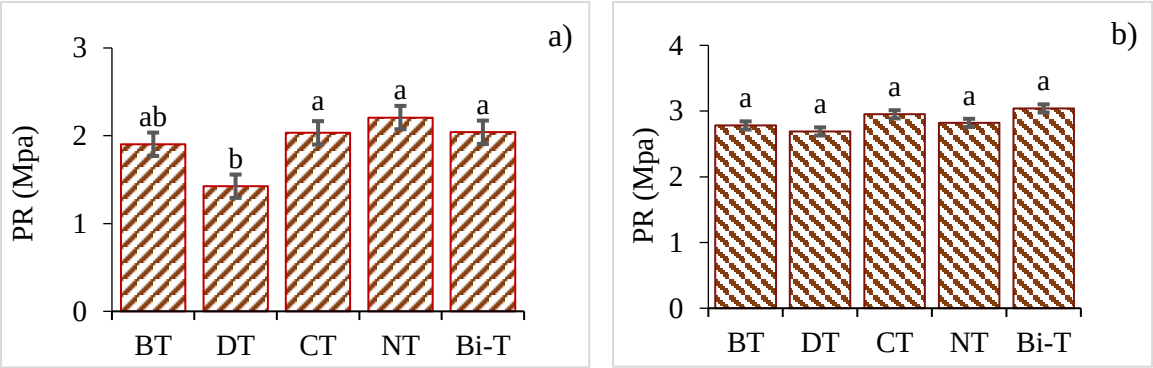

Figure 5. Penetration resistance at 20-40cm (a) and 40-60cm (b)

3.4 Runoff

There was significance difference ($p<0.05$) in runoff depth among the tillage treatments throughout cropping season in both years as shown in Table 3. Mean runoff depth was significantly reduced in deep and *Berken* tillage system as compared to conventional and no tillage systems in both years. The difference in runoff depth produced emanated from tillage treatment were applied. Since the treatment plots were similar in all parameters (nodifference in slope, soil type, fertilizer inputs and crop type) except the tillage system. As reported by Araya et al. (2015 and 2016), annual runoff amounted was significantly higher in conventional tillage (CT) systems (98mm).

Table 3. Effect of tillage systems on runoff depth and runoff percentage

	2016		**2017**	
Treatment	Runoff depth ($mmha^{-1}$)	Runoff percent	Runoff depth ($mmha^{-1}$)	Runoff percent
DT	29.5 ± 11^{b}	3.6 ± 1.6^{b}	102.5 ± 15^{b}	6.4 ± 2.1^{b}
CT	71.5 ± 32^{a}	7.7 ± 3.4^{a}	190.6 ± 21^{a}	11.9 ± 3.0^{a}
NT	98.8 ± 62^{a}	10.7 ± 7.0^{a}	206.5 ± 24^{a}	12.9 ± 3.4^{a}
BT	33.5 ± 14^{b}	3.2 ± 1.2^{b}	97.1 ± 17^{b}	6.1 ± 2.5^{b}
Bi-T	47.1 ± 18.7^{ab}	5.4 ± 2.1^{ab}	152.2 ± 18^{ab}	9.5 ± 2.7^{ab}
CV (%)	42.7	44.9	29	41
LSD	34.3	3.7	58.3	3.6

Mean ± SDfollowed by the different letter in the column are significant (p=0.05); at each tillage treatment with respect to runoff and runoff percent.

3.5 Soil loss

There was significant variation in mean soil loss value among the tillage treatments as shown in Table 4. Soil loss was reduced over 50% and 20% due to the application mechanical (DT & BT) and biological systems, respectively as compared to conventionally treated sub-plots. Contour and deep plowing in BT& DT subplots which retards the momentum of runoff and transported soil materials could be the possible reason. Likewise, strong rooted *Pigeon pea* in Bi-T sub-plot had a potential to pushes the hardpan and promotes infiltration that induced lower runoff and soil loss. A study conducted by Melero et al. (2009), long-term conventional tillage practices may result in significant losses of soil organic matter, thus inducing an increase in soil loss.

Table 4. Effect of tillage systems on soil loss and sediment concentration in 2016 and 2017

Treatment	2016		2017	
	Soil loss (t ha^{-1})	Sediment conc. (g lit^{-1})	Soil loss (t ha^{-1})	Sediment conc. (g lit^{-1})
DT	2.55 ± 1.3^{b}	7.69±1.1	21.2 ± 7.0^{b}	8.90±4.5
CT	5.49 ± 2.3^{a}	8.35±1.8	42.1 ± 12^{a}	12.4±3.4
NT	6.66 ± 2.5^{a}	6.78±1.5	32.2 ± 8.6^{a}	9.14±1.3
BT	2.56 ± 1.3^{b}	7.68±0.9	17.4 ± 5.4^{b}	7.8±2.4
Bi-T	3.89 ± 1.6^{ab}	8.15±1.2	35.4 ± 9.7^{a}	12.6±3.0
CV (%)	44	17.2	30	34.2
LSD	2.48	1.75	11.7	4.1

Mean ± SDfollowed by the different letter in the column are significant (p=0.05); at each tillage treatment with respect to soil loss and sediment concentration.

3.6 Maize yield

There has been a significant difference statistically ($p<0.05$) in terms of grain yield with respect to tillage systems. Grain yield responses nearly were the same on BT and Bi-T treatments, and increased by 5 % and 18 % as compared to CT in both years. The grain yield under NT was reduced by 16% comparing to Abidela*et al.* (2015) experiment. The lower penetration resistance and the higher water infiltration might have a favor to have more available moisture in the soil profile that increased plant transpiration rate and could be the reason for yield difference found in tillage treatments. Similarly, ten-year experiment showed that long term effect of no-till on maize grain yield had a decline tend, 5 t ha^{-1} had been during 1999 and at the end of 2008 has fallen to 1.8 t ha^{-1} (Videnovic*et al.*, 2011).

Table 5. Effect of tillage systems on grain yield (mean) of maize crop

Treatment	Yield (ton/ha)	
	2016	2017
DT	5.6±0.93	6.8±1.53[ab]
CT	5.7±1.46	7.15±2.54[ab]
NT	2.7±0.53	4.2±1.85[b]
BT	6±1.44	8.76±2.85[a]
Bi-T	4.8±2.05	7.14±2.62[ab]
CV	36%	38%
LCD	1.82	3.52

Mean ± SDfollowed by the different letter in the column are significant (p=0.05); at each tillage treatment with respect to grain yield.

4 Conclusions

Biological and mechanical techniques were tested for two consecutive years on experimental plots. Both mechanical and biological treatments positively increased infiltration, soil moisture and reduced penetration resistance, runoff & sediment yield. The agronomic performances (root length & grain yield) have also improved. Therefore, properly implementation of both techniques will have a far reaching impact on crop and water productivity.

Acknowledgment

This research was sponsored by the Innovation Laboratory for Small Scale Irrigation project (#AID-OAA-A-13-000SS) which is funded by Feed the Future through the U.S. Agency for International Development (USAID). The research was implemented under a collaborative partnership between the International Water Management Institute and Bahir Dar University. The contents of the paper are the responsibility of the authors and do not necessarily reflect the views of USAID or the United States government.

References

1. Araya, T., Nyssen J., Govaerts B., Deckers J., Sommer R., Bauer H., Gebrehiwot, K., Cornelis W. M. 2016. Seven years resource-conserving agriculture effect on soil quality and crop productivity in the Ethiopian drylands. Soil and Tillage Research 163, 99–109. DOI:10.1016/j.still.2016.05.011.
2. Araya, T., Nyssen, J., Govaerts, B., Deckers, J., Cornelis, W.M. 2015. Impacts of conservation agriculture-based farming systems on optimizing seasonal rainfall partitioning and productivity on Vertisols in northern Ethiopia. Soil Tillage Res. 148, 1–13.
3. Tebebu T.Y., Steenhuis, T.S., Dagnew, D.C., Guzman, C.D., Bayabil, H.K., Zegeye, A.D.,Collick, A.S., Langan, S., McAllister, C., Langendoen, E.J., Yitaferu, B., Tilahun, S.A. 2015. Improving Efficacy of Landscape Interventions in the (Sub) Humid Ethiopian Highlands by Improved Understanding of Runoff Processes. Front. Earth Sci. 3 (49).
4. Temesgen M, Uhlenbrook S, Belay S, van der Zaag P, Mohamed Y, Wenninger J, Savenije H. H., 2012. Impacts of conservation tillage on the hydrological and agronomic performance of Fanyajuus in the upper Blue Nile (Abbay) river basin. Hydrol. Earth Sys. Sci., 16: 4725–4735.

5. Abidela M., Habtamu M., Seifu T., Prossie N., and Petra S. 2015.Improving Subsurface Recharge through Breaking Restrictive Soil Layers by Mechanical Means, presented at ICAST conference, Bahir Dar University, Ethiopia.
6. Tebebu T. Y., Bayabil, H. K., Stoof, C. R., Giri, S. K., Gessess, A. A., Tilahun, S. A., and Steenhuis, T. S. 2016. Characterization of degraded soils in the humid Ethiopian highlands. Land Degradation and Development. DOI: 10.1002/ldr.2687.
7. Videnović, Ž., Simić M., Srdić, J., Dumanović Z. 2011. Long term effects of different soil tillage systems on maize. PLANT SOIL ENVIRON., 57, 186–192.
8. Rockstrom J., Valentin, C. 1997. Hill slope dynamics of on-farm water flows: The case of rain-fed cultivation of pearl millet on sandy soil in the Sahel, Agric. Water Manage.33:183–210.
9. Chen Y., Cavers, C., Tessier, S., Monero, F., Lobb, D. 2005. Short-term tillage effects on soil cone index and plant development in a poorly drained, heavy clay soil. Soil & Tillage Research 82, 161–171.

Integrated Effect of Mulching and Furrow Methods on OnionYield and Water Productivity in Central Highlands of Ethiopia.

Ashebir Haile*[1], Solomon Gezi[1]and Gebeyehu Tegenu[1]

[1]Ethiopian Institute of Agricultural Research, Debre Zeit Agricultural Research Center, P.O.Box 32, Debre Zeit, Ethiopia, ashu_haile@yahoo.com or haileashebir@gmail.com

Abstract

Proper utilization of water resources is crucial for the purpose of sustainable use and improved water productivity in irrigated agriculture sector of Ethiopia.The objective of this study is to select most effective water saving techniques and improve water productivity of irrigated Onion.The experiment was conducted at Debre Zeit Agricultural Research Center at main station, which about 45 km Southeastern of Addis Ababa. Its geographical extent ranges from08°45'15" to 08° 46'45" N Northern latitude and from 38°59' 45" to 39°01'00" Easternlongitude. The research center is located on a nearly level of a very gently sloping topography with a gradient of zero to 2 % slope. It has low relief difference with altitude ranging from 1610 to 1908 meters above the see level. However in some of the sub sites the altitude ranges from 1520 to 2456 meters above sea level at Koka and Chefie Donsa. The experimental design was in RCBD in split plot with three types of furrow irrigation methods (alternate, fixed and conventional furrow irrigation methods) and mulch typesin three replicationswere used as two factors to evaluate the yield and yield component including water use efficiency of Onion.From the study, it has been observed that different types of irrigation method significantly affected ($p<0.01$) main yield and yield components of Onion. Moreover, Onion growth, yield and yield components weren't significantly influenced ($p<0.01$) due to different mulch types used and also there was no interaction effect between irrigation and mulching type. Significantly highest marketable bulb yield (39.5 t/ha) of Onion was recorded due to conventional furrow irrigation method and followed by alternate furrow irrigation method (34.3 t/ha). However, highest water use efficiency (9.7 kg/m^3) was obtained due to alternate furrow irrigation method when compared with the least water use efficiency of conventional furrow method of 5.7 kg/m^3. Hence, there was 18 to 22% increment of marketable yield and water use efficiency of onion by applying mulching over the conventional non-mulching condition and also 42% improvement of water use efficiency by using alternative furrow irrigation over the conventional furrow type.Therefore, for maximizing marketable bulb yield of onion under no water stress scenario, irrigation of onion with conventional furrow irrigation methods could be used. Whereas under limiting irrigation water resource condition, irrigation of onion could be done by alternate furrow irrigation method with plastic mulch application to minimize evaporation loss and maximize water productivity of onion for similar agro-ecology and soil type.

Keywords: Water use efficiency, furrow method, mulch type and water productivity.

1. Introduction

Water is one of the largest renewable natural resources but fresh water is expected to emerge as a key constraint to future agricultural growth. Globally and more particularly for many developing countries including India, Ethiopia, changing water availability and quality pose complex problems and management options are not easy. The changing situation comes partly from increasing demands such as population, industry and domestic requirements partly from consequences of climatic change. Major concerns on future planetary freshwater resources are the effects of climate change on changing sea temperature and levels, drought and flood events, as well as changes in water quality, and general ecosystem vulnerabilities **[21].** Changes in the extreme climatic events are more likely to occur at the regional level than show in national or global statistics. The unpredictability of climatic events is of key concern to farmers in all countries, particularly in Africa.

Ethiopia has a long history of traditional irrigation systems and yet. Simple river diversion still is the dominant irrigation system in Ethiopia. Awulachew et al. [1] estimates of the irrigation potential of Ethiopia has estimated that 5.3 million hectares. Of the potential 3.7 million ha is from surface water (small, medium and large scale), while the remaining 1.6 million ha is from rain water harvesting technologies and ground water. In terms of utilization, only about 12% (about 857,933 ha) has been irrigated by 2015[7]. So, it is prudent to make efficient use of water and bring more area under irrigation through available water resources. This can be achieved by introducing advanced methods of irrigation and improved water management practices.

Regulated furrow (deficit) irrigation is one way of maximizing water use efficiency for higher yields per unit of irrigation water used in agriculture **[15], [8].** In deficit irrigation application, the crop is exposed to a certain level of water stress either during a particular growth period or throughout the whole growing season, without significant reductions in yields **[5].** The expectation is that the yield reduction by inducing controlled water stress will be insignificant compared with the benefits gained through diverting the saved water to irrigate additional cropped area **[9].** In Ethiopia conditions, results on deficit irrigation level, irrigation level have positively influenced marketable yield of Onion bulb, with bulb yield decreasing as the water deficit level increased as South-northern Ethiopia by **Bekele and Ketema [2] and Mulu and Alamirew[14].** However, previous findings showed that the amount of water applied and method of application varied across the reports by crop and study site.

Mulch in tropics improves nutrient and water retention in the soil, encourages favorable soil microbial activity and worms, and suppresses weed growth. When properly executed, mulching can significantly improve the well-being of plants and reduce maintenance as compared to bare soil culture **[18].** The use of mulch reduces the natural water losses through evaporation on soil surface, thus leading to net return of crops though maximizing yield & water productivity with limited available water **[20] , [12].** Hence, reducing non-productive loss of irrigation water is best achieved through the integrated use of regulateddeficit irrigation along with mulching material for maximum water use efficiency (WUE) in arid and semi-arid lands**[10].**So, to improve crop production to feed the ever increasing population under limiting water resource condition, strategies that conserve moisture in the soil and efficient irrigation techniques should be identified and practiced [**24].**Therefore, this study aimed to select most effective water saving techniques for Onion and evaluate the effect of different furrow irrigation and mulching type on the marketable yield of Onion bulbs.

2. Materials and Methods

2.1.Description of study area

The study was conducted at Debre Zeit Agricultural Research Center, located in the central highlands of Ethiopia. Its geographical extent ranges 08°45’51” (8.760) Northern latitude and 39°00’29” (39.010) Eastern longitude. It has low relief difference with altitude ranging from 1610 to 1908 meters above the see level. The soil at the experimental site was heavy clay in textures with field capacity and permanent wilting point of 35% and 19%, respectively. The area receives an annual mean rainfall of around 810.3 mm with the medium annual variability and bimodal pattern. Seasonal variations and atmospheric pressure systems contribute to the creation of three distinct seasons in Ethiopia: Kiremt (June to September), Bega (October to February) and Belg (March to May). The Kiremt is the main rainy and Belg is the short lasting one while the dry season is attributed to Bega (Selshi and Zanke, 2004). Belg in the study area receives quite small rainfall to support crop production whereasKiremtis known by long rainy season. About 76 % of the total rainfall of the area falls in Kiremt or wet season, about 15% in Belg and the rest is Bega or dry season which needs full irrigation in the area.. The mean maximum temperature varies from 23.7 to 27.70C while mean minimum temperature varies from 7.4 to 12.10C (Table-1). However; maximum and minimum reference Evapo-transpiration (ETo) was recorded as 4.9 and 3.3 mm/day in May and July respectively (Table-2).

Table-4:*The climatedata of 42 years (1975 – 2017) for the study area.*

Month	**Tmax (^{O}C)**	**Tmin (^{O}C)**	**Relative humidity (%)**	**Wind speed (m/s)**	**Sunshine hour (hrs)**	**Solar radiation (MJ/M^2/day)**
January	25.2	8.9	63.0	1.3	9.8	22.0
February	26.3	10.2	46.4	1.4	8.5	21.4
March	27.0	11.3	46.4	1.5	8.1	21.8
April	27.1	11.9	47.7	1.5	7.1	20.4
May	27.7	11.6	46.5	1.6	8.6	22.2
June	26.4	11.4	54.9	1.0	6.3	18.4
July	23.7	12.1	66.4	0.9	4.9	16.4
August	23.9	12.1	67.8	0.9	5.5	17.7
September	24.1	11.5	63.3	0.8	6.7	19.6
October	25.0	9.5	49.9	1.4	8.6	21.7
November	24.6	8.0	47.0	1.3	9.3	21.4
December	24.8	7.4	46.9	1.4	9.4	20.9
Average	**25.5**	**10.5**	**53.9**	**1.2**	**7.7**	**20.3**

Table-5:*Mean Monthly rain fall, effective rainfall and ETo values of study area.*

Month	**Rainfall (mm)**	**Effective Rainfall (mm)**	**ETo (mm/day)**	***Season***
January	9.4	0.0	4.0	Bega
February	24.8	4.9	4.4	
March	31.5	8.9	4.7	Belg
April	44.2	16.5	4.6	
May	41.3	14.8	4.9	
June	88.9	47.1	3.9	Kiremt
July	235.1	164.1	3.3	
August	208.2	142.6	3.5	
September	83.6	42.9	3.7	
October	25.9	5.5	4.3	Bega
November	7.4	0.0	4.1	
December	1.0	0.0	4.0	
Average	**810.3**	**447.3**	**4.1**	

2.2 Experimental design and procedure

The experiment was done in a split plot design with three irrigation water application methods (fixed, alternate and conventional furrow method) in main plot and two mulch types (straw and plastic) and control as no mulch. Each main plot factors (furrow irrigation methods) was assigned randomly within each replication and every sub plot factor (mulching) was randomly assigned inside each main plots.

Plot size of was 3.0 m x 3.0 m which consists of 5 ridges with the spacing 40cm and plant with 5cm spacing interval. Wheat straw mulch with a rate of 6 t/ha was used as mulching types in the sub plots.

The amount of irrigation water applied was calculated using CROP WAT 8.0 software by using necessary input data (crop, soil and long-term climatic data). Irrigation water was applied up to field capacity by monitoring soil moisture content using gravimetric method in the conventional furrow plot. The calculated irrigation depth based on the water holding capacity of the soil in the management allowable depletion level was measured using three-inch Parshall flume before diverted to each sub plots.

2.3 Data collection and analysis

The selected verity of Onion (Var. Nafis) was planted in November for the consecutive three years in Debre Zeit Agricultural Research Center of main station. During the implementation period all agronomic & yield parameters and data of irrigation water was collected following the data sheet including date of 50% emergency, days of 95% maturity, stand count at harvesting, fresh biomass yield, marketable yield , bulb diameter and weight was measured after the sample was sun dried for three days. Water use efficiency was calculated using the following formula.

$$\text{Water use efficiency} = \frac{\text{Marketable Bulb yield } \left(\frac{\text{kg}}{\text{ha}}\right)}{\text{Net irrigation water applied} \left(\frac{\text{m}^3}{\text{ha}}\right)} \quad (7)$$

Where; Water use efficiency (kg/m^3), Marketable bulb yield (kg/ha) and Net irrigation water applied (m^3/ha).

The collected data were analyzed using statistical analysis system (SAS) software procedure of general linear model for the variance analysis. Mean comparisons were carried out to estimate the differences between treatments using Fisher's least significant difference (LSD) at 5% probability level.

3. Result and Discussion

3.1.Marketable yield of onion bulb

The combined analysis of marketable yield data showed that different types of furrow irrigation and application of mulch in agricultural water management was significantly ($p<0.01$) influenced.

3.2.Effect of Furrow Type on Onion Yield

Result analysis showed that different types of furrow method had a significant difference ($p<0.01$) on onion yield as indicated in table-3 below. The maximum Onion yield (39.5 t/ha) were observed at conventional furrow irrigation water application method (Table-3). The maximum marketable Onion yield obtained at conventional furrow irrigation was statistically superior to both alternate and fixed furrow irrigation. However, minimum marketable yield (28.9 t/ha) were obtained at fixed furrow irrigation method. Therefore, the highest marketable yield of onion obtained at conventional furrow irrigation method lead to an improvement of 27 % while alternative furrow was 16% than the fixed furrow irrigation method.

Table-6:*Combined analysis of marketable yield Onion bulb (t/ha).*

Furrow type	Mulch type				
	No	**Straw**	**Plastic**	**Mean**	**$LSD_{0.05}$**
CFI	34.65	41.81	42.04	39.50**a**	**5.45**
AFI	29.51	37.47	35.81	34.26**ba**	
FFI	24.38	32.00	30.24	28.87**b**	
Mean	29.51**b**	37.09**a**	36.01**a**		
$LSD_{0.05}$	**1.98**				
CV (%)	**4.51**				

N.B. *Treatments with similar letter in the column & also in rows are not significantly different; CV: coefficient of variation; LSD: least significant difference; CFI: conventional furrow irrigation; AFI: alternate furrow irrigation; FFI: fixed furrow irrigation.*

3.*3. Effect of Mulching on Onion Yield*

Field experiment of combined analysis result also revealed that different types of mulch on onion yield had highly significant ($p<0.01$) influence as indicated in Table-3. Therefore, maximum marketable yield of onion bulb (37.1 t/ha) were observed at straw mulching condition but the maximum bulb yield obtained at straw mulching condition was statistically similar with that of plastic mulch. Moreover, the minimum (29.5 t/ha) marketable yield obtained at no mulching condition was statistically significant different with both straw and plastic mulching. So, the highest marketable yield of onion bulb obtained at straw followed by plastic mulchingshowed an improvement of 20% and 18% respectivelyover the conventional non-mulching condition.

Even though irrigation water depth is reduced due to different irrigation water management methods like alternate and fixed furrow, the applied depth could be conserved due to reduction of evaporation from soil surface by mulching. The conserved moisture content of soil in the root zone could enhance crop transpiration and nutrient uptake and transportation in the plant body. Similarly, Xu *et al.* [22] reported that plastic mulching improves the accumulation of dry matter, leading to a significantly greater final biomassand an improvement of grain yield of maize by 15-26% both in the dry years. Moreover, Yaseen*et al.* [23] revealed that maximum increase in biomass (29.56%) and grain yield (35.5%) were recorded on mulch and higher irrigation depth treatments. Panigrahi*et al.* [16] also revealed that application of black plastic mulching improves yield of okra plant by 21.4 to 36.9% at different allowable soil moisture depletion level and alternate furrow irrigation method.

Water Use Efficiency (WUE): Water use efficiency was significantly ($p<0.01$) influenced due to different types of irrigation water management methods (Table-4).

3.4. Effect of Furrow type on water use efficiency

Results indicated that the water use efficiency of marketable Onion bulb was significantly influenced by application of irrigation water though furrow type. The highest was recorded under alternate furrow irrigation as compared with conventional and fixed furrow method. Maximum water use efficiency (9.86 kg/m^3) observed at alternate furrow which was statistically superior to both conventional and fixed furrow whereas minimum water use efficiency (5.7 kg/m^3) was recorded at conventional furrow irrigation (Table-3). Therefore, the highest water use efficiency of onion obtained at alternative furrow irrigation showed an improvement of 42% and fixed furrow type 31% over the conventional non-mulching condition.

Table-7: Combined analysis of WUE (kg/m^3) of Onion.

	No	**Straw**	**Plastic**	**Mean**	**LSD$_{0.05}$**
CFI	5.01	6.04	6.06	5.70**c**	**5.45**
AFI	8.45	10.91	10.20	9.86**a**	
FFI	7.07	9.15	8.71	8.31**b**	
Mean	6.84**b**	8.70**a**	8.32**a**		
LSD$_{0.05}$	**1.98**				
CV (%)	**4.51**				

N.B. Treatments with similar letter in the column & also in rows are not significantly different; CV: coefficient of variation; LSD: least significant difference; CFI: conventional furrow irrigation; AFI: alternate furrow irrigation; FFI: fixed furrow irrigation.

3.5 Effect of mulch type on water use efficiency

Application different types of mulch in field experiment had significantly ($p<0.01$) influenced marketable yield of Onion bulb and water use efficiency of the crop. The combined analysisrevealed that, water use efficiency was maximized at straw mulch followed by plastic mulching than no mulch condition. The maximum water use efficiency (8.7 & 8.32 kg/m^3) obtained at straw &plastic mulching was statistically no difference with each other but both are superior to no mulch conditions. Hence, the minimum water use efficiency (6.84 kg/m^3) was observed at no mulch condition. Hence, there was 21.4 % and 21.6% increment of water use efficiency of onion by applying straw and plastic mulching respectivelyover the conventional non-mulching condition.

Generally, different mulching types lead to maximize water use efficiency. Xu *et al. [22]* reported that water use efficiency of maize under plastic mulching (3.27 kg/m^3) was increased by 16% compared to the control treatment without mulching, although the overall evapotranspiration was similar between the two treatments. With reduced soil evaporation, the conserved moisture due to plastic mulching might be allotted to transpiration which improve nutrient uptake and transportation to plant body. Based on different studies in different location, Montazar and Kosari [13] reported that water use efficiency of different crops including onion could be enhance though mulching to conserve moisture in the soil for proper utilization by the plant. The conserved moisture content of soil in the root zone due to mulching could enhance crop transpiration and nutrient uptake and transportation in the plant body with limited available water.

4. Conclusion and Recommendations

Based on the findings of this experiment, application of mulch played a greater role in minimizing evapotranspiration, due to that available water to plants root varied appreciably. Generally, there was 18 to 22% increment ofmarketable yield and water use efficiency of onion by applying mulching over the conventional non-mulching condition and also 42% improvement of water use efficiency by using alternative furrow irrigation over the conventional furrow type.Moreover, the highest onion yield obtained at conventional furrow irrigation method lead to an improvement of 27 % while alternative furrow was 16% than the fixed furrow irrigation method.

Therefore, for increasing marketable bulb yield of onion under no water stress scenario, irrigation of onion with conventional furrow irrigation methods could be used. However, under limiting irrigation water resource condition, irrigation of onion could be done with alternate furrow irrigation method with straw mulch application to minimize evaporation loss and maximize water productivity of onion for similar agro-ecology and soil type.

Acknowledgement

The authors are grateful to Natural Resource Management Research Directorate, Ethiopian Institute of Agricultural Research, for providing funds for the experiment. They are also thankful to technical and field assistance and all staff members of Natural Resource Management Research Process,Debre ZeitAgricultural Research Center for their support and technical assistance in the field experimentation.

Finally, we would like to thank Water Resources Research Center of Arba Minch University and coordinating committee for inviting us to present this research finding on 18th international symposium.

Reference

[1] Awulachew S.B, Merrey D., Van Koopen B, and Kamara A., 2010. Roles, Constraints and Opportunities of Small-Scale Irrigation and Water Harvesting in Ethiopian agricultural Development: Assessment of Existing Situation. ILRI workshop; 2010 March 14-16; Addis Ababa, Ethiopia: International Water Management Institute (IWMI).

[2] Bekele, S., and Ketema T., 2007. Regulated deficit irrigation scheduling of onion in a Semi-arid Region of Ethiopia. Agric water manage 89,148 – 152.

[3] EngidaMersha. 2003. Assessment of Moisture Availability over Semi-arid and Arid Zones of Ethiopia. Ethiopian Journal of Natural Resources 5(2): 165-191.

[4] Enciso, J.; Weidenfeld, B.; Jifon, J., 2009. Nelson, S. Onion yield and quality response to two irrigation scheduling strategies. Sciatica Horticulture, v.120, p.301-305.

[5] FAO (Food and Agricultural Organization), 2000. Socio- Economic Impact of Smallholder irrigation Development in Zimbabwe, FAO Sub-Regional Office for East and Southern Africa, Harare.

[6] FAO (Food and Agriculture Organization). 2011. The State of the world's land and water resources for food and agriculture. Managing systems at risk. FAO, Rome, Italy.

[7] FDRE (Federal Democratic Republic of Ethiopia). 2016. Growth and Transformation Plan II (GIP II). Volume I, Addis Abeba.

[8] Geerts, S., and Raes, D., 2009. Deficit irrigation as an on-farm strategy to maximize crop water productivity in dry areas. Agricultural Water Management. 96, p. 1275–1284.

[9] Gijón, M.C., Guerrero, J., Couceiro, J.F., and Moriana, A., 2007. Deficit irrigation without reducing yield or nut splitting in pistachio. Agricultural Water Management, 96 p. 12-22.

[10] Hanson, B., and D. May. 2004. Effects of subsurface drip irrigation on processing tomato yield, water table depth, soil salinity, and profitability. Agric. Water Manage. 68:1-17

[11] Igbadun, H. E.; Ramalan, A. A.; Oiganji, E., 2012. Effects of regulated deficit irrigation and mulch on yield, water use and crop water productivity of onion in Samaru, Nigeria. Agricultural Water Management, v.109, p.162-169.

[12] Kumar, S.; Imtiyaz, M.; Kumar, A., 2007. Singh, R. Response of onion (Allium cepa L.) to different levels of irrigation water. Agricultural Water Management, v.89, p.161-166.

[13] Montazar, A. and Kosari, H. 2007. Water productivity analysis of some irrigated crops in Iran. In: Lamaddalena, N., Bogliotti, C., Todorovic, M. and Scardigno, A. (eds). Water saving in Mediterranean agriculture and future research needs. Vol.1: Bari: CIHEAM: 109 – 120.

[14] Mulu, A. and Alamirew, T. 2012. Deficit Irrigation Application Using Center Pivot Sprinkler Irrigation for Onion Production. International Journal of Basic & Applied Sciences, pp: 148-159.

[15] Nagaz, K., Masmoud, M.M., and Mechlia, N., 2012. Effects of deficit drip-irrigation scheduling regimes with saline water on pepper yield, water productivity and soil salinity under arid conditions of Tunisia. Journal of Agriculture and Environment for International Development -JAEID 106 (2): 85-103.

[16] Panigrahi, P., Sahu, N.N. and Pradhan, S. 2011. Evaluating partial root-zone irrigation and mulching in okra (Abelmoschusesculentus L.) under a sub-humid tropical climate. J. Agr. Rural Develop. Trop. Subtrop. 112 (2): 169–175.

[17] Ramalan, A. A.; Nega, H.; Oyebode, M. A., 2010. Effect of deficit irrigation and mulch on water use and yield of drip irrigated onions. WIT Transactions on Ecology and the Environment, v.134, p.39-50.

[18] Ramakrishna, A., H.M. Tam, S.P. Wani and T.D. Long., 2006. Effect of mulch on soil temperature, moisture, weeds infestation and yield of groundnut in Vietnam. Field crop 66 Research, 95(2/3): 115-125.

[19] Seleshi Y and Zanke U., 2004. Recent Changes in Rainfall and Rainy days in Ethiopia. International Journal of Climatology 24: 973-983.

[20] Singh, G., Joshi, V.K., Chandra, S., Bhatnagar, A. and Dass, A. 2016. Spring maize (Zea mays L.) response to different crop establishment and moisture management practices in north-west plains of India. Research on Crops. 17 (2): 226-230.

[21] United States Global Change Research Program. 2011. Overview: Water. Available from <http://www.globalchange.gov/component/content/article/52-reports-andassessments/ 481-overview-water> Accessed 07/15/2011.

[22] Xu, J., Li, C., Liu, H., Zhou, P., Tao, Z., Wang, P., Meng, Q. and Zhao, M. 2015. The Effects of Plastic Film Mulching on Maize Growth and Water Use in Dry and Rainy Years in Northeast China. PLoS ONE 10(5).

[23] Yaseen, R., Shafi, J., Ahmad, W., Shoaib, M., Salim, M. and Qaisrani, S.A. 2014. Effect of Deficit Irrigation and Mulch on Soil Physical Properties, Growth and Yield of Maize. Environment and Ecology Research. 2(3): 122-137.

[24] Zaman, W.U., Arshad M., and Saleem, K. 2001. Distribution of nitrate –nitrogen in the soil profile under different irrigation methods. International, J. Agri. Biol., 2: 208-9.

Theme Four: Water Supply and Sanitation

Impact of Coagulant Type and Ion Exchange (IEX) Pretreatment on Floc Strength and Structure at the Kluizen WTP

Gizeshwork Tadesse[1], Prof. dr. ir. Arne Verliefde[2]

[1.]Federal Technical and vocational education and training institute, Addis Abeba Phone: + 251937332891 E-mail: gizesh1999@gmail.com , [2.] Ghent University, Department of Applied Analytical and Physical Chemistry Phone: + 32 (0)9 264 60 02 E-mail: Arne.Verliefde@UGent.be

Abstract

Drinking water supplied to the community should be free of disinfection by-products, which occur when organic matter which is present in surface water reacts with chlorine. Conventional coagulation and flocculation process have therefore been used in water treatment plants as method of removing organic matter from the raw water. Recently, ion exchange followed by coagulation and flocculation has started to gain attention, since it allows considerably improving natural organic matter removal and decreasing coagulant demand. Besides processes to remove organic matter a priori to coagulation/flocculation, the structure/size and strength of the flocs formed in the coagulation and flocculation process also determine the efficiency of NOM removal and the efficacy of downstream processes as well. This study aims to compare floc structures such as floc sizes, floc strength and fractal dimensions, generated from coagulation of raw water and water pretreated with ion exchange obtained from Kluizen WTW (Kluizen, East- Flanders, Belgium). The coagulation was carried out with three coagulants; aluminum chloride ($AlCl_3$), polyaluminum chloride (PACl) and ferric chloride ($FeCl_3$). The working conditions of the water treatment plant were mimicked by adjusting pH and using similar doses of coagulants. In addition, the study also looks at the influence of coagulation mechanism and velocity gradient on floc structure. The floc sizes during growth, breakage and re- growth were measured using (laser) light scattering (Malvern Mastersizer 2000), coupled with jar test equipment. The strength of flocs was evaluated by empirically relating the floc size after breakage to the increased shear rate applied; in addition, the mode of breakage was identified based on strength coefficient obtained. Fractal dimensions of the aggregates were also determined from small angle light scattering using the Mastersizer.

Key word: water; coagulation; natural organic matter; floc size; jar test; Magnetic ion exchange

1. Introduction

Raw surface water often contains dissolved and particulate Natural Organic Matter (NOM), which deteriorates water quality. The presence of NOM in water by itself is not harmful when it is consumed, however its removal from the water is necessary to avoid the reaction of this NOM with disinfectant (chlorine), which results in formation of disinfection by- products that have adverse effect on human health (Singer & Bilyk, 2002; Burton, 2009; Drikas et al., 2011). In many surface water treatment plants for potable water production, coagulation and flocculation processes are used as an essential step to get rid of NOM (Jarvis et al., 2004; Yukselen & Gregory, 2004; Vahedi & Gorczyca, 2011). According to Jarvis et al. (2005b) coagulation is a process of removing natural organic matter and colloids by particle destabilization by double layer compression or charge neutralization of colloids and/or NOM within coagulant precipitates (or chemical reaction or chemical sorption). Since colloids (as well as NOM) in water mostly contain negative charges, coagulant with higher positive charge are mostly added to the water to destabilize the NOM and/or colloids to form aggregates. This step is followed by slow conciliate agitation to form larger aggregates called flocs. It is practically important to study properties of flocs and factors that impact their strength and structure to obtain efficient removal of organic matter (colloidal) from the water. Better understanding of factors such as the influence of the water type (i.e., ionic balance, pH, temperature, etc) and simple fractionation of NOM into hydrophobic and hydrophilic fractions will help to enhance the coagulation and flocculation process. In this study, floc characteristics and mechanisms affecting floc strength and structure will be assessed

1.2. Objective

This research focus on the impact of coagulant type and magnetic ion exchange (IEX) pre- treatment on floc structure, strength and re-growth potential on the raw water of Kluizen WTW, and the raw water. Therefore, following sub-goals were defined:

- Compare NOM removal efficiency of the raw water and IEX pretreated water after coagulation with three coagulants namely; $AlCl_3$, PACl and $FeCl_3$
- Evaluate and compare the floc structures obtained from the two water types and
- Understand the effects of coagulant type & dosage,

- Find out the response of the floc size to the increased shear and understand the breakage mechanism (i.e., investigate floc strength) for the different water types and different coagulants

2. Materials and Methods

The experiments conducted in this study used two water types obtained from the Kluizen Drinking Water Treatment plant, operated by De Watergroep in Flanders, Belgium. All the experiments were carried out in the laboratory at a temperature 20±2ºC

2.1. Raw water before and after the Pre-treatment

The first sample is raw water which is taken directly from the reservoir of Kluizen Drinking Water Treatment plant, where as the second sample is the same raw water, but then pre-treated with an anionic ion exchange resin. The IEX pretreatment was carried out in a pilot plant at the Kluizen site.

Table 1: raw water and Pretreated water characteristics (All samples were kept at room temperature (20 ±2 ºC) until the experiment was performed.)

Parameter	Raw water	Pretreated water
pH	8.16	**7.57**
UV absorbance at 254 nm (m^{-1})	28.34	**11.51**
Turbidity (NTU)	2.98	**3.06**
Conductivity (µS/cm)	647.29	**663.93**
Color (mg/l Pt-Co)	63.64	**38.29**
DOC (mg/l)	11.21	**6.34**
SUVA (m^{-1} mg/l)	**2.53**	**1.81**

2.2 Coagulant types and optimization of coagulant dosage

All the experiments were carried out using liquid coagulants obtained from Kluizen water treatment plant. The following coagulants were tested: Aluminum chloride ($AlCl_3$), Polyaluminum chloride (PACl) and Ferric chloride ($FeCl_3$): Aluminum chloride ($AlCl_3$, 6 weights % as Al), Polyaluminum chloride (PACl Aqualenc F1, 9.6 weight % as Al_2O_3), Ferric chloride ($FeCl_3$, 200g/l of iron). All coagulation experiments were conducted at a corrected pH of 6.8 adjusted by adding 1 molar (M) of sulphuric acid (H_2SO_4). After pH regulation, coagulation experiments were performed with 1L measuring beakers filled with 0.5 l of the selected water. To find the optimum coagulant dose for each treatment

option, doses between 6 mg/l and 22 mg/l was investigated using a series of jar test. Coagulation experiments were carried out with a PB -900 variable speed jar tester. A rapid mixing at 260 rpm for 2 min was applied followed by slow stirring phase at 35 rpm for 15 minutes to let the flocs grow. Samples were taken for the analysis of UV_{254} after a settling of 30 min and a dose which gave the lowest $UV_{254\ value}$ was taken as an optimum dose. $UV_{254\ was}$ measured using UV-Vis spectrophotometer and Zeta potential using Zetasizer (Malvern Instruments, UK).

Figure 1: Experimental set up of coagulation for dose optimization

3.3. Floc size measurements

A Malvern Mastersizer 2000, coupled with the coagulation device by a peristaltic pump, was used to measure floc size as shown in Figure 2. The floc size was measured based on the method explained in Jarvis *et al.* (2005b), in which jar tester and Mastersizer are joined together. The sample water was pumped from the jar tester through the measurement cell of Mastersizer using a peristaltic pump at a rate of 6 liter per hour (l/hr). The water was taken from the jar just above the paddle of the coagulation device. Floc size measurements were performed every minute for all the stages of growth, breakage and re- growth. The median floc size (d_{50}) was obtained from the instrument and logged on the computer for further analysis.

Figure 2: Experimental set up for floc size measurements (Mastersizer coupled with jar tester Coagulation,

Coagulation, flocculation and breakage protocol in jar tester for floc sizes measurement were carried in the jar test with commercial jar tester, one-liter measuring beakers were filled with 0.5L of water sample and an initial rapid mixing of 260 rpm were applied for two minutes where coagulant was added 30 second after the start of the mixing. Flocculation of the suspension was performed after the coagulation phase. The flocculation was done for 15 minutes at a mixing intensity of 35 rpm following the coagulation. During flocculation, the suspension was continuously pumped into the Mastersizer measurement cell to measure floc growth. Following the flocculation phase at slow mixing rate, a variation of different higher shear rate was applied to break the floc. For the flocs coagulated jar tester, a breakage phase of 5 minutes was carried out after flocculation at a mixing speed of 50 rpm, 75rpm, 100 rpm, 150 rpm and 200 rpm corresponding to average velocity gradient of $33s^{-1}$, $61s^{-1}$, $94s^{-1}$,$172s^{-1}$, 265 s^{-1} respectively. The floc size is measured every minute during all the flocculation phases Finally, the floc was allowed to re-grow for 15 minutes after breakage phase, at stirring rate of 35 rpm and size was measured to examine the re-growth potential. The strength and recovery factor were calculated based on (Equation 1 and 2) (Yukselen & Gregory, 2004; Jarvis *et al.*, 2005b; Burton, 2009). The average floc size d_{50} as obtained from the Mastersizer was used to calculate the strength and recovery factors. In Equation 1 and 2; d_1, d_2 and d_3 are the steady state average d_{50} floc sizes at the end of growth phase, breakage phase and re-growth phase, respectively.

$$Strength\ factor = \frac{d_2}{d_1} * 100 \quad (1)$$

$$Recovery\ factor = \frac{d_3 - d_2}{d_1 - d_2} * 100 \quad (2)$$

Another way used to characterize floc strength is the empirical relationship between the applied shear force and the remaining floc size in the suspension at the end of breakage phase (Equation 3).

$$\log d = \log(C) - \gamma * \log(rpm) \quad (3)$$

The slope of the equation (γ) and the intercept (log(C)) indicates floc strength constant and floc strength co-efficient respectively.

3.4. Statistical Analyses

The mean, standard deviation and standard error of the floc size measurements were calculated using Analysis ToolPak of Microsoft Excel.

4. Results and Discussion

4.1. Optimal coagulant dosage (as determined from uv254 removal)

For raw water, coagulation with $AlCl_3$ gave best removal of UV_{254} (0.073) at a dosage of 11 mg/l while $FeC1_3$ gave the lowest UV_{254} (0.033) at a dosage of 9 mg/l for the pretreated water. The choice of best coagulant to be used depends on the type of water used. For all the coagulants and comparable dosage, lower values of UV_{254} were obtained for the pretreated water compared to the raw water. This is mainly because UV_{254} absorbing organics were already removed by the pretreatment of the raw water with IEX.

Table 2: Summary of obtained UV254 result for the three coagulants with different dose with UV absorbance at 254 nm

Dose (mg/l)	UV absorbance at 254 nm (cm^{-1})					
	Raw + $AlCl_3$	Raw + PACl	Raw+ $FeCl_3$	Pretreated + $AlCl_3$	Pretreated + PACl	Pretreated+ $FeCl_3$
6	0.095	0.097	0.134	0.074	0.062	0.034
9	0.088	0.114	0.12	0.073	0.06	0.033
11	0.073	0.11	0.115	0.072	0.059	0.033
14	0.090	0.101	0.108	0.065	0.058	0.034
16	0.090	0.082	0.105	0.066	0.056	0.032
20	0.077	0.082	0.098	0.060	0.047	0.029
22	0.153	0.085	0.080	0.058	0.097	0.067

As shown in Figure 4-2, both water types coagulated with $AlCl_3$ and pretreated water coagulated with PACl have positive zeta potential for the entire dose applied. As a result, it is most likely that hydroxide precipitation and sweep coagulation are responsible for the coagulation. On the other hand, zeta potential for both water types coagulated with $FeCl_3$ changes from negative to positive at a dose close to 16 mg/l as Fe, which is considered as an iso- electric point. The negative zeta potential obtained at a dose of 11 mg/l Fe might indicate that charge neutralization is the main coagulation mechanism Occurring for Fe.

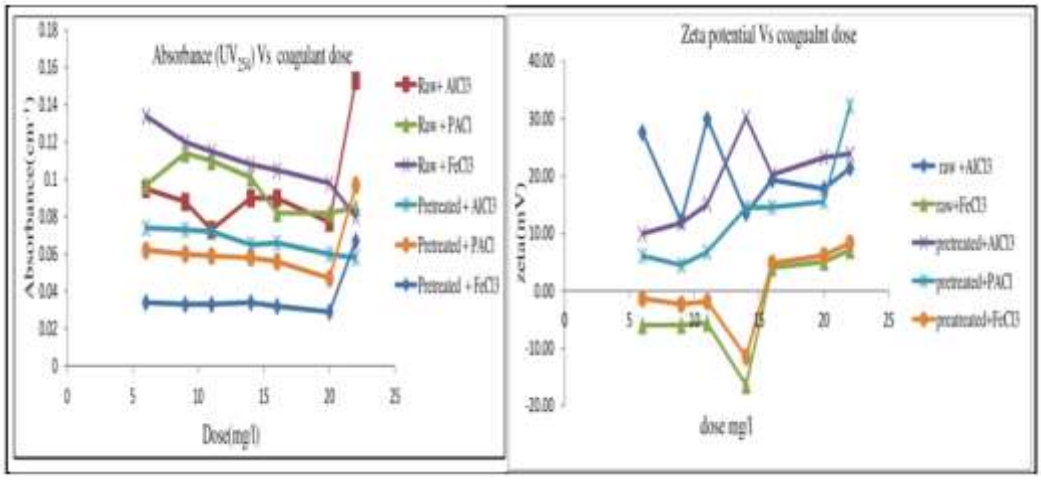

Figure 3 Absorbance and zeta potential as function of coagulant dose for all the coagulant and both water types Floc Size

In measurement of the floc size with different coagulants and water samples, the growth, breakage and re-growth phases of the floc were investigated at a dose of 11mg/l for both raw and pretreated water. As can be seen in Table 4-2 the d50 floc size during the growth phase of flocculation was in following order FeCl3 < PACl < AlCl3, for both water types. For all the coagulants, water floc sizes in the pretreated were higher than for the raw water. After pretreatment, the floc size was increased by 19%, 63% and 64% for the coagulants PACl, AlCl3, and FeCl3 respectively. This result indicates that pretreatment of the raw water with IEX and selections of coagulants have a large influence on the floc size.

Table 3 Floc size of raw water and pretreated water for the three coagulants after 1.5 minutes coagulation at 260 rpm and 15minute flocculation time at 35 rpm

Coagulant	raw water floc average size(d_{50}) during growth	Pretreated water floc average size (d_{50}) during growth	Increase in size after pre-treatment
$AlCl_3$	102 ±13.4µm	167±13.6 µm	63%
PACl	160±9.6 µm	190 ±6.8 µm	19%
$FeCl_3$	219±3.9 µm	357±10.6µm	64%

The floc size during the growth, breakage and re-growth phase for the two water types with the different coagulants is shown in the Figures below (Fig 4-3 to Fig 4-5). The floc size is represented by the volumetric median diameter (d_{50}) as obtained from the Mastersizer. The data shows growth phase of the floc during 15 minutes flocculation at a stirring rate of 35 rpm. Floc size during the breakage phase is measured at different mixing intensities for 5 minutes while the re-growth phase was carried out for 15minute at a reduced intensity of 35 rpm. On the graphs, the first vertical line indicates the point at which increased shear (50 rpm, 75 rpm, 100 rpm, 150 rpm and 200 rpm) was introduced for floc breakage (after 15 minutes of flocculation time). The second vertical line indicates the point where shear was again reduced (35 rpm) for the re-growth of the flocs after 5 minutes of breakage time.

From the Figures, it can be seen that the floc size during the growth phase is different for the two different water types. For all the coagulant, the pretreated water showed consistently higher floc sizes than the raw water.

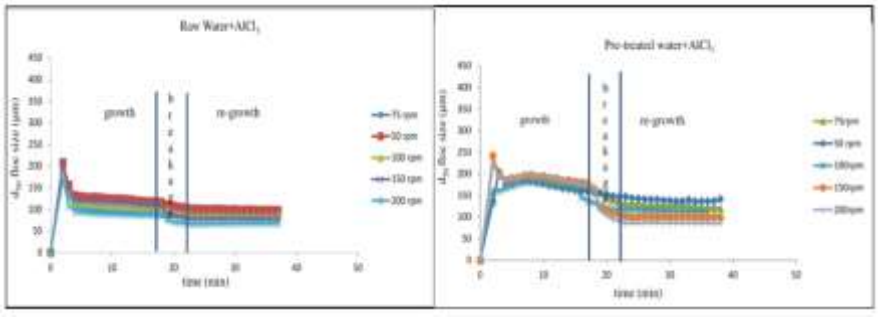

Figure 4 Floc size profile for $AlCl_3$ flocs formed from raw water and pre- treated water upon exposure to different levels of shear (at a dose of 11 mg/l as Al at pH 6.8 for both water types).

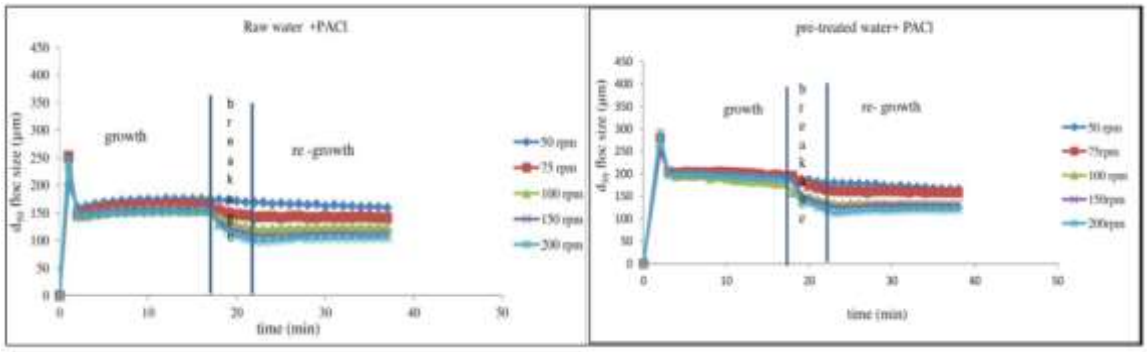

Figure 5: Floc size profile for PACl flocs formed from raw water and pre- treated water upon exposure to different levels of shear (at a dose of 11 mg/l as Al at pH 6.8 for both water types).

For PACl coagulation with both water types, the evolution of the flocs size during growth, breakage and re-growth was similar to that of $AlCl_3$. An increased in floc size was not observed during the flocculation phase after coagulation as can be seen from the steady state curve of the

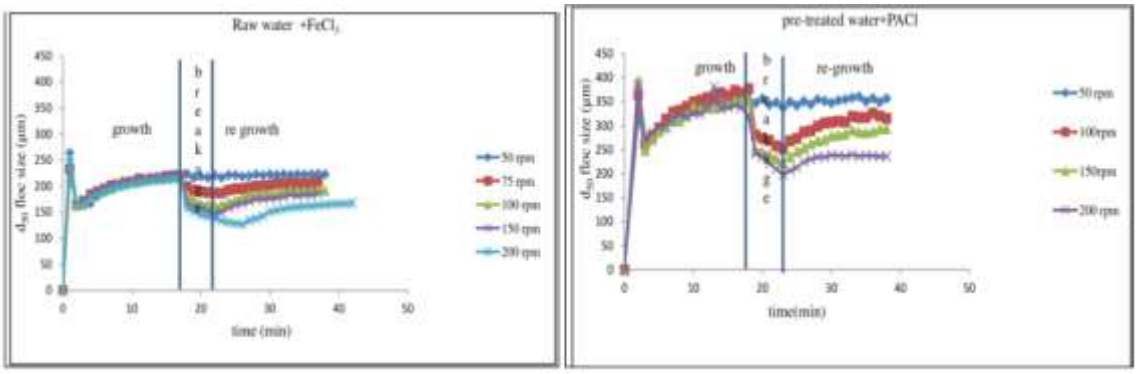

Figure 6 Floc size profile for $FeCl_3$ flocs formed from raw water and pre- treated water upon exposure to different levels of shear (at a dose of 11 mg/l as Al at pH 6.8 for both water types)

It was seen from the result that pre-treatment of the raw water with IEX has a significant impact on the size of the flocs formed during coagulation/flocculation given the same mixing conditions. This concur with the result obtained by Jarvis *et al.* (2004) and Burton (2009) where larger and stronger flocs were observed for the pre-treated water compared to the raw water. This might be as a result of the reduction in the amount of natural organic matter such as DOC after pretreatment with IEX. The modified composition of the water has an impact on floc structure such as size, strength, fractal dimension, since smaller DOC to coagulant ratio has the potential to

produce floc with better structure. The improved floc structure (at lower DOC concentration) is ascribed to the interaction of carbon with floc matrix. At higher DOC concentration, NOM aggregates might be covered with the organic carbons which limit further aggregation or leads to formation of loosely structured aggregates when they are flocculated with inorganic salts. Another reason for the improved floc size after pretreatment could be because IEX pretreatment removes low molecular weight organics. The remaining higher molecular weight fraction polymers have improved binding capacity with flocs leading to larger flocs size (Burton, 2009). Statistically analyzed, there was significant difference in the floc size during flocculation of both water types with the three coagulants (Levene's Test, $p < 0.001$ at 95% confidence interval). Hence the choice of the coagulants and water types has a significant impact on the floc size obtained from the flocculation during growth phase.

It was seen from the results that, the flocculation phase for $FeCl_3$ is different from the other two coagulants. For both water types, the floc continues to grow until the end of the growth phase after coagulation with $FeCl_3$. This might not be explained only by the organic matter to coagulant ratio, but also by the behavior of the coagulant itself. Iro based coagulants have preferential selectivity for organic matter than aluminum-based coagulants (Uyak & Toroz, 2007). This leads to the better aggregation of ferric chloride with organic matter leading to larger flocs formation. This also explains why the pretreated water coagulated with ferric chloride has the lowest UV_{254}. This conforms to the result of Uyak & Toroz (2007) who obtained better removal of UV_{254} by ferric coagulants than aluminum-based coagulant.

It was also observed that application of high shear force during breakage resulted in a decrease in floc size, with the decrease in size becoming larger with higher mixing intensity. In fact, when mixing at 200 rpm, the size decreased largely while mixing at 50 rpm did not change floc size. For $FeCl_3$ the breakage phase observed was similar to that the two other coagulants where broken floc size decreases as breakage intensity increase.

4.2. Floc strength and recovery

The strength of the floc to resist the high shear applied during the breakage phase after flocculation and the ability to grow in size when fewer shear is again applied after breakage, is highly dependent on the intensity of the mixing during breakage and duration of the breakage. Floc size during breakage/after should be inversely related to the intensity of the shear applied (the flocs size decreases as intensity of the shear increase) (Spicer *et al.*,1996; Burton, 2009)

This is because floc size is the net result of aggregation and fragmentation of flocs and an increased shear rate can lead to breakage of more flocs (Yukselen & Gregory, 2004). For breakage at the highest intensity of 200rpm, $AlCl_3$ showed the highest strength factor (81%) followed by PACl (68%) and $FeCl_3$ (62%) for the raw water. For the pretreated water breakage at mixing intensity of 200 rpm, $FeCl_3$ (66%) showed highest strength factor followed by PACl (64%) and $AlCl_3$ (56%). When statistically analyzed, the calculated strength factors did not show significant difference between the two water types (Levene's Test, p= 0.808). Similarly, strength factors did not reveal any significant difference for the different coagulant types (Levene's Test, p= 0.15 There was no recovery seen in floc size for both water with coagulants $AlCl_3$ and PACl after the shear was again reduced to the slow stirring at 35 rpm for. However, $FeCl_3$ flocs obtained from both water types were able to recover after the shear was reduced to 35 rpm and there was increase in floc size as re-growth time increases (Table 4-3). The recovery potential indeed depends on the intensity of the shear applied to break the floc. The floc broken with lower intensity (i.e. 75 rpm) showed larger recovery potential compared to the flocs broken with higher intensities (i.e. 200 rpm). There was no statistically significant difference observed in recovery factor between the raw and pretreated water for all the shear force applied (Levene's Test, p=0.56).

The significant difference seen in recovery factor might be correlated to the charge. Neutralization coagulation mechanism involved with iron coagulants.

This conforms to the result of Zhao *et al.* (2011a) who found higher recoverability for flocs formed by charge neutralization coagulation mechanism. The higher selectivity of iron coagulants to NOM could also be another reason for the higher recoverability of iron flocs after breakage (Burton, 2009).

Another way of characterizing the floc strength is by examining the response of d_{50} floc size to the increased shear rate. This was done by plotting the measured d_{50} size at the end of 5 minute of breakage phase against the rpm of the jar tester on a log- log scale (see material and method section 3.4). The R^2 values for these log-log plots were high (between 0.946 and 0.996) indicating a good Correlation

Shear force (rpm)	Raw water +$AlCl_3$		Raw water + PACl		Raw water+ $FeCl_3$		Pretreated water+ $AlCl_3$		Pretreated water+ PACl		Pretreated water + $FeCl_3$	
	Strength factor (%)	Recovery factor (%)	Strength factor (%)	Recovery factor (%)	Strength factor (%)	Recovery factor (%)	Strength factor (%)	Recovery factor (%)	Strength factor (%)	Recovery factor (%)	Strength factor (%)	Recovery factor (%)
50	97	-244	97	-181	98	154	92	-127	94	-113	99	161
75	**90**	**-86**	**88**	**-25**	**85**	**67**	**82**	**-73**	**84**	**-22**	-	-
100	87	-41	81	-2	75	54	71	-21	76	-13	68	48
150	78	-33	73	-2	68	50	62	-22	68	-2	65	51
200	81	-21	68	3	62	36	56	-21	64	1	66	24

150	78	-33	73	-2	68	50	62	-22	68	-2	65	51
200	81	-21	68	3	62	36	56	-21	64	1	66	24

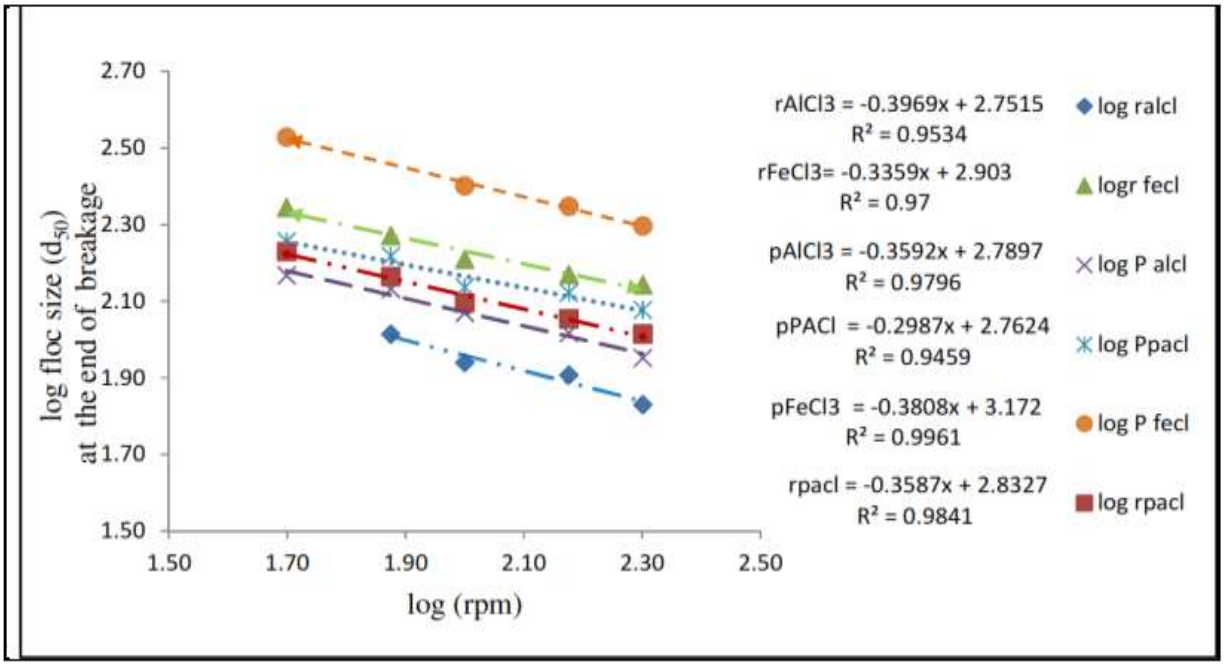

Figure 7: Response of floc sizes after breakage to an increased shear rate. Log- log relationship between floc size (d50) and shear (rpm)

For $AlCl_3$, the floc strength coefficient () is 0.359 for the pretreated water and 0.396 for raw water. The same trend was seen for PACl for which has 0.30 and 0.36 for the pretreated water. Based on these values, it can be concluded that flocs formed with raw water are more prone to breakage than with pretreated water for $AlCl_3$ and PACl. On the other hand, flocs generated with $FeCl_3$ showed higher for pretreated water (0.388) than for raw water (0.336), and thus flocs are easier to break down after pretreatment. This corroborates findings by Burton (2009) for $FeCl_3$. However, for PACl and $AlCl_3$ the trends seen here do not follow results observed by Burton (2009). This disagreement might arise either from the different resin type used for ion exchange pretreatment of the raw water, the variation in water characteristics due to season and the different coagulant dose used with the two studies.

5. Conclusion and Recommendation

5.1. Conclusions

This study examined the overall structural characteristics of flocs generated from raw surface water and water pretreated with IEX obtained from the Kluizen drinking water treatment plant. The growth, breakage and re-growth of flocs generated from the two different water types were assessed for three different coagulants ($AlCl_3$, PACl, and $FeCl_3$).

The result obtained from the laboratory experiment gave the following conclusions:

- Pretreatment of raw water with IEX removed (part of the) DOC and UV254 absorbing organics from the raw water which lead to improved water quality. As a result, Optimum coagulant dose was decreased.
- The flocs generated using PACl as coagulant were found to be strongest based

  on the lower value of γ and the higher fractal dimension of the microflocs (floc aggregates smaller than 2.5μm).
- Flocs generated using $FeCl_3$ as coagulant show higher recovery factors (i.e., the

  re-grow better after breakage), which was explained by the higher selectivity of Fe to organic matter and by the charge neutralization coagulation mechanism involved with Fe coagulant.
- Higher floc sizes were obtained after pretreatment with IEX, because of the decreased concentration of lower MW substances after IEX. The higher MW polymer like substances left in the water gave an increased floc sizes when coagulated.

5.2. Recommendations

For future work, it would be important to consider the following points: Further research is necessary on the influence of mixing intensities/velocity gradients during coagulation on floc properties. The interaction between coagulants and different NOM constituents should be examined to better understand effects of IEX pretreatment on coagulation. There should also be more research to clearly understand why different coagulants behave differently for both water types. Seasonal variations on the efficiency of the coagulation /flocculation should be considered since the water quality and temperature will change with respect to the season

References

Boller, M. & Blaser, S. (1998). Particles under stress. *Water Science and Technology* 37, 9-29.
Burton, V. (2009). Impact of MIEX pre-treatment on floc strength and structure. *Msc Thesis*.

Drikas, M., Dixon, M. & Morran, J. (2011). Long term case study of MIEX pre-treatment in drinking water; understanding NOM removal. *Water Research* 45, 1539-1548.

Francois, R. J. (1987). Strength of aluminium hydroxide flocs. *Water Research* 21, 1023-1030.
Jarvis, P., Parsons, S. A. & Jefferson, B. (2004). The Impact of Natural Organic Matter on FlocStructure *PHd dissertation*.

Jarvis, P., Jefferson, B. & Simon, A. P. (2005b). Measuring floc structural characteristics. *Environmental Scienceand Bio-Technology* 4, 1–18.

Jarvis, P., Jefferson, B. & Parsons, S. A. (2006). Floc structural characteristics using conventional coagulation for a high doc, low alkalinity surface water source. *Water Research* 40, 2727-2737.

Kim, S.-H., Moon, B.-H. & Lee, H.-I. (2001). Effects of pH and dosage on pollutant removal and floc structure during coagulation. *Microchemical Journal* 68, 197-203.

Li, T., Zhu, Z., Wang, D., Yao, C. & Tang, H. (2006). Characterization of floc size, strength and structure under various coagulation mechanisms. *Powder Technology* 168, 104-110.

Singer, P. C. & Bilyk, K. (2002). Enhanced coagulation using a magnetic ion exchange resin. *Water Research* 36, 4009-4022.

Spicer, P., Pratsinis, S., Trennepohl, M. & Meesters, G. H. M. (1996). Coagulation and Fragmentation: The Variation of Shear Rate and theTime Lag for Attainment of Steady State. *Industrial and engineering chemistry research* 35, 3074-3080.

Uyak, V. & Toroz, I. (2007). Disinfection by-product precursors reduction by various coagulation techniques in Istanbul water supplies. *Journal of Hazardous Materials* 141, 320–328.

Vahedi, A. & Gorczyca, B. (2011). Application of fractal dimensions to study the structure of flocs formed in lime softening process. *Water Research* 45, 545-556.

Wang, Y., Gao, B.-Y., Xu, X.-M., Xu, W.-Y. & Xu, G.-Y. (2009). Characterization of floc size, strength and structure in various aluminum coagulants treatment. *Journal of Colloid and Interface Science* 332, 354-359.

Yukselen, M. A. & Gregory, J. (2004). The reversibility of floc breakage. *International Journal of Mineral Processing* 73, 251-259.

Zhao, Y. X., Gao, B. Y., Rong, H. Y., Shon, H. K., Kim, J. H., Yue, Q. Y. & Wang, Y. (2011a).

The impacts of coagulant aid-polydimethyldiallylammonium chloride on coagulation performances and floc characteristics in humic acidâ€“kaolin synthetic water treatment with titanium tetrachloride. *Chemical Engineering Journal* 173, 376-384.

Theme Five: Climate Variability, Change, and Impacts

Modeling Impact of Climate Change on Future Projections of Temperatures and Precipitation in Shaya Watershed, Genale-Dawa Basin, Ethiopia

Sintayehu Fetene[1] and Meseret W/Yohannes[2]

[1]PhD Candidate in Climate Smart Agriculture and Biodiversity Conservation at Haramaya University, Lecturer at Kotebe Metropolitan University demessie1986@gmail.com, +251912431189, [2]Kotebe Metropolitan University, College of Natural and Computational Science

ABSTRACT

Predictions of the impacts of climate variables at small watershed level on the intensity, amount, and spatial and temporal variability of rainfall and temperature are required for solving the potential water resource management problems. The main aim of this study was to downscale the Global Circulation Model (GCM) output in particular, temperature and precipitation to watershed level for analyzing the impact of climate change on water resources variabilityof Shaya River Watershed. The HadCM3A2a and HadCM3B2a (Hadley Centre Climate model 3), output of Global Circulation Model (GCM), scenarios of climate change were used for predicting the future climates of the study area. Statistical Downscaling Model (SDSM 4.2) was used to downscale large scale predictors into finer scale resolution. To estimate the level of impact of climate change, climate change scenarios of precipitation and temperature were divided into three time windows of 30 years each from 2011-2099. The Soil and Water Assessment Tool (SWAT) was used to simulate the hydrological response. SWAT was first calibrated and validated using observed data and the SDSM downscaled climate outputs were used as an input into the SWAT model to assess the hydrological responses of Shaya River due to climate change. The period from 1977-2000 were taken as a base period against which a comparison was made. The results showed that the SWAT calibration and validation reveals a good agreement with R^2=0.89 during calibration and R^2=0.69 during validation whereas NSE= 0.86 during calibration and 0.63 during validation. The monthly downscaled precipitation, maximum and minimum temperature in the future time horizons did not show systematic increase and decrease i.e. increases in some months and decreases in some other months. Annually, the temperature showed increasing trends while the precipitation showed decreasing trends but not significant in all future time horizons (Precipitation decreases up to 5.77% while temperature increases up to a maximum of 2.01^0c). Therefore, the change in the amount and distribution of rainfall and level of temperature would affect the agricultural productivity and water utilizations in the region.

Keywords: Climate change, Shaya River, SWAT, GCM, PrecipitationTemperature.

1 1. 1. **1. Introduction**

Climate change is real and happening now. Where the impact has the potential to undermine and even, undo progress made in improving the socio-economic well-being of human livelihood. This is compounded by many factors, including widespread poverty, human diseases, and high population density, estimated to double high demand for food, water, and livestock forage within the next 30 years (Davidson *et al*., 2003). Water resource is also one of the main sectors that will be adversely affected by climate change. Many of the most critical impacts of global climate change will manifest themselves through the hydrologic system. There is already strong evidence that climate change is having an impact on the world's water resources. These impacts include changing precipitation and temperature patterns that may result in more severe drought or floods, changing snow pack amount and elevation, varying stream flow patterns, and rising sea levels along the coasts.

Even though Africa is widely held to be highly vulnerable to future climate change, Ethiopia is often cited as one of the most extreme examples. Both instrumental and proxy records have shown significant variations in the spatial and temporal patterns of climate in Ethiopia. The United Nation Development Programme (UNDP) Climate Change profile for Ethiopia shows that the mean annual temperature increased by 1.3°C between 1960 and 2006, at an average rate of 0.28°C per decade while, rainfall behavior shows no marked emergent changes (Conway and Lisa, 2010).

The results of Intergovernmental Panel on Climate Change (IPCC's) mid-range emission scenario show that compared to the 1961-1990 average mean annual temperature across Ethiopia will increase from 0.9 and 1.1°C, 1.7 to 2.1°C and 0.5°C to 3.6°C by the years 2030, 2050 and 2080 respectively and annual precipitation shows a change of between 0.6% and 4.9% and 1.1% to 18.2% for 2030 and 2050, respectively (NMA, 2006).

(Conway and Lisa, 2010), reported that Ethiopia's economy basis on rain-fed agriculture is highly exposed to climate variability and extremes supporting roughly 42% Gross Domestic Product (GDP) and 85% employment. Over the years the most devastating Ethiopian droughts are associated with late onset, early offset or due to failure of rainfall during the growing season. Despite this situation, fundamental understanding of the patterns and causes of the seasonal-to-inter annual variability of the rainfall seasons have remained conspicuously absent, which is crucial for Ethiopia's food security (Degefu, 1987; Gissila et al., 2004). Moreover, Mc Sweeney *et al*., (2008) argued that climate change

will be a major challenge against the country's efforts towards achieving food security and environmental sustainability.

In spite of the fact that the influence of different climate change scenarios are projected at a global scale. The exact type and magnitude of the impact at a small watershed scale remains untouched in most parts of the world. So, identifying localized impact of climate change at a watershed level and quantitative estimates of hydrologic effects of climate change are essential for understanding and solving the potential water resource management problems; Future water resource planning, reservoir design and management, and for protection of the natural environment with the changing environment. All this gives an opportunity to define the degree of vulnerability of local water resources to climate change and plan appropriate adaptation measures that must be taken up front. Additionally, this study provided an adequate amount of time/chance to reflect possible future threats in all levels of water resource development projects.

1.1. Research Objectives

The general objective of this study was to downscale the Global Circulation Model (GCM) output in particular temperature and precipitation to watershed level for analyzing the impact of climate change on Shaya River.

The specific objectives of the study include:

- To simulate the hydrological processes of Shayariver watershed using ArcSWAT model, and
- To develop temporal climate change scenarios (precipitation and temperature), for Shayariver watershed, for the future until year 2099,

2. Materials and Methods

2.1 Description of the Study area

Shaya watershed is found in south-eastern part of Ethiopia in Oromia Regional State, Bale Zone. The watershed is situated in Genale-Dawa basin at the upper most parts of the Weyb basin, located between 6°52'-7°15'N latitudes and 39°46'-40°02'E longitudes as shown in figure 1.

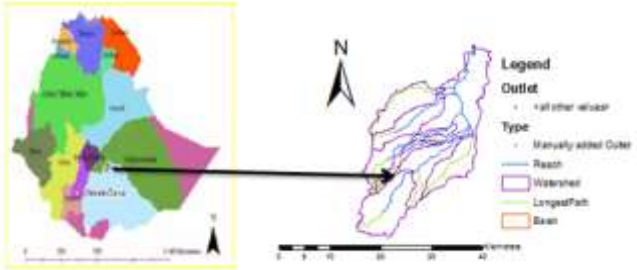

Fig 1: Location of study area

3. Methodology

3.1. Modeling Approaches

The modeling approaches were divided in to two major parts. The first part was climate changemodeling approach, and the second was hydrological modeling approach.

3.1.1. Climate Change Modeling Approach

General Circulation Model (GCM) outputs*:* Global Circulation Model (GCM) derived scenarios of climate change were used for predictingthe future climates of the study area based on criteria proposed by the Intergovernmental Panelon Climate Change (IPCC).

Among the wide range of GCM models HadCM3, (Hadley Centrefor Climate Prediction and Research, England), was selected for the impact study. Besides, the HadCM3 GCM output was chosen since themodel was widely used for climate change impact assessment and the results of HadCM3 can beeasily downscaled using SDSM (Dile*et al*., 2013). For HadCM3 the model result is available for A2 (medium-high) and B2 (medium-low) emissionscenarios. For this study the ensemble "a" was considered for A2a and B2a experiments (the "a"in A2a and B2a refers the ensemble member in the HadCM3 A2 and B2 experiments).

Downscaling Techniques: For this study SDSM 4.2- a decision support tool forthe assessment of regional climate change impacts developed by Wilby and Dawson (2007) wasused to downscale large scale predictors and it was freely downloaded from http://www.sdsm.org.uk.

SDSM develops statistical relationships, based on multiple linear regression techniques, betweenlarge-scale (predictors) and local (predictand) i.e. precipitation, and maximum and minimumtemperature for this study which could be used as input for hydrological modeling.

Predictor Variables: Large-scale predictor variable information was freely obtained from the Canadian climate impactscenario group with web address of: http://www.cics.uvic.ca/scenarios/sdsm/select.cgi/. TheNational Center for Environmental Prediction (NCEP_1961-2001) reanalysis data and HadCM3 predictor variables for the A2a and B2a were downloaded for grid boxes representing the study watershed area. Large-scale predictor variable information i.e. National Center for Environmental Prediction(NCEP_1961-2001) reanalysis data set were used for the calibration and validation of SDSMwith the observed precipitation, maximum and minimum temperature at Robe station and HadCM3 (Hadley centre Climate Model 3) GCM (H3A2a_1961-2099 and H3B2a_1961-2099 data were used for the baseline and climate scenario generation.

Screening Predictor Variables: Identifying the empirical relationships between gridded predictors and single site predictands (such as station precipitation, maximum, and minimum temperature) is central to all statisticaldownscaling methods, and is often the most time-consuming step in the process (Wilby andDawson, 2007). Several analyses were made by selecting a maximum of six out of 26 predictor variables at a timetill best predictor-predictand correlations were found even though up to 12 predictors were possible to select at a time (Wilby andDawson 2007). The strength of the individual predictors varies on a month by month basis. Hence the mostappropriate combination of the predictors with the predictand was chosen by looking the analysisoutput of all months. The Correlation matrix was done to investigate inter–variable correlations for annual sub–periods to identify the amount of explanatory power that was unique to each predictor.

SDSM calibration, weather generator and validation: Forthe current study, the calibration was done for the period of 10 years (1977-1986) at a monthly model type in order to see the monthly temporal variations. The downscaling process is Unconditional for daily temperature value and Conditional forprecipitation. Since for conditional processes in which the distribution of predictand values isskewed, the Fourth root transformations were applied.

Ensembles of synthetic daily weather series were produced using NCEP re–analysis atmosphericpredictor variables and regression model weights produced by the Calibrate Model operation. The Weather Generator can also be used to reconstruct predictands or to infillmissing data. An independent predictand variables from 1977-2000 at Robe station were used formodelvalidation.

Scenario generation and bias correction methods: Hence for this study, the HadCM3A2a and HadCM3B2a were the two GCM output files used for the scenariogeneration. The regression weights produced during the calibration process were applied to thetime series outputs of the GCM model. This is based on the assumption that the predictorpredictandrelationships under the current condition remain valid for future climate conditions. Twenty ensembles of synthetic daily time series data were produced for each of the two SRESscenarios for a period of 139years (1961 to 2099). Finally, the mean of the twenty ensembles forthe specified period was produced for maximum and minimum temperature and precipitation. The period from 1977-2000 were considered as a base period whereas the period from 2011-2099 were considered as future periods. The future periods were divided into three-time horizons from 2011-2040, 2041-2070 and 2071-2099 and analyses were made for each timehorizons.

During this study Linear Scaling (LS) method was adapted to correct the model errors due to itssimplicity. Precipitation is typically corrected with a multiplier and temperaturewith an additive term on a monthly basis. The correction factors derived during the base period (1977-2000) were applied for the future period (2011-2099).

4. Results and Discussion

The results and discussion of the climate change model results were shown using both statistically and graphically and discussed in detail accordingly. Moreover, the hydro-climatologically conditions of the catchment from the period 1977 to 2000 were analyzed using observed hydrological and meteorological data. Moreover, the change in precipitation and temperature of the catchment from the period 1977 to 2000 were analyzed using observedmeteorological and modeled data.

Hydro- Climatological Conditions of Shaya River Watershed/Catchment from 1977-2000.: Mostly the observed daily precipitation at Robe station showed that the maximum amount of precipitation occurred within the major parts of the rainy season. In most of the year, the average monthly precipitations are found between 1.98 mm and 2.70 mm as shown in the figure 7. More or less the observed daily precipitation in each year is uniform.

However in the year 1993 and 1994 the most extreme events were occurred i.e. 3.0 mm, 3.07 mm respectively. The highest and the lowest value of average monthly precipitation was recorded in the year 1994 (3.07 mm) and 1983 (1.45mm) respectively.

Moreover, the trend line of observed average monthly precipitation from 1977-2000 shows slightincrements. Unlike that of precipitation, the observed average monthly maximum and minimum temperaturedid not show large variation from year to year. Figure 8 showed that, in most of the year theaverage monthly maximum temperature are found between 21.30^0C (1977) and 22.37^0C (1994) while for minimum temperature the average monthly values are found between 7.89^0C (1988) and 8.78^0C (2000). In the year 1985 the lowest average monthly maximum temperature was observed (21.05^0C). The trendline of minimum temperature showed slight increments while it is more or less constant for maximum temperature.

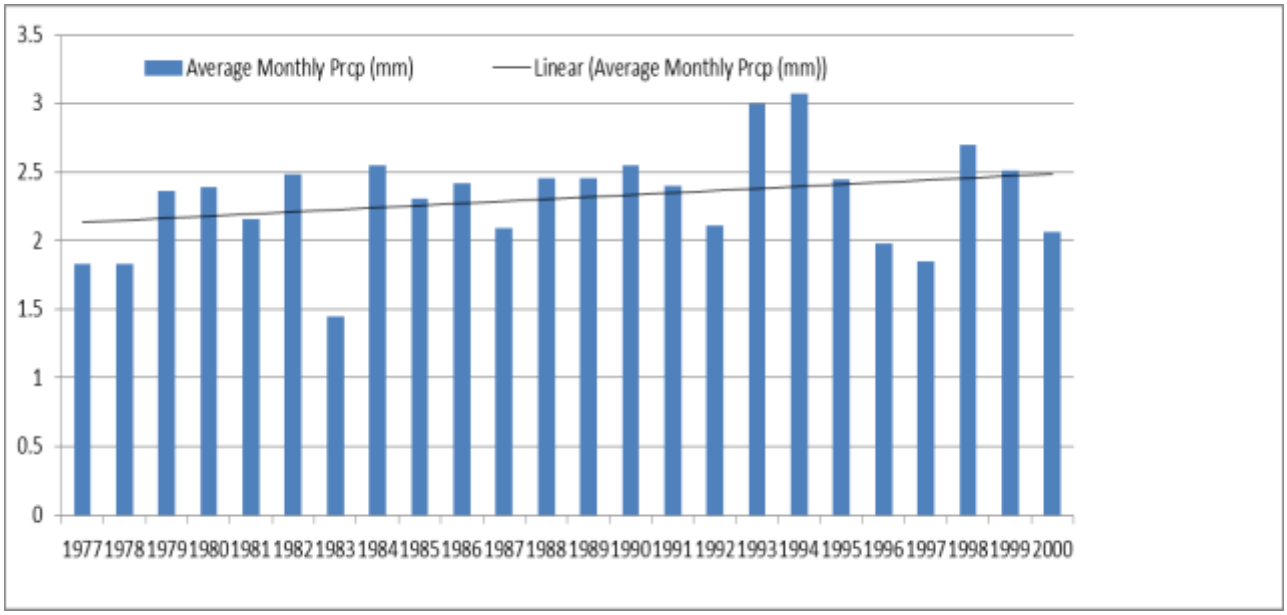

Figure 8. Observed Average Monthly Precipitation at Robe Station (1977-2000) (mm)

Figure 9 shows the average monthly flows of Shaya River. As it can be shown from thefigure the flow patterns more or less correspond with the pattern of average monthly precipitation even if the trend line does not show a slight increment as that of the average monthly precipitation (figure 7). In most of the year the average monthly flows are found between 3.92m^3/s and 5.33m^3/s. However, in the year 1993 and 1994 the most extreme flows were occurred in which theaverage monthly flow reaches to a maximum of 7.31m^3/s and 7.37m^3/s respectively.

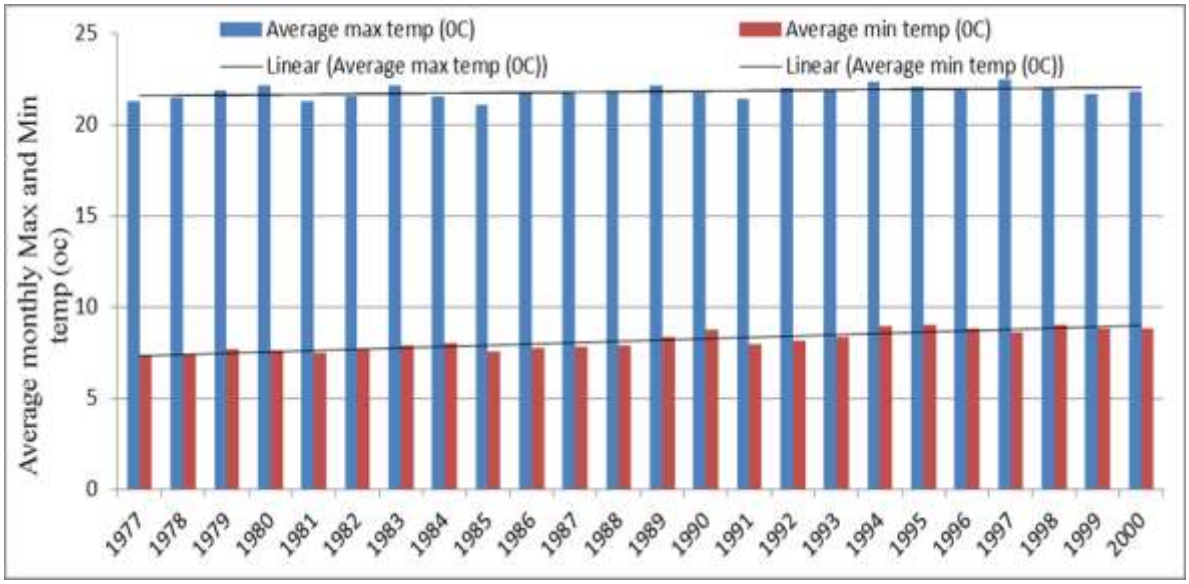

Figure 9.Observed Average Monthly Max and Min temperature at Robe Station (1977- 2000) (^{0}C).

These twoextreme values occurred due to the corresponding high values of precipitation (figure 7) in thesame years. The lowest flow of the River was recorded in the year 1980 (2.31m^3/s) and this alsocorresponds with the lowest value of precipitation within the same year. The trend line of theaverage monthly flow of the River also shows slight increments.

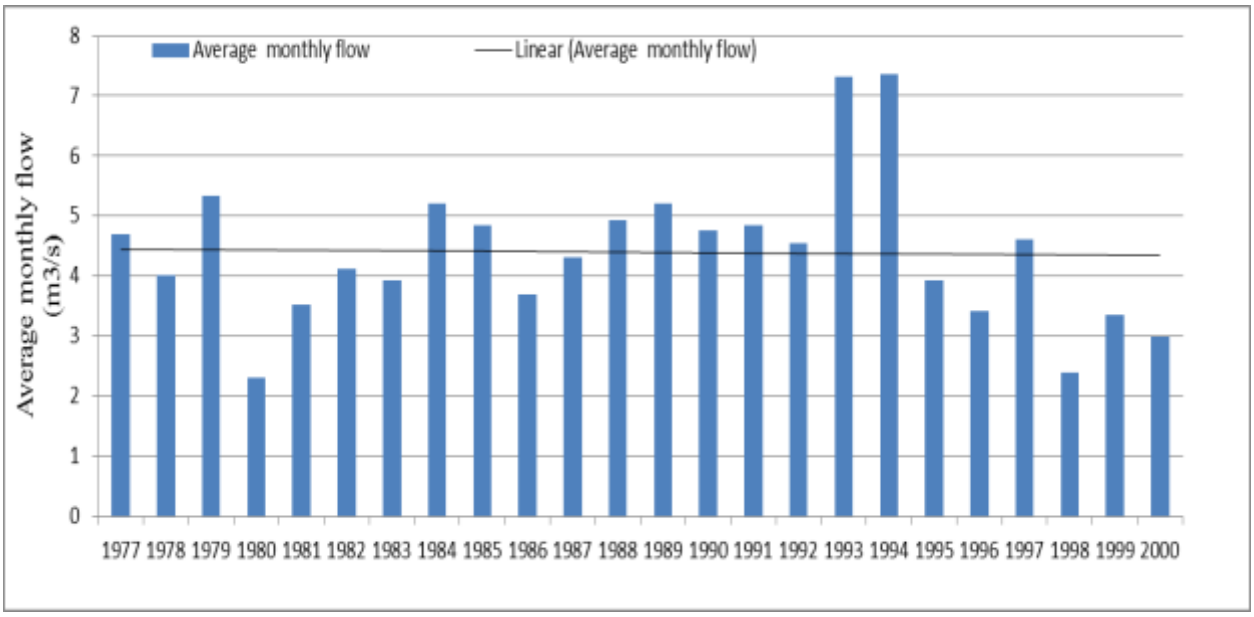

Figure 10.Observed Average Monthly Flows at Shaya River Gauge Station (1977-2000) (m^3/S)

Climate Change Model Outputs: Comparisons of the results of observed data among different stations for quality control, thecalibration and validation of SDSM model, selection of predictor variables and scenariogenerations for base period and for the future time period were discussed below.

Selection of Predictor Variables: The first step in the downscaling procedure using SDSM was to establish the empiricalrelationships between the predictand variables (minimum temperature, maximum temperature, and precipitation) collected from stations and the predictor variables obtained from the NCEP reanalysisdata for the current climate. It involves the identification of appropriate predictorvariables that have strong correlation with the predictand variable. The correlation matrixbetween predictor variables were used to investigate the association strength between them.

Higher value of correlation static's indicates strong association. Therefore, in the screening ofpredictor variables the partial correlation coefficients was used as selection criteria. Up to sixpredictors were selected at a time and analyzed to investigate the percentage of varianceexplained by specific

predictand–predictor pairs, then those predictors that have high explainedvariance was selected. Then after using the selected predictors the correlation matrix was done toinvestigate inter variable correlations for annual sub periods. Finally, predictors with better spatial and temporal correlations were selected.

Predictor variables that have better spatial and temporal correlation with the predictand at Robeweather station at significance level of less than 0.05 were presented in Table 5.

The application of these empirical predictor-predictand relationships of the observed climate is todownscale ensembles of the same local variables for the future climate. This is based on theassumption that the predictor-predictand relationships under the current condition remain validunder future climate conditions.

The Partial correlations indicate that on average relative humidity at 850 hPa has the strongestassociation with local precipitation once the influence of all other predictors has been removed, whereas maximum and minimum temperatures are strongly correlated with mean temperature at 2m, which shows their heavy dependence on regional temperatures.

Table 8.List of predictor variables that have better spatial and temporal correlation with thepredictands at Robe.

Predictands	Predictors/Notation	Descriptions	Partial r
	ncepr850af	Relative humidity at 850hPa	+0.35
	ncepp8uaf	850hPa zonal velocity	+0.03
Precipitation	Necptempaf	Mean temperature at 2 M	+0.024
	Necprhumaf	Near surface relative humidity	+0.3
	ncepr850af	Relative humidity at 850hPa	+0.13
	Necptempaf	Mean temperature at 2 M	-0.174
Maximum Temperature	Necpmslpaf	Mean sea level pressure	-0.068
	ncepp5_uaf	500hPa zonal velocity	+0.051
	Ncepshumaf	Surface specific humidity	-0.063
	necpp_zhaf	Surface divergence	+0.074
	necpp500af	500hPa geopotential height	+0.235
Minimum Temperature	necpp8_faf	500 hPa air flow strength	-0.103
	ncepp8zhaf	850 hPa divergence	+0.175
	Ncepshumaf	Surface specific humidity	+0.155

The partial correlation coefficient (r) shows the explanatory power that is specific to each predictor. All aresignificant at p = 0.05, hpa – is a unit of pressure, 1 hPa = 1 mbar = 100 Pa = 0.1 kPa

4.1. Calibration and Validation of SDSM Outputs

The calibration was done for the period of 10 years (1977-1986) at a monthly model type inorder to see the monthly temporal variations. Monthly precipitation, maximum temperature, andminimum temperature values were generated based on the above selected predictor variables ofthe NCEP data. Twenty ensembles (runs) were generated and the average of these ensembleswas taken as a simulated result for each predictand variable. The conditional and unconditionalprocesses were selected for daily rainfall and daily temperature (maximum and minimum) valuesrespectively and since for conditional processes in which the distribution of predictand values isskewed, the Fourth root transformations were applied. The calibration and validation statisticsfor all the three predictand variables after bias correction are shown in Table 6.

These results show that the simulated precipitation, maximum temperature and minimumtemperature have good agreements with the observed results. Precipitation is a conditionalprocess (dependent on other intermediate processes like on the occurrence of humidity, cloudcover, and/or wet-days) and high spatial variability. Due to this reason the calibration andvalidation results are comparatively less than the maximum and minimum temperature (Lijalem,2006, Dile*et al*, 2013). However for this study a good agreement between generated andobserved precipitation was resulted (R^2=0.67) during calibration and this might be due to lessspatial variability of precipitation on Shaya watershed. Hence the SDSM model resulted insatisfactory multiple regression equation parameters for precipitation, maximum and minimumtemperature (Table 6). Thus, it may be inferred that future projections may also be wellreplicated. However, the calibration results after bias corrections showed better agreements forall the three predictands, the model under estimates in some months and over estimates in someother months as shown in the figure 10 and 11. To correct this under/over estimation, a linearscaling bias correction method was applied and it perfectly matches the observed predictandswith generated values as shown in (table 6).

Table 9.Calibration statistics of daily precipitation, maximum temperature, and minimum temperature after bias correction at Robe Station with the Reanalysis data.

	Bias Corrected R^2	
Predictands	**Calibration**	**Validation**
Precipitation	0.67	0.98
Maximum Temperature	0.99	0.98
Minimum Temperature	0.99	0.99

Figure 10 (a, b) also shows the calibration results between observed and generated mean dailymaximum and minimum temperature after bias correction. As it can be shown in thefigure, the generated values of both maximum and minimum temperature have the same trendsas the observed values. For maximum temperature, the model slightly over estimates from month January, June and July and slightly under estimates in month February, May, August and September. While in the remaining months the generated and observed values are more or lesssimilar. The model also over estimates the minimum temperature inApril and May and under estimates in month January, March and October. While in the remaining months the values are more or less similar.

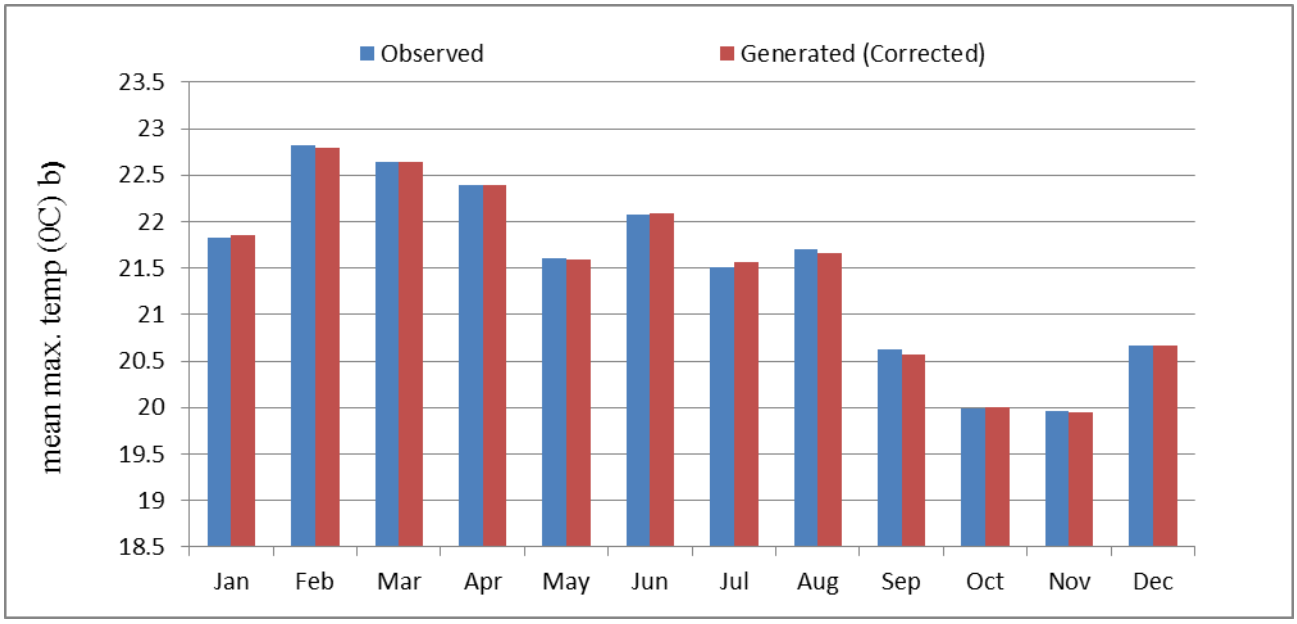

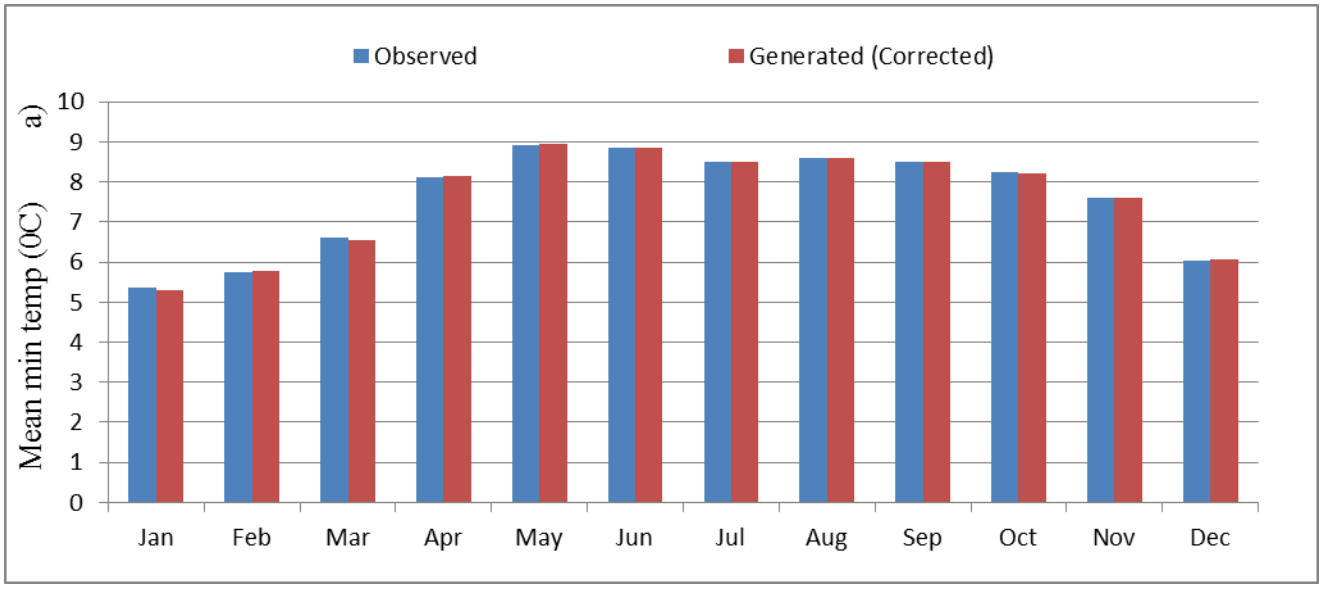

Figure 11.Calibration results after bias correction between observed and generatedmean daily maximum temperature (^0C) (a) and mean daily minimum temperature (^0C) (b), in the time step for the Robe station.

Figure 11 shows the calibration results of precipitation. As shown in the figure, the model slightly overestimates only in month June and underestimates in most of the other months. However, the overall agreement was good (Table 6)

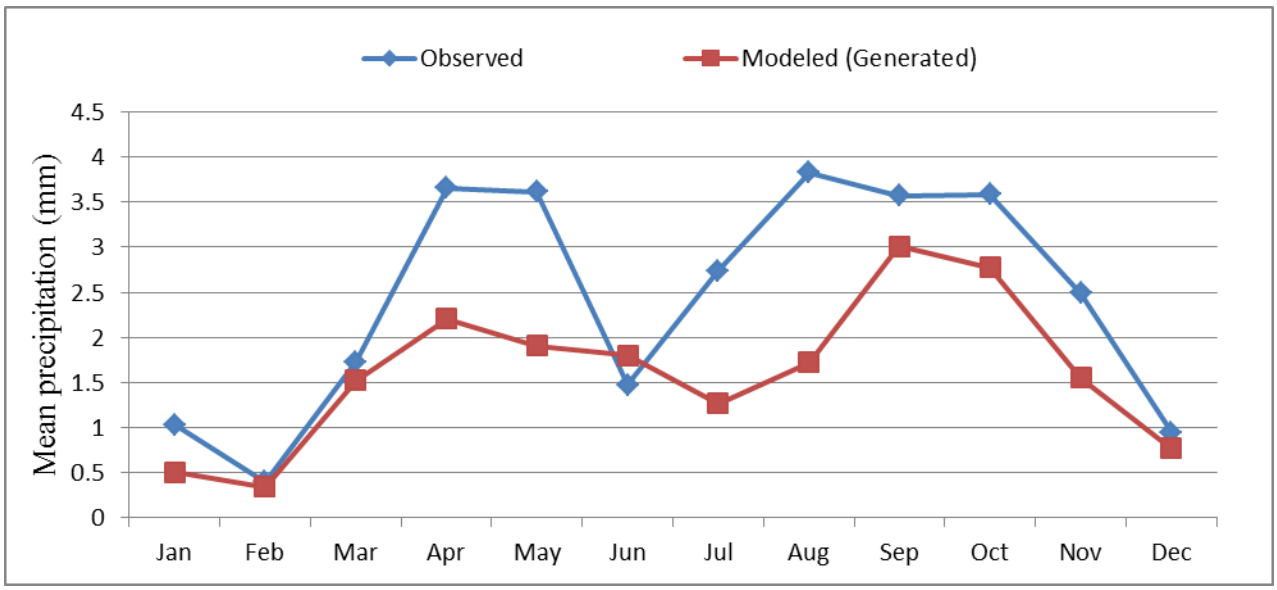

Figure 12.Calibration results between observed and generated mean daily precipitation (mm) in the time step for the Robe station.

Validation was done using an independent observed data for the period of five year from 1987 to 1991. Here also twenty ensembles (runs) of daily values were generated and the averages ofthese ensembles were taken for the comparison. The correlation coefficients after biascorrection that were found during the calibration are also maintained during the validation as shown in the Table 6. A good agreement was also found between the observed and simulatedprecipitation (R^2=0.98) though it is a conditional process and for minimum temperature (R^2 =0.99) duringvalidation.

The model underestimates the maximum temperature during validation in most of themonth except in the second moth (February) as compared to the observed data as shown in the figure 12 but the overall agreement between simulated and observed is good. In the month of April, May, August and October the simulation results were exceptional in which the model results were highlydeviated from the measured values in minimum temperature during validation. The model underestimates the precipitation

during validation in the most of the months. But this might be due to the conditional process ofprecipitation and its high temporal and spatial variability. However as that of calibration, thevalidation results also found to be good agreements between generated and observedprecipitation, maximum and minimum temperature which proofs the SDSM models ability togenerate weather variables for Shaya watershed under a given set of model parameters. As that of calibration, to correct the model errors the bias correction was applied and it perfectly matchesthe observed and generated values.

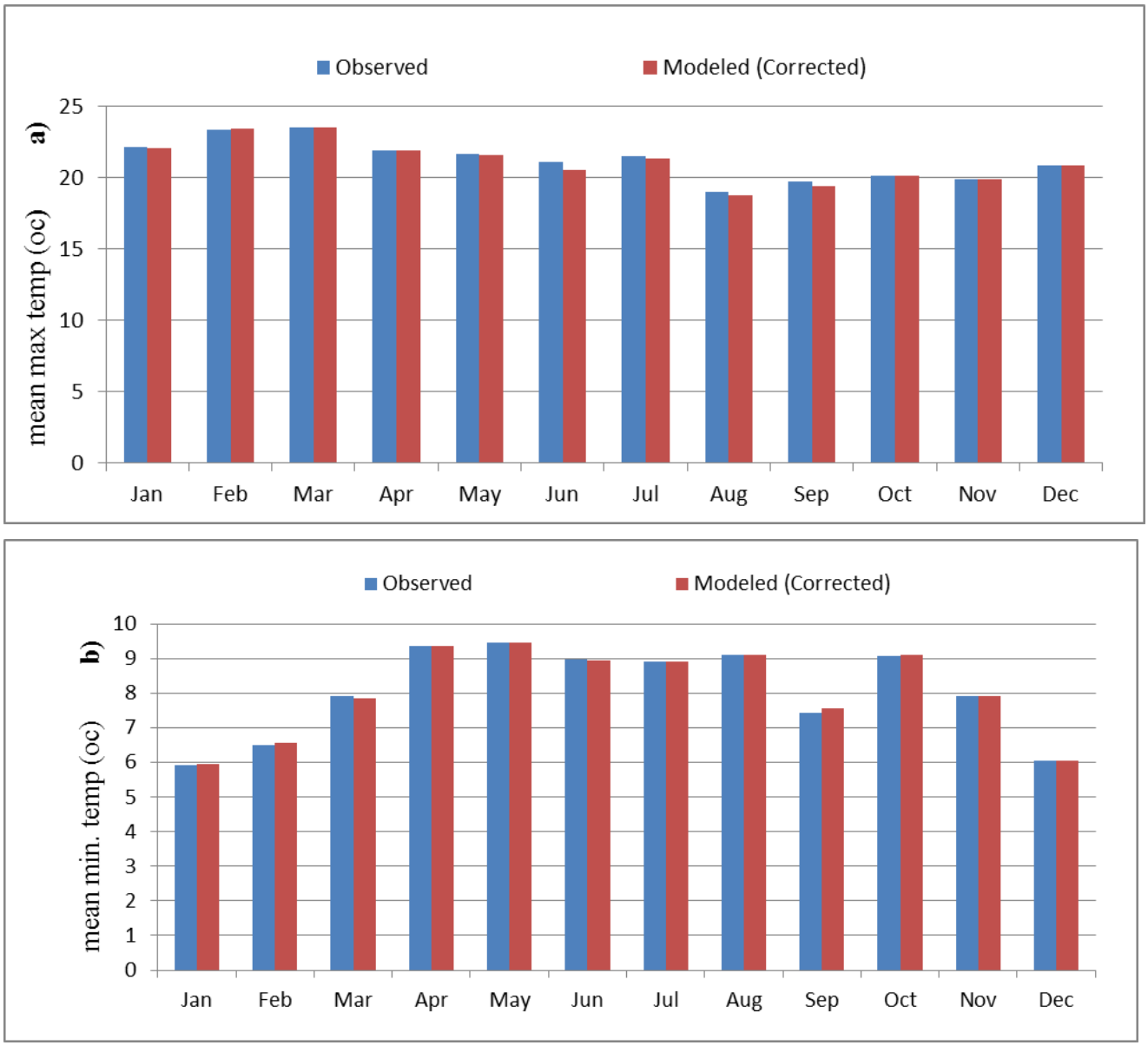

Figure 13.Validation results after bias correction between observed and generated mean daily maximum temperature (^0C) (a) and mean daily minimum temperature (^0C) (b).

4.3. Scenarios Generated

One of the criteria commonly used in evaluating the performance of any useful method is whether the historic condition can be replicated or not. For this study, theHadCM3A2a and HadCM3B2a were the two GCM output files used for the scenario generation. The regression weights produced during the calibration process were applied to the time seriesoutputs of the GCM model based on the assumption that the predictor-predictand relationshipsunder the current condition remain valid for future climate conditions.

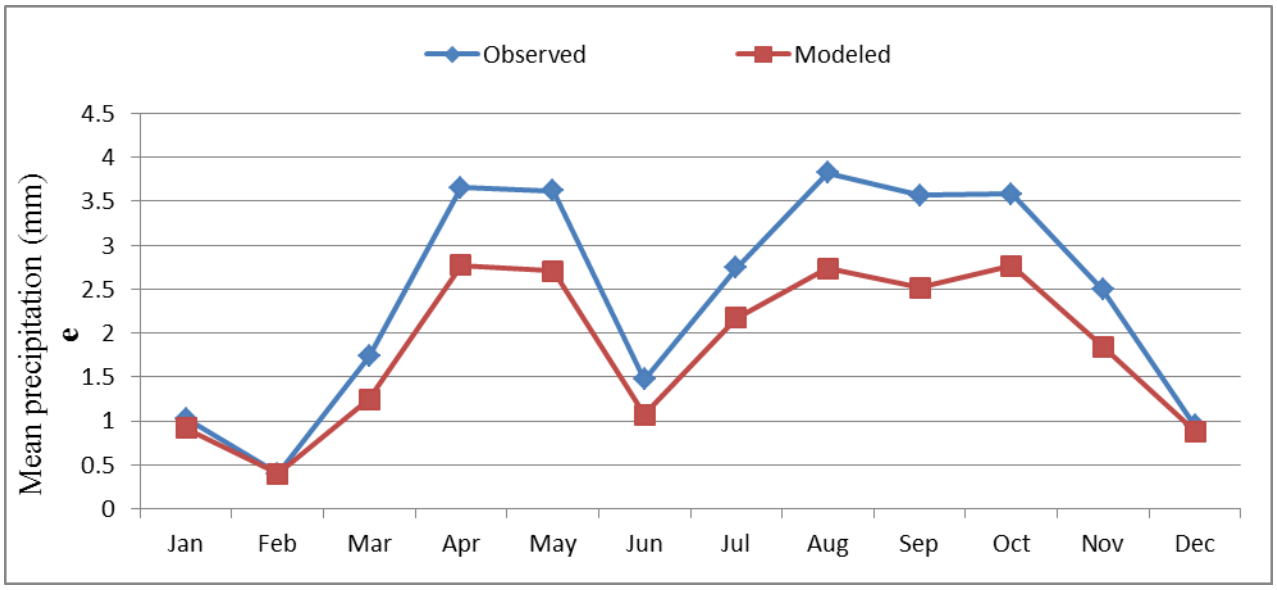

Figure 14. Validation results between observed and generated mean daily precipitation (mm) in the time step for the Robe station.

Twenty ensembles ofsynthetic daily time series data were produced for each of the two SRES scenarios for a period of 139years (1961 to 2099). Finally, the mean of the twenty ensembles for the specified period wasproduced for maximum and minimum temperature and precipitation

The climate scenario for the future period was developed from statistical down scaling using theGCM predictor variables for the two emission scenarios for 90 years based on the mean of 20ensembles and the analysis was done based on 30 years period from 2011-2040, 2041-2070 and 2071-2099. The IPCC recommends 1961-1990 as a climatological base period inimpact assessment. Hence, for this research the period from 1977-2000 was taken as a baseperiod. Likewise, (Wilby and Dawson, 2007) suggested

that Stationmeteorological data prior to 1st January 1961 or after 31st December 2000 will have no preparedpredictor variables.

4.3.1 Scenarios Developed for the Future periods (2011-2099)

For future scenarios, the climate signal (difference between future and baseline climates) wasfirst removed before the correction is adjusted. Then the future simulated results were added(temperature) and multiplied (precipitation) with the changing factor obtained in the baselinecorrection for each month. Then, initially removed climate signal is added back to create a biascorrected precipitation and temperature scenario for the future.

i. Maximum Temperature

The mean monthly and annual change in maximum temperature for the future period (2011-2099) for both A2a and B2a emission scenarios are shown in the figure 14. (a, b). As itcan be seen from figure, the overall results (2011-2099) for annual mean maximum temperatureshowed an increasing trend for both scenarios (A2a and B2a). During 2011-2099 the mean annualincrement of maximum temperature ranges between 0.17^0C (2011-2040) and 0.30 ^{0}C (2071-2099)for A2a emission scenarios while for B2a emission scenarios, itranges between 0.14^0C (2011-2040) and 0.26 ^{0}C (2071-2099) and the increment is not worth forboth scenarios based on IPCC-TGICA (2007) in which the globally averaged surface airtemperature is projected to warm 1.4 °C to 5.8°C by 2100.

Moreover, on monthly basis, the maximum temperature increases in February (2001-2099), August - November (2001-2099), in March (2011-2040) and in June (2011-2099) for both scenarios andthe increment was highest in September by 2.01^0C (2041-2099) for A2a scenario whereas for B2ascenario the highest increment was found in the same month (September) by 1.71^0C(2071-2099). Additionally in A2a scenarios the maximum temperature increases in March (2041-2070).

In January (2011-2099), March (2071-2099), April-May (2011-2099) and in December (2011-2099) maximum temperature shows a decreasing trend from 0.21-0.40^0c (2011-2099), 0.03^0c (2071-2099), 0.38-0.64^0c (2011-2099) and in 0.2-0.25^0c (2011-2099) respectively for A2a scenario.

In addition in January (2011-2099), March (2041-2099), April-May (2011-2099) and in December (2011-2099),maximum temperature shows a decreasing trend from 0.14^0c-0.35^0c (2011-2099),in 0.04 ^{0}c (2041-2099), 0.49-0.64^0c (2011-2099) and 0.18-0.29^0c (2011-2099) for B2a scenario respectively. The maximum temperature increases almost in equal proportions in July for allfuture periods. Monthly and annual increase in maximum temperature for A2a scenario is greater thanB2a scenario because A2a

scenario represents medium to high scenario which produces moreCO2 concentration than B2a scenario which represents low to medium emission scenarios.

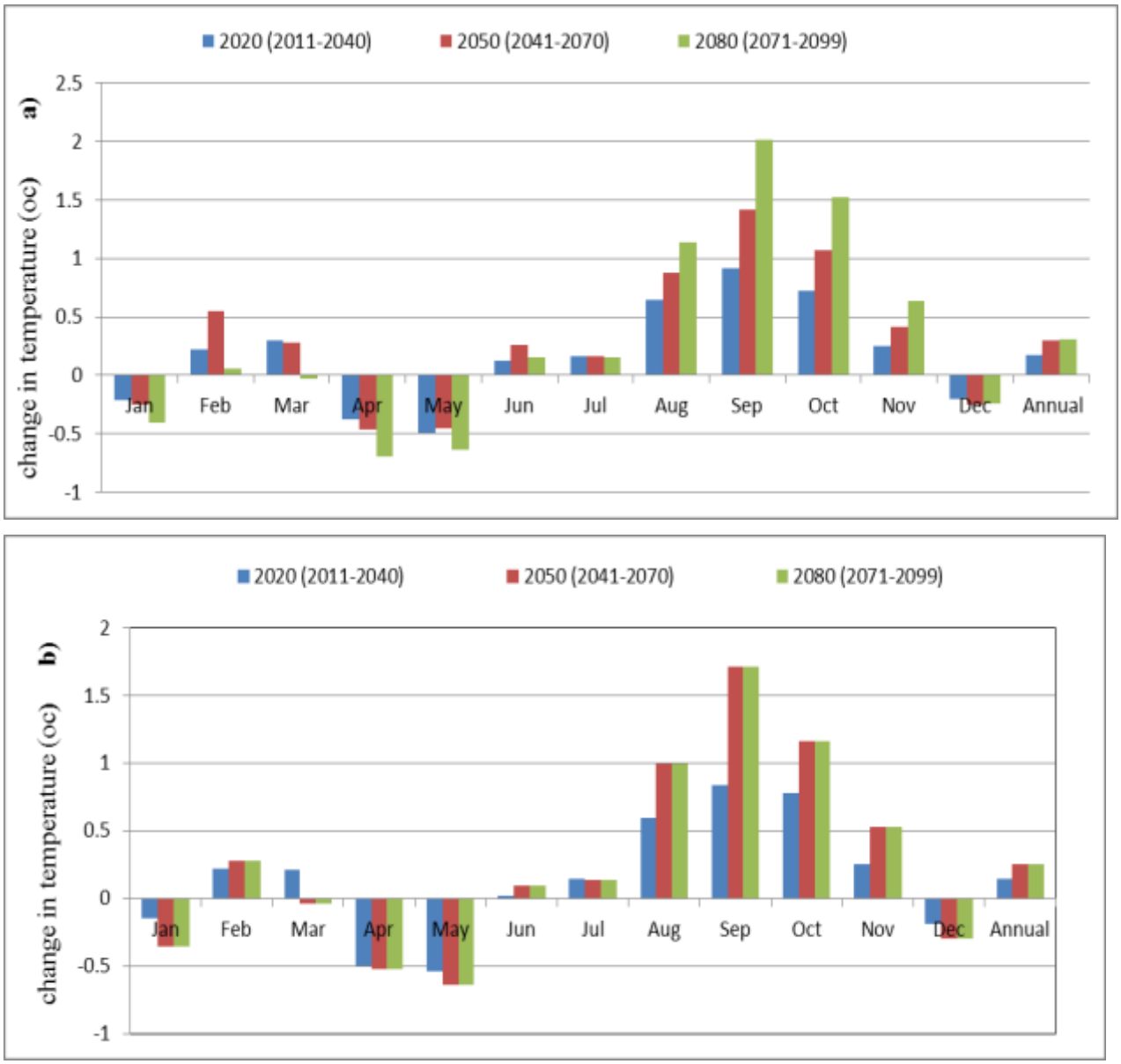

Figure 15.Change in average monthly and annual maximum temperature in the future (2011- 2099) for A2a scenario (a) and B2a scenario (b) from the base period.

Figure 15 shows the general trend of maximum temperature for the future periods as comparedto the base period. The figure 4.9 reveals that even though the increase or decreases ofmaximum temperature are not systematic on monthly and seasonal basis (figure 14., a & b), theaverage annual maximum

temperature shows a slightincrement trend for the future period for bothA2a and B2a scenarios and the trend line shows positive relation.

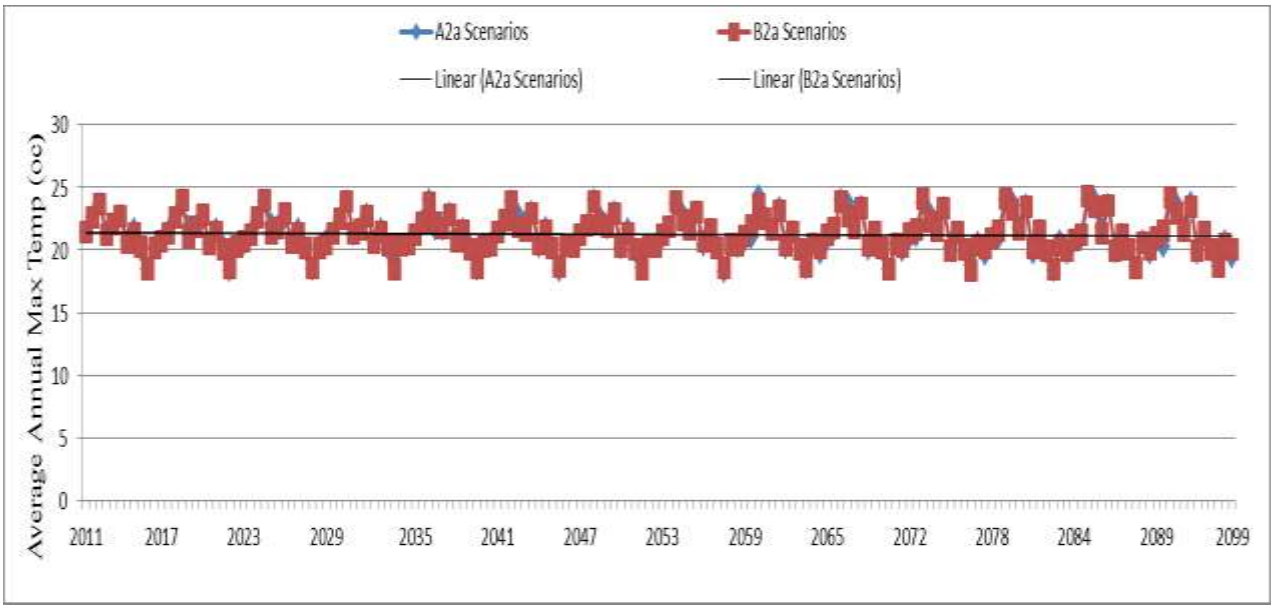

Figure 16.Trend of downscaled maximum temperature (2011-2099).

ii. Minimum Temperature

Figure 16. (a, b) shows the mean monthly and annual changes of minimumtemperature for the future periods (2011-2099) for the two emission scenarios (A2a and B2a) ascompared to the base period. The minimum temperature shows increasing trends for the future periods (2011-2099) in January (2041-2099), in march (2011-2099), in April (2011-2040), in June (2011-2099), in August (2071-2099), September (2041-2099) and December (2071-2099 for both A2a and B2a emissionscenarios except in December in which the temperature shows a decreasing trend from the period 2041- 2070 and a slight increment of the same period in B2a and A2a scenario respectively. The minimum temperature decreases almost in equal proportions in July for allfuture periods.

The increment of minimum temperature varies from 0.93-2.55^{0}C in January (2041-2099), 0.16-0.86^{0}C in March (2011-2099), 0.18^{0}C in April (2011-2040), 0.10-0.51^{0}C in June (2011-2099), 0.32^{0}C in August (2071-2099), 0.25-0.69^{0}C in September (2041-2099) and 0.09-1.09^{0}C in December (2072-2099) for A2a scenario. For B2a scenario it varies from 0.36-1.47^{0}C in January (2041-2099), 0.27^{0}C -0.72^{0}C in March (2011-2099), 0.12^{0}C in April (2011-2040), 0.02^{0}C-0.40^{0}C in June (2011-2099), 0.05^{0}C in August (2071-2099), 0.13^{0}C- 0.39^{0}C in September (2041-2099) and 0.35^{0}C in December (2041-2070).

InJanuary the increment of minimum temperature is higher for the period 2071-2099, while in May and November the minimum temperature is extremely decreasing from the period (2071-2099) forboth scenarios.

The decreasing of minimum temperature varies from 1.04^0C-1.4^0C in February (2011-2099), 0.32^0C in January (2011-2040), 0.27^0C to 3.37^0C from April (2041-2099) –May (2011-2099), 0.2^0C-0.3^0C in August (2011-2070), 0.07^0C in September (2011-2040), 1.17^0C to 3.38^0C fromOctober-November (2011-2099) and 0.4^0C-0.5^0Cin December(2011-2040) the minimum temperaturedecreases with different ranges ascompared to the base period for A2a scenarios.

For B2a scenario the decrements of the minimum temperature varies from 0.94^0C-1.11^0C in February (2011-2099), 0.33^0Cin January (2011-2040), 0.16^0Cto 2.38^0Cfrom April (2041-2099)-May (2011-2099), 0.09^0C-0.25^0Cin August (2011-2070), 0.07^0Cin September (2011-2040), 1.2^0C to 2.69^0Cfrom October-November (2011-2099) and 0.4^0C-0.5^0Cin December (2011-2040). The overall results (2011-2099) for annual mean minimum temperature decreases forboth scenarios (A2a and B2a).

Figure 17. Shows the future trend of minimum temperature. As shown in the figure, there arehigh fluctuation of minimum temperatures for both A2a and B2a scenarios. However, the overallaverage annual minimum temperature shows a slight increasing trend line for the future timeperiod.

iii. Precipitation

As it can be seen from the figure 18 (a, b) the overall results (2011-2099) for annual percentagechange in precipitation showed a slight decrement trend for both scenarios (A2a and B2a). The decreasing trend of annual percentage change of precipitation ranges from 5.77% (2041-2099) to 0.33% (2071-2099) for A2a scenario and for B2a scenario the decrement ranges between 7.10% (2041-2099) and 6.01% (2071-2099). As described in the IPCC Third Assessment Report (McCarthy *et al*., 2001), the projected future changes in mean seasonal rainfall in Africa are less well defined. The diversity of African climates, high rainfall variability, and a very sparse observational network make the predictions of future climate change difficult at the sub regional and local scales.

On monthly basis, the percentage change in precipitation is not systematic i.e. precipitationincreases in some months and decreases in some other months. The percentage changes inprecipitation increases from January-May, in August and in November (2041-2099) and decreases from June-July, from September-November (2011-2040) and in December for the future (2011-2099) periods as compared to the base period.

Theincrement is most dramatic in March from the period 2071-2099 for A2a and from the period (2041-2070) for B2a scenariosin which the precipitation increases by 146.84% and 143.59% respectively.The decrease inprecipitation reaches to a maximum of 99.0% (2071-2099) for A2a scenario and 95.36% (2071-2099) for B2a scenario.

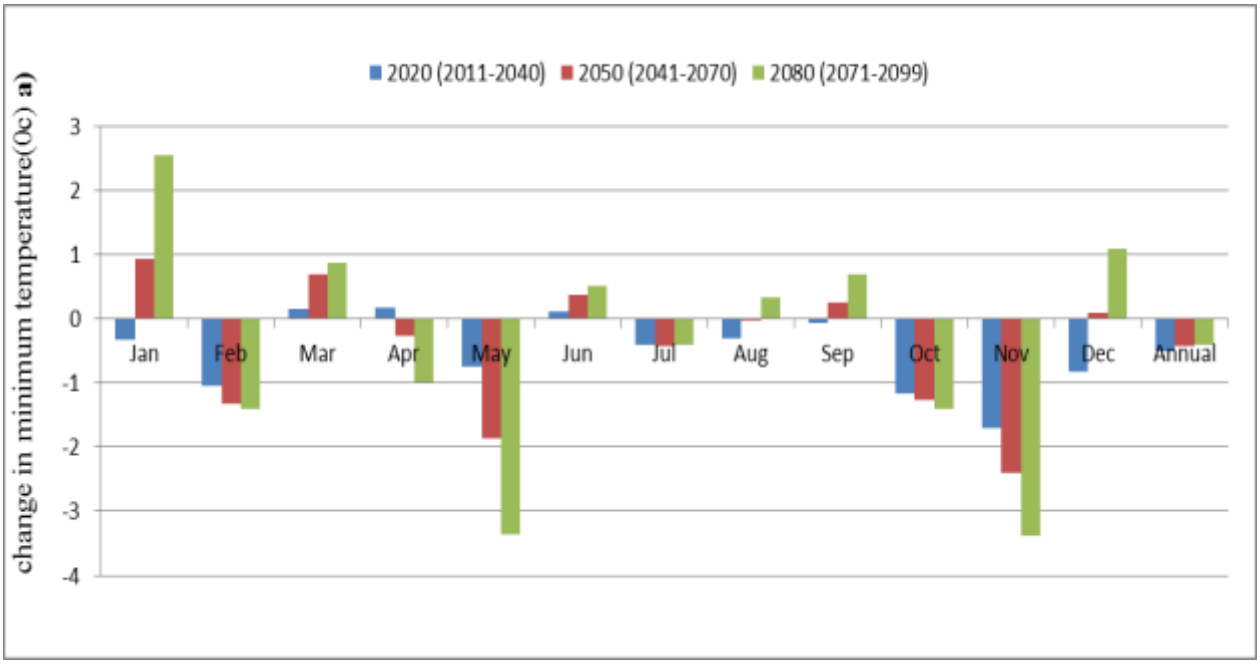

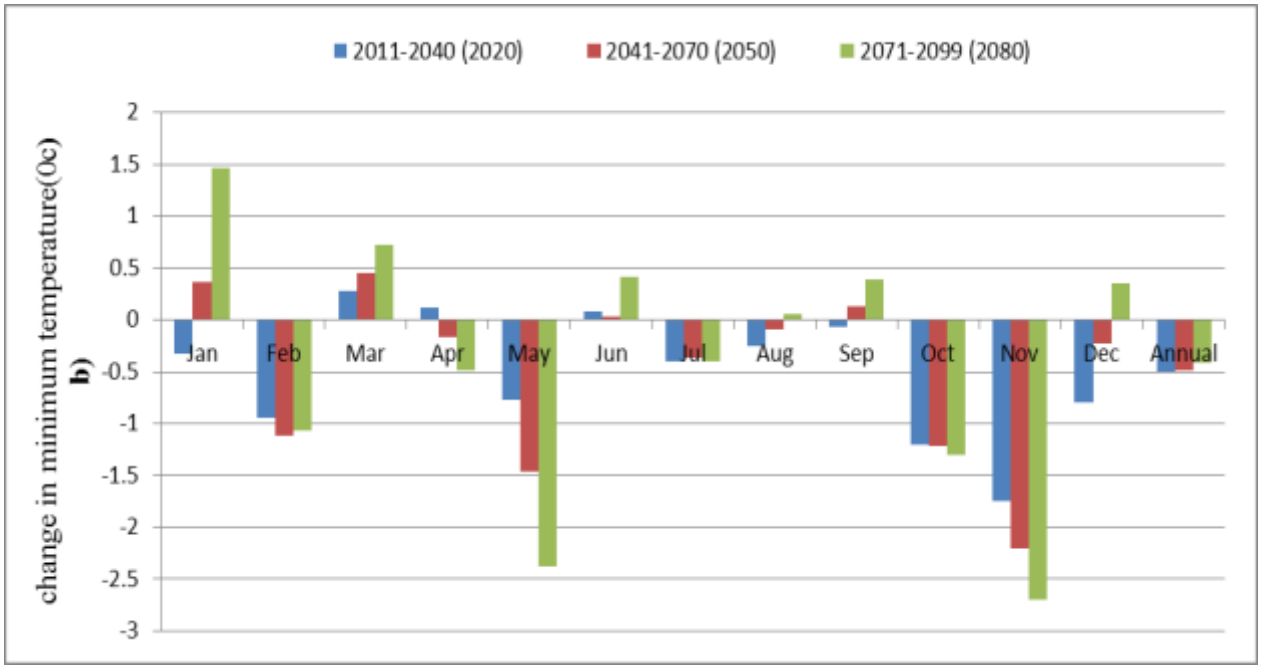

Figure 17.Change in average monthly and annual minimum temperature in the future (2011- 2099) for A2a scenario (a) and B2ascenario (b) from the base period.

In East Africa, Faramarzi*et al*. (2013) report a generallywetter climate and a large spatial variation from a decrease of 25–50% to an increase of 25–50%. Generally, increase of rainfall comparatively higher in the Dry season which might have positive impact on pastoral region of the study area and it might affect the highland areas negatively due to this season is specifically main crop harvesting period.

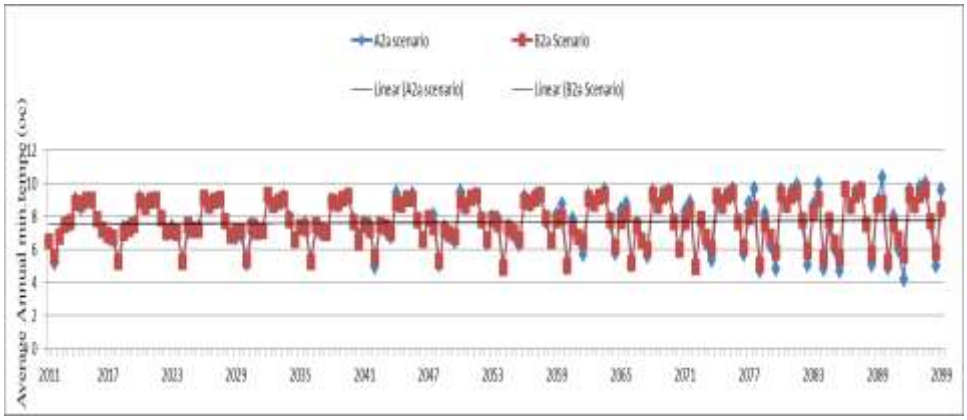

Figure 18.Trend of downscaled minimum temperature (2011-2099).

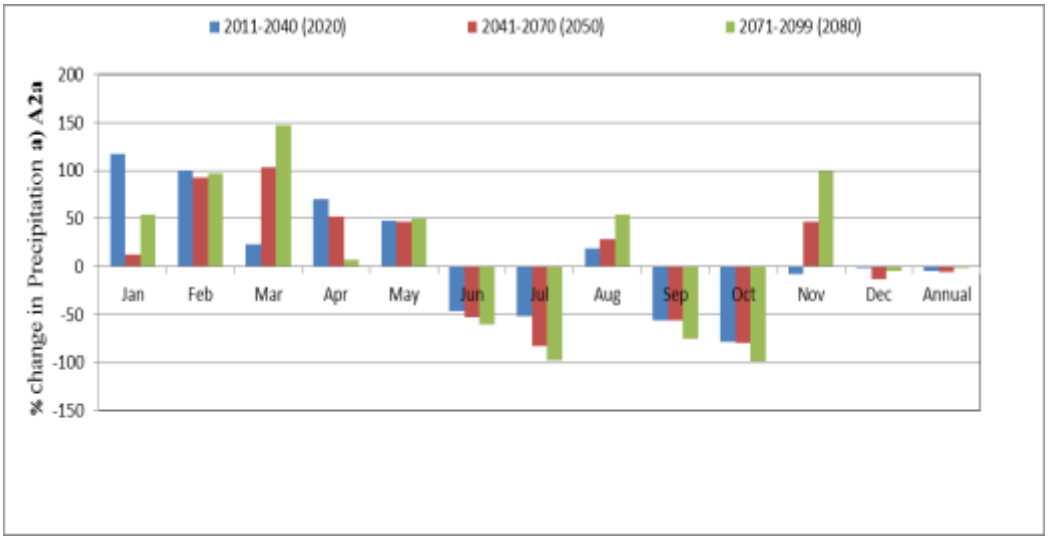

Figure 19.Percentage Change monthly and annual precipitations in the future (2011- 2099) for A2a scenario (a) and B2ascenario (b) from the base period.

The generated future scenarios for annual precipitation generally show a slight decrement trend withrespect to the base period and this is also in line with the previous third assessment reports of IPCC (McCarthy *et al*., 2001).

5. Conclusion

The tremendous importance of water in both society and nature underscores the necessity ofunderstanding how a change in global climate could affect the availability and reliability of waterresources at a catchment scale. Human beings, at the larger scale, are vulnerable to climatechange as recurrent floods and droughts continue to bring misery and keep on claiming manylives all over the world. Regarding to the design and management of water resource systems, it isrequired to make indicative predictions of the impacts of climate change on the spatial andtemporal variability of rainfall and temperature and their influences on stream flows.

6. Recommendation

Water resources are vulnerable and have the potential to be strongly impacted by climate change, with wide-ranging consequences for human societies and ecosystems. Precipitation andtemperature are highly affected by climate changes and in turn, the change of these climaticvariables affects the stream flows, the recurrent floods and droughts. Hence, it is recommendedto intensify such kind of researches at the catchment level to give insight for decision makers, planners and stockholders.

References

Bale Mountains National park general Management Plan (BMNP GMP). (2007) Bale Mountains National Park General Management Plan.(Frankfurt Zoological Society, eds.), Ethiopia.

Conway and E. Lisa,2010. Adaptation to climate change in Africa: Challenges and opportunities identified from Ethiopia, a School of International Development, University of East Anglia, UK Tyndall Centre for Climate Change Research, University of East Anglia, UKc Stockholm Environment Institute, Bangkok, Thailand.

Davidson, O., K. Halsnaes, S. Huq, M. Kok, B. Metz, Y. Sokona, and J. Verhagen. 2003. The development and climate nexus: the case of sub-Saharan Africa. Climate Policy 3S1: S97-S113

Degefu, Workineh. 1987. 'Some aspects of meteorological drought in Ethiopia.' In Michael H.Glantz (Ed), *Drought and Hunger in Africa*. Cambridge: Cambridge University Press.

Dile YT, Berndtsson R, Setegn SG, 2013. Hydrological Response to Climate Change forGilgelAbay River, in the Lake Tana Basin - Upper Blue Nile Basin of Ethiopia. PLoSONE 8(10): e79296. Doi: 10.1371/journal.

DilnesawAlamirew, 2006. Modeling of Hydrology and soil Erosion of Upper AwashRiver Basin.PhD Thesis, University of Bonn.

Faramarzi M. , Abbaspour K. C., Vaghefi S. A., Farzaneh M. R., Zehnder A.B., Srinivasan R. and Yang H. (2013). Modeling impacts of climate change on freshwater availability in Africa. *J. of Hydrology* 480 (2013) 85–101.

Farm Africa-SOS Sahel Ethiopia, 2007.Participatory Natural Resource Management Programme and Oromia Bureau of Agriculture and Rural Development, Six Months Report. 45p.

Gissila, E. Black, D. I. F. Grimesc and J. M. Slingo,2004. Seasonal forecasting of the Ethiopian summer rains, a *National Meteorological Services Agency, Addis Ababa, Ethiopia,* b *Centre for Global Atmospheric Modelling, University of Reading, Reading, UK,* c *Department of Meteorology, University of Reading, Reading, UK.*

HailemariamKinfe, 1999. Impact of climate change on the water resources of Awash River Basin, Ethiopia.*Climate Research Journal*, 12: 91-96.

LijalemZeray, 2006. Climate change impact on Lake Ziway watershed water avialability, Ethiopia. MSc Thesis. University of applied sciences Cologne, Germany. 123p.

McCarthy, J. J., Canziani, O. F., Leary, N. A., Dokken, D. J. & White, K. S. (2001). Climate Change 2001: Impacts, Adaptation, and Vulnerability Contribution of Working Group II to the Third Assessment Report of the Intergovernmental Panel on Climate Change.

Neitsch S.L., J.G. Arnold, J.R. Kiniry, J.R. Williams, 2009. Soil and Water Assessment Tool (SWAT). Theoretical Documentation, Version 2009, Grassland Soil and Water Research Laboratory, Agricultural Research Service, Black land Research Center, TexasAgricultural experiment Station.

NMA. 2006. National Adaptation Programme of Action of Ethiopia (NAPA). National Meteorological Agency, Addis Ababa.

Shawul A. Alemayehu, Alamirew, T., and Dinka, M. O. (2013). Calibration and validation of SWAT model and estimation of water balance components of Shaya mountainous watershed, Southeastern Ethiopia, Hydrol. Earth Syst. Sci. Discuss., 10, 13955-13978, doi:10.5194/hessd-10-13955-2013.

Wilby, R.L. and Dawson C.W., 2007. Statistical downscaling model (SDSM 4.2) – A decision support tool for the assessment of regional climate change impacts, version 4.2, user's

Hydrological Responses of Climate Change on Lake Ziway Catchment, Central Rift Valley of Ethiopia:

Tesfalem Abraham[a*], Brook Abate[b], Abraham Woldemicheal[a]and Alemayehu Muluneh[a]

[a]School of Biosystems and Environmental Engineering, Hawassa University, EthiopiaP.O. Box. 05, Hawassa, Ethiopia., [b]School of civil and construction technology, Addis Ababa Science and Technology University, P.O. Box. 1176, Addis Ababa, Ethiopia.

*Correspondence to: Tesfalem Abraham, School of Biosystems and Environmental Engineering, Hawassa University, Ethiopia, Tel: +251 960956896; E-mail: atesfalem@gmail.com P.O. Box. 05, Hawassa, Ethiopia

Abstract

This study predicts future runoff conditions under changing climate using multi model outputs from Coupled Model Intercomparison Project Phase 5 (CMIP5) over Lake Ziway Catchment in the Central Rift Valley of Ethiopia. Bias corrected precipitation, maximum and minimum temperature data from HadGEM2-ES, CSIRO-MK-3-6-0 and CCSM4models under representative concentration pathways RCP8.5 and RCP4.5 were used as future climate. Soil and Water Assessment Tool (SWAT)is used to simulate the future inflows from Katar River and Meki River towards Lake Ziway. Maximum and minimum temperature increased under RCP8.5 and RCP4.5 scenarios however, precipitation showed reduction. The percentage change in monthly average precipitation showed extremes for HadGEM2-ES model which range between -51.19% during 2050s and +23.15% during 2080s under RCP8.5. The model output showed an annual decrement in runoff depth from Katar River up to 19.45% on RCP8.5 on CSIRO MK-3-6-0 model and maximum reduction was recorded on RCP4.5 at 17.49% for CCSM4 model. Meki River showed maximum annual reduction of 20.28% during 2080s on RCP8.5 for HadGEM2-ES model. Due to future reduction of River flow on the region optimal allocations for water use purposes at all levels of water resource development projects are crucial for future water planning and management.

Key words: CMIP5; Lake Ziway Catchment; RCP; Runoff Estimation; SWAT model.

1. Introduction

In recent decades, changes in climate have caused impacts on natural and human systems onall continents and across the oceans. Whatever its cause, natural and human systems have become sensitiveto climate change (IPPC, 2014). Increased anthropogenic activities on industries and population expansion towards forested areas has increasedthe concentration of carbon dioxide on Earth's atmosphere hasraised global surface temperature andaffected precipitation amount (IPCC, 2014;NASA, 2010).

Lake Ziway serves for wide range of socio-economic activity in Ethiopia. Different water use sectors have recently increased their pressure on the water balance of Lake Ziway which is recharged by precipitation and two rivers namely Katar and Meki Rivers.Climate variability in the frequency and intensity of extreme events over the Ethiopian Rift Valley (Legesse et al., 2010; Mechal et al., 2015)has increased due to climate change. Changes in flow magnitude, variability on long-term mean annual stream flow and water availability issues in the regionhave been studied frequently (Seyoum et al., 2015; Ayenew, 2007; Alemayehu, 2006; Legesse et al., 2010).Existing studies have focused on IPCCs fourth assessment report to assess the future water potentials and little is known about the potential impacts on River flows from the Climate Model Intercomparison Project Phase 5 archive (CMIP5) outputs (Taylor et al., 2011).

Possible future changes in the precipitation and temperature extremes can be predicted by global circulation models (GCMs) (Gebre et al., 2015). On the Central Rift Valley, GCM simulations for daily data was collected from the Climate Model Intercomparison Project Phase 5 archive (CMIP5) (Taylor et al., 2011). These downscaled data provide a basis of Intergovernmental Panel on Climate Change (IPCC) Fifth Assessment Report (AR5). Representative concentration pathways (RCP) have beenalso introduced in the CMIP5 ensemble data, which are more comprehensive than Special Report on Emission Scenarios (SRES).

Lake Ziway catchment covering a total area of about 6991 km^2 contains Lake and River systems, where two Rivers namely Katar and Meki flowing towards Lake Ziway and one outflow River Bulbula flowtowards Lake Abiyata. The flow scheme in the region passes through a densely populated area where water use for commercial farming, fishing and recreation by state and private sectors is gigantic. The outflow of Lake Ziway is an important source of the downstream terminal Lake Abiyata, whose quantity and quality is controlled by the outflow from Lake Ziway(Seyoum et al., 2015).Evaluation of climate change impacts on regional hydrology would greatly benefit policy makers and other stakeholders for better preparedness in the region. In this study, we used bias corrected climate model output of CMIP5 ensembles (HadGEM2-ES, CSIRO-MK-3-6-0and CCSM4) for simulation of river flows for impact evaluation. Soil and Water Assessment Tool (SWAT) (Arnold et al., 1998; Neitsch et al., 2011) was tested over Lake Ziway catchment to generate future inflows under RCP 4.5 and RCP 8.5scenarios for Katar and Meki Rivers respectively, using sequential uncertainty fitting algorithm (SUFI-2) (Abbaspour, 2013) and impact analysis was made using metrics that are useful for decision makers.

2. Materials and Methods

2.1.Study Area

Lake Ziway is located between 7°51'N to 8°7'N Latitude and 38°43'E to 38°57'E Longitude. It has an open water area of 434 km^2 with an average depth of 4 m and an elevation of 1636 m.a.s.l. Lake Ziway catchment falls in between 7°15'N to 8°30'N Latitude and 38°E to 39°30'E Longitude covering a total area of about 6991 km^2 (Figure1).

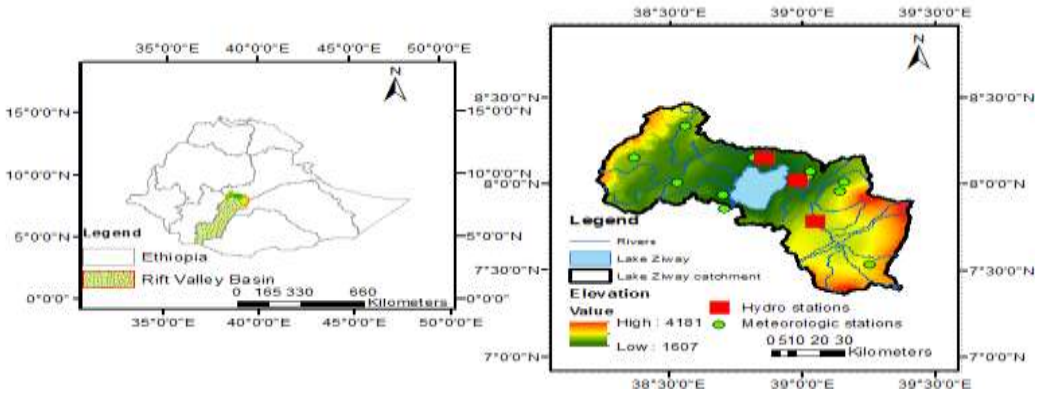

Figure 1: The study area showing the rift valley basin, lake Ziway, lake Ziway catchment with hydro meteorological gauging locations and rivers.

It starts from the highlands of the Eastern part from which Meki River is originating, passes through the central parts of the East Shoa Zone where the Lake Ziway is located, and ends up in the Western Highlands of the Arsi Zone from which the Katar River is originating.

2.2.Climate projection

Horizontally gridded CMIP5 model group outputs were employed to predict the past and the future climatic conditions of the area. Observed precipitation and temperature dataset at monthly time scale from 1980 to 2005 are downloaded from the model group web pages (https://climexp.knmi.nl/select.cgi). Coupled model output data (precipitation and surface air temperature) of a historical run from 1850 to 2005 and two future projection simulations from 2010 to 2099 under two Representative Concentration Pathways were obtained. The RCP4.5 represents a moderate mitigation scenario (van Vurren et al., 2011), while RCP8.5 represents the higher stabilization pathway, where wider range of radiative forcing across the RCP extensions are provided (Moss et al., 2010). Hence RCPs are required for planning the adaptation and mitigation option for the response of river flow by changing climate.

Outputs of coupled climate models, three GCMs were employed over Lake Ziway catchment, as shown in Table 1.The selection of the GCM model was based on how well models represent the past and the present climate, their resolution and other studies related to the impact of climate change on the Ethiopian Rift

Valley and adjacent plateau.HadGEM2-ES, CSIRO-MK-3-6-0and CCSM4 models are recognized as being capable of reproducing the precipitation and temperature pattern on the Ethiopian Rift(Asaminew et al., 2017; Negash et al., 2013; Jury, 2015).

The daily precipitation, Tmax and Tmin from 1980 to2099, was extracted from grid cells covering Lake Ziway Catchment. The period from 1980 to 2005 was defined as the baseline period. While the future periods that are covered by this study are 2010–2040, 2041–2070, and 2071–2099 (denoted by the 2020s, 2050s, and 2080s, respectively) relative to the baseline period (1980–2005).Future climate time series were constructed using the delta change method (Fowler et al., 2007; Biniyam, 2017) which involves observed climate time series by mean changes (differences or ratios of changes) simulated with GCMs. The changes were determined as monthly temperature changes (in °C) and monthly precipitation changes (in %) from the base period (1980-2005) values.

CMIP5 GCM models were selected based on how well models represent the past and the present climate. Inthis regard bias correction of precipitation data has employed a nonlinear methodwhich corrects coefficient of variation (CV) and the mean (Kahsay et al., 2018) Eqn. (1) while temperature correction isdone by calculating monthly systematic biases (Biniyam, 2017; Negash et al., 2013) Eqn. (2).

$$P^* = aP^b \quad (1)$$

Where; P* is the simulated data in the projection period, where ‘a’ and ‘b’ are the parameters obtained from calibration in the baseline period and subsequently applied to the projection period. They are determined by matching the mean and coefficient of variation (CV) of simulated data with that of observed data.

$$Tc = Tom + \frac{\partial o}{\partial r} * (Tr - Trm) \quad (2)$$

Where; Tc is bias corrected future temperature, Tom is mean of observedtemperature in base period, Trm is mean of RCPs temperature in base period and Tr is RCPs temperature of base period δ_r, and δ_o, represent the standard deviation of the daily RCPs output and observations in the reference period respectively.

Table 1: Description of the climate models used in this study.

Model name	**Model center**	**Resolution (Lon* Lat)**
HadGEM2-ES	Hadley Centre for Climate Prediction and Research, Met Office, United Kingdom	1.875° * 1.25°
CCSM4	National Center for Atmospheric Research	1.25° * 0.9°
CSIRO-MK-3-6-0	Commonwealth Scientific and Industrial Research Organization, Australia	1.9° * 1.9°

2.3.SWAT model

SWAT model is a physically based distributed model designed to predict the impact of land management practices on water, sediment, and agricultural chemical yields in large complex watersheds with varying soil, land-use, and management conditions over long periods of time (Neitsch et al., 2011). SWAT divides the catchment into a number of sub watersheds or sub-basins. Sub-basins are further partitioned into hydrological response units (HRUs) based on soil types, land-use types, and slope classes that allow a high level of spatial detail simulation, where HRUs consist of unique combinations of homogenous soil and land use properties in each sub-basin (Arnold et al., 2012). The model predicts the hydrology at each HRU using the water balance Eqn. (3).

$$SWt = SWo + \sum_{i=1}^{t}(Rday - Qsurf - Ea - Wseep - Qgw) \quad (3)$$

where SWtis the final soil water content (mm H2O), SWo is the initial soil water content on day i(mm H_2O), t is the time (days), Rdayis the amount of precipitation on day i(mm H_2O), Qsurfis the amount of surface runoff on day i(mm H_2O), Eais the amount of evapotranspiration on day i(mm H_2O), *W*seepis the amount of water entering the vadose zone from the soil profile on day i(mm H_2O), and Qgwis the amount water return flow on day i(mm H_2O).

A detail description of the different model components can be found in the SWAT Theoretical Documentation (Neitsch et al., 2011). The input data required for SWAT include weather data (1993-2013), a land-use map, a soil map, a Digital Elevation Map (DEM) (Table 2). Discharge data are also required for calibration of streamflow. Monthly flow data (1993-2007) measured at the Katar river, and Meki were used for the calibration of streamflow. This data was obtained from the Hydrology Department of MoIWE.

Table 2: Data sources used in the initial setup of the SWAT model for the Lake Ziway Catchment.

Data type	Data description	Scale	Data sources
Topography	Elevation	20 m	Aster GDEM
Land-use	Land-use classification such as agricultural land, forest, and urban	1 km	MoIWE
Soil	Soil types and physical properties	10 km	FAO
Meteorology	Daily precipitation, minimum and maximum temperature, relative humidity, radiation	Daily	NMSA

2.4.SWAT-CUP model

The SWAT-CUP tool (SWAT Calibration and Uncertainty Procedures) is a program that interfaces with ArcSWAT, to perform calibration, validation and sensitivity analysis of the SWAT model. The execution of the SWAT-CUPmodel involves the use of output files generated by SWAT model inArcSWAT (Abbaspour, 2011). From the five different algorithms associated to SWAT, the SUFI-2 strategy is applied in this research since it cansupply the widest marginal parameter uncertainty intervals ofmodel parameters. The goodness of fitin SUFI-2 is quantified by the coefficient of linear correlation (R^2), the coefficient of Nash-Sutcliffe efficiency (NSE) and the coefficient of Percent bias (PBIAS) between the observed data and the best simulation. The formulas of these coefficients are given in the following equations:

$$R^2 = \frac{(\sum[Qsi - Qsi_{av}][Qob - Qob_{av}])^2}{\sum[Qsi - Qsi_{av}]^2 \sum[Qob - Qob_{av}]^2} \quad (4)$$

$$NSE = 1 - \frac{\sum(Qob - Qsi)^2}{\sum(Qob - Qob_{av})^2} \quad (5)$$

$$PBIAS = \frac{\sum_{i=1}^{n} Yi^{obs} - Yi^{sim}) * 100}{\sum_{i=1}^{n} (Yi^{obs})} \quad (6)$$

NSE is a normalized dimensionless statistic that implement the comparative size of the residual distinction compared to the measured data variance- (Nash & Sutcliffe, 1970). It shows how well the plot of observed versus simulated data fits the 1:1 line. PBIAS measures the average tendency of the simulated data to be larger or smaller than their observed counterparts (Gupta et al., 1999). It is the perversion of information being evaluated, expressed as a percentage. In addition, Yi obsis the i^{th} observation for the constituent being evaluated, Yi sim is the i^{th} simulated value for the constituent being evaluated, Ymeanis the mean of observed data for the constituent being evaluated, and n is the total number of observations.

2.5.Basin delineation and HRU definition:

The Lake Ziway watershed was delineated with an outlet point at the downstream sites of the Katar and Meki rivers. The overall watershed was further broken down into sub-basins based on the Algorithms provided by the SWAT model. With this information the model automatically delineates the Katar river basin area of 3241.6 km^2 in to 13 sub basins in this study and Meki river basin in to 2033 km^2 in to 9 sub basins. The Katar river basin results in 75 HRUs and Meki river basin results in 73 HRUs in the basin.

3. Results and Discussions

3.1.Analysis of Monthly and Seasonal Future Climate on Lake Ziway Catchment

For this study, monthly and seasonal analysis was taken for Ethiopian local season of Belg (March, April and May), Kiremt (June, July, August and September) and Bega (October, November, December, January and February) over Lake Ziway Catchment.

Maximum Temperature: There is a general increasing trend for maximum temperature from baseline period under RCP 4.5 and RCP 8.5 except for the months of March and September in all time periodsunderRCP 4.5 for HadGEM2-ES and CSIRO-MK 3-6-0 model.The maximum amount of average annual temperature is projected from HadGEM2-ES model under RCP 8.5 during 2080s and the minimum average annual temperature is projected from CSIRO-MK 3-6-0 model under RCP 4.5 during 2020s.The same trend has been also reported on the projected average annual temperature by (Belay et al., 2012; Monireh et al., 2013)where, increased extreme daily temperature events prevailed for future scenarios (Negash et al., 2013).Maximum amount of temperature change from RCP 8.5 is due to the fact that RCP 8.5 produces more greenhouse gas as compared to RCP 4.5, which is medium in greenhouse gas production (Riahi et al.,2011).

Minimum Temperature: For minimum temperature, there is a general increasing trend from baseline period under RCP 4.5 for the three models except on March for HadGEM2-ES, October on CSIRO-MK 3-6-0 and July CCSM4.

Precipitation: The overall result revealed that, percentage change in monthly average precipitation might range between -51.19% during January 2050s and +23.15% during February 2080s underRCP8.5 for HadGEM2-ES model (Figure 2). However, for RCP4.5precipitations is projected to increase in amount by 2.69% on 2020s and decrease by 2.7%, and 1.6% during 2050s and 2080s, respectivelywhichis having similar projection by (Monireh et al., 2013).However, seasonally maximum precipitation reduction is projected during the Ethiopian local rainy season of 'Kiremt' in all the model outputs. Furthermore, inter-annual and intra-seasonal rainfall variability in the Central Rift Valley is accompanied by a significant warming trend in temperature and reduction of rainfall can add stress to crop growth during this season.The occurrence of warming across Ethiopia is reported (Conway, 2000)and decline in precipitation up to 25%is also shown by(Monireh et al., 2013).

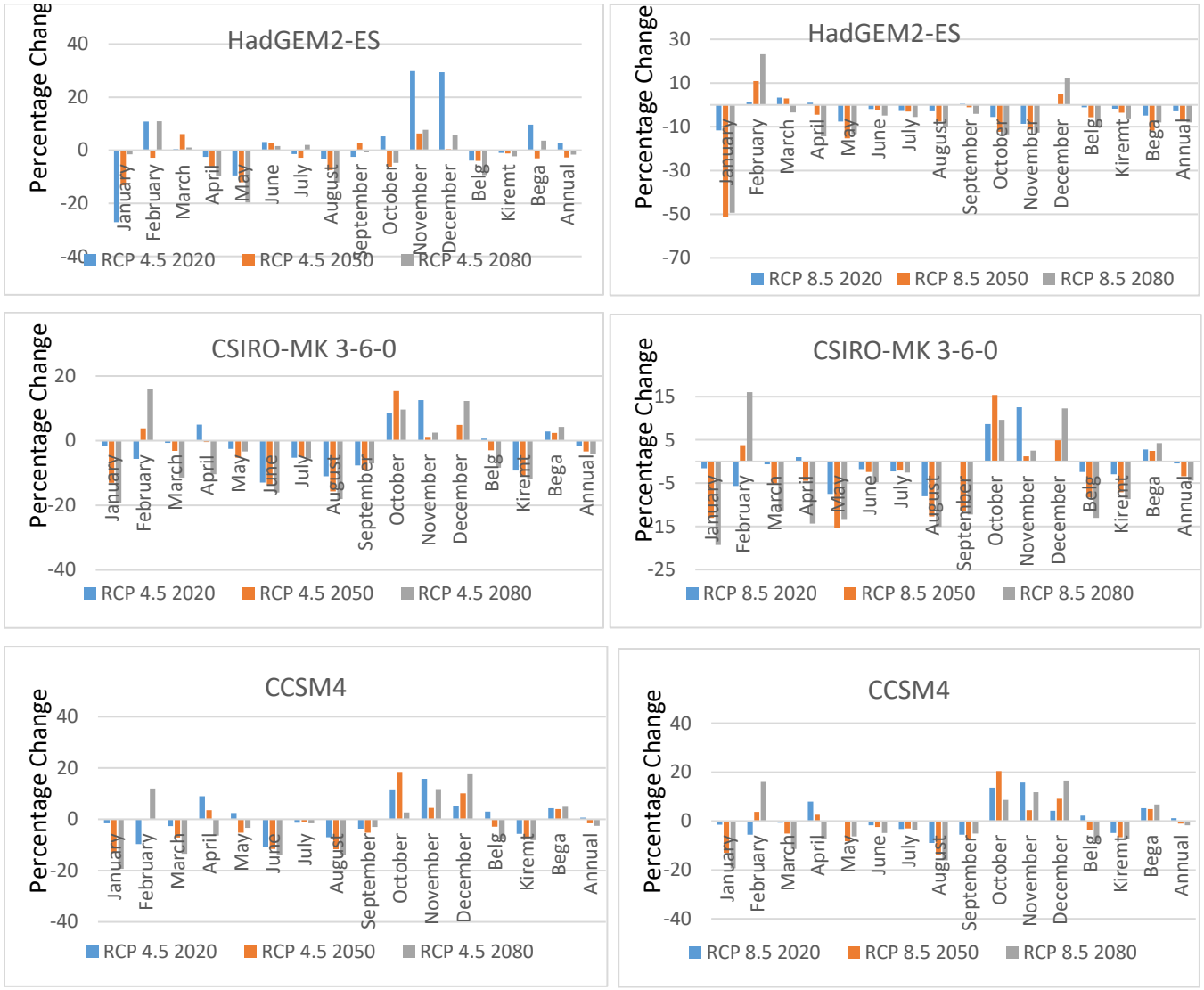

Figure 2: Percentage change in mean monthly and seasonal precipitation at different time horizon under RCP 4.5 and RCP 8.5 for the future period (2010-2099).

3.2.Hydrological Model Calibration and Validation Results

Sensitivity analysis: SWAT sensitivity analysis for lake Ziway Watershed indicates for flow calibration, about 11 parameters was reported as sensitive in different degree of sensitivity. Among these 11 parameters, only 9 & 8 of them have effect on the simulated result when changed on Katar river and Meki rivers respectively. So, on category specified by sensitivity classes, the parameters changed for flow calibration were those of from very high to small sensitivity class for both watersheds based on lower p-value and higher t-stat value are rankedTable 3.

Table 3: Calibrated parameters of flow and their fitted values and rank for Katar and Meki river

	Katar River				Meki River			
Rank	Parameter_Name	Fitted_Value	Min_value	Max_value	Parameter Name	Fitted Value	Min_value	Max_value
1	8:R_SOL_K(..).sol	-0.99998	-1.00014	-0.99981	1:R_SOL_Z(..).sol	-0.6453	-0.6454	-0.6452
2	2:V_ALPHA_BF.gw	0.037093	0.035176	0.038984	6:R_CN2.mgt	-0.2437	-0.2835	-0.2322
3	9:V_SFTMP.bsn	-0.65711	-0.75149	-0.49173	5:R_ESCO.bsn	0.32996	0.32986	0.32997
4	1:R_CN2.mgt	-0.16251	-0.16425	-0.16191	7:V_ALPHA_BF.gw	0.03857	0.03692	0.0408
5	11:R_OV_N.hru	-0.26289	-0.26547	-0.26176	8:V_GWQMN.gw	130.614	130.613	130.616
6	3:V_GW_DELAY.	308.4943	308.3842	309.2767	2:R_REVAPMN.gw	292.689	290.581	292.743
7	4:V_GWQMN.gw	821.1171	817.2775	823.3721	4:R_SOL_AWC (..)	-0.2116	-0.2117	-0.2116
8	7:R_SOL_AWC(..)	0.31291	0.312876	0.314902	3:R_BIOMIX.mgt	0.53562	0.5356	0.53563
9	6:V_ALPHA_BNK.	-0.00982	-0.01151	0.02219				
10	10:R_HRU_SLP.hr	0.150725	0.148563	0.151471				
11	5:V_ESCO.hru	0.043773	0.039845	0.044991				

Model Calibration: The model calibration was done from (January, 1993-December, 2001) for Katar as well as Meki independently. Calibration resulted after simulation from (January, 1994-December, 2001) found a coefficient of determination (R^2) of 0.71 & 0.73 and Nash–Sutcliffe efficiency (NSE) of 0.64 & 0.7, for Katar and Meki respectively showing a good agreement between measured and simulated monthly flows. The calibration result demonstrates SWAT's ability to predict realistic flow for bothcatchmentsFigure3 and Figure 4.

Model Validation: Like Model calibration, the model performance evaluation parameters were calculated and checked weather the model perform very well or not and within this the monthly stream flow of (R^2= 0.79 and NSE= 0.65) for Katar river and (R^2= 0.8 and NSE= 0.74) for Meki river.

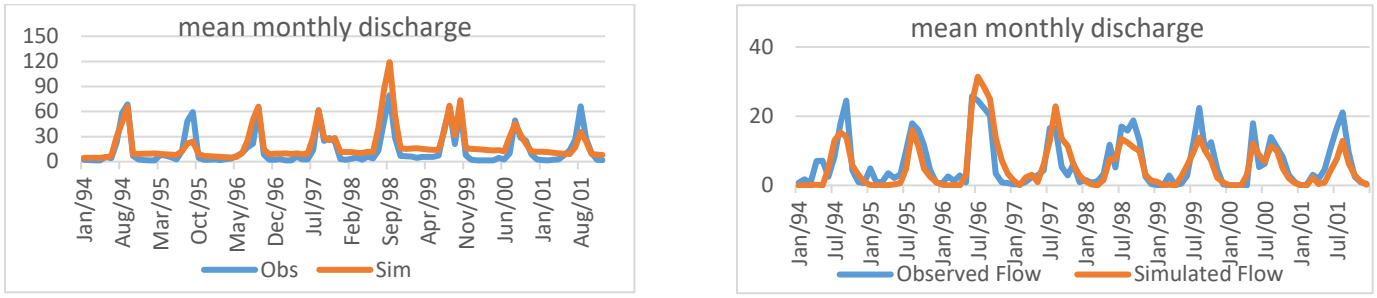

Figure 3: Monthly simulated and measured streamflow on calibration period (1994 – 2001) for Katar (left) and Meki (right) Sub-basin

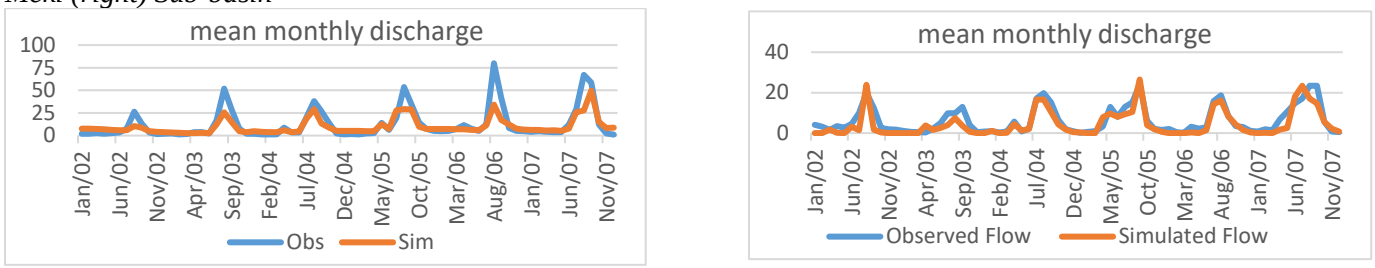

Figure 4: Simulated and measured monthly streamflow on during the validation period for Katar (left)Meki (right) Gauging Station (2002-2007)

3.3.Impact on Seasonal and Annual Flow of Katar River

For the HadGEM2-ES model maximum flow reduction was observed during the rainy season 'Kiremt' on average. It shows reduction of 10.78%, 17.58% and 19.23% for the periods of 2020s, 2050s and 2080s respectively under RCP 8.5 Figure5. Generally, flow reduction from this model corresponds with the reduction in precipitation on the same season. CSIRO-MK 3-6-0 model has also shown maximum flow reduction during the rainy season 'Kiremt' on average basis. Generally, flow reduction from the model groups is also shown by previous study on the neighboring Awash River Basinranging between 10% to 34% using different GCM outputs (Hailemariam, 1999). Annually, flow shows reduction for both scenarios has complied with the precipitation reduction. Therefore, the River flow is found to be very sensitive to variations in precipitation than temperature changes. The study done in the rift floor (Mechal, 2015) indicated that under high or low warming trends a very slight proportional change in evapotranspiration resulted in high relative change in ground water recharge and surface runoff. Also decrease in ground water recharge is reported on the northern part of Ethiopiaon Tekeze river basin under future scenarios of RCP2.6 and RCP4.5 (Kahsay et al., 2018). This result shows the maximum flow reduction during rainy season of Kiremt that comply with previous study on the area (Zeray, 2007).

3.4.Impact on Seasonal and Annual Flow of Meki River

Flow reduction on Meki River was observed during 'Belg' season across all the model groups. Maximum flow reduction reaches40.27% for the periods of 2050s under RCP 8.5 for the HadGEM2-ES model. A slight flow increment is observed during the local dry season of 'Bega' on HadGEM2-ES model for both concentration pathwaysFigure 6. Other slight increment is also predicted during the 2080s from CCSM4 model output under RCP 4.5 scenarioduring Belg and Kiremt which represents a range of technologies and strategies for reducing GHG until 2100 (van Verrun et al., 2011).

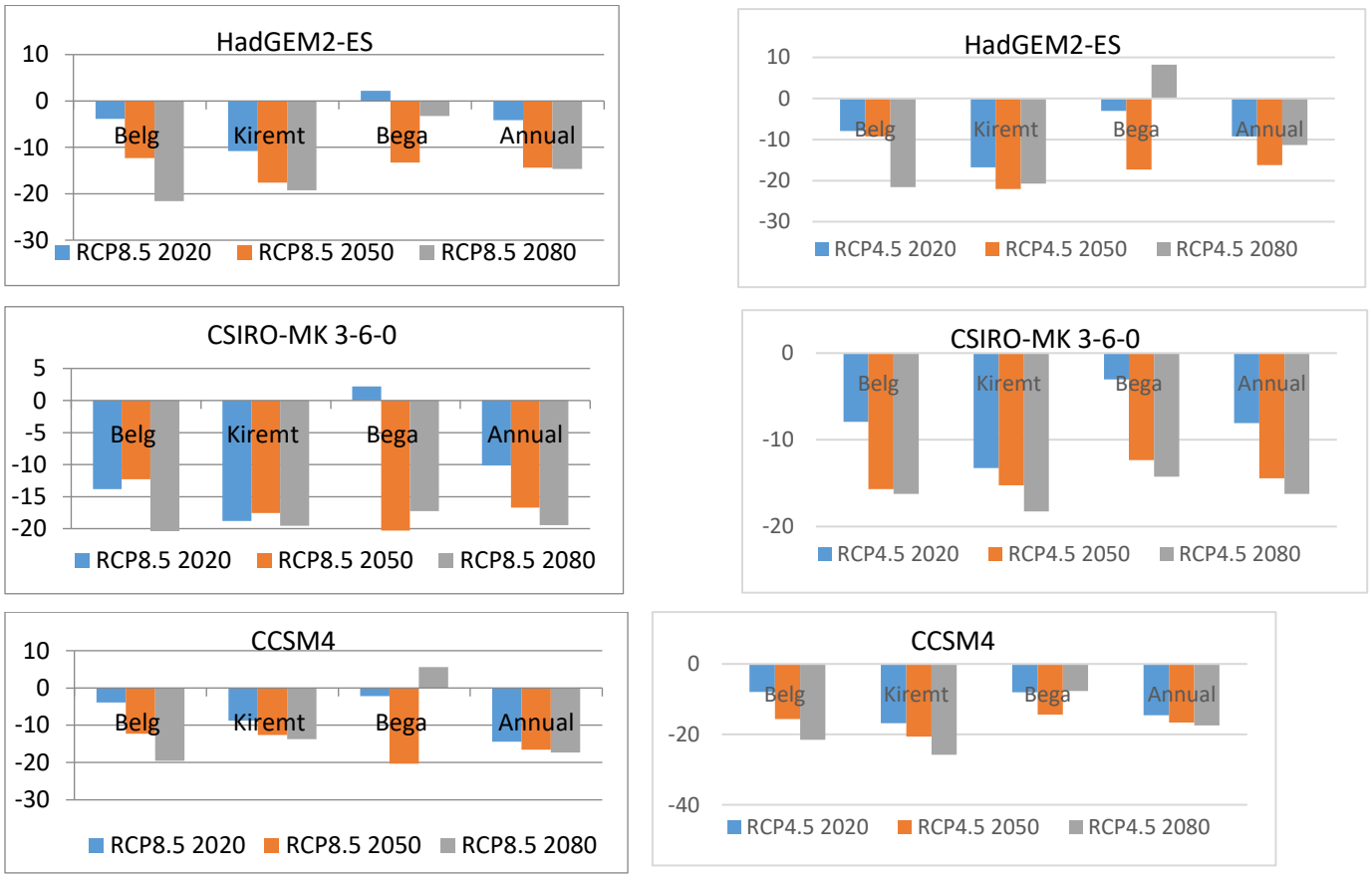

Figure 5: Percentage change in seasonal and annual inflow at Katar River with respect to baseline period for the HadGEM2-ES, CSIRO-MK 3-6-0 and CCSM4 model.

Flow reduction from this model furthermore has correspond with the reduction in precipitation on the same season. Annually maximum reduction is projected from model by 20.28% during 2080s from HadGEM2-ES model under RCP 8.5. On the other hand, CCSM4 model has shown minimum flow reduction by 1.1% during 2080s under RCP 4.5 (Figure 6).

Seasonal change in flow volume from Katar and Meki rivers will have implication on the socio-economic conditions with respect to reduction for irrigation potential, Lake level (Seyoum et al., 2015)and on out flow river. Increased Bega stream flow for indicated periods and scenarios is desirable to exploit the irrigation potential of the sub-basins thereby improving the irrigated agricultural production in the area. Kiremt flow volume might show highest decrease for Katar River and Belg seasons show the highest reduction from Meki River for both scenarios, which will greatly affect Lake Ziway level. This effect has also been indicated by (Zeray, 2007; Alemayehu, 2006) drop on lake level that may rich up to two third of a meter, surface area might also shrink by 25.3 km^2, which is about 6% of the base period lake surface area.

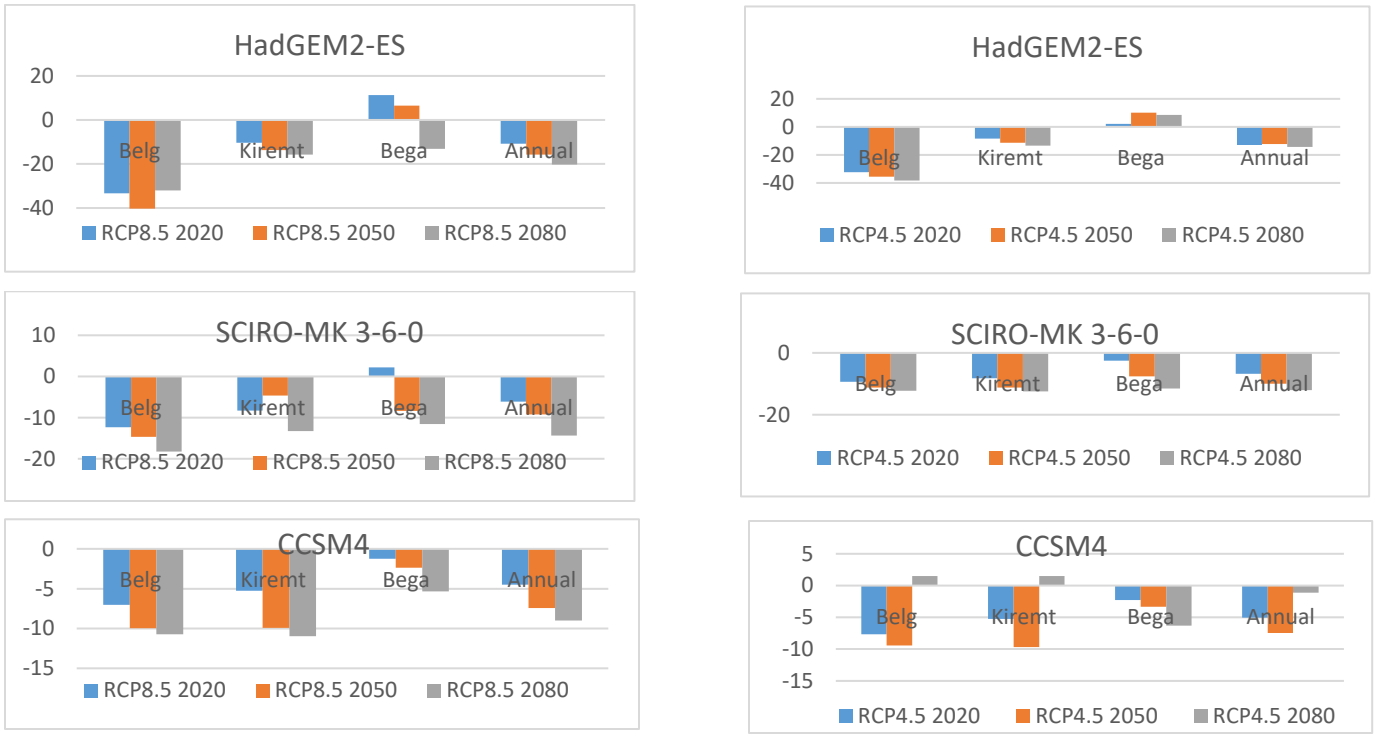

Figure 6: Percentage change in seasonal and annual inflow at Meki River with respect to baseline period for the HadGEM2-ES, CSIRO-MK 3-6-0 and CCSM4 model.

On Central Rift Valley (CRV) human impacts contributed to the changes in the hydrology of Lake Ziway and Lake Abiyata causing a decrease in lake storage and prolonged dry periods(Seyoum, 2015). This shows a worsening trend of the recent lake level fluctuation and aerial coverage contraction. This combined with the unbalanced supply-demand equation in the watershed is expected to have significant impact on the lake water balance. Other clear indicator is the fate of Bulbula River flowing out of Lake Ziway, recently its flow is observed to be intermittent and number of state and private farms that were operating on it were closed up. Hence, it is imaginable to predict its complete existence on future for indicated inflow scenarios.

The increasing water abstractionfor industrial and agricultural activities (Seyoum, 2015)due to economic development and population growth(Legesse, et al., 2010)is also likely to further reduce seasonal flows(Hailemariam, 1999)and downstream Lake Abiyata surface area (Seyoum, 2015).Furthermore, (IPCC, 2014) reported climate change over the 21st century is projected to reduce renewable surface water and groundwater resources in driest subtropical regions, intensifying competition for water among sectors. As this region is largely occupied by rural settlers they are expected to experience major impacts on water availability and supply, food security, infrastructure and agricultural incomes, including shifts in the production areas of food and non-food crops around the world (IPCC, 2014).Therefore, in Lake Ziway catchment, runoff is likely to decrease in the future and insufficient to meet future demands for water of the ever-increasing population in the region.Therefore, the region requires integrated basin-wide water management practice(Alemayehu, 2006).

4. Conclusions

CMIP5 model outputs from IPCC 5th assessment report has been used to assess the response of Katar and Meki River and their implication to Lake Ziway that was projected by using three GCMs and a semi distributed hydrologic model (SWAT). Projection of the three GCMs HadGEM2-ES, CSIRO-MK 3-6-0 and CCSM4 pointed out that temperature will increase and precipitation reduced for future periods denoted by 2020s, 2050s and 2080s.

The SWAT model output showed that HadGEM2-ES, CSIRO-MK 3-6-0 and CCSM4 modelsshowed flow reduction during the rainy season ‘Kiremt’ on extreme case under RCP 8.5 on Katar River. CCSM4 model has shown maximum flow reduction by 25.75% during 2080s under RCP 4.5 which is the extreme as compared with the above model groups. On Meki River seasonally flow reduction was observed during ‘Belg’ across all the model groups. Maximum flow reduction reaches 40.27% for the periods of 2050s under RCP 8.5 for the HadGEM2-ES model. A slight flow increment is observed during the local dry season of ‘Bega’ on HadGEM2-ES andCCSM4 model. Despite uncertainties on GCM and hydrological models, the result suggestearly decrease in water use from different water use sectors in Lake Ziway Catchmentas the best water resource management strategy. Furthermore, the integratedwatershed development in Lake Ziway Catchmentshould be considered, to reduce the adverse impact of climate change particularly during localrainy seasononrain fall dependent agriculture. Therefore, projected scenarios on River flow and climate change would significantly affects the livelihood of farmers and water using sectors in the area. Thus, concern for climate change and water management strategies should have to be given priority to mitigate the

impacts. Furthermore, this study need to be extended to see the role of other climate model groups and use of new assessment reports, and further investigations on impact of other water sources like groundwater has to be done to fill the gap.

Acknowledgements

The authors wish to thank Hawassa university for their grant support for handling this research activity. We are also grateful for the support from the National Meteorological Services Agency, Ministry of Water Irrigation and Electricity of Ethiopia and Rift Valley Basin Development Regional Office for providing us the required data and information. All our colleagues, who participated by providing material support, consultation and proof reading of the manuscript are greatly acknowledged.

References

Abbaspour, K. (2013). SWAT-CUP 2012: SWAT Calibration and Uncertainty Programs — A User Manual 103 pp.

Abbaspour, K. C., Yang, J., Maximov, I., Siber, R., Bogner, K., Mieleitner, J., et al. (2007). Spatially distributed modelling of hydrology and water quality in the Pre-Alpine/Alpine Thur watershed using SWAT. Journal of Hydrology, 333, 413–430.

Alemayehu, T. (2006). Hydrogeochemical and Lake level changes in the Ethiopian Rift valley. J. Hydrol 316,290-300.

Arnold, J., Srinivason, R., Muttiah, R., Williams J. (1998). Large area hydrologic modeling and assessment. Part I: model development. J. Am. Water Resour. Assoc. 34, 73–89.

Arnold, J. G., Moriasi, D. N., Gassman, P. W., Abbaspour, K. C., White, M. J., Srinivasan, R., … Jha, M. K. (2012). SWAT: model use, calibration, and validation. Transactions of the ASABE, 55, 1491–1508.

Asaminew, T.G., Araya, A., Atkilt, G., Solomon H. (2017). Modeling the Potential Impact of Climate Change on Cotton (*Gossypiumhirsutum*) Production in Northeastern Semi-Arid Afar and Western Tigray Regions of Ethiopia. J. Earth Sci.Clim. Change 8: 390.

Ayenew, T.(2007).Water management problems in the Ethiopian Rift: challenges for development. Journal of African Earth Sciences 48,222-236.

Belay, T.K., Rötter,R.P., Hengsdijk, H., Asseng, S., Van Ittersum,M.K.,et al. (2012).Climate variability and change in the Central Rift Valley of Ethiopia, challenges for rain fed crop production.The Journal of Agricultural Science 152, 58-74.

Biniyam, Y., Kemal, A. (2017). The Impacts of Climate Change on Rainfall and Flood Frequency, The Case of Hare Watershed, Southern Rift Valley of Ethiopia. J. Earth Sci.Clim. Change 8, 383.

Conway, D. (2000). Some aspects of climate variability in the North-East Ethiopian highlands-Wollo and Tigray. SINET, Ethiopian Journal of Science 23, 139–161.

Fowler, H.J., Blenkinsop, S., Tebaldi, C. (2007). Linking climate change modelling to impacts studies, recent advances in downscaling techniques for hydrological modeling. Int.J. Climatol27,1547–1578.

Gebre, S.L., Tadele, K., Gebre-Mariam, B. (2015). Potential Impacts of Climate Change on the Hydrology and Water Resources Availability of Didessa Catchment, Blue Nile River Basin, Ethiopia. J. GeolGeosci 4,1.

Gupta, H. V., Sorooshian, S., &Yapo, P. O. (1999). Status of automatic calibration for hydrologic models, comparison withmultilevel expert calibration. Journal of Hydrology Engineering, 4(2), 135–143.

Hailemariam, K. (1999). Impact of Climate Change on the Water Resources of Awash RiverBasin, Ethiopia.Climate Research International and Multidisciplinary Journal 12, 91-96.

IPCC. (2014) Climate Change 2014, Synthesis Report. Contribution of Working Groups I, II and III to the Fifth Assessment Report of the Intergovernmental Panel on Climate Change [Core Writing Team, R.K. Pachauri and L.A. Meyer (eds.)]. IPCC, Geneva, Switzerland, 151 pp.

Jury, M.R. (2015). Statistical evaluation of CMIP5 climate change model simulations for the Ethiopian highlands. Int. J. Climatol 35, 37–44.

Kahsay, K.D, Pingale, S.M, Hatiye, S.D. (2018) Impact of climate change on ground water recharge and base flow in the sub-catchment of Tekeze basin, Ethiopia. Ground water for sustainable development 6, 121-133.

Legesse, D., Abiye, T.A., Vallet-Coulomb, C., Abate,H. (2010). Streamflow sensitivity to climate and land cover changes, Meki River, Ethiopia. Hydrol. Earth Syst. Sci 14, 2277–2287.

Mechal, A., Wagner, T., Birk, S. (2015). Recharge variability and sensitivity to climate, The example of Gidabo River Basin, Main Ethiopian Rift. J. Hydrol, Reg Studies 4,644–660.

Monireh,F., Karim, CA., Saeid, AV., Mohammad, RF., Alexander, JBZ., et al. (2013). Modeling impact of climate change on fresh water availability in Africa. J. Hydrol 480, 85-101.

Moss, R.H, Edmonds, J.A, Hibbard, K.A, Manning M.R, Rose, S.K, et al. (2010). The next generation of scenarios for climate change research and assessment. Nature 463, 747–756.

NASA. (2010)Description of global climate change key indicators. Retrieved from http,//climate.nasa.gov/key indicators/

Negash, W.,Jain,M.K., Goel, N.K.(2013).Effect of Climate Change on Runoff Generation, Application to Rift Valley Lakes Basin of Ethiopia. J. of Hydrologic Engineering 18, Issue 8.

Neitsch, S.L., Amold, J.G., Kiniry, J.R, Srinivasan, R., Williams, J.R. (2011). Soil and Water Assessment Tool SWAT Theory. USDA Agricultural Research Service and Texas A & M Black land Research Centre Temple, TX, pp. 476.

NMSA. (2015). National meteorological service agency. Addisababa, Ethiopia.

Riahi, K., Rao, S., Krey, V., Cho, C., Chirkov, V., et al. (2011) RCP 8.5- A scenario of comparatively high greenhouse gas emissions. Climatic Change 109,33.

Seyoum, W.M, Milewski, A.M, Durham, M.C (2015). Understanding the relative impacts of natural processes and human activities on the hydrology of the Central Rift Valley lakes, East Africa. Hydrol. Process 29, Issue 19.

Taylor, K.E, Stouffer, R.J, Meehl, G.A. (2011). An overview of CMIP5 and the experiment design. Bull. Am. Meteorol. Soc 93, 485–498.

Van Vurren, D., Edmonds, J., Kainuma, M., Riahi, K., Thomson, A. et al. (2011). The representative concentration pathways, an overview. Climatic Change 109, 5-31.

Zeray, L. (2007) Climate Change Impact on Lake Ziway Watershed Water availability, Ethiopia. Proceedings of the International Joint Conference on Catchment and Lake Research.

Development of Rainfall Intensity-Duration-Frequency (IDF) curve for Lower Omo-Gibe River Basin under changing climate

WozaderWoldeKachama *[1]; Mamuye Busier Yesuf[2] ; Fiseha BehuluMuluneh[3]

*[1] Aksum University, School of Water Technology, E-mail: wozwolde@gmail.com, Aksum, Ethiopia, [2]Jimma University (JiT), School of Civil and Environmental Engineering, E-mailmamuyebusier@yahoo.com, Jimma, Ethiopia, [3] Addis Ababa University (AAiT), School of Civil and Environmental Engineering, E-mail: fiseha.behulu@aait.edu.et, Addis Ababa, Ethiopia

* Corresponding Author Email: wozwolde@gmail.com Cell Phone: +251916070386

Abstract

Rainfall Intensities-Duration- Frequency (IDF) curves have got important role in planning and designs of storm water projects and other water related infrastructures. The reliability of IDF is highly associated with the appropriate choice of rainfall data. However, high emissions of greenhouse gasses exert pressure on atmospheric processes and now a day affects rainfall characteristics. In different water resources development activities, one means of adaptation to climate change is through updating (IDF) curves developed from historical datasets with respect to possible future climate change scenarios. This study is aimed to assess the impact of climate change on IDF curves of selected cities namely, Bulki (Mindre), Jinka and Arba Minch in lower Omo-Gibe River basin. Observed historical rainfall data of 34 years (1980-2013) were used as an input. In order to evaluate the climate change impact, the most recent data from Coordinated Regional Climate Downscaling Experiment (CORDEX) data scenarios were used as additional source. The CORDEX data were thoroughly evaluated and appropriate bias correction using power transformation method was undertaken. Daily based data were disaggregated to 5, 10, 20,30,60,90,120 minutes to define IDF curve appropriately. Projected data period (2040-2069) of three scenarios were examined for evaluations of potential impact of climate change. IDF curve from comparative evaluation of all scenarios showed that there will be likely increase in intensities in the future for all cites. Therefore, future water infrastructure development of the selected cities can be designed by utilizing the approaches developed in this study.

Key Words: Climate Change, CORDEX, IDF Curve, Lower Omo-Gibe River Basin, Rainfall

1. Introduction

Degradation of water quality, property damage and potential loss of life due to flooding is caused by extreme rainfall events (De Paola et al., 2014).Historic rainfall event statistics (in terms of intensity, duration, and frequency) are used to design storm water management facilities, erosion and sediment

control structures, flood protection structures, and many other civil engineering structures involving hydrologic flows (Prodanovic and Simonovic, 2007).

The reliability of IDF curve is highly associated with the appropriate choice of rainfall data.However, during the last century the concentration of carbon dioxide (CO_2) and other greenhouse gases (GHGs) in the earth's atmosphere has risen due to increased industrial activities (Prodanovic and Simonovic, 2007). This increment in GHG concentrations now a day exerts pressure on atmospheric processes so that affects rainfall characteristics and other meteorological parameters. As long as rainfall characteristics are used to design water infrastructures, reviewing and updating rainfall characteristics (i.e., Intensity–Duration–Frequency (IDF) curves) for future climate scenarios is necessary (Mirhosseini et al., 2013). The need for considering the potential effect of changing climate when working with IDF curve has been suggested by many scholars in many parts of the world(Mirhosseini et al., 2012 ; De Paola et al., 2014; Shrestha et al., 2017). The need for such understanding comes from the fact that the existingdrainage systems are designed to cope with past records of rainfall events and as such they may be insufficient to accommodate future rainfall characteristics. Hence, development of appropriate present and future Intensity–Duration–Frequency (IDF) curves assist in hydrological study for the urban drainage system performance analysis, design and operation (Shrestha et al., 2017).Therefore, the objective of this study isto assess the impact of climate change on IDF curves of selected cites namely, Bulki (Mindre), Jinka and Arba Minch in lower Omo-Gibe River basin.

2. Study area and data Sources

The analysis has been performed on two cities locate with in lower valley of Omo-Gibe river basin and Arba Minch city outside's ridge of the basin which are characterized by different rainfall pattern.

Table 1 Characteristics of meteorological stations and corresponding RCM grid point of cities

S. N	Stations	Grid Code	Latitude	Longitude	Elev. (m)
1	Bulki (Mindre)	GP[3]109208	6.16	36.52	1196.30
2	Jinka	GP109207	5.72	36.52	1017.39
3	Arbaminch	GP111208	6.16	37.40	1637.79

Observed daily time series rainfall of a period (1980-2013) for the three stations were collected from National Meteorological Agency (NMA). On the other hand, climate data model for future climate projection isfrom Coordinated Regional Climate Downscaling Experiment (CORDEX) data set. For this study, dynamically downscaled outputs by the recent version of the Rossby Centre Regional Climate Model—RCA4 were used. The model is developed in Swidish Meteorological and Hydrological Institute (SMHI). Spatially, the RCA4 simulations cover the CORDEX-Africa domain at resolution of 0.44° × 0.44° (~50 km × 50 km) for the 1951–2100 time period which is divided into two: historical (1951–2005) and scenario (2006–2100) periods. Data sets of three climate model scenarios namely RCP 2.6, RCP 4.5 and RCP 8.5 were considered which is a cumulative measure of all anthropogenic emissions of GHG's from all source expressed in Watts per square meter, by 2100(Van Vuuren *et al.*, 2011).RCP 2.6 scenario is characterized by low emissions consistence with ambition of GHG emission reduction over time and become zero at 2100(Van Vuuren *et al.*, 2011).RCP 4.5 is intermediate scenario which is a stabilization without overshoot pathway to 4.5 W/m^2 at stabilization after 2100 through the use of various policies and technologies to minimize greenhouse gas emissions (Thomson *et al.*, 2011). Whereas RCP 8.5 is characterized by comparatively high greenhouse gas emissions and absence of climate change policies resulting to a radiative forcing of 8.5 W/m^2 in 2100(Riahi *et al.*, 2011).

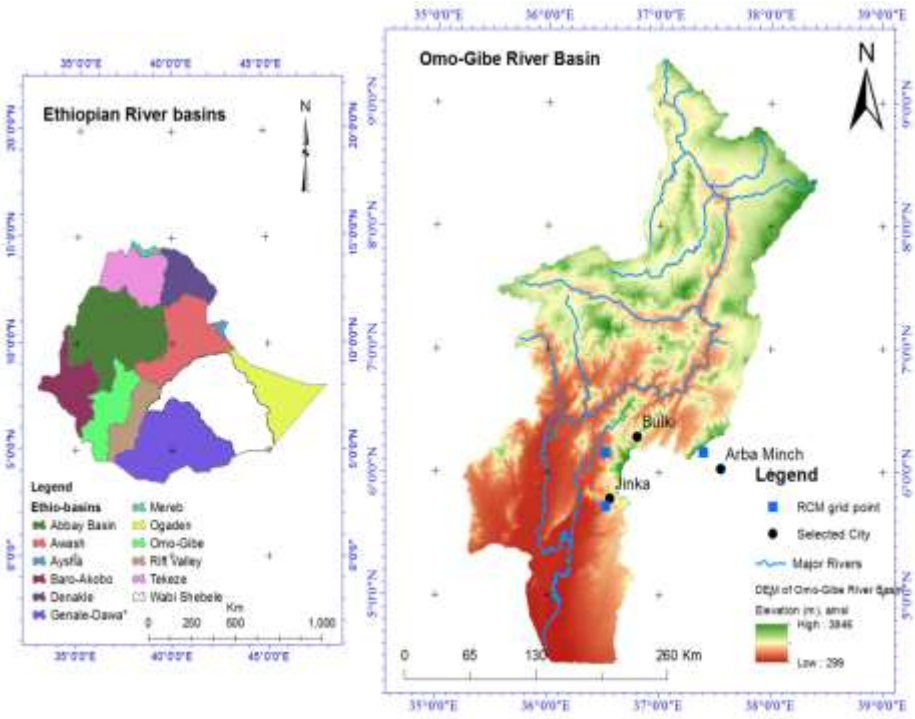

Figure1, Geographical location of the study area

3. Methodology

3.1 Observed rainfall Data

Observed raw data collected from NMA passed through quality control techniques.Nearest neighbormethod was adopted for data gap filling, given that aspecial attention for rainy season (Jun to September) as well as (March to May). Data period of (1980-2013) were used for developing IDF curves of baseline period. For validating raw RCM data with observed data, data series of a reference period (1980-2005) were used.

3.2 Bias correction

Data from RCM were not directly used for the analysis as it may have systematic error introduced from considered boundary condition and downscaling steps. In order to match quantiles of simulated RCM rainfall data withrespect to point scalerainfall data series, bias correction was applied. In this study, power transformation method was employedwhich could adjust the mean as well as the variance statistics of a precipitation time series(Lenderink *et al.*, 2007; Teutschbein and Seibert, 2012). The method also adopted on Hare watershed, southern rift valley of Ethiopia (Biniyam and Kemal, 2017).

$$p^{*} = a\, p^{b} \tag{1}$$

Where; P^{*} is corrected daily data in the projection period; a & b are parameters obtained from calibration in the baseline period and then subsequently applied to the projection period; whereas, p is daily precipitation amount of scenario data. TheFuture projection was made for mid-21st century by using data of a time slice ranges (2040-2069).

3.3 Outlier test

Outliers are data points which depart significantly from the trends of remaining data. The test was carried for both lower and higher outliers and the threshold was determined according to Water Resources Council technique. Because, outliers significantly affect the magnitude of statistical parameters computed from the data series(Water Resources Council, 1981). Graphical approach‘s was adopted for easy detection of both outliers in the data series of baseline and projected period.

3.4 Probability distribution function

The annual maximum rainfalls were fitted into Gumbel's distribution, Log Pearson type III distribution and lognormal distribution. The goodness of fit (GOF) testwere carried byusing Kolgomorov-Smirnov (K-S), Anderson–Darling and Chi-Squared.

Log Pearson type III probability distribution was found to be best fit for all stations based on overall rank of GOF tests earned from computed parameters.Basically, this distribution is the standard distribution for frequency analysis of annual maximum floods in the United States (Benson, 1968).

Its probability density function is given as;

$$f(x) = \frac{\alpha^{\beta}(y-\gamma)^{\beta-1}e^{-\alpha(1-\gamma)}}{x\Gamma(\beta)}; \log x \geq \gamma \tag{2}$$

$$\alpha = \frac{\delta_y}{\sqrt{\beta}}$$

$$\beta = \left[\frac{2}{C_s(y)}\right]^2$$

Where, $\gamma = \overline{Y} - \delta_y\sqrt{\beta}$ (3)

$y = \log x$ and assuming $C_s(y)$ is positive

Where α, β and γ are the scale, shape and location parameters of the distribution and y= log(x), assuming the skewness$C_s(y)$ is positive.

The methodology used in this study to estimate events for varies return period was based on Hershfield technique, (Chow *et al.*, 1987)

$$X_T = \boldsymbol{X}_{avg} + \Delta\boldsymbol{X}_T \tag{4}$$

Where, $\Delta\boldsymbol{X}_T = K_T\delta$ is departure of the variate from the mean. δ is standard deviation and $K_T$referrers to frequency factor commuted as; (Kite, 1977)

$$K_T = z + (z^2-1)k + \frac{1}{3}(z^3-6z)k^2 - (z^2-1)k^3 + zk^4 + \frac{1}{3}k^5 \tag{5}$$

Where, $k = \frac{C_s}{6}$ Where $C_s \neq 0$, (Kite, 1977)

The intensity is time rate of rainfall which is rainfall depth (d) per unit time (t). The average intensity is commonly expressed as;

$$i = d/t \quad (6)$$

*Disaggregation:*Short duration rainfall data in sub hourly time series is required to define IDF curves appropriately.So that,it is necessary to disaggregate precipitation data collected on highertimescale (e.g., daily) to a different, shorter timescale (Fadhel *et al.*, 2017)**.**Disaggregation in this study followed technique adopted in Ethiopian Road Authority's drainage design manual (ERA, 2013).

3.5 Creating IDF Curve

The process of creating IDF curves consists of the following steps.

i. Extract annual maximum daily time series of rainfall depth form the quality controlled raw data;

ii. Fit the data to the commonly available theoretical probability distributions;

iii. Extrapolate precipitation magnitude for different return periods by using the best fit distribution (Log- Pearson Type III in our case);

iv. Repeat the thirdsteps for different return periods (2, 5, 10, 25, 50 and 100) years

v. Disaggregate output of the fourthstep data series in to (5, 10, 20, 30, 60, 90, and 120) minutes time series;

vi. Compute corresponding time rate of rainfall

vii. Plot the IDF curve

However, for creating future IDF curve, the above steps must be adopted after bias correction techniques are applied to RCMrainfall data series of a period 2040-2069.

4. Results and Discussions

4.1 Rainfall frequency analysis

Events for different return periods were extrapolated from annual maximum of baseline period as well as projected data for a period (2040-2069) by using best fit frequency distribution. Simple comparison

was made between baseline period and projected period. The comparison was made on rainfall depthof base period and three scenarios (RCP 2.6, RCP 4.5 and RCP 8.5) of different return period.

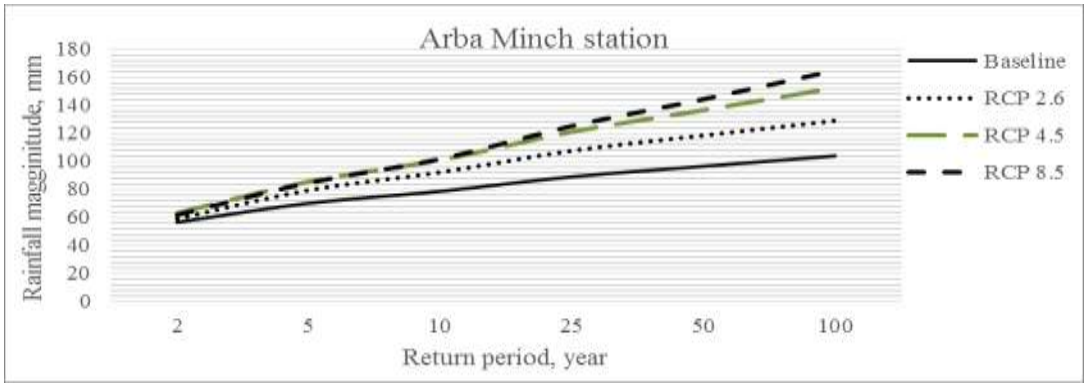

Figure 2, Extrapolated rainfall magnitude ofArba Minch for different return period

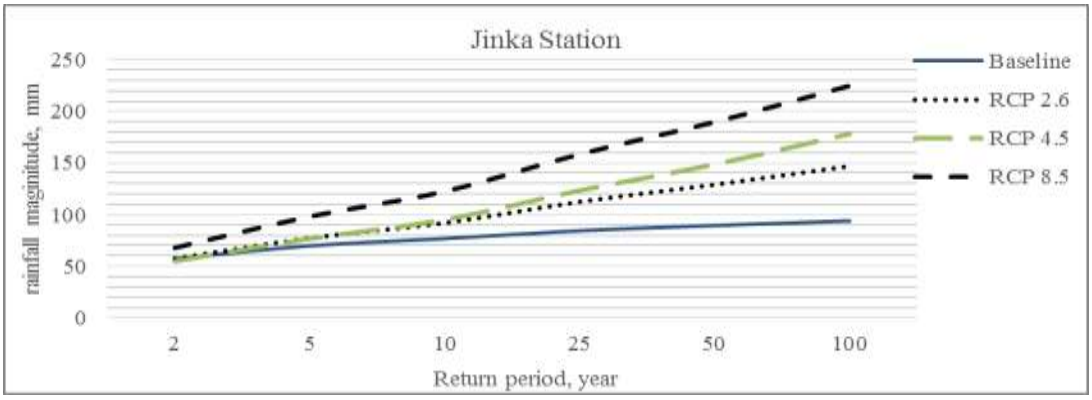

Figure 3, Extrapolated rainfall magnitude ofJinka for different return period

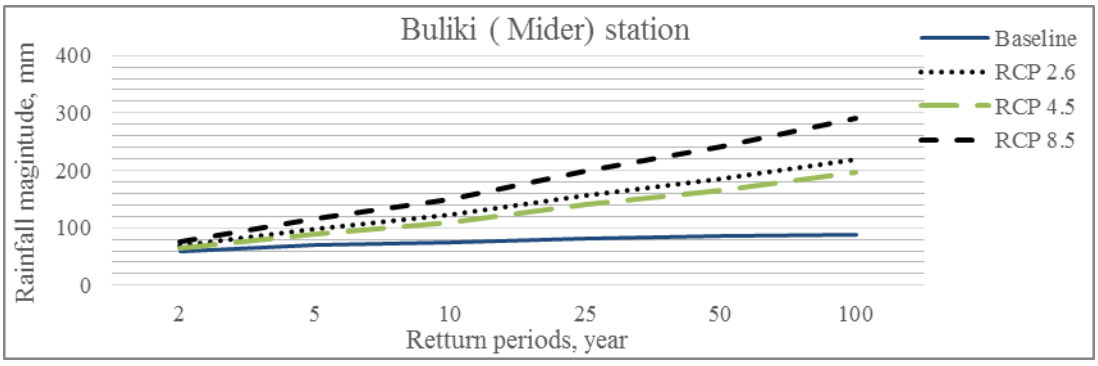

Figure 4, Extrapolated rainfall magnitude ofBulki for different return period

Figure 1-4, shows comparison between rainfall magnitudes of historical and future period of different recurrence intervals projected under changing climate scenarios. Accordingly, the three scenarios projected increased rainfall magnitude above baseline period for the three cities depending on the return

periods. RCP 8.5 scenario predicted more high value than projection under RCP 2.6 and RCP 4.5 scenarios for all cities. The projection under RCP 8.5 scenario for Arba Minch match with study conducted on Hare watershed which indicates future severe rainfall is subjected to increasing under changing climate condition(Biniyam and Kemal, 2017).

4.2 IDF curves

For developing IDF curve, durations up to 120 minutes were considered as short duration maycause flash flood events (De Paola *et al.*, 2014).However, for simple demonstration of impact of changing climate on future IDF curve, rainfall intensity with 25 and 50 years recurrence interval is plotted for Arba Minch, Bulki andJinka.

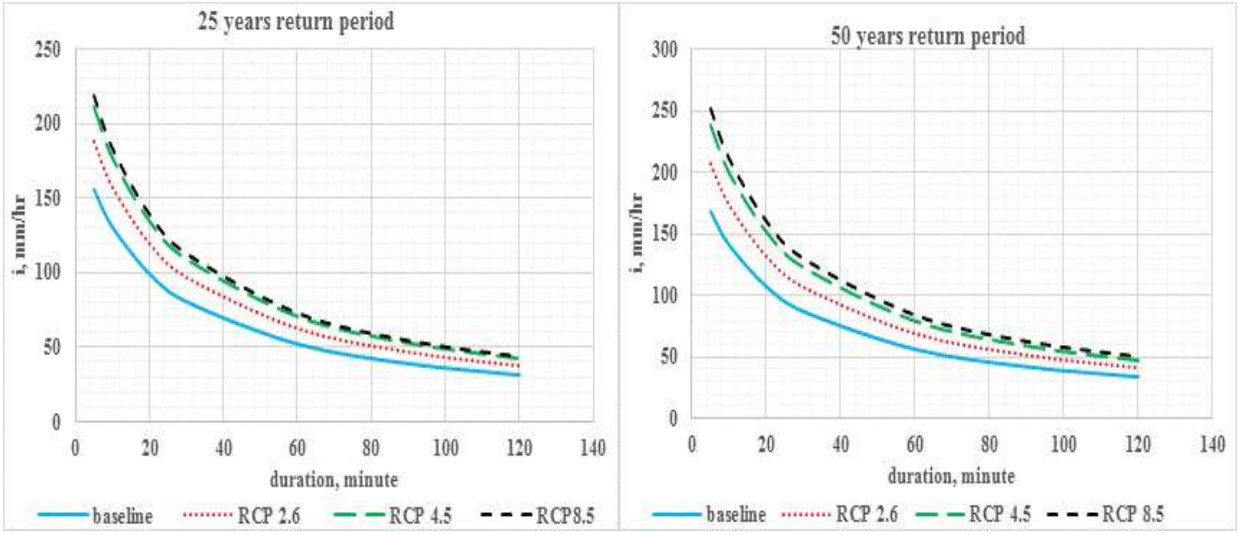

Figure 5, IDF curvesunder baseline and projected period forArba Minchcity

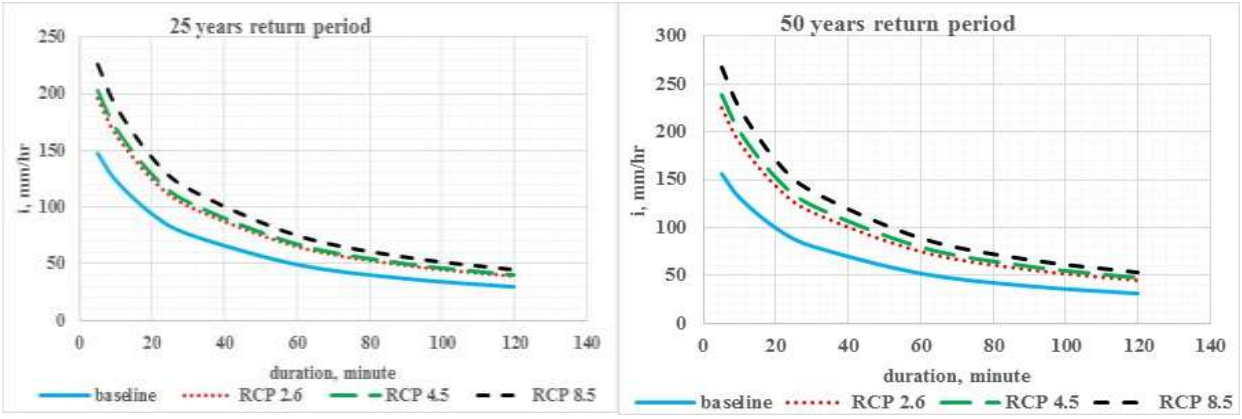

Figure 6, IDF curvesunder baseline and projected period forJinkacity

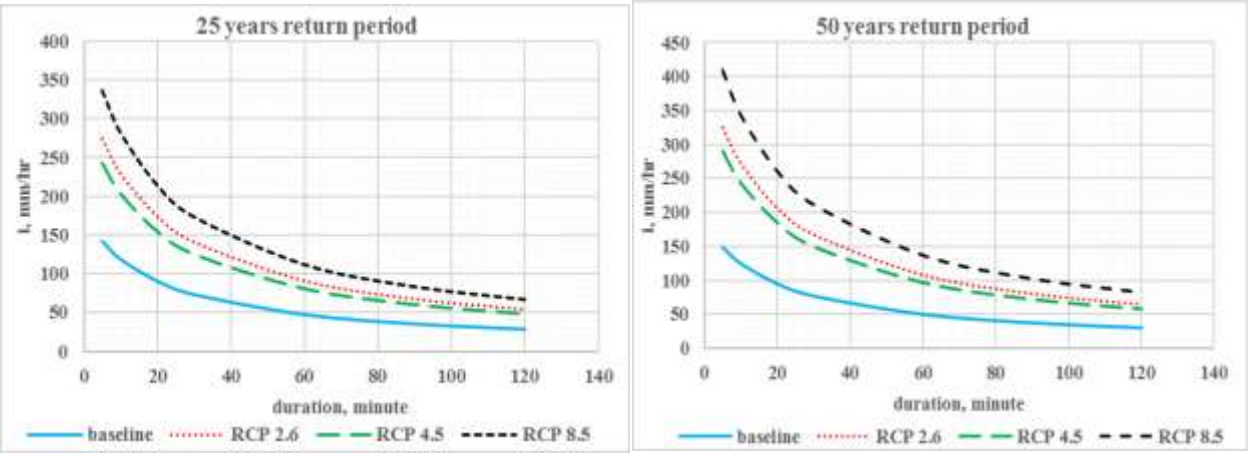

Figure 7, IDF curvesunder baseline and projected period forBulkicity

Figure 5-7 illustrates thata possible potential increment of rainfall intensities for all citiesunder different changing climate scenarios. For Arba Minch, RCP 4.5 and RCP 8.5scenarios projected somewhat similar and a little bit higher than projection under RCP 2.6 scenario. On the other hand, RCP 2.6 and RCP 4.5 scenarios have shown almost similar projection for Jinka relative to RCP 8.5 scenario. However, RCP 8.5 projection has shown substantial deviation when compared to projection under RCP 2.6 and RCP 4.5 for Jinka and Bulki.Other important thing demonstrated from the analysis is RCP 8.5 scenarioprojected higher value for all cites which clearly showssignificant consequencesassociated to no policy changes to reduce GHG emissions.Accordingly, the potential over estimation under RCP 2.6 scenario ranges in percent (20.8-23); (36-41) under RCP 4.5 scenario and (40-49) under RCP 8.5 scenario for Arba Minch. For Jinka, the percentage increment ranges (33-44) under RCP 2.6 scenario; (37-52.8) for RCP 4.5 scenario and (52-81.2) under RCP 8.5 scenario. However, for Bulki the increment goes above 70 percent under RCP 2.6 and RCP 4.5 scenarios; and extends as high as beyond its double value under high emission scenario. Generally, overall outcome of the study indicates that, future IDF curve has shown significant deviation from that of baseline period for all citiesregardless of the realizations under consideration. Therefore, it can be certainly taken from this investigation that changing climate condition could likelyexert stress on future IDF curve and may tend to increasing in magnitude depends on the return period.

In forth coming manuscript under preparation, evaluations were carried to see spatial variability of IDF curve as well asthe effect of changing climate on future IDF curve for the entire Omo-Gibe river basins.

5. Conclusion

This study comparatively evaluates IDF curves developed under climate changing scenarios with the IDF curves of baseline climatefor three cities. To investigate the potential effect of changing climate on future IDF curves, bias corrected rainfall data projected for a period (2040-2069) were used from three RCP's scenarios. The analysis result from climate model projection shows that future severe rainfall intensities could be subjected to increasing depending on the return period. This could affect Engineering infrastructures and poses problem on existing municipal storm water management system. In line with the outcome of this study, it can be concluded that future water infrastructure development of the selected cities can be designed by utilizing the approaches developed in this study. However, to draw strong conclusion, additional climate model should be incorporated to get more realistic information about potential effect of climate change on future IDF curve. Therefore, appropriate recommendation could be drawn as adaptation mechanism for the selected cities.

References

BENSON, M. A. (1968) Uniform flood-frequency estimating methods for federal agencies, *WaterResour. Res.*, vol. 4, no. 5, pp. . 891-908, [Cross reff).

BINIYAM, Y. & KEMAL, A. (2017) The Impacts of Climate Change on Rainfall and Flood Frequency: The Case of Hare Watershed, Southern Rift Valley of Ethiopia. *J Earth Sci Clim Change*, 8.

CHOW, V. T., MAIDMENT, D. R. & MAYS, L. W. (1987) *Applied Hydrology*, New york, St. Louis San Francisco Auckland Bogota, Mc Graw-Hill International Edition: Civil Engineering Series.

DE PAOLA, F., GIUGNI, M., TOPA, M. E. & BUCCHIGNANI, E. (2014) Intensity-Duration-Frequency (IDF) rainfall curves, for data series and climate projection in African cities *SpringerPlus*, 3/133; Doi 10.1186/2193-1801-3-133.

ERA (2013) Ethiopian Road Authority: Drainage Design Manual federal democratic republic of Ethiopia. Addis Ababa, Ethiopia.

FADHEL, S., RICO-RAMIREZ, M. A.&HAN, D. (2017) Uncertainty of Intensity–Duration–Frequency (IDF) curves due to varied climate baseline periods. *Journal of Hydrology*, 547**,** 600–612: http://dx.doi.org/10.1016/j.jhydrol.2017.02.013.

KITE, G. W. (1977) *Frequency and Risk Analysis in Hydrology*. *Water Resources Publications, Fort Collins, Colo. [CrossRef]*.

LENDERINK, G., A. BUISHAND & DEURSEN, W. V. (2007) Estimates of future discharges of the river Rhine using two scenario methodologies: direct versus delta approach. . *Hydrology and Earth System Sciences Discussions, European Geosciences Union,*, 11**,** 1145-1159, [Cross ref].

MIRHOSSEINI, G., SRIVASTAVA, P. & STEFANOVA, L. (2012) The impact of climate change on rainfall Intensity-Duration-Frequency (IDF) curves in Alabama: ; USA. . *Reg Environ Change***,** 1-9; DOI 10.1007/s10113-012-0375-5.

MIRHOSSEINI, G., SRIVASTAVA, P. & STEFANOVA, L. (2013) The impact of climate change on rainfall Intensity-Duration-Frequency (IDF) curves in Alabama. *Reg Environ Change,* 13**,** 25-33.

PRODANOVIC, P. & SIMONOVIC, S. P. (2007) Development of rainfall intensity duration frequency curves for the City of London under the changing climate. Department of Civil and Environmental Engineering, . *Report 058* London, Ontario, Canada,, The University of Western Ontario.

RIAHI, K., RAO, S., KREY, V., CHO, C., CHIRKOV, V., FISCHER, G., KINDERMANN, G., NAKICENOVIC, N. & RAFAJ, P. (2011) RCP 8.5—A scenario of comparatively high greenhousegas emissions. *Springer: International Institute for Applied Systems Analysis (IIASA), 2361 Laxenburg, Austria*

SHRESTHA, A., BABEL, M. S., WEESAKUL, S. & VOJINOVIC, Z. (2017) Developing Intensity-Duration-Frequency (IDF) Curves under Climate Change Uncertainty: The Case of Bangkok, Thailand:. *water, MDPI,* 9**,** 1-22

TEUTSCHBEIN, C. & SEIBERT, J. (2012) Bias correction of regional climate model simulations for hydrological climate-change impact studies: Review and evaluation of different methods. *Journal of Hydrology*, 456–457 12-29.

THOMSON, A. M., CALVIN, K. V., SMITH, S. J., KYLE, G. P., VOLKE, A., PATEL, P., DELGADO-ARIAS, S., BOND-LAMBERTY, B., WISE, M. A., CLARKE, L. E. & EDMONDS, J. A. (2011) RCP4.5: A Pathway for Stabilization of Radiative Forcing by 2100. *Climatic Change*.

VAN VUUREN, D. P., EDMONDS, J., KAINUMA, M., RIAHI, K., THOMSON, A., HIBBARD, K., HURTT, G. C., KRAM, T., KREY, V., LAMARQUE, J.-F., MASUI, T., MEINSHAUSEN, M., NAKICENOVIC, N., SMITH, S. J. & ROSE, S. K. (2011) The representative concentration pathways: an overview. *Clamatic change*, 109**,** 5−31: DOI 10.1007/s10584-011-0148-z.

WATER RESOURCES COUNCIL (1981) now called Interagency Advisory Committee on Water Data), Guidelines for determining flood flow frequency, . *bulletin 17B, available from Office of Water Data Coordination,,* U.S. Geological Survey, Reston, VA 22092.

Theme Six: Emerging Challenges

Regional Initiatives for Drought Monitoring in the Horn of Africa

Luke O. Olang; Markus Disse; Zheng Duan

Technical University of Munich, Chair of Hydrology and River Basin Management, Germany

ABSTRACT

Reducing rainfalls and increasing temperatures consequent of changes in climate is a threat to water and food security in Africa. In the Horn of Africa, scarcity of water resources to support subsistence agriculture particularly during the crop growing rainfall seasons is a major cause of recurring droughts. The current approaches for monitoring the climatic trends, however, are limited in part due to lack of reliable and sufficiently representative in-situ observation datasets. Operational seasonal forecasting often relies on statistical regressions that provide little information for drought assessment and forecasting. There is hence the inevitable need for improved monitoring strategies emphasizing on integrated approaches to support regional policy and community-based adaptation. Recent advancements in seasonal climate monitoring coupled with large-scale model predictions consequent of global satellites data systems have provided the ability to improve drought monitoring and early warning. The African Flood and Drought Monitor exploiting these capabilities has recently been developed for the evaluations of near real-time terrestrial water cycles based on ensemble dynamical and statistical forecasts conditioned on climate indices. We demonstrate the application of the system for drought monitoring in medium catchments in the Horn of Africa. We further illustrate how auxiliary datasets can be re-analyzed in conjunction with in-situ datasets where available, to reveal the climatological trends of stream flows, rainfalls and drought severity indices in the Greater Horn of Africa.

1. Introduction

In the arid and semi-arid regions of the Horn of Africa, drought remains a major cause of food insecurity due to the existence of marginal lands and over-reliance on rain-fed agriculture (Gan et al. 2016; Sandstrom & Juhola 2016). Despite existing interventions by the concerned national agencies, water and agricultural sectors still lag behind, thereby posing a significant threat to the economic development of the region (Cervigni & Morris 2016; Tadesse et al. 2018). With continued climate change and variability effects, exacerbated by eminent poverty and disproportionate increases in human population, the economic development of the Greater Horn of Africa (GHA) depends on its ability to vibrantly adapt, while at the same time investing on development options that directly improves the health of it rural population (Lyon 2014; Ouma et al. 2018). To this end, the concerned regional institutions have

recently advocated for the application of improved management strategies, emphasizing more on accurate predictions of the environmental related challenges to promote improved management (Awange et al. 2016). However, the shift in paradigm is already being hampered by technological and political contraints undermining the development, testing and adaptation of integrated approaches capable of promoting seamless utility across various scales within the vulnerable groups (Otzelberger 2015).

A majorty of national and regional institutions in the GHA today recognize that the impacts of droughts consequent of climate extremes are largely felt at community levels (i.e. by the water resources users and management communities; farming and agriculture based communities). It is hence important that such vulnerable groups are supported to appropriately plan and adapt in good time before the disasters strike (Berger 2009; Arndt et al. 2015). And because the effects of the drought events occur through hazards that may be historically familiar, and for which the communities often had a rich repertoire of adaptive strategies, there is also the need for solution based approaches that incoperate local skills and experiences to expedite the adaption and recovery process (Gogoi et al. 2014; Ouma et al. 2017). Yet, some of the key challenges constraining the attainment of such integrated approaches include limited institutional coordination at national, regional and international levels to mainstream and guide robust management strategies applicable across the geo-political zones. Also, there is lack of good quality measured datasets, be it hydro-meteorological and/or socio-economic data, to enable the testing of improved monitoring tools. More often, there exists mistrusts and hence the inability amongst concerned stakeholders to share the existing in-situ measurements. This is because most countries in the region do not have robust data sharing policies capable of protecting any abuse of the shared datasets as its utility spreads horizontally across the users (Sheffield et al. 2014).

Despite these national and regional challenges however, some scientific tools for monitoring drought status across the globe have been developed. The development has been boosted by increased proxy datasets consequent of advances in satellite remote sensing, and hence the urgent need for consolidated environmental management (Olang et al. 2012; Chaney et al. 2014). Such tools ingest the spatial datasets to provide near real- time estimates of various water balance fluxes known to influence the development and recovery of drought conditions. Since most of the tools were developed elsewhere, and sometimes for targeted local applications, there is the inevitable need to test the model estimates against the existing data for enhanced application in supporting policy at local levels. Some of the

existing global tools available for monitoring of drought include the Global Integrated Monitoring and Prediction System, and the African Flood and Drought Monitor (AghaKouchak 2015). Other global tools for understanding the socio-economics of drought effects are the FAO's Global Information and Early Warning System on Food and Agriculture (GIEWS), the Humanitarian Early Warning Service (HEWS) operated by the World Food Programme (WFP) and the FEWS-Net (Famine Early Warning System - Network) amongst others (Trambauer et al. 2014). These compact tools provide near real time information, conditioned on climate-based indices, obtained by employing a number of global-input datasets capable of estimating meteorological, hydrological, agricultural, socio-economic forms of droughts (Agutu et al. 2017).

Very few studies in the GHA, however, have been undertaken to compare and validate these global model estimates to understand their reliabilities (Masih et al. 2016**)**. In this contribution, we demonstrate a straightforward validation approach within two medium River basins with relatively poor quality of datasets. The simulated and observed hydrographs and selected drought indices are compared to enable the plausibity checks and to further understand the predictive skill of the African Flood and Drought Monitor (AFDM) recently operationalised at some regional centers in Africa (Sheffield et al. 2014).

2. Study areas and Data basis

2.1 The River Basins of Study

Figure 1 illustrates the two basins where the study was carried out. The Transboundary Mara basin spans the countries of Kenya and Tanzania covering an area of about 13,800 km^2 between longitudes 33° 47’ E and 35° 47’E, and latitudes 0° 38’ S and 1° 52’ S. About 65% of the basin lies in Kenya. The 365km Mara River drains the basin, which is of world Heritage status famous for the Wild Beast migration. The altitudes range from 2950 m (above mean sea level) at its source in the Mau Escarpment to about 1000 m downstream at the final outlet into Lake Victoria. Rainfall in the area varies with altitude, with mean annuals ranging from 1000-1750 mm within the uplands, 900-1,000 mm in the midlands and 700–850 mm in the lowlands regions. Meteorological drought is a common phenomenon in the midland region with mean annual temperatures ranging between 30-35° Celsius. Stream flow based hydrological droughts however are generally prevalent between the months of December and February during low flow conditions (Mati et al. 2008).

The Transboundary Mara River Basin

The Kafu River Basin in Uganda

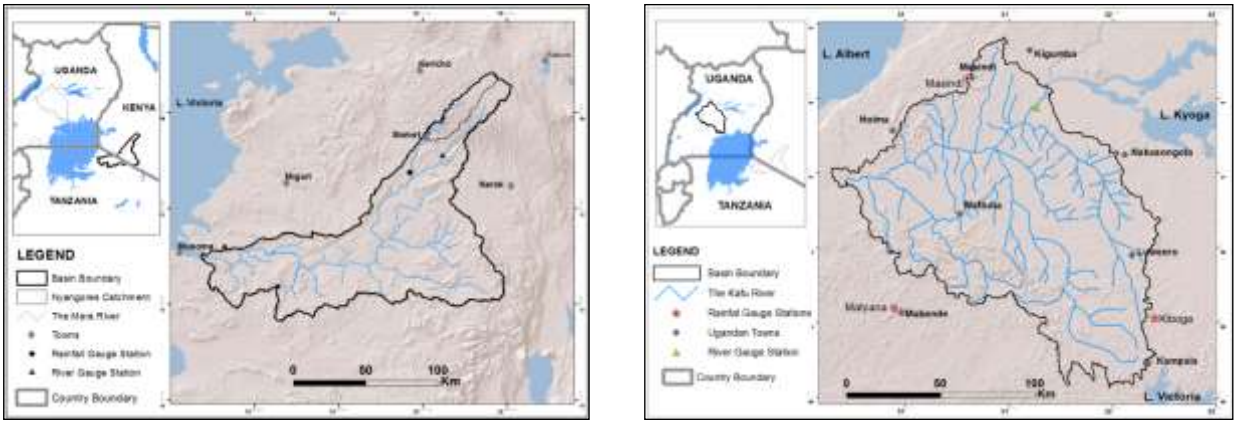

Figure 1. Location of the River Basins of study

The Kafu River Basin covers an area of 12,950 km^2 in central to mid-western part of Uganda. The River has a total length of about 180km; originating from a swamp located approximately 12km northeast of the village of Kitoma in Western Uganda. At its source, River Kafu has an altitude of approximately 1100m. At its point of entry into the Nile River, the altitude is about 1,040 m. On its course generally described as eastwards, northeastwards and northwards, the river traverses the districts of Hoima, Kyankwanzi, Nakaseke, Nakasongola District and Masindi. The region is largely located in the humid areas, with mean annual rainfall rainfalls between 1500-1800 mm per year, and mean monthly temperatures of 17-30 degrees Celsius. The region experiences more or less seasonal agricultural droughts consequent of rainfall variability mainly (Sutcliffe & Parks 1999).

2.2 Data Basis and Assessment

For this pilot study, spatial and hydro-meteorological datasets were necessary. The Shuttle Radar Topographic Mission (SRTM) Digital Elevation Model (DEM), geographical locations of the gauges, the catchment boundaries and administrative centers located around the basins were used to derive topological and morphometric characteristics of the basins (Figure 1). The analysis data supported by automated procedures in a spatial information system (GIS) (Burrough & McDonell 1998; Reuter et al. 2007). The major hydro-meteorological datasets collated were point measurements of rainfall and discharges for assessing time series trends of the hydrological droughts for study. For the Mara River Basin (like most basins in the GHA), it was not possible to obtain the data downstream of the basin, and consequently, data from two stations namely the Nyangores-Bomet Bridge streamflow station, and Amala-Kapkimolwa Bridge stream flow station were acquired from the local water user's association

(WRUA). Table 1 illustrates the data characteristics for the study basins. However, it was not possible to acquire long-term temperature data for the basins.

Table 1 Characteristics of the hydro-meteorological data

ID	Code	Gage	Location		Data Period			Lowest Q	Highest Q
			Lat.	Long.	Start	End	% missing	(m^3/s)	(m^3/s)
83213	-	Kafu Discharge G. Rd	1.54	32.04	1952	2014	12	0.4	190
107052	1LB02	Amala Discharge K.B.	-0.90	35.44	1955	1995	28	0	168
107032	1LA03	Nyangores Discharge	-0.79	35..255	1963	1992	10	0.3	29
9035265	-	Bomet WS Rain Stn	-0.78	35.35	1967	2009	12	-	-
-	-	Masindi Rainfall Stn	1.68	31.71	1980	2010	3	-	-

Streamflow and rainfall data for the Kafu River Basin (KRB) were obtained from the Uganda Meteorological authorities. The stream flow gauges provided relatively longer period of the datasets. Rainfall data from three stations namely Masindi, Kiboga, and Mityana could be obtained, but only datasets from Masindi was used due to its longer time span and close proximity to the discharge gauge station (Table 1).

3. Tools and Methods

3.1 The African Flood and Drought Monitor

The African Flood and Drought Monitor (AFDM) is macro scale hydrologic modeling system that ingests global input data to provide real-time assessment of the water cycle and drought conditions, put in the context of the long-term record back to 1950 (Sheffield & Wood 2011). Development of the model has been supported by GWADI - African experts, regional centers in consultation with UNESCO for operational and research use in flood and drought studies over Africa. The model has been operationalized at AGRHYMET for the Western African region, ICPAC for the IGAD region, and SADC for the Southern African region (Sheffield et al. 2014). In outline, the AFDM comprises of two parts. First, a historic reconstruction (1950 – 2008) of the water cycle forced by a merged reanalysis/observational meteorological data set. This forms the climatology against which current conditions are compared. Second is a real-time monitoring system (2009 – present) driven by remote sensing precipitation and atmospheric analysis data that tracks drought conditions in near real-time.

The historic and real-time data are calculated using the Variable Infiltration Capacity (VIC) land surface hydrological model, which is run at a daily time step at ¼ degree spatial resolution for the whole of Africa. For the historic reconstruction, the model is forced by meteorological data derived from a

blending of reanalysis (NCEP/NCAR) and gridded observation-based datasets including: the Climate Research Unit TS3.1 monthly precipitation and temperature data set, the NASA Tropical Rainfall Measurement Mission (TRMM), the monthly gridded precipitation and temperature data set of Willmott and Matsura, and the Global Precipitation Climatology Project (GPCP) monthly data set (Liang et al. 1994; Sheffield et al. 2006).

The VIC model estimates drought primarily from soil moisture, which is then provided as a drought index based on soil moisture percentiles. Using the model, multiple hydrologic variables and drought products are estimated for over 800 catchments over Africa corresponding to the Global Runoff Data Center (GRDC) network and Food and Agriculture Organization (FAO) reservoir database. The variables include: simulated discharge and basin averaged water cycle fluxes, including precipitation, evaporation, surface runoff, baseflow, and the soil moisture drought index. Some of the capabilities of the tool, including the data sources, drought types, indices and their spatial attributes are provided in Table 2 (Sheffield et al. 2014).

Table 2: Capabilities of the AFDM

Index	**Data Source**	**Drought Type**	**Attributes**
Standardized Precipitation Index (SPI)	Bias corrected TMPA (2009-present), hybrid observational /reanalysis (1950-2008)	Meteorological drought	0.25-degree, SPI-1,3,6,12
VIC - Soil Moisture Index	VIC land surface model (1950-present)	Agricultural drought	0.25-degree, daily
SMOS Soil Moisture Index	SMOS retrievals (2010-present)	Agricultural drought (top 5cm of soil)	0.25-degree, daily
NDVI/EVI	GIMMS NDVI (1982-2008); MODIS EVI (2000-present)	Ecological drought (optical-based)	8km/0.5-degree, bi-monthly/daily
VOD Index	SSM/I,TRMM,AMSR-E VOD (1987-2008); AMSR-E VOD (2000-present)	Ecological drought (passive microwave)	0.25-degree, daily
dB Index	QuickSCAT (1999-2009), ASCAT (2009-present)	Ecological-hydrological drought (active microwave)	0.25-degree, 2/4 days
Streamflow percentiles	VIC land surface model (1950-present)	Hydrological drought	streamflow gauges, daily/monthly
Cumulative streamflow deficit	VIC land surface model (1950-present)	Hydrological drought	streamflow gauges, daily/monthly

3.2. Validation of the Model Discharges

Several approaches for model testing and validation in hydrology have been proposed (Boyle et al. 2000; Refsgaard & Henriksen 2004). These goodness of fit (GOF) measures for comparing observed and simulated estimates are commonly classified as either visual (if they rely on expert judgment of the time-series hydrological fluxes) or statistical (if they employ empirical relationships between state variables). For this study, the both approaches were important considering the relatively weak data states. Emphasis was therefore not on the need to obtain a perfect fit, but rather on the overall trend and temporal transition over the seasonal scales. Visual assessment provided an opportunity to compare the model estimates across various spatial scales. Validation of the discharges at the point locations assumed the same spatial trends exists within the study entire basins. The selected statistical GOF measures used included (**1**). the Volumetric Efficiency (VE) (**2**). Pearson correlation coefficient (r) (**3**). Index of Agreement (d) (**4**). Product of coefficient of determination and slope of the linear regression (br2) and (**5**) Visual assessment of the residuals (Krause et al. 2005; Criss & Winston 2008).

3.3. Comparison of the Drought Indices

The SPI is a straightforward method recommended by WMO for quantifying rainfall deficits at several time scales (Mozafari et al. 2011; WMO 2012). Table III summarizes the categories of drought intensities-based SPI cumulative probabilities. Another index tested here was the simulated Drought Index (DI), which commonly provides an indication of severity of agricultural droughts (Nijssen et al. 2001; Liang et al. 1994). Lower values of the DI generally indicate severe droughts. Using the simulated DI, the spatial trends and transition of the simulated drought events across the study regions were mapped and visually assessed.

Table 3: Classification of drought Risk based in SPI values

SPI Value	Class of Drought	Probability of Occurrence
SPI ≥ 2.0	Extremely wet	0.977 – 1.000
1.5 ≤ SPI < 2.0	Very wet	0.933 – 0.977
1.0 ≤ SPI < 1.5	Moderately wet	0.841 – 0.933
-1.0 < SPI < 1.0	Near Normal	0.159 – 0.841
-1.5 < SPI ≤ - 1.0	Moderately dry	0.067 – 0.159
-2.0 < SPI ≤ -1.5	Severely dry	0.023 – 0.067
SPI ≤ -2.0	Extremely dry	0.000 – 0.023

4. Results and Discussion

4.1 preliminary data analysis

Plotted daily observations against model simulations for the Kafu basin are shown in Figure 2. The simulations generally over-estimated the observed daily flow discharges. However, the low-flows that provide an indication of the drought discharges were sufficiently captured by the model. Since it was not easy to discern such drought discharges from the daily time series, and because droughts manifest more at monthly time-scales, detailed assessment of the data was important to select monthly seasonal periods to use in further analysis.

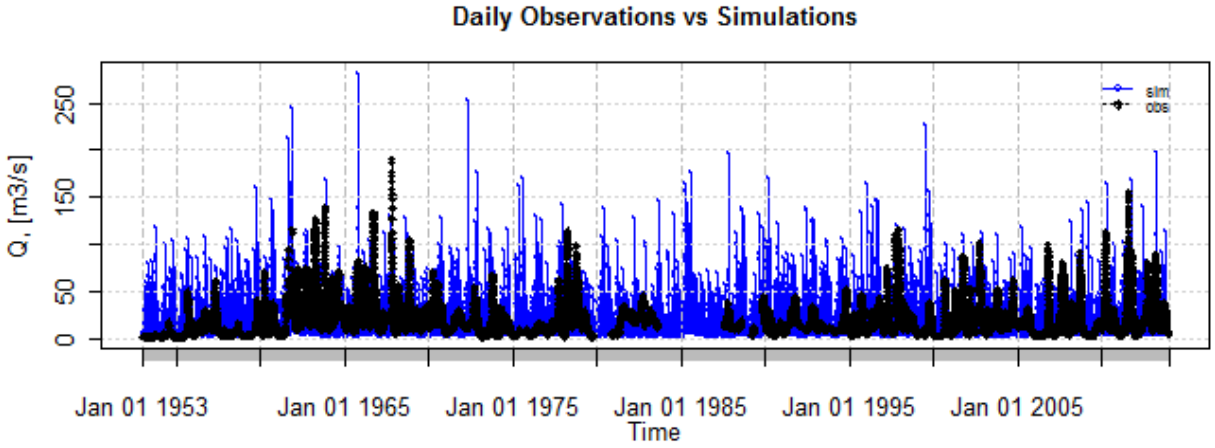

Figure 2. Daily stream flow hydrographs for the Kafu River Basin

To achieve this, the time series plots of the acquired stream-flows for all the basins were plotted for plausibility checks. Because the Nyangores and Amala sub-basins lie adjacent to each other within the Mara basin, we used the hydrograph trends to identify common low flows periods that could befit the seasonal drought analysis approach envisaged. Figure 3 illustrates the selected dry periods from the discharge plots.

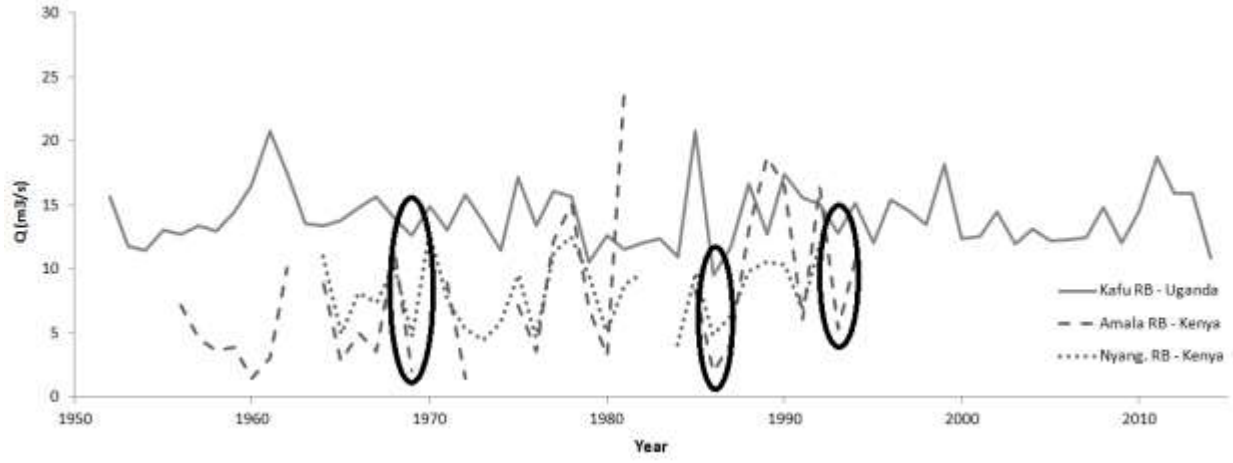

Figure 3: Comparison of stream-flow hydrographs for the basins

From the plots, three windows in 1969, 1986 and 1993 were identified. The Kafu River Basin exhibited low flows when its discharge fell below 13.0 m3/s. The Amala and Nyangores equally revealed hydrological drought at discharges less than 5.0m3/s and 6.0m3/s, respectively. Further analysis of the data indicated that low flows in the Kafu Basin were prevalent between December-February (DJF), with the lowest peak of about to 7m3/s being realized in January 1986. An almost a similar trend was noted in Mara basin where discharges as low as $3m^3/s$ were recorded during the DJF period. Based on these assessments, the study selected the periods between October – March to characterize drought events of study. Figure 4 provides mean monthly estimates for the basins for the period of data collected.

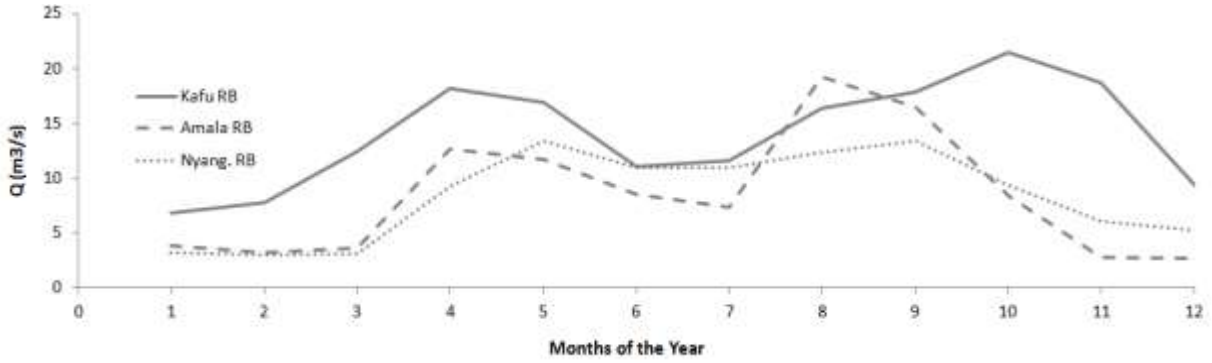

Figure 4. Mean monthly discharges for the entire data periods of the basins

4.2 Validation of the Discharges

4.2.1 The Kafu River Basin

The validation results for Kafu River Basin for selected periods are illustrated in Table 4. It should be noted here that the validations were achieved by allowing the GOFs to warm-up to the first 30% of the data period. This warm-up period was important for sufficient parameterization of the GOFs to provide good validation of estimates. See also section 3.4.1 for the measures**.**

Table 4: Estimated GOFs from the validations.

Year	GOF Measures			
	VE (%)	r (%)	d (%)	br2 (%)
Oct. 69 - Mar. 70	58	83	66	42
Nov.93 - Mar. 94	67	74	56	51

Generally, the hydrographs for basins produced acceptable comparisons and a good indication of above average simulation capability by the model. The Pearson product or Pearson correlation coefficient (r) produced the highest value indicating a good strength and direction of linear relationships based on the covariances of the data. However, lower values were generally obtained when the product of coefficient

of determination and slopes of the linear regression (br2) were calculated (Criss & Winston 2008). This was attributed to the discrepancies in the magnitudes and dynamics of the two hydrographs due to over prediction of the actual state. In terms of the residuals, the results provided in Figure 5 were obtained.

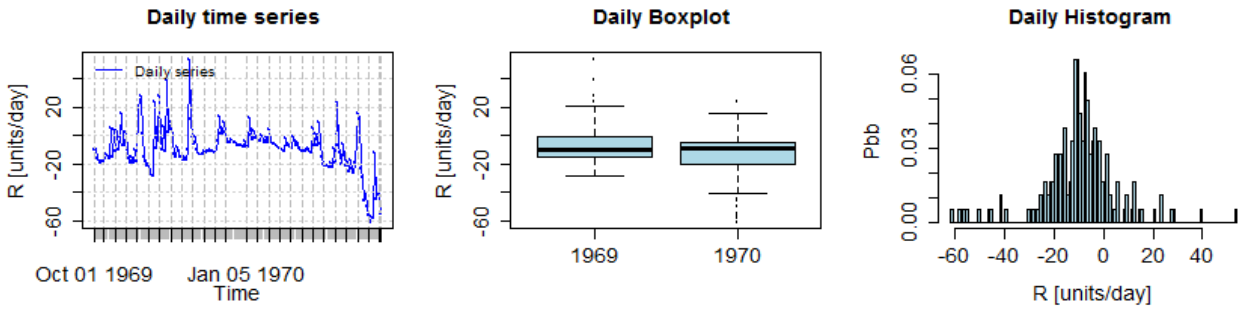

Figure 5. Residual of the Kafu River Basin validation data in mm/day

In outline, the period of 1969 generally exhibited acceptable level of homogeneity and normality based on clusters and time-series distribution of the residual (Figure 5). This is unlike the data for the 1993, when random error was apparent from the histogram, perhaps indicating a violation of model assumption requiring auxiliary investigations to verify. The Standard Precipitation Indices for the Kafu Basin were derived from the observed rainfall datasets at 1-, 3-, 6-months periods based on Gamma distribution. The derivation was achieved using the R-package SPEI, and aimed at visual comparison of plots from the observed and simulated indices. In outline, the Kafu basin indicated an SPI value of about -1.3 (Moderately dry) based on the AFDM model estimates. This was much more than the -0.6 (near normal) exhibited by the observed datasets for the same month of January for 1994 period. It is worth noting, however, that the SPI is an indicator of meteorological droughts, which often has some lead-time to hydrological droughts depending on the large responses (Maidment, 1993). Generally, from the SPI plots, it could be concluded that the simulated estimates overestimated the SPI from the observed datasets. This conclusion calls for more investigations into the precipitation input datasets for the model.

4.2.2 The Mara River Basin

Despite the apparent no-data periods in observed datasets for this basin, it was noted that the simulated trends compared fairly well. From the daily time series, going by the general trends of the simulated baseflows, the model generally overestimated the low-flows of the basin. In terms of the GOFs, relatively lower values were obtained; with an average *VE* value of 52%, *r* of about 65%, *d* of about 53% and *bR2* of 48%.

Considering the overall data quality used for the validation, however, these values were considered above average and acceptable. Though further investigations may be important with good datasets from a number of observations in the basin. In terms of the residuals (Figure 6), clearly apparent from the monthly plots was the random error due to lack of stability in the histogram. The residuals increased in values from December to February, peaking in March over the study period. However, a critical assessment of the observed data quality and the model estimates maybe important to further deduce more information from the residual plots.

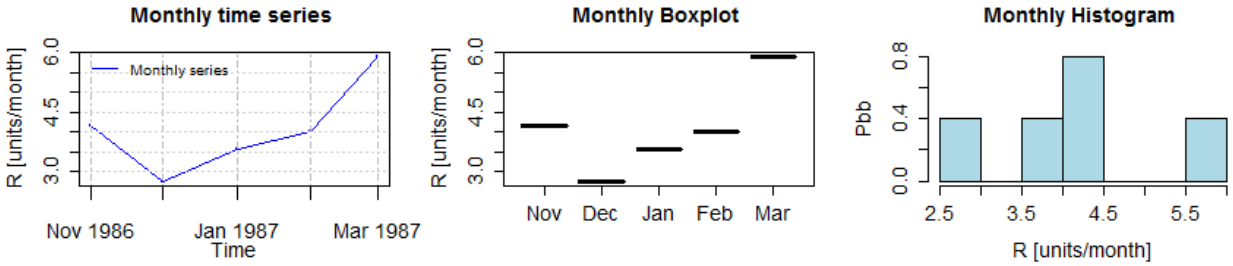

Figure 6. Residual for the Amala River Basin

Using the monthly rainfall data from Bomet Water Supply station, which had relatively good datasets, the equivalent SPIs were developed and compared with simulated SPIs from the AFDM (Figure 7). From the results, a fairly good comparison in the general trends, except in February 1994 when mild near normal drought was predicted by the model instead of near normal wet conditions. However, the model tended to underestimate the SPI index, perhaps indicating non-stationarity in the precipitation time series used in the SPI calculation. Generally, except for February, when the basin experienced a moderately dry condition (SPI of 1.3), the rest of drought months could be classified as near normal in the figure below.

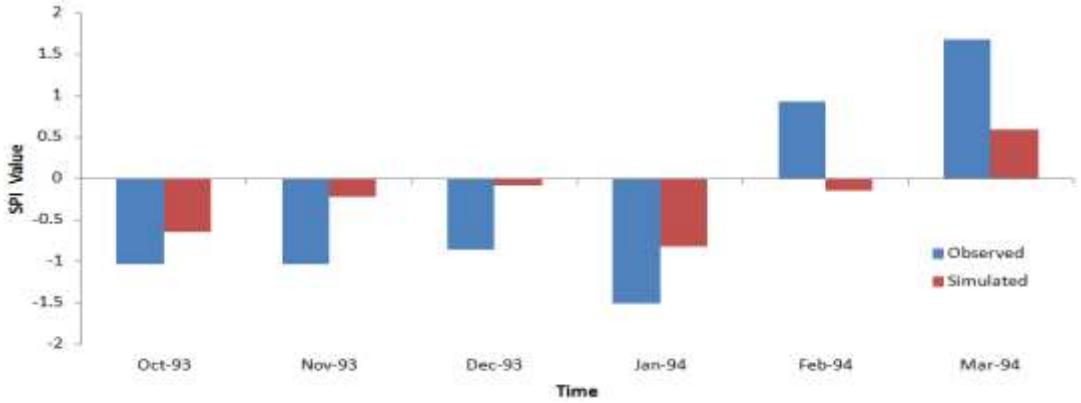

Figure 7. SPI comparison for the Bomet Water Supply Station

4.3 Comparison of the Model performance in the River Basins

Within the context on this study, the Kafu River Basin was selected to represent a medium catchment with humid to semi-humid conditions, while the Nyangores and Amala sub-basins of the Mara basins used in this were relatively small, with some parts in the semi-arid zones. The Kafu basin provided sufficiently good quantity and quality of streamflow data compared to the Mara basin, which had better quality of rainfall datasets. Consequently, from the validation results, the Kafu basin provided better estimates based on the GOFs produced. In terms of SPI values which relied more on rainfall datasets, the Nyangores of the Mara Basin provided better comparison to the AFDM simulations. Based on the Drought Index (DI) from the AFDM model, the spatial trends from simulated estimates for 1985/1986 drought events in both basins are illustrated in Figure 8. Generally, lower Drought Index (DI) values often signify severe droughts. From the maps, therefore, the Mara Basin could be seen to be more effected spatially in February 1986, with the Northern upstream parts being highly affected, as the drought front spreads south-wards of the basin. .

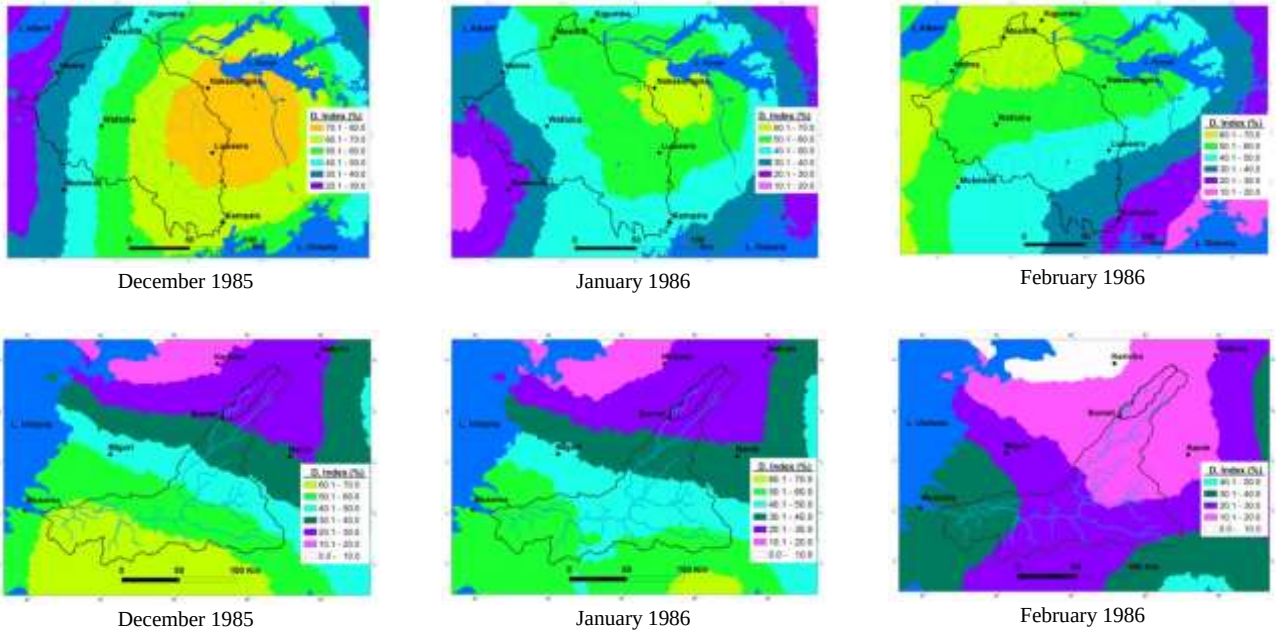

December 1985 January 1986 February 1986

December 1985 January 1986 February 1986

Figure 8. Comparison of the spatial trends of the droughts

5. Conclusion and Recommendation

Today, a majority of the existing regional tools for drought monitoring employ physical datasets obtained largely from remote sensing data sources. In the GHA, however, there exist significant geophysical and geopolitical disparities likely to influence the occurrence and management of drought.

It is hence critical to localize and test the existing global tools to promote ownership and build confidence towards policy support. In this study, we attempted to demonstrate a straightforward validation procedure that can be reproducible across the region considering the poor data status. The results also indicate that the AFDM regional tool has the potential to replicate the general trends and drought characteristics across the scales. Monthly seasonal periods were used to understand the response of the basins, considering that drought events exhibit seasonal variations are often difficult to capture from the existing data quality we obtained for the study. In outline, African Flood and Drought Monitor provide many other products that can be tested further against observed datasets, or at best in limited to no data cases, compared with other regional national tools. Such products include, daily wind speeds, temperature (min and max), net radiation, evaporation, and vegetation indices *etc*. It is equally important that the validation procedures be carried out in several river basins to understand and appreciate their reliabilities towards supporting drought studies across various scales, and especially under conditions of a continually changing climate.

References

AghaKouchak A. (2015). A multivariate approach for persistence-based drought prediction: Application to the 2010–2011 East Africa droughts. Journal of Hydrology, 526, 127–135. DOI: 10.1016/j.jhydrol.2014.09.063

Agutu N.O., Awange J. L., Zerihun A., Ndehedehe C.E., Kuhna M., Fukuda Y. (2016). Assessing multi-satellite remote sensing, reanalysis, and land surface models' products in characterizing agricultural drought in East Africa. Remote Sensing of Environment, 194 287–302. https://doi.org/10.1016/j.rse.2017.03.041

Arndt C., Chinowsky P., Fant C., Gebretsadik Y., Neumann J.E., Paltsev S., Schlosser C.A., Strzepek K., Tarp, F., & Thurlow, J. (2015). Climate change and developing country interests. United Nations University - World Institute for Development Economics Research (UN-WIDER). https://www.wider.unu.edu/sites/default/files/WP2015-116-.pdf

Awange J.L., Khandu, Schumacher M., Forootan E., Heck B. (2016). Exploring hydro-meteorological drought patterns over the Greater Horn of Africa (1979 - 2014) using remote sensing and reanalysis products. Advances in Water Resources, 94,45-59. https://doi.org/10.1016/j.advwatres.2016.04.005.

Berger R. (2009). Linking adaptation planning and implementation from community level to national level. Bangkok: United Nations Economic and Social Commission for Asia and the Pacific (UNESCAP).

Boyle D.P., Gupta H.V., Sorooshian S. (2000). Toward Improved Calibration of Hydrologic Models: Combining the Strengths of Manual and Automatic Methods. Water Resources, 36(12): 3663–3674. https://doi.org/10.1029/2000WR900207

Burrough P.A., Mc Donnel R.A. (1998). Principles of Geographical Information System. Oxford University Press: New York.

Cervigni R., Morris M. (2016). Confronting Drought in Africa's Drylands: Opportunities for Enhancing Resilience. World Bank Publications, 2016. ISBN: 9781464808180.

Chaney N.W., Sheffield J., Villarini G., Wood E.F. (2014). Development of a high resolution gridded daily meteorological data set over sub-Saharan Africa: spatial analysis of trends in climate extremes. Journal of Climate, 27, 5815-5835. DOI: 10.1175/JCLI-D-13-00423.1

Criss, R. E. and Winston, W. E. (2008), Do Nash values have value? Discussion and alternate proposals. Hydrological Processes, 22: 2723-2725. DOI: 10.1002/hyp.7072

Gan T.Y., Mari Ito, Hülsmann S., Qin X, Lu X.X., Liong S.Y., Rutschman P., Disse M., Koivusalo H. (2016). Possible climate change/variability and human impacts, vulnerability of drought-prone regions, water resources and capacity building for Africa, Hydrological Sciences Journal, 61:7, 1209-1226, DOI: 10.1080/02626667.2015.1057143

Gogoi E., Dupar M., Jones L., Martinez C., McNamara L. (2014). Enablers for delivering community-based adaptation at scale. Climate and Development, 6(4), 368-371. DOI:10.1080/17565529.2014.918869

Krause, P., Boyle, D. P., and Base, F.: Comparison of different efficiency criteria for hydrological model assessment. Adv. Geosci., 5, 89-97, 2005. https://doi.org/10.5194/adgeo-5-89-2005

Liang X., Lettenmaier D.P., Wood E.F., Burges S.J. (1994). A simple hydrologically based model of land surface water and energy fluxes for general circulation models. J. Geophys. Res., 99(D17), 14415–14428. https://doi.org/10.1029/94JD00483

Lyon B. (2014). Seasonal Drought in the Greater Horn of Africa and Its Recent Increase during the March–May Long Rains. Journal of Climate, 7, 7953-7975. DOI: 10.1175/JCLI-D-13-00459.1

Maidment D.R. (1993). Handbook of hydrology. McGraw Hill, New York, USA.

Masih I., Maskey S., Mussá F.E.F., Trambauer P. (2014). A review of droughts on the African continent: a geospatial and long-term perspective. Hydrol. Earth Syst. Sci. 18 (9), 3635–3649. http://dx.doi.org/10.5194/hess-18-3635-2014.

Mati B.M., Mutie S., Gadain H., Home P., Mtalo F. (2008). Impacts of land-use/cover changes on the hydrology of the trans-boundary Mara River, Kenya/Tanzania. Lakes & Reservoirs: Research & Management, 13: 169–77. DOI: 10.1111/j.1440-1770.2008.00367.x

Mozafari G.A., Khosravi Y., Abbasi E., Tavakoli, F. (2011). Assessment of Geostatistical Methods for Spatial Analysis of SPI and EDI Drought Indices. World Applied Sciences Journal, 15 (4): 474-482.

Nijssen B.N., Schnur R., Lettenmaier D.P. (2001). Global retrospective estimation of soil moisture using the Variable Infiltration Capacity land surface model, 1980-1993, J. Clim., 14(8), 1790-1808. DOI: 10.1175/1520-0442(2001)014<1790:GREOSM>2.0.CO;2.

Olang L.O., Kundu P.M., Ouma G., Fürst J. (2012). Impacts of Land Cover Change Scenarios on Storm Runoff Generation: A Basis for Management of the Nyando Basin, Kenya. Land Degradation and Development, 25(3), 267-277. DOI: 10.1002/ldr.20

Otzelberger A., Percy F., Ward N. (2015). Strengthening Adaptive Capacity to Climate Change: Learning from Practice. Cooperative for Assistance and Relief Everywhere (CARE). Online Publications. http://careclimatechange.org/publications/adaptive-capacity-practitioner-brief

Ouma J.O., Olang L.O., Ouma G.O., Oludhe C., Ogallo L., Artan G. (2018). Magnitudes of Climate Variability and Changes over the Arid and Semi-Arid Lands of Kenya between 1961 and 2013 Period. American Journal of Climate Change, 7, 27-39. https://doi.org/10.4236/ajcc.2018.71004

Ouma G.O., Dieye A.M., Ogallo L.O., Olang L.O. (2017): Institutional challenges in scaling-up climate change adaptation actions: experiences from rural communities in Senegal and Kenya, Climate and Development. DOI: 10.1080/17565529.2017.1372261

Refsgaard J.C., Henriksen H.J. (2004). Modelling guidelines—terminology and guiding principles. Advances in Water Resources **27**: 71–82. DOI: 10.1016/j.advwatres.2003.08.006.

Reuter H.I., Nelson A., Jarvis A. (2007). An evaluation of void filling interpolation methods for SRTM data. International Journal of Geographic Information Science 21(9): 983-1008. DOI: 10.1080/13658810601169899

Sandstrom S., Juhola S. (2016) Continue to blame it on the rain? Conceptualization of drought and failure of food systems in the Greater Horn of Africa, Environmental Hazards, 16:1, 71-91. DOI: 10.1080/17477891.2016.1229656

Sheffield J., Goteti G., Wood E.F. (2006). Development of a 50-yr, high resolution global dataset of meteorological forcings for land surface modeling. Journal of Climate, 13, 3088-3111. https://doi.org/10.1175/JCLI3790.1

Sheffield J., Wood E.F. (2011). Drought: Past Problems and Future Scenarios. London: Earthscan.

Sheffield J., Wood E.F., Chaney N., Guan K., Sadri S., Yuan X., Olang L., Amani A., Ali A., Demuth S. (2014). A drought monitoring and forecasting system for Sub-Sahara African water resources and food security. Bulletin of the American Meteorological Society, 95(6), 862-882. https://doi.org/10.1175/BAMS-D-12-00124.1

Sutcliffe J.V., Parks Y.P. (1999). The Hydrology of the Nile. IAHS Special Publ. no. 5

Tadesse T., Wall N., Hayes M., Svoboda M., Bathke D. (2018). Improving National and Regional Drought Early Warning Systems in the Greater Horn of Africa. Bull. Amer. Meteor. Soc. DOI: 10.1175/BAMS-D-18-0019.1. In press.

Trambauer P., Maskey S., Werner M., Pappenberger F., van Beek L.P.H., Uhlenbrook S. (2014). Identification and simulation of space–time variability of past hydrological drought events in the Limpopo River basin, southern Africa. Hydrology and Earth System Sciences. https://doi.org/10.5194/hess-18-2925-2014

WMO [World Meteorological Organization] (2012). Standardized Precipitation Index User Guide (M. Svoboda, M. Hayes and D. Wood). (WMO-No. 1090), Geneva.

Adaptive capacity of community to drought in Upper Gana watershed, southern Ethiopia

Kassaw Beshaw Tesema[a], Alemseged Tamiru Haile[b]

[a]*Arba Minch Water Technology Institute (AWTI), Arba Minch University, P. O. Box 21, Ethiopia,*
[b]*International Water Management Institute (IWMI), P. O. Box 5689, Addis Ababa, Ethiopia*

*Correspondence: beshawkassaw@yahoo.com

Abstract

The adaptive capacity of communities in small watersheds is not well documented in literature. In this study, we evaluated the adaptive capacity of the community to drought in Upper Gana watershed in southern Ethiopia. The adaptive capacity was determined using primary data which was derived using a household survey. We used a stratified random sampling to identify the households to be surveyed. The watershed was divided in to three parts: lower, middle and upper part. Fifty-one households were interviewed from each of the watershed parts. A total of 153 households were surveyed. Interview of each respondent lasted for an average time of 30 minutes. The adaptive capacity of the community was determined by composite index which has sub-indices called human, financial, social and physical capital. Each of the sub-indices was estimated from a set of indicators which were derived from the household survey data. The adaptive capacity of the community was rated from extremely low to extremely high. The results of this study can be used to identify interventions that improve adaptive capacity and as input to study the vulnerability of community whereas the approach can be tested in other watersheds in Ethiopia.

Key words: adaptive capacity, adaptation, agricultural water, community, watershed, Upper Gana, Ethiopia

1. Introduction

Drought has a huge negative impact on livelihood of the communities at local and global scale particularly these who live in semi-arid and arid regions (Keshavarz et al., 2017; Martin et al., 2014). The diverse effect of drought on a community livelihood in terms of its duration, frequency and severity is immense. Drought is one of climate events which can have a capacity to make the community system

more exposed, sensitive and vulnerable to various external stress (Keshavarz et al., 2014, Sulieman and Elagib,2012).

Vulnerability of the system is a function of exposure, sensitivity, and adaptive capacity (Smit and Wandel, 2006; Engle, 2011). When the system is affected by the external stresses such as drought, flood, climate change, occurrence of diseases and other factors, we call it exposure. Then the system will have a certain feeling for the external stresses and the phenomena is called sensitivity.

The combined effect of exposure and sensitivity resulted in to negative or positive potential impact on the system. This produces potential impact fully or partially resisted by the system with a change or temporal adjustment of itself. The process is called adaptive capacity (Smit et al., 2001;Adger et al., 2007). If there are unbalance between the potential impact created by the external stress and the adaptive capacity, the surplus potential impact will be the cause of vulnerability. Figure 1 shows the interrelationship between the three components of vulnerability.

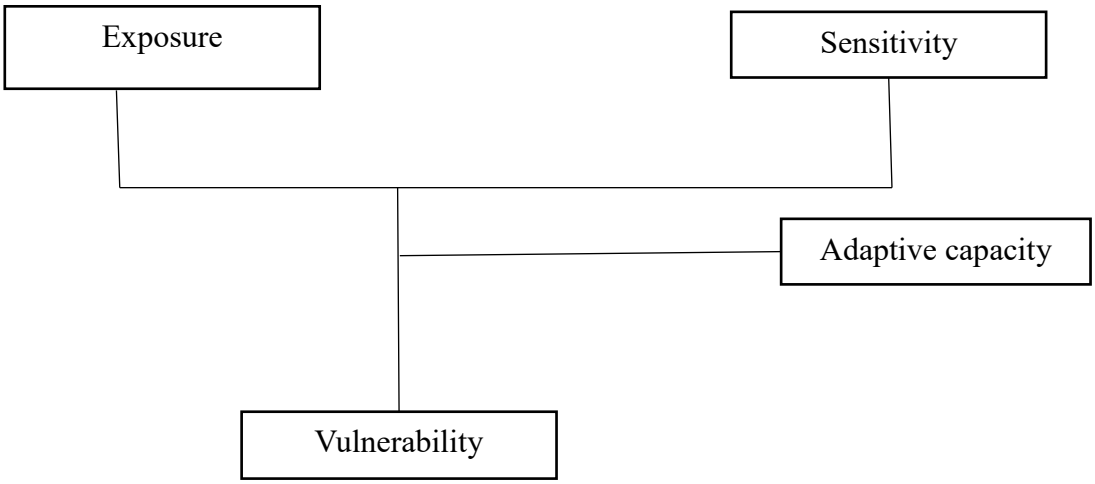

Figure 1. Interrelationship between vulnerability and its components: exposure, sensitivity, and adaptive capacity

Adaptive capacity of the system or the community have been defined in various ways with respect to different objectives, targets and purposes. We pick one of its definition as follows. Adaptive capacity is defined as the ability or the capacity of the system to modify or change its characteristics or behavior so as to cope better with existed or anticipated external stress (IPCC,2001; Burton et al.,2002; Anger et al., 2003). It is a function of different factors such as human, physical, financial, and social capital (Keshavarz et al., 2017). These factors are very helpful as indicators and sub indicators for the evaluation of the adaptive capacity of community to drought.

Upper Ganawatershed is densely populated with high competitionfor water and land resources, high stress on the environment. The aim of this research is to investigate community capabilities to deal with external stress such as drought in Upper Gana. This can provide a guidanceto make targeted intervention which improves adaptive capacity of community.

2. Material and Methods

2.1.Description of study area

The study was conducted at a small upland watershed that covers an area of 1690 ha. Its geographic location is at 7º34'45.915''N latitude and 37º45'12.957''E longitude (Figure 2). The population density is 45 households per km^2 (personal communication with kebele leaders).

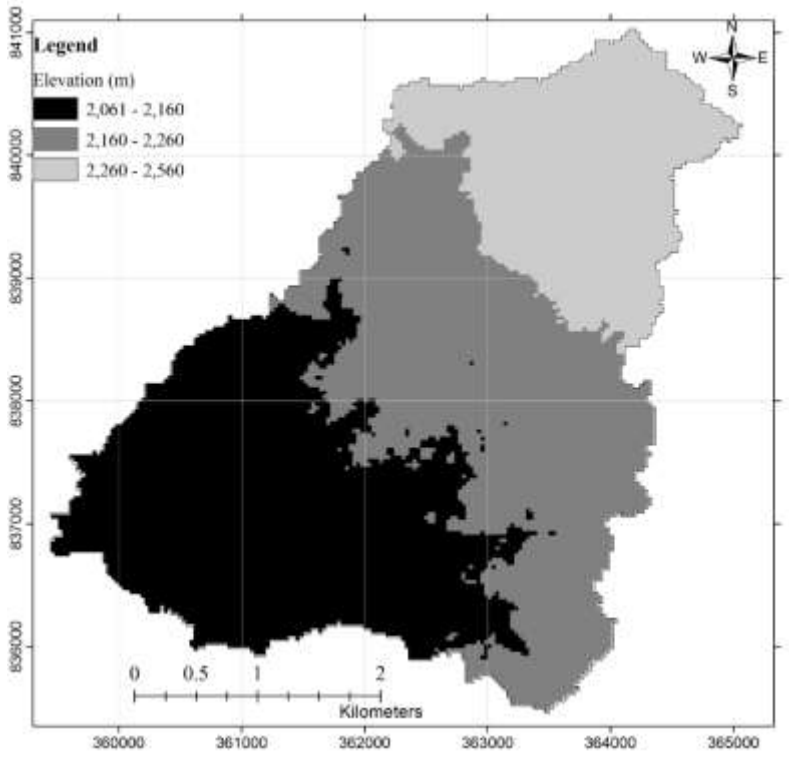

Figure 2. The three elevation zones of Upper Gana Watershed.

Average temperature : The annual variation of the temperature of the area is averaged from three years of climate data of the area. The data was measured using Automatic Weather Station (AWS) which is installed in the watershed. The maximum and minimum monthly average temperature are 20.45 ^{O}C and 16.84 ^{O}C respectively. The maximum was recorded in May and the minimum in July and August which are the main rainy season (Figure 3).

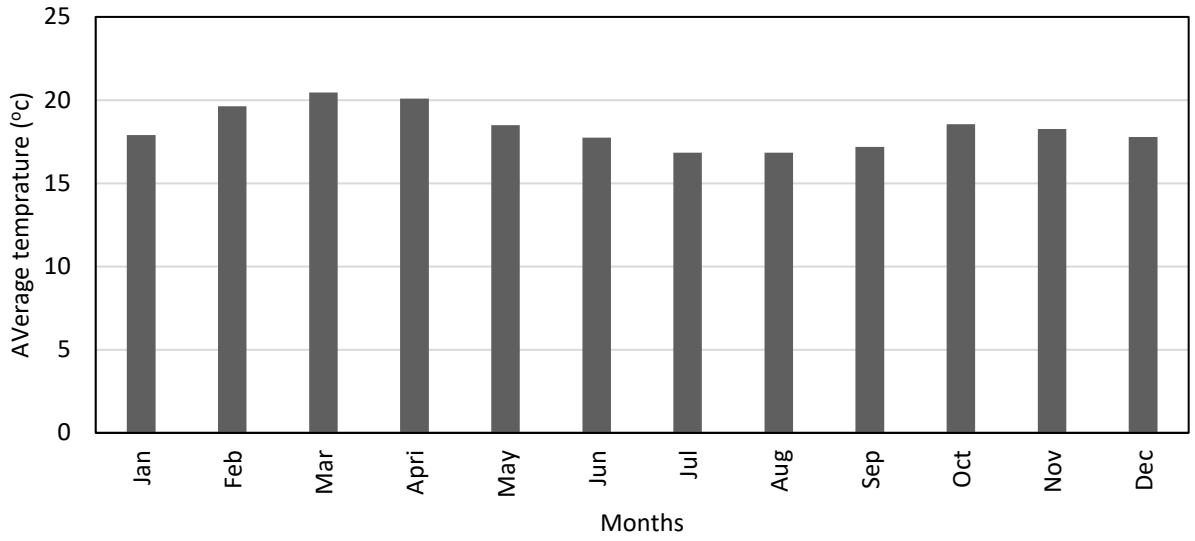

Figure 3. Average monthly temperature of the study area. (it was averaged using the annual data of the year 2015, 2016, & 2017)

Rainfall anomaly: Rainfall anomaly was computed from 23 years of rainfall data which wasobtained from the nearby weather station of Hosanna town. The deviation of annual rainfall from the 23-year average rainfall was calculated and plotted against corresponding year (Figure 4). The figure shows that 48 % of the time, the annual rainfall deviated from the average of 23 year by at least±5%. Out of which 22% are greater and 26% are less than the average rainfall. Therefore, temporal variability of rainfall in the area is high which cause some uncertainty and irregularity which in turn affect the livelihood of the community.

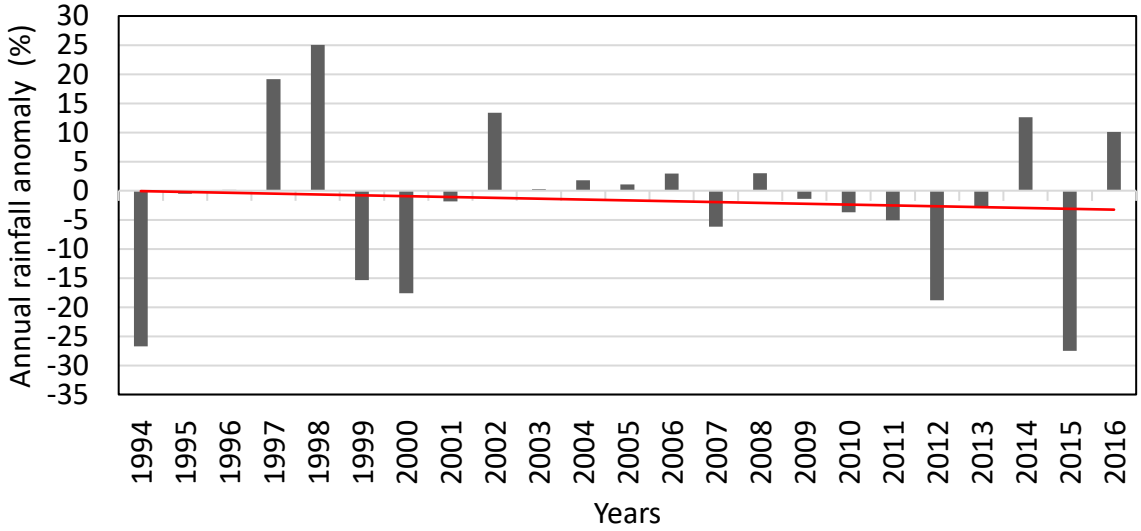

Figure 4. Rainfall anomaly which was calculated from 23 years of rainfall data.

Data collection and surveying: The first activity of data collection was preparation of interview questionnaires which comprises of all-important aspects such as humans, physical, social and financial factors collectively determine the adaptive capacity of the community. The prepared questionnaires were pre-tested and a revision work was done to make it very clear, brief, understandable and less time consuming.

Figure 5. a photo which was taken during pre-testing of household survey questionnaires with the supervisor

Then we follow stratified random sampling strategy to select the respondent head of households. The watershed is divided as lower, middle and upper part and a total of 153 respondents were interviewed about 78 are used for this analysis. We tried to keep uniformity of surveying throughout the whole watershed area.

Adaptive capacity determination: Table 1 shows the indices and sub indicators which were used to evaluate the adaptive capacity of community for drought. We defined four indices which represent human, physical, social and financial capital. The value of each index was estimated as aggregated values of multiple sub-indices. The four indices were aggregated to estimate the adaptive capacity. We assigned scores to each indicator to attach quantitative value to the household data (Table 2). The respondents answer was assigned a certain value according to the contribution to adaptive capacity. The values range from 1 (representing very low adaptive capacity) to 5 (representing extremely high adaptive capacity).

Table 1. Indicator of community adaptive capacity

Indices	Sub indices	Description
Human capital	Education	Educational grade level of HH head
	HH size	Total family member of the HH
	Illiteracy ratio	Percent of family member without primary education
	Adult ratio	Percent of adults within the age 18 to 65 years
Physical capital	Farm size	Total hectare of land owned by the farmer
	Livestock	Number of livestock owned by HH
	Water source in dry	Type of source (tap water, stream, shallow groundwater or spring)
	Water accessibility in dry	Distance from the water source
Financial capital	Income	Annual income generated from both on farm and off farm activity
	Income diversification	Practices that may diversify the income of HH
Social capital	Support from relatives	Percent of their total income which is received from their relatives
	Social network	Membership of social network such as "edir and "Iqub"
	Support from organizations	Support from governmental and non-governmental organizations when drought occurred

The score of each sub index component averaged to obtain the adaptive capacity of the community in terms of main indices using the following equations.

$$AC_i = \frac{1}{n}\left(\sum_{j=1}^{n} SI_j\right) \quad (1)$$

Where AC_i is the adaptive capacity with respect to a particular index (i), n is number of sub-indexes corresponding to a certain index, SI_i is the score of j^{th} indicator of the sub-index. Finally, value of all main indices was averaged to obtain the adaptive capacity of the community to drought.

Table 2. Score assigned for adaptive capacity of indicators

	Adaptive capacity scores				
	very low	low	good	high	Extremely high
Human capital Physical capital Financial capital Social capital	1	2	3	4	5

3. Results &discussion

The adaptive capacity of the communities to drought stress at Upper Gana watershed was evaluated using composite index of capital assets such as human, physical, social and financial. The average aggregated adaptive capacity of community to drought at Upper Gana watershed is 2.919 (58.4%) which ranks the adaptive capacity of rural agricultural watershed community under moderate range.

The main indicator which lowers average AC of community to drought is social capita.The contribution of each main indices to adaptive capacity of community are shown in Figures 6. The highest contributors of adaptive capacity are physical capital (3.575) and financial capital (3.424) while the lowest contributor is social capital (1.485). This suggests that the need to first target the social capital if the adaptive capacity is to be increased.

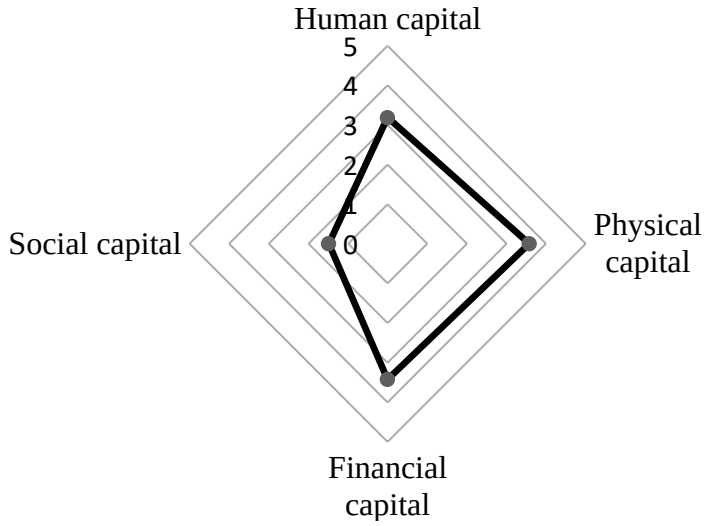

Figure 6. Adaptive capacity of community with respect to main indices

The contribution of the sub-indices to adaptive capacity of community are evaluate and presented in Figure 7. With regard to human capital, illiterate ratio performs least (2.443) and family size score is the highest (4.709). Particularly the uneducated members of the household and the educational level of the head of household play an important role in reducing the overall score of human capital. This indicates the policy maker and other relevant actors should first target education to enhance human capital of the community.

Regarding physical capital ownership, there is noticeable difference between the contribution of the different indicators. Livestock ownership and average farmland holding are not satisfactory. The community are highly populated which is manifested by small number of livestock and very small size of land owned.

Scores from water related criteria is more than satisfactory which greater than 4.253. This is well supported by the public fountains which are distributed throughout the watershed that supply water to the community on daily bases. In addition, small streams in the watershed have perennial flow.

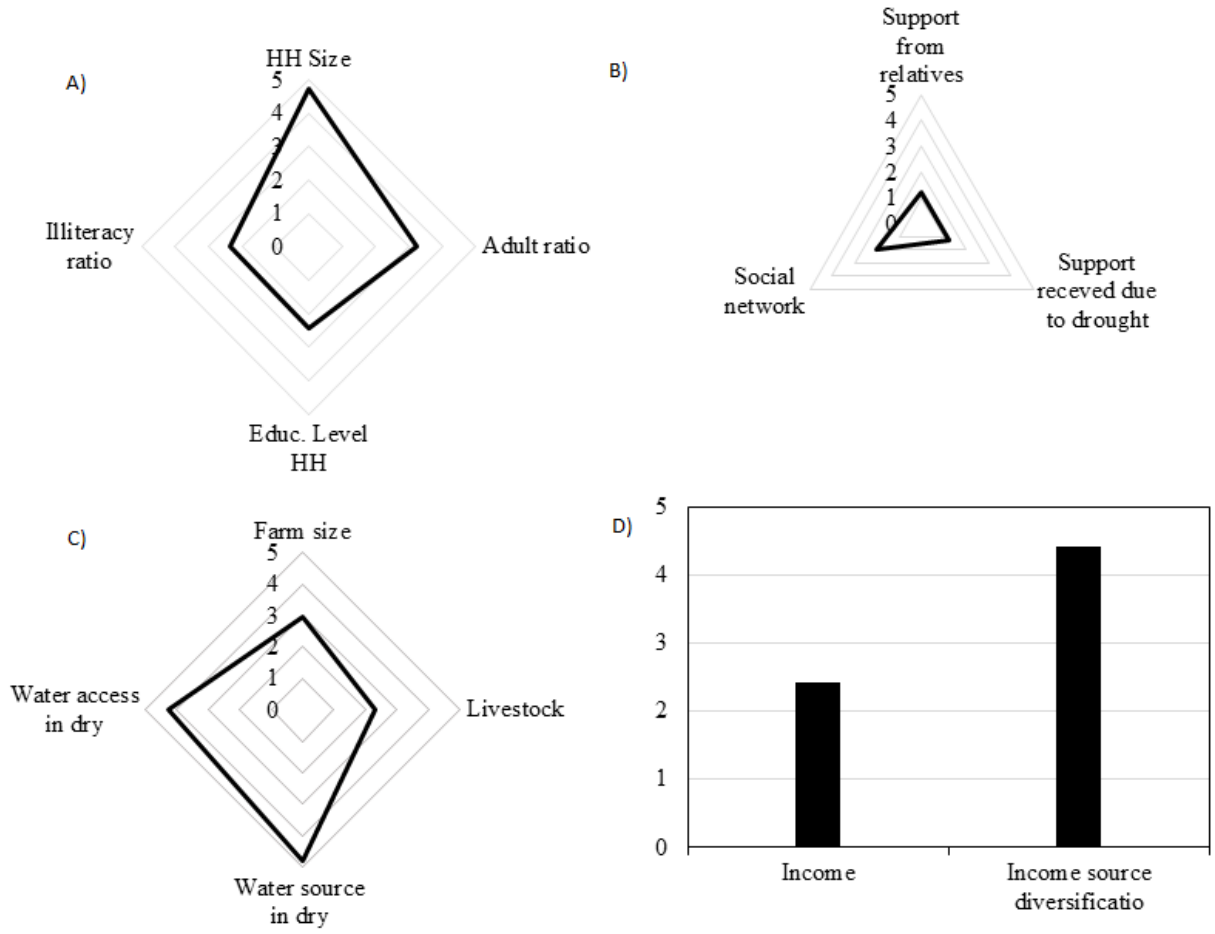

Figure 7. Adaptive capacity of community with respect to sub indicators. Note that A, B, C, D stands for the components of human, social, physical and financial capital respectively.

Land accessibility and livestock ownership can be improved through the implementation of highly intensified farming system which enable the community to produce more livestock and agricultural product on limited amount of land resource.

The scores of all social capitalindicators are low which ranges between 1.228 to 2. The contribution of support from relatives and various governmental and none governmental organizations during the occurrence of drought stress is not satisfactory.

Annual income and its diversification are categorized under the financial capital. The scores of incomes and its diversification are 2.418 and 4.430 respectively. From this, we can conclude that communities in the watershed are engaged a very diversified source of income. However, the income is small which is manifested with its score.

4. Conclusion and Recommendation

Based on the results of our analysis, the following conclusions are drawn.

- Adaptive capacity of the community is not high which needs to be improved

- There is a variation in contribution of each adaptive capacity sub-index to the entire adaptive capacity.
- The contribution of social capitalis the lowest and therefore should be targeted first to increase the adaptive capacity of the community.
- The community has diverse income generation mechanisms but the total income is too low to lead to high adaptive capacity. Therefore, special attention is required to increase the total income of households.

Future work should focus on community consultation to assign scores and weight to indicators.

References

Adger, W.N., Huq, S., Brown, K., Conway, D., Hulme, M. (2003). Adaptation to climate change inthedeveloping world.Progress in Development Studies, 3(3), 179–195.

Adger, W.N., Agrawala, S., Mirza, M.M.Q., Conde, C., O'Brien, K., Pulhin, J., Pulwarty, R., Smit,B., Takahashi, K. (2007). Assessment of adaptation practices, options, constraints and capacity. Climate Change 2007: Impacts, Adaptation and Vulnerability. Fourth Assessment Report of the Intergovernmental Panel on Climate Change, Cambridge University Press, Cambridge, UK, pp: 717-743.

Burton, I., Huq, S., Lim, B., Pilifosova, O., Schipper, E.L. (2002). From impacts assessment to adaptation priorities: the shaping of adaptation policies, Climate Policy, 2, 145-159.

Engle, N.L. (2011). Adaptive capacity and its assessment. Global Environmental Change, 21, 647-656.

IPCC- Climate Change (2001). Impact, adaptation and vulnerability. Contribution of working group II to the third assessment report, Cambridge University press, Cambridge, UK.

Keshavarz, M., Maleksaeidi, H., Karami, E. (2017). Livelihood vulnerability to droughts: A case of rural Iran. International Journal of Disaster Risk Reduction, 21, 223 – 230.

Keshavarz, M., Karami, E. (2014). Farmer decision making process under drought. Journal of Arid Environment, 1080,43 – 56.

Martin, R., Linstadter, A., Frank, K., Muler, B. (2014). Livelihood security in face of drought: Assessing the vulnerability of pastural household. Environmental Model Software, 75, 414 – 423.

Smit, B.,Wandel, J. (2006). Adaptation, adaptive capacity and vulnerability. Global Environmental Change, 16 (3), 282–292.

Smit, B., Pilifosova, O., Burton, I., Challenger, B., Huq, S., Klein, R.J.T., Yohe, G., Adger, N., Downing, T., Harvey, E., Kane, S., Parry, M., Skinner, M., Smith, J., Wandel, J. (2001). Adaptation to climate change in the context of sustainable development and equity. In: McCarthy, J.J., Canziani, O.F., Leary, N.A., Dokken, D.J., White, K.S. (Eds.), Climate Change 2001: Impacts, Adaptation and Vulnerability. Contribution of Working Group II to the Third Assessment Report of the Intergovernmental Panel on Climate Change. Cambridge University Press, Cambridge, UK.

Sulieman, H.M.,Elagib, N.A. (2012). Implications of climate, land-use and land-cover changes for pastoralism in eastern Sudan. Journal of Arid Environments, 85, 132–141.

Structural measures for Kulfo River Flood mitigation

Abdella K.[1], Mekuanent M.[2*]

[1] Faculty of Hydraulics and Water Resources Engineering, Arba Minch Water Technology Institute (AWTi), Arba Minch University, Arba Minch, Ethiopia, P.O. Box 21., [2] Water resource research centre, Arba Minch Water Technology Institute (AWTi), Arba Minch University, Arba Minch, Ethiopia, P.O. Box 21. Email: mulunehmekuanent@gmail.com
*Corresponding author

Abstract:

Flood is one of life-threatening events in different part of Ethiopia. The causes of flood might vary from place to place, for instance rates of deforestation, agriculturalization, urbanization, wet land drainage, climate change, siltation of river bed and several other types of land use change might be the cause for flood in different rivers banks. This study aims to assess, investigate and design suitable river training works on lower Kulfo river reach. The study reach has been seriously affected by extreme floods due to the above reasons. For minimizing the loss due to flood, and to use the advantage of flood for different developmental activities various flood control measures should be adopted. The flood control measures which should more correctly be termed as "flood management" can be planed either through structural engineering measure or non-structural measures. Structural measures comprise retarding structures which stores flood water, channel improvements which increase flood carrying capacity of the river, embankments and levees which keep the water way from flood prone area, detention basin which retards and absorbs most of the flood water. Within identified 6 km reach, field investigation including secondary data collection has been done to predict the flood extent using 1D hydro dynamic model, HECRAS and HEC Geo RAS. Estimated flood depth and extent helped us in fixing the dimension of different river training structures selected. The modelling result indicates a maximum channel bed flood depth of 4.3m and flood plain flood depth 2.3m obtained using a 100-year return flow. Analysis of soil samples indicate that the lower reach of Kulfo river is gravel and sand dominated meandering river, with estimated scour depth up to 3.41m along the river course. Levees has been designed in conjunction with Groynes to protect the Upstream farm located at prison and upper part of the Limat households. Frequent floods happening near both bridges shall be reduced by using Guide banks without influencing the bridges and diversion structures. Consideration is given for the ecosystem to stay in equilibrium, by providing suitable outer slopes so that plantation is possible on top and side slope of the levees and guide banks.

Key Words: Kulfo, Structural Measures, River Training, HEC-Geo RAS, HEC-RAS

1. Introduction

Rivers have always played an important role in human development and in shaping civilisations. Primary function of a river is the conveyance of water and sediment. Rivers, except when flowing through well-defined narrow sections confined by high and stiff banks, have also generally caused problems of flooding; change of course, banks erosion etc. The morphology of river changes considerably on account of natural causes. Besides, changes made by man in an attempt to harness a river strongly influences behaviour of the river.

The behaviour of a river is mainly affected by the characteristics of the sediment-laden water flowing in the river. The available energy of the flow is utilised in transporting the sediment load as well as in overcoming the resistance due to the viscous action and the roughness of bed and sides. On account of the interdependence of the factors affecting the flows, there is an inherent tendency of these rivers to attain equilibrium. As such, whenever the equilibrium of a river is disturbed by man-made structures or natural causes, the river tends to attain a new equilibrium condition by scouring the bed or by depositing the sediment on the bed or by changing its own plan-form. These changes can be either local or extended over a long reach. The behaviour of a river can, therefore, result in the variation of the shape of the river cross section and/or its plan-form. Aggradation, degradation, scour and deposition of sediment around bends, and meandering are a few examples of such changes.

Flood risks have been a threat to human lives and property ever since people settled on river banks for early agricultural civilizations. The state of affairs remains the same in this day and age. Flood is a very common type of natural disaster, and they cause substantial amounts of property damage and losses of life. Damages from the floods may include: direct damage on properties, Indirect damage from lost services and businesses, secondary damages from hardships to those who depend on the outputs from the damaged properties or hindered services, Intangible damages like environmental quality, social well-being and aesthetic values and uncertainty damages due to uncertainty in flooding. Flood warning system using structural and non-structure methods will be very helpful to prevent the damages of human life and property that can be caused by excessive flood magnitudes.

Significant progress has been made in terms of assessing the risk of flood damage, designing and implementing efficient flood protection works to safeguard the live and property of mankind. However, the inherent hydrologic risks involved in these methods persist. In addition, manmade activities on flood plains of rivers alter the scenarios, there by flood patterns, and pauses a threat to previously unaffected areas. In prevention of such problems and getting benefits from river flooding human kind tried to assess

different river training methods. River training measures aim at achieving flood protection, navigation and guiding the flow.

Upstream catchment of the Kulfo Watershed is characterized by high upland erosion. The deposition mainly occurs on lower course of the river, changing the morphology and resulting in reducing the carrying capacity of the channel. This in turn result on overflow of water to nearby area during heavy rainy periods. Historical flood events were recorded on Limat sub city and outflanking of old bridge (Figure 20). Dredging activities has been conducted to increase the carrying capacity of the channel in addition of gabion construction upstream of new bridge. But those measures are not scientifically approved hence this project will assess the possible measures to protect the nearby area from flooding in scientifically approved way.

Figure 20: Kulfo flooding problems: Failure of Gabion upstream of New bridge (Left); Photograph of Kulfo Bridge after its failure during the October 1997 flood (Right)

The overall objective of this project is set methods to regulate the Kulfo flood by designing different river training works like retaining structures and gabions in order to maximize the resultant social and economic welfare of the community in participatory and equitable manner.

The specific objective of this sub project includes:

a) To plan and design river training and hydraulic structures to protect human lives and property from flood damages,

b) To control the depth and course of the river for aesthetic, recreational and ecological purposes,

c) To set mechanisms that stabilize the banks to facilitate safe and efficient intakes and control sedimentations.

d) To protect the upper and lower bridges from outflanking and the direct attack of flow thereby to assure the long-term stability of these hydraulic structures.

2. Materials and Methods

2.1. Description of the study area

The study area, Kulfo River Watershed, is located in the Abaya-Chamo sub-basin of the Southern Ethiopian Rift Valley and drains to Lake Chamo. This watershed is located to the west of Hare catchment (Fig. 2). The watershed area of Kulfo is about 392km^2 and located between 5°55'N and 6°15'N latitude and 37°18'E and 37°36'E longitude. Nearly 41% of the watershed area is used for settlements and agriculture. The area is characterized by remarkable elevation difference that reaches from 3490 masl at the peak of the Wisha Ridge to 1180 masl at the confluence to Lake Abaya. This head difference together with unsustainable land use system is the driving force for serious soil erosion and flooding of the lower Kulfo planes during rainy seasons

The Kulfo River basin has especial importance because: (1) it is the major tributary of Lake Chemo, (2) in its pathway to the lake it flows through ground forest harbouring biodiversity and the 40 springs, (3) it drains Arba Minch town, one of the rapidly growing towns in the region and situated in the lower reach of watershed, (4) sources of livelihood for thousands of people living in rural and pre-urban areas of the watershed including Arba Minch town.

The study was carried out in Kulfo basin, for lower stretch of Kulfo River. A small reach of the river including 128 C-sections and two bridges with a total length of about 5 km was used for a 1D hydrodynamic approach. Google map result in fig 2 represents the reach where the study conducted.

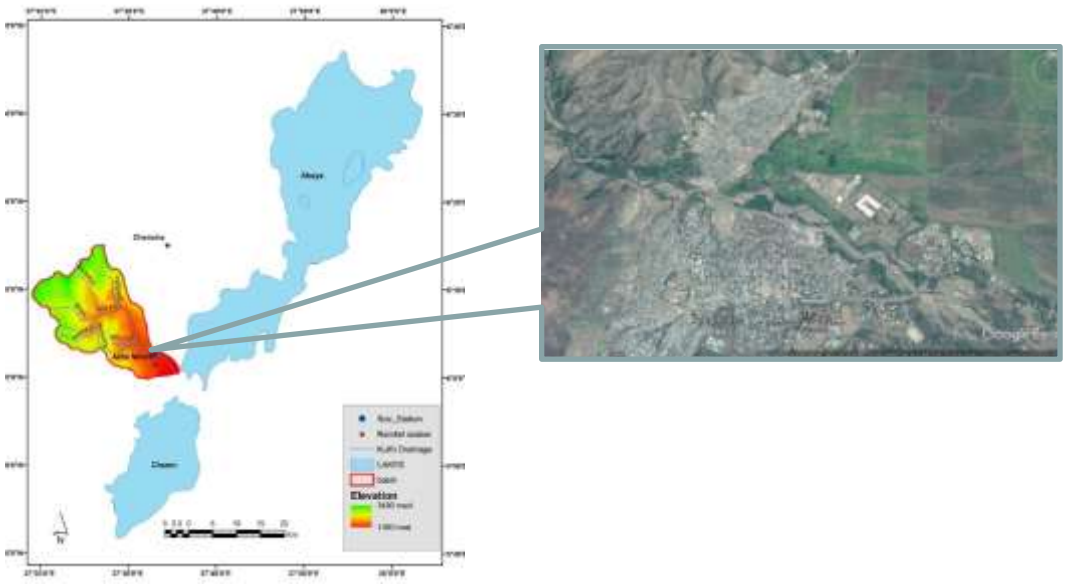

Figure 2: Location of Kulfo Catchment and Study Reach

2.2. HEC-RAS Model description

Hydrologic Engineering Center River Analysis System (HEC-RAS) is a one-dimensional model, intended for hydraulic analysis of river channels. The model is comprised of a graphical user interface, separate hydraulic analysis components, data storage and management capabilities, graphics and reporting facilities. The HEC-RAS system includes four river analysis components. They include the steady flow water surface profile computations, unsteady flow simulation, sediment transport computations and water quality analysis. In addition to these components, the model contains several hydraulic design features that can be invoked once the basic water surface profiles are computed. HEC-RAS applications include floodplain management studies, bridge and culvert analysis and design, and channel modification studies (Brunner, 2010).

The main inputs to the model are:

- River geometric data: width, elevation, shape, location, length,
- River floodplain data: length, elevation,
- The distance between successive river cross-sections,
- Manning 'n' value for the land use type covering the river and the floodplain area,
- Boundary conditions e.g. slope, critical depth,
- Stream discharge values.

The outputs from the model include

- Water surface elevations
- Rating curves
- Hydraulic properties i.e. energy grade line slope and elevation, flow area, velocity
- Visualization of stream flow, which shows the extent of flooding

2.3. Data collection and evaluation

For the successful achievement of this study we have collected the necessary information (data) using the following two major categories of data gathering techniques.

a) Field Survey to collect primary data such as land use/cover near to the river banks for estimation of runoff coefficient, sediment samples and cross section of the river at different locations using GPS and total station (Figure 12).
b) Gathering secondary data legally from different agencies and literatures.

This study involved the use of a Hydrodynamic model (HEC-RAS) that requires extensive hydro-meteorological and spatial data. These data types are indicated in table 1 including their potential sources and description.

HEC-RAS Calibration Approach: The goal of this project is to create a floodplain and water surface elevation model for the lower Kulfo River basin. This will be carried out in HEC-RAS by setting up a hydraulic model which is to able to simulate recorded peak flow water elevations with reasonable accuracy. Once this is completed, the model can be used for floodplain modelling and designing of the dimensions of river training structures.

Table 1: Data requirement for the study

Data type	Sources/Method	Description
Climate data	NMA	Daily rainfall and temperature data of Arba Minch station (1990-2012)
Hydrology	MWIE	Daily flow data of Kulfo river at Arba Minch town (1976-2013)
Land use maps	MWIE	Cover types of the Kulfo catchment
Top maps	EMA	20m contour interval geofenced tiff files of the Kulfo catchment
DEM	USGS website	30m by 30m Georeferenced Tiff files representing elevation of the area
Other spatial data	Google earth	Three images collected during past and present to validate land use types and study river morphology change
Cross sectional data	Filed Survey	932 surveying points including three bridge dimensions for study reach
Soil samples	Filed Survey	12 sediment sampling points on the study reach (collected during two periods)
Ground truthing	Filed Survey	25 location points describing land use of the study reach
Photo and Video	Filed Survey	About 50 pictures collected from study reach for verification

The activities of the river training theme are illustrated in the following hierarchal structure (Figure 3).

2.4. Kulfo River- Ungauged flow estimation of the study reach

There was one flow gauging station within the study reach, just under the foot bridge. Currently both the gauging station and the foot bridge were removed. The gauging station had long records of daily stream flow data (1976-2013). Two commonly used methods to determine streamflow values at an ungagged location include: 1) application of regression equations that relate flows to basin characteristics, and 2)

use of a drainage area-ratio adjustment for existing flow data in the same drainage basin. For the study, the drainage area-ratio method was used to determine stream flows for the study reach.

The drainage area-ratio method (Parrett and Johnson, 2004) assumes that peak flows at the ungagged site are equivalent per unit area to the peak flows at the gaged site. The method is most effective at estimating peak flows for locations on the same stream or within the same drainage basin as the gaging station(s). The drainage area-ratio method should only be used when the ratio of drainage areas between the ungagged and gaged sites is within a range of 0.5 to 1.5, otherwise the results may not be reliable. The following equation is used to calculate flows at the ungagged site:

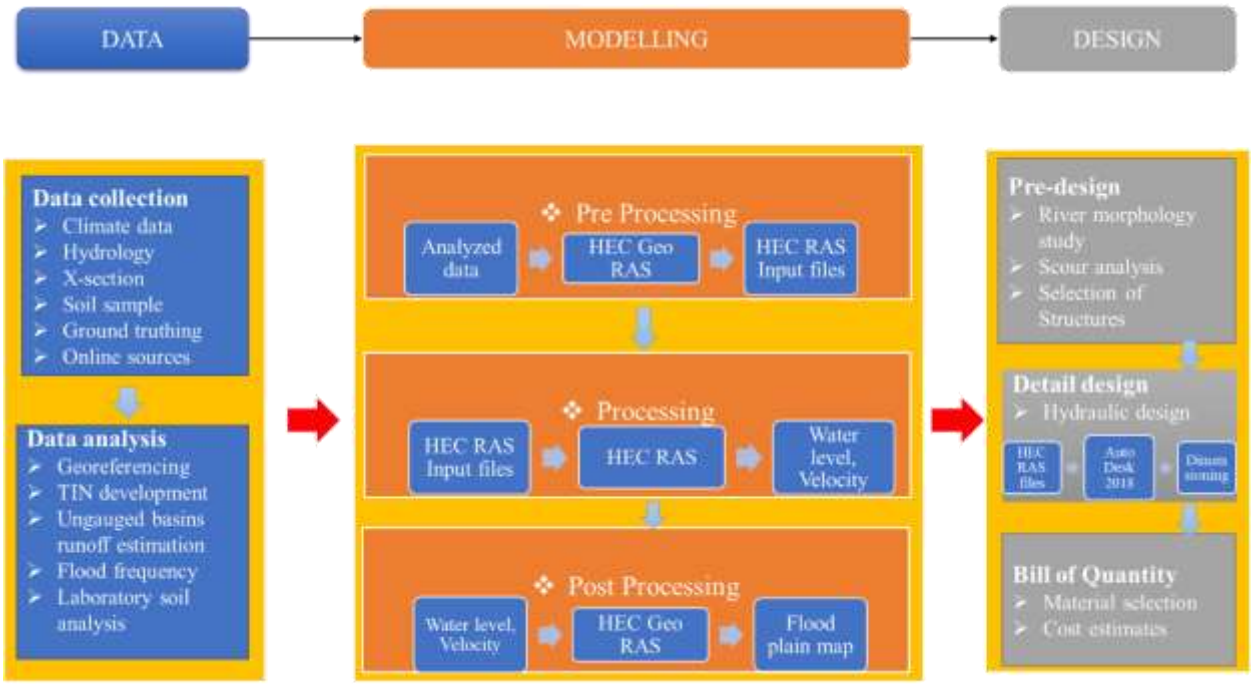

Figure 3: Flow chart indicating the activities to be carried out in river training work modelling and design

$$Q_u = Q_g * \left(\frac{A_u}{A_g}\right)^{expT} \quad (1)$$

Where, Qu = discharge at the ungagged site, Qg = discharge at the gaged site, Au = drainage area at the ungagged site, Ag = drainage area at the gaged site and expT = regression coefficient for a simple ordinary least squares (OLS) regression relating the log of T-year flood to the log of drainage area.

2.5. Estimation of design flood

Annual maximum flood events were first extracted from instantaneous daily flow that spans from 1976-2013. Data year with missing flow were removed to reduce the uncertainty during flood estimation. The T years return flood was estimated using generalized Pareto Distribution cumulative density function G(x) as follows

$$G(x) = 1 - (1 + \Upsilon\frac{x-x_t}{\beta})^{-1/\Upsilon} \quad \text{if} \quad \Upsilon \neq 0 \tag{2}$$

$$G(x) = 1 - \exp(-\frac{x-x_t}{\beta}) \quad \text{if} \quad \Upsilon = 0 \tag{3}$$

Where β and x_t can be approximate for Gumbel distribution (Υ=0) as

$$\tilde{\beta} = s_x\sqrt{\frac{6}{\pi^2}} \tag{4}$$

$$x_t = \bar{x} - 0.577216\tilde{\beta} \tag{5}$$

The theoretical return period can be calculated as

$$T = \frac{n}{t}\left(\frac{1}{1-G(x)}\right) \tag{6}$$

The peak flood for any return period can be estimated as

$$x_T = \tilde{\beta}(\ln(T) - \ln\left(\frac{n}{t}\right)) \tag{7}$$

2.6. Laboratory soil analysis

To determine the scouring effect of heavy flood, the bed load samples were collected from the field in two different periods and averaged to import the data in HEC RAS. The collected samples were passed through different sizes of sieve opening to obtain percent of passing. The modelling output of sediment data were used to determine the foundation of the river training structures.

3. Result and discussion

3.1. Pre-processing and data importing into HEC RAS

Channel Geometry - Field Survey: A surveyor collected field survey data used to create the channel geometry. The survey data was captured in UTM Zone 37N WGS 1984. Cross sections locations were selected by a Hydraulic engineer in 2014. A total of 138 cross sections (Fig 4) were surveyed on the study reach. All of the surveyed cross sections were used in the hydraulic analysis.

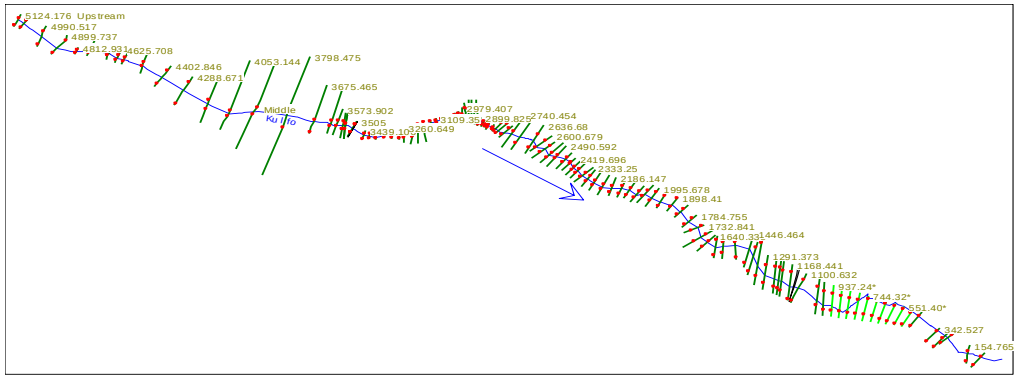

Figure 4: Cross sections developed using HEC RAS

Overbank Geometry (Topographic Data): For the overbank geometry a Triangulated Integrated Network (TIN) was developed using topographic map provided by Ehiopian Mapping Agency (EMA). The TIN (Fig 13) accompanied with HEC-GeoRAS was used to extract cross sections, stream length, and overbank floodplain flow lengths.

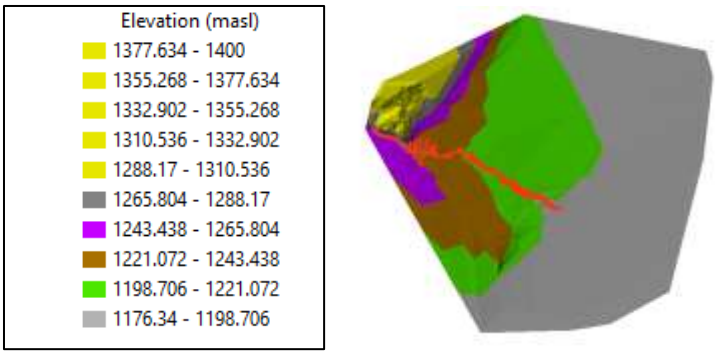

Figure 5: TIN of the study reach

Final HEC-RAS Cross Sections: Final HEC-RAS cross sections were created using the field survey data and the TIN. The field survey cross sections were created by exporting the field points along the cut line from AutoCAD (Autodesk, Inc. 2018) into Excel. The TIN cross sections were cut using HEC-GeoRAS in ArcGIS. The geometric data from HEC-GeoRAS was then directly imported into HEC-RAS for hydraulic modelling (Figure 6).

Flow Resistance or Roughness: Manning's n values for the HEC-RAS model were determined by field reconnaissance and engineering judgment. A hydraulic engineer walked the channels of the reach and estimated roughness values for every surveyed cross section. The HEC-RAS User's Manual (USACE, 2008), "Roughness Characteristics of Natural Channels"(Barnes, 1967), and "Open Channel Hydraulics", (Te Chow, 1959) provided tables of roughness coefficients for different surfaces (see

annex). The investigation determined for the study reach that a Manning's n of 0.10 to 0.125 was acceptable for the overbank value and 0.034 was appropriate for the channel values along most of the project reach (Fig 6). A sensitivity analysis of varying Manning's n values was also completed to further ensure appropriate values were used.

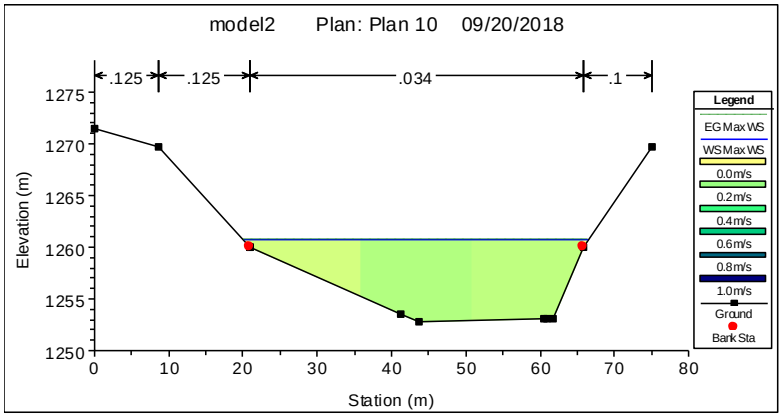

Figure 6: Sample cross section in the study reach exported from HEC-GoeRAS to HEC RAS after flood modelling

Hydraulic Structures: There were two bridges modelled, on the study reach. From downstream to upstream, the old bridge (Sta.1132.756) and the new bridge (Sta. 3502.996). Survey crews captured structure geometry of the bridges (table 4) and this was used in combination with field notes and photographs to provide model inputs. Currently the foot bridge is removed, hence it is not considered in modelling.

Table 2: Geometry of bridges

S NO	Name of Bridge	Pier Circ. (m)	Distance B/N Piers (m)	Length (m)	Width (m)	Remark
1	Foot Bridge	1.1 x 2.6	7	31	2.6	Not considered
2	New Bridge	3.2	17	50	31	Considered
3	D/S Old Bridge	3.75	12.95	63.3	13	Considered

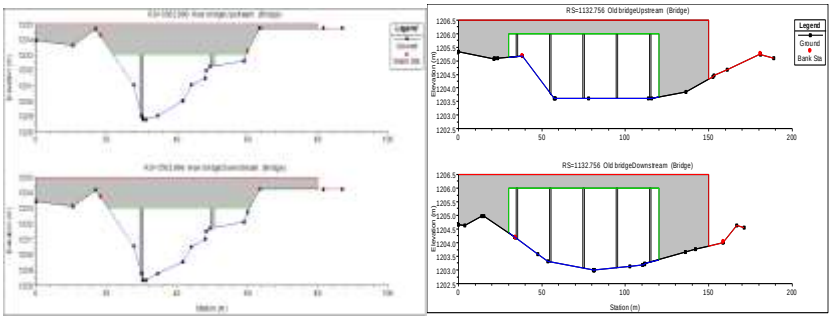

Figure 7: Bridge modelling using HEC RAS (Left: New bridge upstream and downstream cross sections; Right: old bridge upstream and downstream cross sections)

Boundary Conditions: The HEC-RAS models were executed under the assumption of subcritical flow. Normal depth was the chosen downstream boundary condition. Normal depth computations are based on energy slope which was approximated by channel slope of the downstream reach as determined from topographic data. Two calibration cross sections were placed downstream of the limit of the study to further ensure accuracy of the downstream boundary condition used for the model. The friction slope is taken as 0.000625m/m, which is the bottom slope between the last two cross sections. The upstream and lateral boundary conditions are derived from ungauged flow estimation (see figure 8)

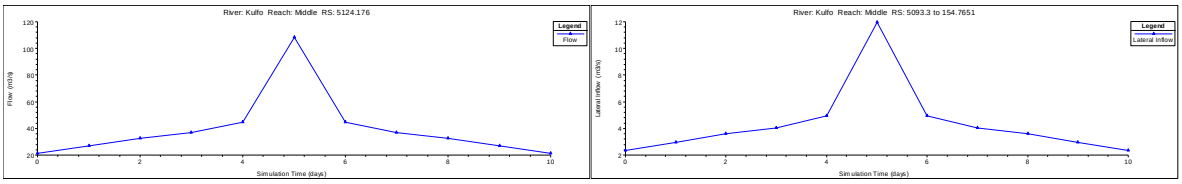

Figure 8: Upstream (Left) and Uniform Lateral (Right) flow boundary conditions

Ineffective Flow Areas: Ineffective flow areas are areas of the channel that contain water which is not actively conveyed. Ineffective flow areas were added to the model cross sections located just upstream and downstream of each hydraulic structure per the HEC-RAS Hydraulic Reference Manual (USACE, 2008). Ineffective flow areas were also added in overbank areas that are acting as storage, with no conveyance of flow.

Sensitivity Analysis: The study reach of the Kulfo River has a low gradient and a coarse bed of boulders and cobbles. The flow resistance is very high in this type of channel. The flow depth in an open channel is directly proportional to the roughness; the greater the roughness, the greater the flow depth. It was difficult to estimate flow resistance through the study reach and there was some uncertainty in the final values. To address this uncertainty and to increase our confidence in the model results we used a previous flood event to "check" or confirm our final roughness values. The flood event of July/2001 was a 10-year event in the study reach and provided a good opportunity to check model assumptions. During the event some observations are made and photographed the flooding extent and water surface elevations relative to landmarks. The most useful of these observations was made at the new Bridge. The community reported in personal communications that the water surface elevation of the Kulfo River, several hours before the peak flow, was equal to the new bridge deck and that floodwaters were just starting to crest the bridge. Several photographs confirmed these observations. To check the model, we run the estimated flood discharge from the 2001 event and compared the modelled water surface

elevation to the observed and found that they were in good agreement. In addition to comparisons to known water surface elevations several model runs were completed with adjusted roughness values to determine how sensitive the water surface elevation was to different values. While the model did respond to changes in roughness values the change in water surface elevation was very small.

3.2. Design discharge and synthetic hydrograph

The estimated flood events for different years return periods are as shown in table 3. The 100-year flood is selected for designing the river training works after fitting it (fig 9).

Table 3: Design discharge for different return periods

T	200	100	50	10	5	2	1
X_T (m^3/s)	123.03	113.61	104.19	82.31	72.89	60.43	51.01

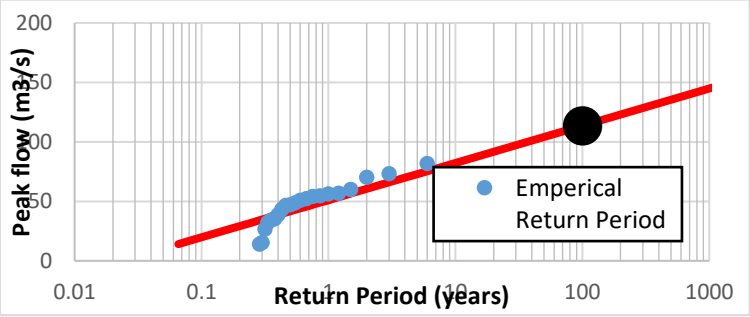

Figure 9: 100-year design flood fitted using Generalized Pareto Distribution

The tabulated flood events are used to run steady flow simulation in HEC-RAS, while synthetic design storms (Fig 10) are prepared to run unsteady flow simulation

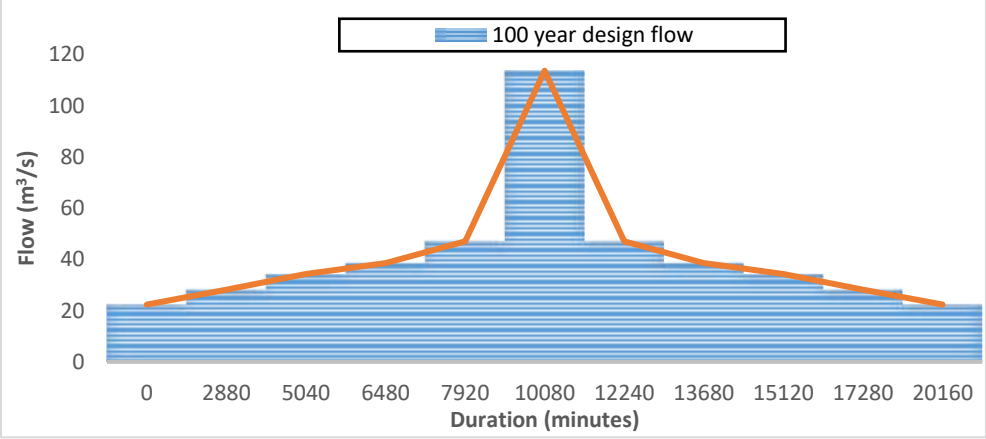

Figure 10: Synthetic design storm for unsteady flow simulation

Finally, the flood plain was mapped using HEC Geo RAS, as indicated in in Fig 22. The maximum water depth estimated to be 4.3 m, in the channel and 1.2m in the flood plain. To design the river training works along the river course, site investigation and verification is conducted and the detail design of the river training structures are presented on the next section. From supplementary cross-sectional plots (fig 11), it is observed that both bridges will be overtopped by the flood, hence guide banks should be designed to pass the coming peak flood. For most part of the river course, the flood level exceeds the right and left bank levels, hence we come up with an idea to design levees on both only leaving the first 224m of the left bank, where the bank is connected to the mountain. This area is just opposite side of the prison, where it is not necessary to construct river training structures. Along the prison, where peak flood jumps into the farm, attracting groynes are designed to protect the convex levee from high water current. Just below the quarry side, where we found a natural retaining wall, we proposed a gabion to protect the fall of the wall due to high water pressure, and peak rainfall event. Starting from this point to a few meters downstream of old bridge, we proposed a levee to continue as designed for prison and upstream Limat township. A special consideration is given to protect the upstream bridge, where we proposed masonry structure on the left bank levee. Levee designed downstream of the new bridge is also used to low water training, where navigation is possible with latter adjustments. It is observed that there is a 10m elevation difference between the two bridges, so that check dams shall be designed to make the river navigable.

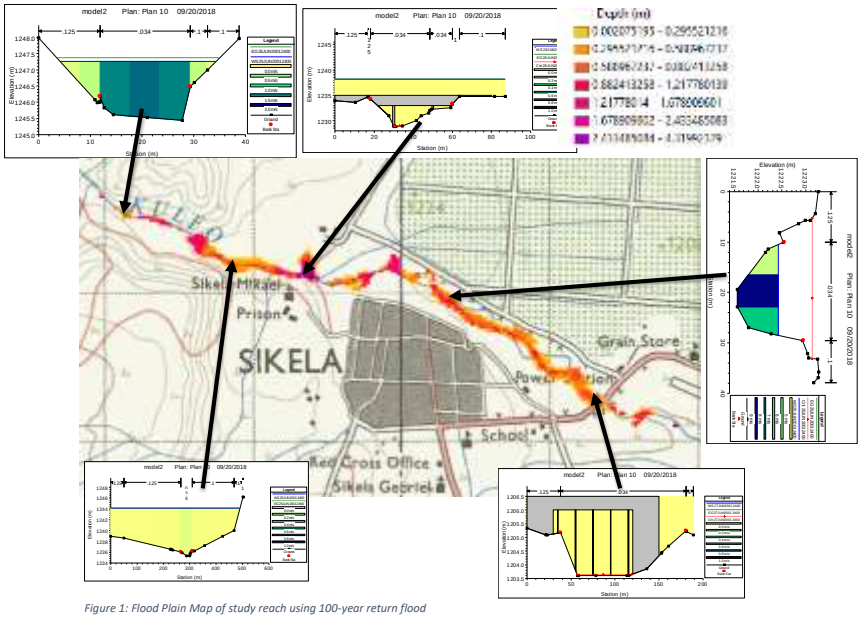

Figure 1: Flood Plain Map of study reach using 100-year return flood

Figure 11: Flood plain map of the study area using 100-year return flood

3.3. Design of Levee embankment

Embankment hydraulic design is the dimensioning of the embankment based on the river's hydraulic parameters.

Step 1: Determine the design flood water height H:
Using the design discharge Q_T (i.e. Q_{100}) computed and the hydraulic and geometric characteristic of the river at the site, compute the flood height H. For wide streams
or rivers:

$$Q_T = \frac{1}{n} B H^{\frac{5}{3}} \sqrt{S} \quad (8)$$

Where; B= stream width (61m assuming Lacey's water way $P = 4.75\sqrt{Q_{100}}$ and allowing 20% for bridge piers), n= Manning's coefficient of roughness (estimated to be 0.06 for natural channel with boulders and gravels), S= stream bed slope (and estimated to be 0.018 near the bridge. But to be more conservative 1% is used.
The above equation is solved in iterative way and the flood depth for design flood has been estimated about 1.2m.

Step 2: Determine the freeboard F:
The freeboard is defined as the vertical distance between the crest of an embankment and the maximum flood level. It protects embankments and dams from overflow caused by wind induced tides and waves. Depending on the importance of the structure, the amount of freeboard will vary in order to maintain structural integrity and the estimated cost of repairing damages resulting from overtopping.

Freeboard is generally estimated based on maximum probable wind conditions. Three basics considerations are generally used in establishing freeboard allowance viz. wave characteristics, wind setup, and wave run-up. The minimum height of the freeboard for wave action is generally taken as $1.5h_w$, where h_w is given by:

$H_w = 0.032\sqrt{(V.F)} + 0.763 - 0.271\,(F)^{3/4}$ for F<32 km and,
$H_w = 0.032\sqrt{(V.F)}$ for F>32 km (9)

Where: H_w=height of water from top of crest to the bottom of trough in meters, V= wind velocity in km/hr (Long time average wind speed of Arba Minch station is about 2.5 km/hr) and F= Fetch or straight length of water expansion in km. Using a design flood of normal event, and fetch length of 31.9 km, a freeboard of 0.3 m is used. The height of the embankment is hence calculated as H+F=1.5m.

Step 3: Determine the embankment side slopes V: H.

For levees that do not exceed height of 4 m, and have no particular foundation problem, the recommended river-side slope is 1:3 – 1:3.5, and land-side 1:2 – 1:2.5. The recommended values of side slopes for earth dams given by Terzaghi (table 4) can be used for flood embankments.

Table 4: Recommended side slopes for earth dams (Source: Garg, 2005)

Type of Material	U/S (V:H)	D/S (V:H)
Homogeneous well graded	1:2.5	1:2
Homogenous course silt	1:3	1:2.5
Homogenous sillty clay		
Height less than 15m	1:2.5	1:2
Height more than 15m	1:3	1:2.5
Sand or sand and gravel with central clay core	1:3	1:2.5
Sand or sand and gravel with R.C. diaphragm	1:2.5	1:2

The minimum side slopes are assumed to design the levee based on the given criteria. i.e. the river side slope is taken as 1:3 and land side slope is taken as 1:2.5 for sand and grave with central clay core taking in account that plantation if possible, in land side of the levee.

Step 4: Determine the seepage line V:H

The seepage line depends on the soil type and its compaction. It starts 0.3 m above the design water level with the following slopes: Clayey Soil 1V:4H; Clayey sand 1V:5H and Sandy Soil 1V:6H. The embankment section should be designed in such a way to keep the seepage line inside the body of the embankment well below the top surface of the embankment. In Ethiopia, seepage line of **1:6** is used with no failure for many years. This is attributed to the soil type and wetness conditions (intermittently wet).

Step 5: Determine the embankment Crest width B

Embankment crest width (B) is width necessary to keep the seepage line well within the embankment at the design water level and road width on embankment crest. For designing the levee, crest width of 2.4m is used. In designing flood embankments wetness conditions are very important. Two types should be distinguished viz. always wet or intermittently wet. The differences in the design of the two types are summarized in the following paragraphs. Case b is selected taking account that flood happens rarely.

a. The embankment is always wet:

Should be design as an earth dam embankment;

1. Design the embankment using seepage line slope as recommended by MoWIE (1V:7H);
2. Design an upstream filter for relieving the pore pressure;

3. Downstream filter is optional;

4. Diaphragm embankments with clay core can be used.

b. Embankments subject to wetness intermittently

1. Seepage failure is rare. Therefore, they can be designed using textbooks seepage line slope (clay1:4, clayey sand 1:5 and sandy soils 1:6).

2. Use homogenous soils;

3. Avoid the use of clay cores as the clay will crack when dry leading to embankment failure

4. Upstream filters are not necessary.

In designing flood embankments in urban areas where space limitations exist, steeper slopes can be used provided that adequate slope protection is used. Seepage cut-off walls can also be used. Stability berms can be used to avoid very steep side slopes for more economic design.

Detail design of the levee on both sides, including channel modification is as shown in figure 12. In this case, a trapezoidal channel with a bottom width of 50m is designed taking in account that the river side slope of the levee to be 1:3, and land side slope of the levee to be 1:2.5, top width of the levee to be 2.4m, and the maximum bottom width of the levee to be 10.65 m assuming the river bed and flood plain lies on the same elevation level.

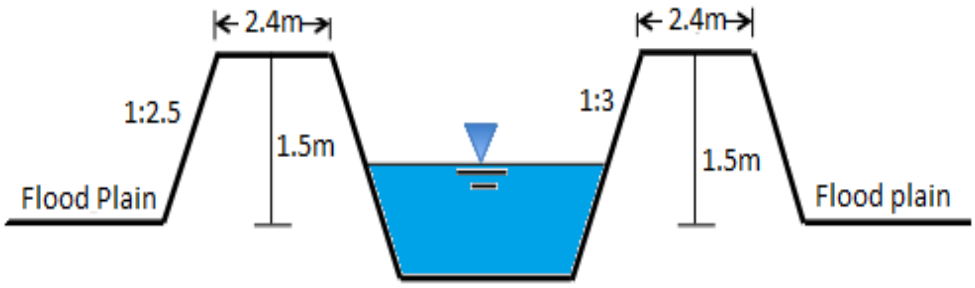

Figure 12: Dimensions of Levee on right and left side of the river: {Crest width B=2.4 m, Freeboard F=1.2 m, Design water Height H=1.5 m, Side Slope (Sin 1:3, Sout 1:2.5) Seepage line 1:7}

The Levee dimension shall be modified taking in account that the height of the Levee should be always 1.5m from the flood plain, not from the river bed.

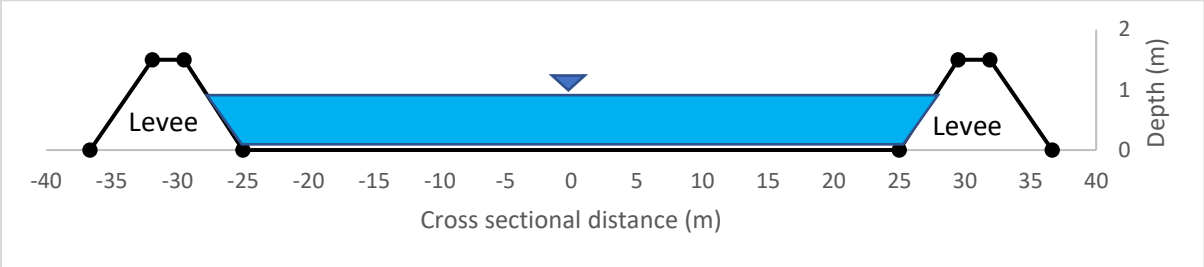

Figure 13: Dimensions of Levee on right and left side :(scaled)

Gabions are made of stone baskets of wire or plastic netting. The most commonly used steel wire may be woven or welded. Nominal mesh size varies from 440x60 mm to 100x120 mm. The filter stone must have its nominal diameter as 1.5 times mean mesh size. Individual units are assembled before placing them in position.

3.4.Dyke layout and location

Levees or dykes designed as a part of flood protection works which also include channel regulation and alignment viz. river training the axes of the levee can follow the river alignment as shown in figure 14. Left and Right Levees has been designed in conjunction with Groynes to protect the Upstream farm located at prison and upper part of the Limat households. Frequent floods happening near both bridges shall be reduced by using Guide banks without influencing the bridges and diversion structures. Consideration is given for the ecosystem to stay in equilibrium, by providing suitable outer slopes so that plantation is possible on top and side slope of the levees and guide banks

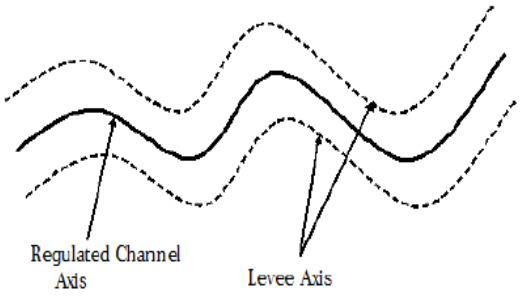

Figure 14: Levee alignment in regulated smaller river

Figure 21: proposed Levee system of Kulfo River: The centre line representing the river, and the other two lines representing 25m offset to start the levee embankment (Left); Plan design of guide banks for upstream bridge)

3.5. Construction aspects and cost estimates

The construction materials include earth, sand, gavel, rock, geotextile and gabions. The location of such materials is identified based on structure requirement throughout the reach length. Alluvial clays and silts are common source of fill material.

The summary of materials required (Volume) is indicated in table 5. It is indicated that including gabion and masonry, it requires 30,418m^3 of stone for pitching and 98,460m^3 of selective materials for embankment core. Core materials can be obtained from nearby quarry site and volume of cute made during dredging activity.

The costs are estimated based on current market values as follows (Table 6). This estimation excludes still bars, and shall be included in detail cost analysis.

Table 5: Construction material requirement

Item	**m^3**
Volume cut from river bed	451,339.3
Volume of stone per meter run	7
Stone required	30,418.7
Volume of core per meter run	21
Core material required	98,460.5

Table 6 Cost estimate of Kulfo River training work

Item	Unit	Quantity	Unit Rate (ETB)	Total Amount (ETB)
Construction cost	m^3	98460.54	250	24,615,134.59
Stone	m^3	30418.78	188	5,718,729.86
Cement	kg	5000	2.5	12,500.00
Fine aggregate	m^3	1000	112	112,000.00
Coarse aggregate	m^3	1000	324	324,000.00
Mesh	m^2	240	400	96,000.00
Total Amount (ETB)				**30,878,364.45**

To minimize the cost of construction, the know-how and local experiences need to be explored before starting the construction. The main target group are the skilled labourer and builders to be contracted on daily-paid bases.

Before starting construction, the followings need to be considered: a) Foundation should be excavated to a depth of at least 1 m and possibly deeper depending on soil conditions (Topsoil is not the optimal foundation to build on); b) Clearing the site from any debris and pushes, if exist; c) A good route between the borrow pit and the embankment site needs to be prepared.

Embankment geometry varies according to type of material used and construction history. Ideally, an embankment should have a crest width of greater than 2.5m to allow access along the crest for operations and maintenance vehicles. Whilst the slope of inward and outward embankment faces might sometimes exceed 1 in 2 (according to construction material), stability problems will be encountered as the face is steepened. Poorly controlled maintenance activities can result in bank steepening through excessive removal of soil when cutting vegetation.

4. Conclusion

The HEC-RAS model is a one-dimensional hydraulic model that can be used to analyse river flows. Version 5.0.3 of the HEC-RAS model was released by the U.S. Army Corps of Engineers Hydrologic

Engineering Centre in September 2016 and it supports water surface profile calculations for steady and unsteady flows, including subcritical, supercritical, or mixed flows. Profile computations begin at a cross-section with known or assumed starting condition and proceed upstream for subcritical flow or downstream for supercritical flow. The model resolves the one-dimensional energy equation. Energy losses between two neighbouring cross sections are computed by the use of Manning's equation in the case of friction losses and derived from a coefficient multiplied by the change in velocity head for contraction/expansion losses. For areas where the water surface profile changes rapidly (e.g., hydraulic jumps, bridges, river confluences), the momentum equation is used (US Army Corps of Engineers 2001).

A HEC-RAS model and available flow records for the Kulfo River at foot bridge was used to simulate flows at cross-section sites within the study reach. The initial form of the Kulfo River HEC-RAS model was developed and modified using cross-section data acquired. Data required for performing HEC-RAS simulations included geometric data and steady-flow data. Geometric data used for our analyses consisted of connectivity data for the river system, cross-section elevation data for 138 cross-sections, reach length, energy loss coefficients due to friction and channel contraction/expansion, stream junction information, and hydraulic structure data, including information for bridges and river training works. Required steady-flow data included the gage records, boundary conditions, and peak discharge information. Elevation data (in meter above the WGS of 1984) for the 138 cross-sections were derived from filed surveys, a topographic map and a digital elevation model of the Kulfo River.

Known water surface elevations were used as downstream boundary conditions and a rating curve, supplied by USGS, was used to calibrate the HEC-RAS model to the Kulfo River near Prison.

Calculations for subcritical flow in the HEC-RAS model begin downstream where a boundary condition is applied. For the Kulfo River, a known water-surface elevation, calculated from a stage-discharge relationship at Kulfo river routed from gage was used as a downstream boundary condition. The energy equation is then solved between the first and second (most downstream) cross sections. Once this is achieved, the model repeats this process working its way upstream balancing the energy equation (or momentum equation if appropriate) between adjacent cross-sections until the most upstream cross-section is reached. Model accuracy is evaluated by comparing calculated water-surface elevations at any gage location with a stage-discharge relationship derived from historic data for the location. The model is calibrated by adjusting factors in the model until calculated results closely approximate the observed

relationship between stage and flow. While expansion and contraction coefficients can be altered, the major parameter altered during the calibration process is typically Manning's roughness coefficient (n), which describes the degree of flow resistance. Flow resistance is a function of a variety of factors including sediment composition, channel geometry, vegetation density, depth of flow and channel meandering. For the Kulfo River HEC-RAS model, a rating curve at the most upstream gage site was not available from Ministry of Water, Irrigation and Energy. Calibration measures were made against the existing data for this site.

The Kulfo River HEC-RAS model calculates profiles for a total of 7 steady flow rates derived from historical flow data measured in the river. The boundary conditions were specified with known water surface elevations for each flow rate at the downstream boundaries. The HEC-RAS model was considered calibrated when calculated water surface elevations were within plus or minus 0.15 m, in keeping with standard practices where this range of error is based on the potential error associated with using data collected to a 20m contour interval aerial mapping standard for model development (Lewelling, 2004). The greatest error associated with the model is likely to be the accuracy of the cross-sectional data.

High riverine floods cause massive damages to property along Kulfo River. Mountainous Flash floods in the urban areas is a second source of flooding, which causes extensive damages, in particular if synchronizes with riverine flooding. It seems that, the frequency of high river floods has increased in the last 2 to 3 decades. This has exacerbated the suffering of the poor farmers and residents living along the rivers.

A recommendation to sustainability of the river training structure to function until its design period is to treat the upstream catchment using watershed management practices. Upstream watershed treatment decreases sediment erosion and increase soil infiltration. This in turn will increase the performance of the modified channel and efficiency of the river training structure.

References

Barnes, H.H., 1967. Roughness characteristics of natural channels. US Govt. Print. Off.,.

Brunner, G.W., 2010. HEC-RAS river analysis system: hydraulic reference manual. US Army Corps of Engineers, Institute for Water Resources, Hydrologic Engineering Center.

GC, E., Adhikary, R.P., Shrestha, A.B., Rai, S.K., 2012. Physical Methods for River Training. ICIMOD.

HASHEMI, N.S.F.A., AYOUBZADEH, S.A.L.I., DEHGHANI, A.A., 2008. Experimental investigation of scour depth around L-head groynes under clear water condition.

Higaki, D., Karki, K.K., Gautam, C.S., 2005. Soil erosion control measures on degraded sloping lands: A case study in Midlands of Nepal. Aquat. Ecosyst. Health Manag. 8, 243–249.

Julien, P.Y., Klaassen, G.J., Ten Brinke, W.B.M., Wilbers, A.W.E., 2002. Case study: bed resistance of Rhine River during 1998 flood. J. Hydraul. Eng. 128, 1042–1050.

Lewelling, B.R., 2004. Extent of areal inundation of riverine wetlands along five river systems in the upper Hillsborough River watershed, west-central Florida. Citeseer.

McCullah, J., Gray, D.H., 2005. Environmentally sensitive channel-and bank-protection measures. Transportation Research Board.

Parrett, C., Johnson, D.R., 2004. Methods for estimating flood frequency in Montana based on data through water year 1998. US Department of the Interior, US Geological Survey.

Safarzadeh, A., Salehi Neyshabouri, S.A.A., Ghodsian, M., Zarrati, A.R., 2010. Experimental study of head shape effects on shear stress distribution around a single groyne, in: River Flow 2010, Proceedings of 5th International Conference on Fluvial Hydraulics. pp. 651–657.

Singh, G., Singh, G., 1980. Irrigation engineering. Standard Book House, Delhi.

Staff, U., 2008. HEC-RAS River Analysis System, User's Manual Version 4.0. US Army Corps Eng. Hydrol. Eng. Cent. Publ. 733p.

Te Chow, V., 1959. Open-channel hydraulics. McGraw-Hill New York.

Varshney, C.K., 1983. Water pollution and management. Wiley Eastern Limited.

Yankoupe, R.F., 1991. American River Watershed Investigation, California, Feasibility Report. Part 1. Main Report. Part 2. Environmental Impact Statement/Environmental Impact Report. ARMY ENGINEER DISTRICT SACRAMENTO CA.

Poster Presentations

Evaluation Of Climate Change Impact On The Magnitude Of Rainfall and Flood Frequency: The Case Of Hare Watershed, Ethiopia

Biniyam Yisehak*[1] and Abdella Kemal[2]

*[1]Institute of Climate and Society,Mekelle University,Ethiopia Email: b1n1y21@gmail.com, [2]Institute of Water Technology, Arba Minch University,EthiopiaEmail:abdellabz@gmail.com

Abstract:

Ethiopia will be more vulnerable to climate change. Because of the less flexibility to adjust the economic structure and being largely dependent on agriculture, the impact of climate change has far reaching implication in Ethiopia. The study aims to evaluate climate change impact on the magnitude of rainfall and flood frequency of Hare watershed. In the study the daily data values of rainfall and discharge from 1980-2006 was used based on stream flow measurements carried out by MWIE. The downscaled climate data such as, RCP4.5 and RCP8.5 was used for the future period assessment. Both rainfall and flood frequency analysis were performed using Log-Pearson type III distributed methods for return periods (T) of T = 2 yrs, 5 yrs, 10 yrs, 25 yrs, 50 yrs and 100 yrs. The annual peak flow frequency analysis has been carried out for the future (2020s, 2050s and 2080s) periods using HEC-SSP software. RCP8.5 scenario for all return period by 2050s and 2080s predicted an increasing the change in rainfall magnitude. RCP4.5 scenario for all return period by 2020s and 2050s predicted decreasing rainfall magnitude. RCPs scenario predicted the 100-years flood of the current climate seems to increase to a flood return period of (2 yrs, 5 yrs, 10 yrs, 25 yrs and 50 yrs). The rainfall frequency analysis shows climate change will have impact on the frequency and magnitude of rainfall intensity. The future change in rainfall magnitude clearly governs in peak flow magnitude and frequency.

Keywords: Climate change; RCPs; Flood frequency; Rainfall frequency; HEC-SSP

1. INTIRODUCTION

The IPCC finding indicates that developing countries, such as Ethiopia more vulnerable to climate change, because of the less flexibility to adjust the economic structure and being largely dependent on agriculture, the impact of climate change has far reaching implication in Ethiopia. Increased industrial activity and excessive deforestation during the last century and a half has increased concentration of

carbon dioxide in Earth's atmosphere. This has in turn initiated large-scale atmospheric processes resulting in change of global temperature and precipitation (among other variables). Changes in Earth's climate system can disrupt the delicate balance of hydrologic cycle and can eventually lead to increased occurrence of extreme events (such as flood droughts, heat waves, summer, and ice storms, etc.).

Extreme rainfall events and the resulting floods usually could cause significant damage to agriculture, ecology and infrastructure, disruption to human activities, injuries, and loss of lives [2]. Determination of frequencies and magnitudes of these events would enhance the management of water resources applications as well as the effective utilization of water resources. Such information can also be used for flood plain management and applied to the planning and designing of water resources related engineering, such as reservoir design, flood control work, drainage design, and soil and water conservation planning, etc. All these works require the rainfall data as a design basis. Though the nature of rainfall is erratic and varies with time and space specially during global warming, yet it is possible to predict the pattern of rainfall accurately for certain return periods using various probability distributions. Frequency analysis of rainfall data has been carried out at different places in Ethiopia without giving attention to the current word wide problem of climate variability [15].

Assessment of these extreme rainfall events is important in hydrological risk analysis and design of urban infrastructures. The increasing trend of rainfall extremes has quantifiable impacts on rainfall frequency relations and an increase in the intensity and frequency of extreme rainfall events may result in the flooding of urban areas.

Floods in Dire Dawa occur because of prolonged heavy rainfall causing rivers to overflow and inundate areas along the river banks in lowland plains. Flooding due to rainfall is probably the most severe among hydro meteorological hazards that cause damages to roads, bridges, residential, and agricultural areas [10]. Therefore, planning and protection of these basins, requires estimate of expected discharge from rainfall events of different magnitudes based on the current global problem of climate change. At the same time, the economic design of bridges, culverts, dams, and other hydraulic structures demands good knowledge of the likely floodswhich the structure would have to withstand during its estimated economic life. However, reliable estimates of flood frequency in terms of peak flows and volumes remain a current challenge in hydrology [9]. Besides this, the evaluate climate change impact on the magnitude of rainfall and flood frequency is one sort of challenge to hydrologists.

In this climate change impact study, the rainfall frequency analysis has been employed by fitting the observed and futureprojected rainfall into a probability distribution function.Next flood frequency analysis has been employed by fitting the observed and simulated future stream flow into a probability distribution function.Finally, carry out climate change impact on the magnitude of rainfall and flood frequency**.**

2. Material and Methods

2.1.Hydro Meteorological Data

Required long year daily precipitation data were collected from three meteorological stations such as, Arba Minch, Chencha, and Mirab Abaya. Daily maximum and minimum temperature data were collected from Arba Minch station. The historical weather data for above three station were obtained from National Meteorological Service Agency (NMSA) from 1980 to 2006 and long year daily stream flow data ware obtained from Ministry of Water Irrigation and Energy (MWIE) from 1980 to 2006.

2.2.Projected Climate Data

Projected ensemble of 20 GCM of rainfall and temperature for the period 1951-2100 have been obtained from CORDEX-Ethiopia database. The data correspond to three RCP scenarios- RCP2.6, RCP4.5, and RCP8.5. In order to best conduct a future climate change study, RCP 4.5 and RCP 8.5 forced scenarios were selected from 2010 to 2099 for three climate stations.

2.3.Rainfall and Flood Frequency Analysis

This study included climate change impact on the magnitude of rainfall and flood frequency of the watershed for T-return periods (2, 5, 10, 25, 50, and 100 year). The rainfall frequency analysis has been employed by fitting the observed and futureprojected rainfall into a probability distribution function. The observed rainfall data for current and future periods using RCPs outputs were used in the rainfall frequency analysis. The flood frequency analysis has been employed by fitting the observed and simulated future stream flow into a probability distribution function. The extreme events magnitude of T-return periods has been assessed for watershed by following the statistical property of that probability distribution. The flow data series simulated using SWAT model for current and future periods using downscaled RCPs data were used in the flood frequency analysis.

The annual peak flow frequency analysis has been carried out for the current (1980-2006) and future (2020s, 2050s and 2080s) periods using the U.S. Army Corps of Engineers Statistical Software Package (HEC-SSP). The input of this analysis was the simulated annual peak flow time series by current and future period. The statistical analysis of peak flow data was computed by HEC-SSP. In this software, the Bulletin 17B "Guidelines for determining peak flow frequency" (1982) and a generalized frequency analysis method have been employed for performing the peak flow frequency analysis. There are a number of two and three-parameter distributions described in literature exceedance [17]such as Gumbel, General Extreme Value Generalized Logistic, Log-Normal, Gama and Log-Pearson III. However, the Log-Pearson III method is generally recommended for analysis of annual flood series in HEC-SSP[9].

2.4.Log-Pearson Type III Probability Distribution

The log-Pearson Type III distribution is a statistical technique for fitting frequency distribution data to predict the design flood for a river at some site. Once the statistical information is calculated for the river site, a frequency distribution can be constructed. The probabilities of floods of various sizes can be extracted from the curve.

$$f(x) = \frac{x^{\beta}(x-x_{\circ})^{\beta-1}\ell^{-x(x-x_{\circ})}}{\Gamma(\beta)}, x \geq x_{\circ} \quad (1)$$

Where x = mean, Γ = gamma function y = reduced variate

$$y = \frac{(x-x_o)}{\beta} \quad (2)$$

$$\bar{x} = x_o + \beta y \quad (3)$$

$$\beta = \frac{\sqrt{v}}{\sqrt{\gamma}} \quad (4)$$

$$\gamma = \left[\frac{2}{g}\right]^2 \quad (5)$$

Where β=Standard deviation, v=variance, g=skewness

Because the problem with most hydrologic data is that an equal spread does not occur above and below the mean as the lower side is limited to the range from the mean to zero (although in many cases

theminimum may be well above zero) while there is theoretically no limitation on the upper range, it contributes to what is called a skewed distribution [13] The coefficient of skew (g) being mathematically defined by:

$$g = \frac{N\sum_{i=1}^{N}(x_i-\bar{x})^2}{(N-1)(N-2)\sigma^3} \quad (6)$$

Where σ=Standard deviation

Pearson (1930) proposed a general formulation that fits many probability distributions including the normal, beta and gamma distribution. A form of the Pearson probability distribution called the Pearson type III has 3 parameters that include the skew coefficient (equation 6), as well as the mean and standard deviation. The Pearson Type III distribution is represented by equation (7) [5].

$$x = \bar{x} + k\sigma \quad (7)$$

Where k = frequency factor determined from Tables. The model parameters,$\bar{x}$standard deviation and the skew coefficient (g) are computed from n observations x, with the following formula

$$\bar{x} = \frac{1}{n}\sum_{i=1}^{n} x_i \quad (8)$$

$$\sigma = \left[\frac{1}{(x-1)}\sum(x_i - \overline{x)^2}\right]^{0.5} \quad (9)$$

$$g = \frac{n\sum_{i=1}^{n}(x_i-\bar{x})^2}{(n-1)(n-2)\sigma^3} \quad (10)$$

However, the Log Pearson Type III distribution of x which has been widely adopted to reduce skewness is equivalent to applying Pearson Type III to the transformed variable log X and it is represented in the literature as:

$$\log x = \overline{\log x} + k\sigma\log x \quad (11)$$

Where x is the flood discharge value of some specified probability, log(x) is the average of the log(x) discharge values, K is frequency factor. σ log(x) is the standard deviation of log x values. The frequency factor K is a function of skewness coefficient and return period and can be read from

published tables developed by integrating the appropriate probability density function. The flood magnitude for various return periods are found by solving the general equation. The mean, standard deviation of the data and skewnesscoefficient can be calculated using the following formulae

$$\overline{\log x} = \frac{\sum \log x_i}{n} \tag{12}$$

$$\vartheta_{\log x} = \left[\frac{\sum(\log x_i - \overline{\log x})^2}{n-1}\right]^{0.5} \tag{13}$$

$$g = \frac{n\sum(\log x_i - \overline{\log x})^3}{(n-1)(n-2)\sigma^3 \log x} \tag{14}$$

Where n is the number of entries of X the flood of some specified probability $\log x_i$ is the average of the log x discharge values

3. Results and dissection

3.1.Rainfall Frequency

The rainfall frequency analysis of the watershed may give different outcomes based on the time scale of future climate scenario. The rainfall frequency curve for current (base period) and different time period are presented in the Figure 1. The change in percentage of rainfall magnitude increase from the current period corresponding to different return period (2, 5, 10, 25, 50, and 100) for RCP4.5 by the 2080s and RCP8.5 by 2050s and 2080s as shown in the Table 1. The RCP8.5 scenarios were better estimated that of RCP4.5 in the period of 2050s.

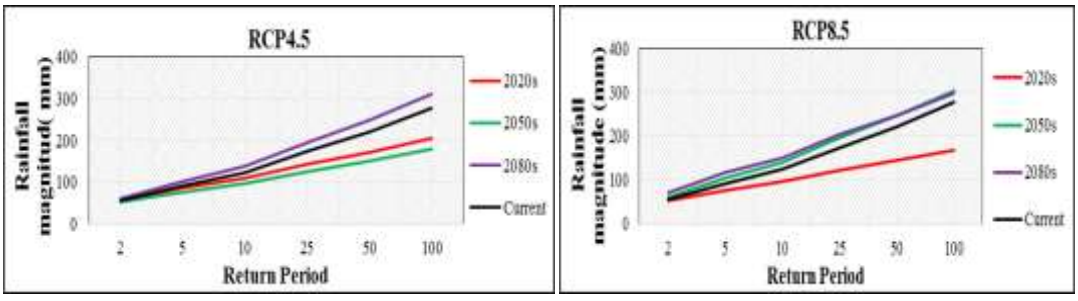

Fig. 1. Rainfall frequency curve of RCP4.5 and RCP8.5 emission scenarios

As shown in the Table 1, for all return period by 2020s and 2050s RCP4.5 scenario predicted decreasing rainfall magnitude. Whereas by 2080s predict increasing rainfall magnitude. For all return period by

2050s and 2080s RCP8.5 scenario predicted increasing the change in rainfall magnitude. Whereas by 2020s the change in rainfall magnitude predicted a decreasing.

Table 1. Changes in rainfall magnitudes of RCP4.5 and RCP8.5scenarios

RCP4.5		Change in rainfall magnitude (%)						RCP8.5		Change in rainfall magnitude (%)					
Return Period		2	5	10	25	50	100	Return Period		2	5	10	25	50	100
	2020s	-0.1	-6.3	-11.1	-17.4	-21.8	-26.1		2020s	-7.34	-16.8	-22.8	-30	-34.9	-39.3
Period	2050s	-6.4	-16	-21.9	-27.8	-31.7	-35.2	Period	2050s	9.96	13.9	14.2	12.97	11.45	9.48
	2080s	7.7	10.6	11.7	12.43	12.73	12.84		2080s	27.2	25.84	22.45	16.81	12.21	7.46

3.2.Flood Frequency

The change in magnitude of flood frequency under RCP4.5 scenarios by 2020s and 2050s were negative. Whereas RCP8.5 negative only by 2020s. Both RCPsemissionscenario.

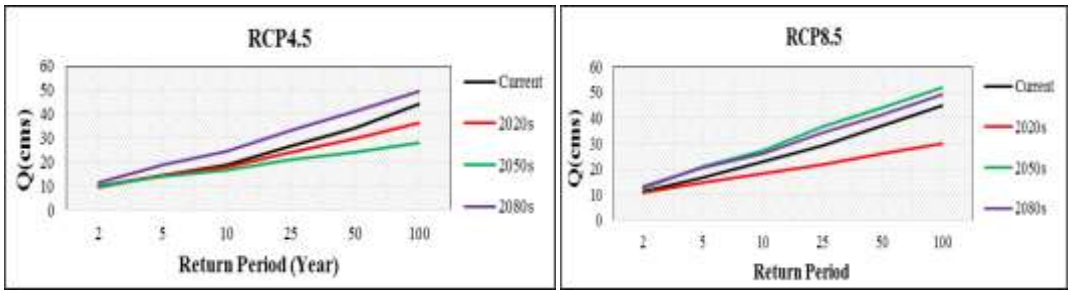

Fig 2. Flood frequency curve of RCP4.5 and RCP8.5 emission scenarios

As shown in the Table 2, for all return period by 2020s and 2050s RCP4.5 scenario predicted a decreasing flood magnitude. Whereas by 2080s predicted an increasing flood magnitude. For all return period by 2050s and 2080s RCP8.5 scenario predicted an increasing flood magnitude. Whereas by 2020s predicted a decreasing flood magnitude.

The effects of climate changes on the frequency and intensity of rainfall and flood is expected to increase the challenges for water and flood management. Change in flood magnitude from the current period of Akaki river corresponding to different return periods (5, 10, 20, 50, and 100) by 2080 average increase in flood event [1]. So, this is true, there is an increasing flood event Hare watershed in the next

100yrs. Black and Silver Creek sub-basin, using current period data, the peak flow magnitude for 100yrs return period is about 17.7 to 26.9 cms [14].

Table 2. Changes in Flood magnitudes of RCP4.5 and RCP8.5scenarios

RCP4.5		Change in rainfall magnitude (%)						RCP8.5		Change in rainfall magnitude (%)					
Return Period		2	5	10	25	50	100	Return Period		2	5	10	25	50	100
	2020s	-2.6	-0.6	-4.38	-9.73	-13.7	-17.4		2020s	-3.56	-13.1	-20.9	-25.1	-29.6	-32.8
Period	2050s	-3.2	-3.1	-10.7	-21.3	-29.1	-36.5	Period	2050s	10.9	24	19.26	24.66	19.35	16.28
	2080s	17.5	29.8	30.3	25.44	19.58	12.7		2080s	18.6	22.14	14.44	17.76	12.41	9.72

The simulation result abridged is linear relationship between the magnitudes of rainfalland peak flow frequency of the two RCPs scenarios. It also exposes that low return period floods are more sensitive to climate change than high return period floods. This might be due to the degree of dampness of the watershed at different flood frequencies. The percentage increase in peak flow (from the current period) in Saguenay watershed corresponding to different return period (20, 50, and 100) by the 2080s [12].

4. Conclusion

The study investigated evaluation of impacts of climate change climate change impact on the magnitude of rainfall and flood frequency of the Hare watershed by using downscaled RCPs climate data. The rainfall frequency analysis shows climate change will have impact on the frequency and magnitude of rainfall intensity. The future change in rainfall magnitude clearly governs in peak flow magnitude and frequency.

The 100yrs flood of the future climate seems to increase a flood event 20 to 50yrs return period by the 2080s. This implication in the design of hydraulic structure in the Hare watershed.

The flood frequency studies can be used as a guide in determining the capacity of a structure e.g. highway bridges, culverts, storm drains when it is permissible to take a means of estimating the probable flood damage prevented by a system of flood protection works over a period of years usually equal to the estimated economic life of the works.

References

1. Abayneh Alemu (2011). Evaluation of Climate Change Impact on Extreme Hydrological Event Case study: Addis Ababa and surrounding catchment

2. Ashley, R.M., Balmforth, D.J., Saul, A.J., Blanskby, J.D., 2005. Flooding in the future predicting climate change, risks and responsesin urban areas. Water Sci. Technol. 52 (5), 265–273.
3. Cunnane, C (1987). Review of Statistical Methods for flood frequency Estimation, in Hydrologic Frequency Modeling.
4. GeremewSahiluGebrie (PhD and AgizewNigussieEngida (PhD) (2015) Climate Modeling of the Impact of Climate Change on Sugarcane and Cotton for Project on 'a Climate Resilient Production of Cotton and Sugar in Ethiopia'.
5. Haan, C.T. (1977) Statistical methods in Hydrology, Iowa State University Press, Ames, Iowa, USA.
6. Ho, C.K., Stephenson, D.B., Collins, M., Ferro, C.A.T., Brown, S.J., 2012. Calibration strategies: a source of additional uncertainty in climate change projections. Bull. Amer. Met.Soc. 93,21–26.
7. IPCC, 2007a: Climate Change 2007: The Physical Science Basis. Contribution of Working Group I to the Fourth Assessment Report of the Intergovernmental Panel on Climate Change [Solomon, S., D. Qin, M. Manning, Z. Chen, M. Marquis, K.B.M.Tignor and H.L. Miller (eds.)]. Cambridge University Press, Cambridge, United Kingdom and New York, NY, USA, 996 pp.
8. Kassa, T. (2009): Watershed Hydrological Responses to Changes in Land Use and Land Cover, and Management Practices at Hare Watershed, Ethiopia.DemFachbereichBauingenieurwesen der Universität Siegen vorgelegte Dissertation.
9. Leander, R., and T. A. Buishand (2007). Resampling of regional climate model output for the simulation of Extreme River flows. Hydrol.,332(3–4), 487–496, doi: 16/j.jhydrol.2006.08.006.
10. Moges SA, Merrakeffale N (2011) Rainfall intensity duration frequency (RIDF)relationships under the changing climate case study on upper Blue Nile riverbasin, Ethiopia.
11. Nigatu, M. (2011). Rainfall Intensity Duration Frequency (RIDF) Relationships under the Changing Climate Case study on Upper Blue Nile River Basin, Ethiopia. Department of Hydraulic Engineering.M.sc thesis. Addis Ababa University, Addis Ababa Institute of Technology.
12. Paulin, C., and B.D. Yonas (2004). Downscaling Global Climate model output for Flood Frequency Analysis in the Seguenay River System. Departement of Civil Engineering/School of Geography and Geology. McMaster University Hamilton, ON L8S 4L7.Projectno. S02-15-01.
13. Prasuhn, A. (1992), Fundamentals of Hydraulic Engineering. Oxford University Press New York
14. Shamarokh, A. (2012). Hydrological Impact of Climate Change in Semi-Urban Watershed. M.sc thesis. Civil and Environmental Engineering (Bangladesh Univ. of Engg. & Tech.)
15. Tamiru, G. (2009). Regional Flood Frequency analysis for upper Omo-Gibe sub-basin. M.Sc. Thesis. Addis Ababa University, Ethiopia.
16. Yidenkachew, A. (2008). Flood Frequency Analysis for lower Awash Sub basin [tributaries from northern Wollo high lands] using SWAT 2005 model. M.Sc. thesis. Addis Ababa University, Ethiopia.
17. Yohannes.G.(2013). Development of one day probable maximum precipitation (pmp) and isohyetal map for Tigray region, Ethiopia. M.Sc. Thesis.Haramaya University, Ethiopia

Optimal coupling combinations between deficit irrigation levels and agronomic practice for furrow irrigated maize grown in semiarid environment

Kidane Welde*, Hintsa Libsekal Gebremariam, Kiflom Degif Kahsay

Tigray Agricultural Institute (TARI), Alamata Agricultural Research Center P.O.Box 56, Alamata, Ethiopia

*E-mail: kidanew2009@gmail.com

Abstract

In Southern Tigray region, water deficit during the growing season is a major factor limiting maize production. Therefore, optimizing irrigation has crucial importance in achieving the ideal irrigation water use efficiency (IWUE) in this region. This study investigated IWUE, crop yield and yield components of maize irrigated with furrow irrigation systems in 2016. Two patterns of maize planting: one row and alternate two row and three levels of irrigation depth: 80, 75 and 100% of crop water requirement (CWR) arranged in factorial randomized complete block design (RCBD) with three replications were considered.The highest average grain yield (40.43 qt/ha) and biomass yield (206.91 qt/ha) were obtained from the alternate two row planting and one row planting respectively while the level of irrigation was full CWR (100% CWR). The IWUE for maize ranges from 0.69 kg/m^3 to 1.03 kg/m^3 for the two type of planting pattern and different depth irrigation water applied. The highest IWUE was obtained from alternate two row method of planting with 35% deficit irrigation level while the lowest was found in one row planting with 20% deficit irrigation. Variance analysis of the plant height, number of cobs per plant and grain yield data indicated that the interaction of planting pattern and level of deficit irrigation not significantly affected the yields. But it showed significant advantage in biomass yield and IWUE. Practical implications of this study is that application of deficit irrigation with some improved planting pattern of maize may improve IWUE and the need for sustainable use of limited irrigation water without significant reduction in yield.

Key words: Agronomic practice, Deficit irrigation, IWUE, Maize yield

1. Introduction

In semi-arid regions water has a precious value that is often limited and costly (Oktem, 2008). Irrigation agriculture is the primary consumer of fresh water on earth (Longo and Spears, 2003). At the same time expansion of irrigated agriculture is essential to maximum production of cropsand returns for the farmers for their food security. As irrigation water availability is also limited and costs are increasing, there is an urgent need to save water and reduce water waste while still maintaining adequate yields (Panda et al., 2004). Proper irrigation water management is therefore very important to minimize yield damage caused by water stress or over irrigation. Several suggestions are being made by irrigation stakeholders on how to irrigate for maximizing production with minimum water input. Application of deficit irrigation through identifying sensitive growth stages to water stress and supporting it with better agronomic practices is one way to improve crop productivity with less water (Jalota et al., 2006).

Deficit irrigation is a scheduling method where irrigation is decisively made not to fully meet water needs of the crop, and crops are deliberately allowed to sustain some water deficit which may consequently lead to yield reduction (Zhang et al. 2004; Prichard et al. 2004). Deficit irrigation for maize production has been widely studied and applied for optimum maize yield and improving irrigation water use efficiencies (IWUE) (Dagdelen et al. 2008; Henry et al. 2008; Wang et al. 2001). In literatures, the effects of deficit irrigation on maize production is also widely reported (Stone et al. 2001; FAO 2002). However, less attention is given supporting deficit irrigation with deferent agronomic practices for its effectiveness. In addition, there are variations in literature showing the effect of deficit irrigation on crop yield and IWUE. This variation in report could imply that the effect of moisture stress may vary across locations, climates and soil types for the same crop.

Maize is among a high-water demanding crop throughout its all growing stages of physiological development (Traore et al., 2000). But under the limited source of irrigation water the large area of the Raya rift valley is used for growing maize annually and surface irrigation is utilized in most of it. This makes maize the most competent crop for irrigation water with horticultural crops in the district. Hence in addition to adaptation of deficit irrigation system agronomic practice that can improve irrigation water productivity of maize is important for the area. Therefore, it is very important to carry out some comprehensive assessment on effect of deficit irrigation scheduling for any location before recommendation and advice can be made on deficit irrigation scheduling methods to be adopted in any specific area. Moreover, a study is required what agronomic practices for the specific crop are important

to support deficit irrigation. Such assessment will help to generate results that can be used to convince farmers and other water resource stakeholders of the benefits associated with irrigation scheduling and the possible limits irrigators could go in terms of reducing the amount of water used in crop production. The objective of this study was to determine effect of planting patterns of maize and some level of deficit irrigation on yield and yield components as well as IWUE of irrigated maize crop in the Raya rift valley, Ethiopia.

2. Materials and methods

2.1.Description of the study area

Maize dominantly cultivated at low land area of southern zone of Tigray but it has also considerable coverage in irrigation scheme of the high land part of the zone. Hence, the field experiments of this study were conducted at the Alamata Agricultural Research center experimental site during the cropping season of 2016. Particularly the research center experimental site is geographically located at 12.69^0 N latitude and 39.66^0 E longitude (Fig. 1).

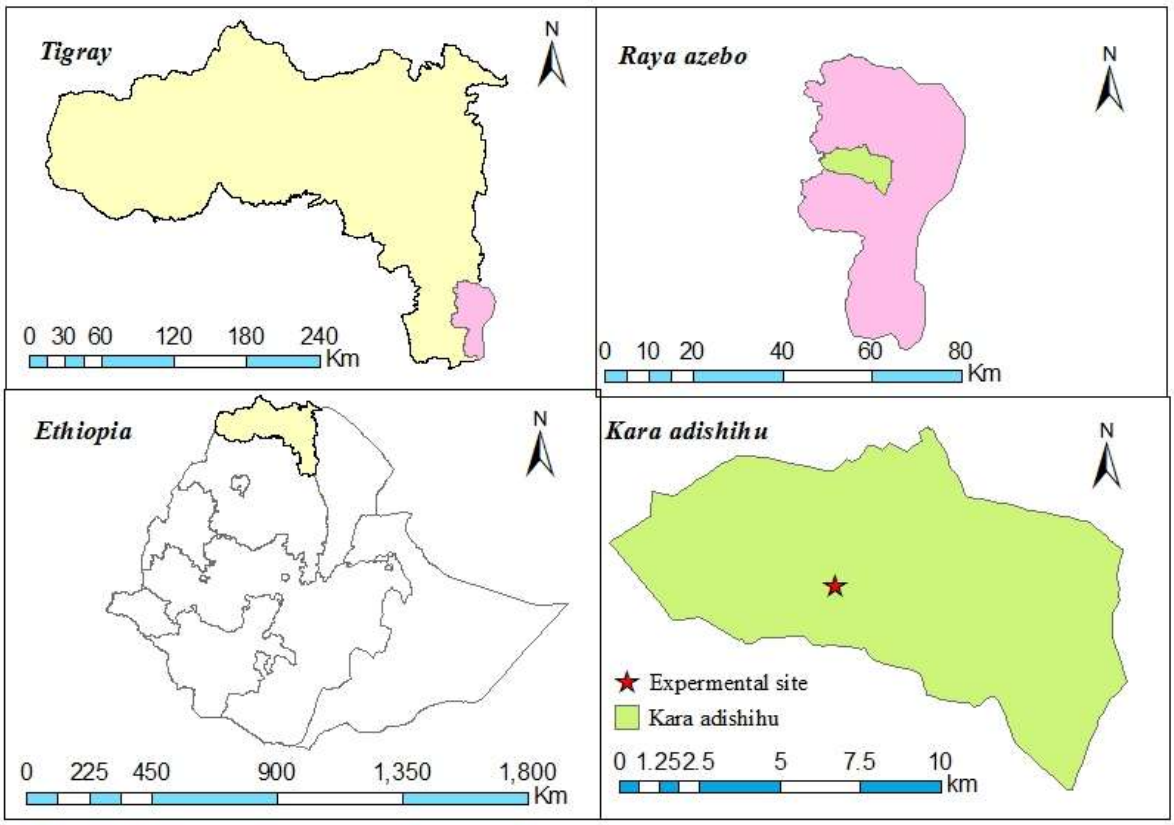

Fig1: Location map of the study area

The maximum infiltration rate of the soil is 40 mm/day. During irrigation application water was applied to refill the soil to field capacity. Some physical and chemical properties of the soil of the experimental site are given in Table 1.

Table 1: Physical and chemical properties of different soil layers of Kara adishabo site

Soil depth	Particle size distribution (%)			Texture class	PH	EC (dsm^{-1})	SAR	Captions ($me\ l^{-1}$)	
	Sand	silt	clay					Na^{+}	$Ca^{++}+Mg^{++}$
0-30	54	32	15	SL	7.86	0.87	2.8	5.2	6.5
30-60	56	28	16	SL	7.93	0.74	2.2	4	6.5
60-90	44	34	22	L	7.94	.86	4.9	6.2	3.1

The climatic condition of the research site is semi-arid. The minimum and maximum temperature of the region is 16 ^{0}C and 29 ^{0}C, respectively. The average annual precipitation of the area also shows 546 mm (Fig 2).

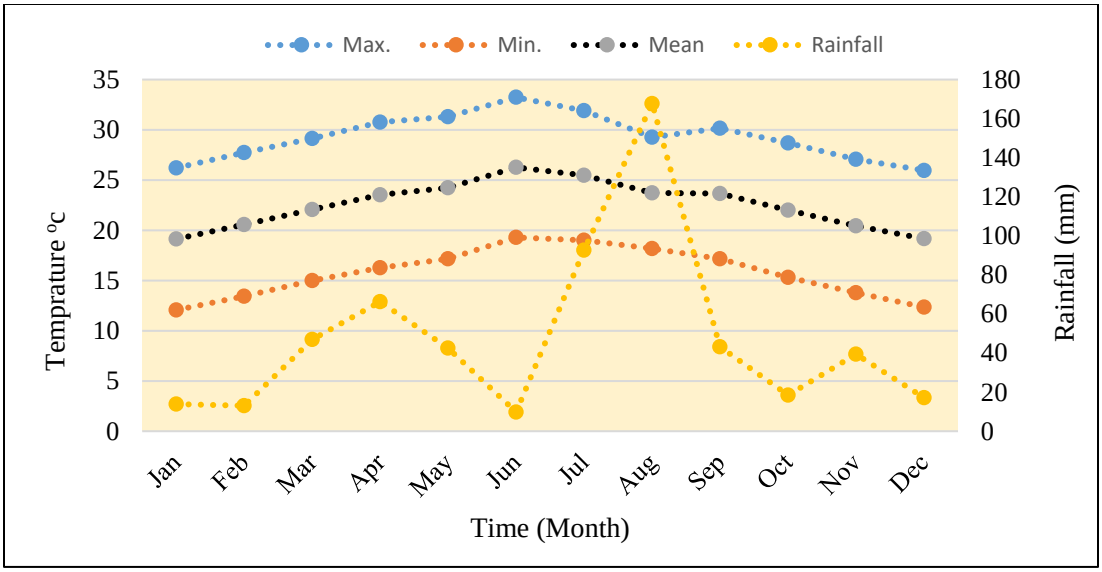

Fig 2: Long term mean monthly temperature and rain fall of the study area (2010-2016)

2.2.Experimental treatment, design and management

In order to investigate irrigation water use efficiency (IWUE) and yield of maize planted in different patterns and level of deficit irrigation, the study was designed in randomized complete block design (RCBD) with three replications. Two types of planting pattern and three level of deficit irrigation with a

total of six treatments were included in the study (Table 2). Spacing between blocks and plots were 2m and 1m respectively with 3.5*4 m^2 plot area. The spacing between furrow and plants were also 70 cm and 20 cm respectively. Furrow irrigation was the method water application for each plots. The first irrigation events took place on 27 December 2016, just 7 days after planting.

Table 2: Treatment setting and codding

Method of planting	Level of deficit irrigation	Treatment code
One row	20% deficit	T1
	35% deficit	T2
	Full crop water requirement	T3
Alternate two row	20% deficit	T4
	35% deficit	T5
	Full crop water requirement	T6

Fertilizer applications were based on soil analysis recommendations of the research site. All treatment plots received the same amount of total fertilizer (300 kg/ha DAP and 150 kg/ha urea). DAP was applied during planting but urea was applied both during planting and three weeks after planting and it was ploughed at least up to 20 cm depth three times before planting. Both fertilizers was applied in ways that minimize loss and maximize the nutrient use efficiency (row application). Weed management is also an important issue as certain weeds may be more problematic in computing water and nutrient (Irena and Clarence 2001). Hence the experimental site was monitored carefully for weed pressure and was employed appropriate management solutions.

2.3.Data measurement and analysis

Climate variables required by CROPWAT8 (minimum and maximum temperature, relative humidity, wind speed, sunshine hours and rainfall) were downscaled using New_LockClim 1.10 software for the particular site and calibrated with nearby meteorological station. ETo of the study areas was then estimated using penman-monteith method from the climatic data by using CROPWAT 8 capability options. Effective rainfall was also calculated using USDA soil conservation service formula. But unfortunately, there was no rainfall event during the experiment season. The crop data required for crop water requirement estimation (Kc value at each growth stage) was collected from different publications and FAO recommendations (Fig 3).

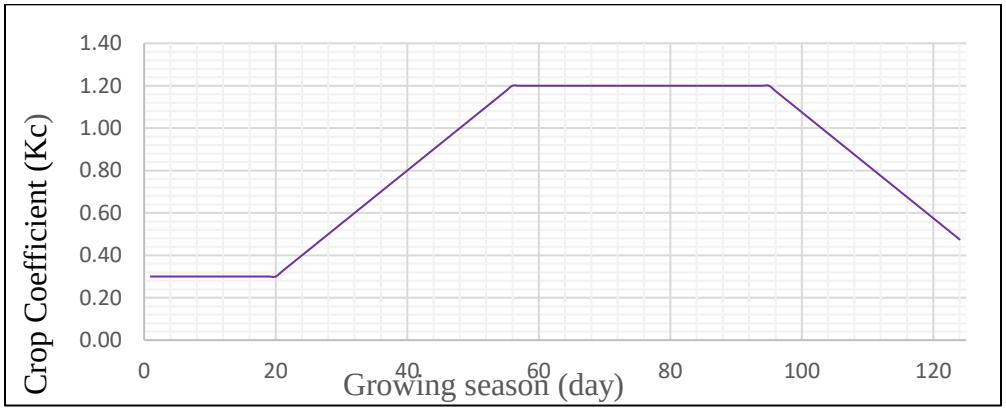

Fig 3: Crop (maize) coefficient throughout the growing season.

Composite soil samples were collected from experimental sites and soil textural class, soil bulk density, field capacity, permanent wilting point of the soil and soil PH were analyzed. After all necessary input datas were collected crop water requirement, irrigation water requirement and irrigation scheduling were estimated. Irrigation water irrigated and saved at each irrigation event were also measured. The amount of water irrigated to each experimental plot was measured using two inch partial-flume per irrigation event. Yield components (Plant height, number of cobs per pant and biomass yield) were collected from each plot. Gran yield was also measured for each harvested plot. Irrigation water use efficiency (IWUE) was calculated as the ratio of obtained grain yield and the total water consumption for the whole season (Stanhill, 1986). All data were presented as means and statistically analyzed using R 3.3.1 software (R Core Team., 2016). All the mean yields and IWUEs results of treatments were compared to each other for any significant differences using the least significant difference (LSD) method. LSD was calculated from data, where the differences among means were tested. Separate analyses were performed for each data at the probability level for determination of significance P = 0.05. The amount of water saved without significantly affecting yield was also be taken in to account as the base point of the study is deficit irrigation.

3. Result and discussion

3.1.Irrigation water applied and seasonal water consumption

Water requirement was determined using CROWAT 8 software. As there was no any rainfall event throughout the growing season the crop water requirement of the crop (CWR) was supplied though application of irrigation. The irrigation depths varied from 9 to 101 mm for the full CWR treatment. Seasonal water amounts applied in this study are almost in agreement with the results of Szeles et al.

(2012) in irrigated maize in Eastern Hungary for the full CWR. Variations of evapotranspiration of plant (ETc) along with the irrigation scheduling of the experiment throughout the growing season is shown in Figures 4. Number of irrigation applications, irrigation depths and seasonal water consumption (ETc) values of the crop are also presented in Table 3.

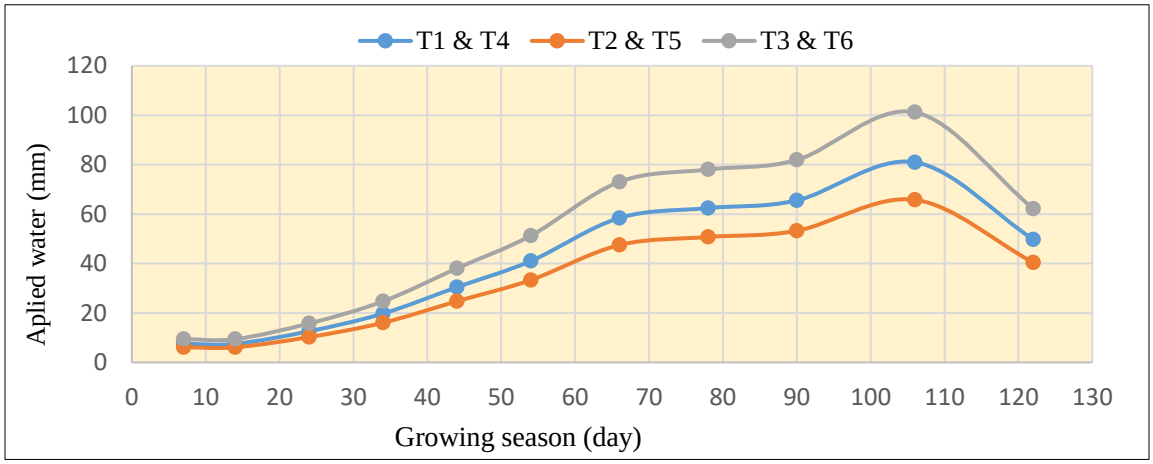

Fig 4: Variations water application to treatments in growing season

Table 3: Depth of irrigation water applied for each treatment

Treatment	Description	Amount of water (mm)	Total water applied (m3/ha)	No. of irrigation
T1	One row planting and 20% deficit irrigation	436	4362	11
T2	One row planting and 35% deficit irrigation	354	3544	11
T3	One row planting and full CWR application	545	5452	11
T4	Alternate two row planting and 20% deficit	436	4362	11
T5	Alternate two row planting and 35% deficit	354	3544	11
T6	Alternate two row planting and full CWR	5452	5452	11

3.2.Plant Height and Number of Cobs per Plant

The effect of the treatments on yield components (plant height and number of cobs per plant) didn't show significant difference (at p = 0.05). But plant height tended to be higher (222 cm) at one row planting and full CWR application (Table 4). The in significant difference might be due to biasness in random sampling of plants from each plot when taking measurements of plant height and number of cobs per plant. Even though the treatments and the environment are different, the results of this study are

supported by those ofMohammad and Afshin, 2011; Farré and Faci, 2009; Kidane and Hintsa et al., 2016 which both reported non-significant on yield components.

Table 4: Effect of treatments on plant height and number of cobs per plant

Treatments	Plant height (cm)	Number of cobs per plant
One row planting and full CWR application	222.08	1.33
One row planting and 20% deficit irrigation	218.25	1.33
Alternate two row planting and full CWR application	215.42	1.25
One row planting and 35% deficit irrigation	214.42	1.5
Alternate two row planting and 20% deficit irrigation	213.00	1.5
Alternate two row planting and 35% deficit irrigation	210.75	1.42
LSD	ns	ns
CV (%)	4.68	16.64

3.3.Grain and biomass yield

The maize grain yield differed between treatment was insignificant (at P = 0.05). The average grain yield of maize was maximum (40.43 qt/ha) foralternate two row planting and full CWR application and minimum grain yield (28.02 qt/ha) was obtained from one row planting and 35% deficit irrigation (Table 5). This agrees with the results of Mohammad and Afshin (2011) investigated water use efficiency and yield in maize irrigated with drip (tape) and furrow irrigation systems and planted in one or two rows in Ghazvin, Iran. In this study, increasing water amounts produced a relatively higher yield for both planting patterns.

Bio mass yield was significantly affected (p = 0.05) by the levels of irrigation water application and method of planting (Table 5). Similar result was reported by Ali, et al., 2008 in an arid region. There was a significant reduction in marketable yield of over 56 qt/ha as compared one row planting and full CWR application with one row planting and 35% deficit irrigation. Under the conditions of the experimental field maximum bio mass yield (206.9 qt/ha) was obtained from the one row planting method and full CWR application. But minimum bio mass yield (150.7 qt/ha) was scored from one row planting and 35% deficit irrigation. At the same level of deficit irrigation (35% deficit) statistically shows insignificant in bio mass yield. But the alternate two row planting gives higher bio

mass yield (182 qt/ha) as compared to one row planting method (151 qt/ha) at the same level of deficit irrigation.

Table 5: Effects of irrigation depth and planting pattern on grain and bio mass yield of maize

Treatments	Grain yield (qt/ha)	Bio mass yield (qt/ha)
One row planting and full CWR application	38.14	206.91[a]
One row planting and 20% deficit irrigation	30.24	170.48[ab]
Alternate two row planting and full CWR application	40.43	198.34[a]
One row planting and 35% deficit irrigation	28.02	150.71[b]
Alternate two row planting and 20% deficit irrigation	34.73	186.43[ab]
Alternate two row planting and 35% deficit irrigation	36.37	181.91[ab]
LSD	ns	44.09
CV (%)	26.53	13.28

Note: levels not connected with similar letter are significantly different

3.4.Harvest index and irrigation water use efficiency

The data in Table 6 indicate that in significant difference among the treatments (at P = 0.05) in % harvest index of maize. This result of harvest index as compared to the different planting pattern and level of irrigation was not attributed to computation of plant nutrients and irrigation water utilization for maize crop grain fill. Numerically, maximum percent of harvest index (25 %) was obtained from the alternate two row planting method and full CWR application. But minimum percent of harvest index (21 %) was obtained from one row planting and 20% deficit irrigation.

IWUE of maze significantly affected by the use of different depth of water application with different planting patterns (p = 0.05). This confirms the results obtained by Salah et al., 2008. The IWUE ranges from 0.69 kg/m^3 obtained from one row planting and 20% deficit irrigation to 1.03 kg/m^3 obtained from alternate two row planting and 35% deficit irrigation (Table 6). This shows as the volume of water application decreases and the method of planting changed from one row to alternate two row the IWUE increase proportionally. The high volume of water which promotes excessive water percolation due to the limited soil water holding capacity of the soil played an important role in the reduction of IWUE results significantly. In general, IWUE was increased by 49% as compared using alternate two row planting and 35% deficit irrigation with one row planting and 20% deficit irrigation. The implication of this result is continuing irrigation practices of maize at different planting pattern could have an immense effect on the efficient utilization of the limited irrigation water.

Table 6: Effects planting pattern and level of deficit irrigation on percent of harvest index and IWUE of maize

Treatments	Harvest index (%)	IWUE (kg/m^3)
One row planting and full CWR application	22.56	0.70^{b}
One row planting and 20% deficit irrigation	21.41	0.69^{b}
Alternate two row planting and full CWR application	25.32	0.74^{ab}
One row planting and 35% deficit irrigation	23.41	0.79^{ab}
Alternate two row planting and 20% deficit irrigation	23.79	0.80^{ab}
Alternate two row planting and 35% deficit irrigation	25.12	1.03^{a}
LSD	ns	0.30
CV (%)	21.73	20.79

Note: levels not connected with similar letter are significantly different

4. Concussion

Our findings indicated that planting pattern and level of deficit up to 35% of CWR did not affect the yield components (plant height & number of cobs per plant) and grain yield of maze. However, both bio mass yield and IWUE have a significant effect as the planting pattern and level of deficit varies. The result showed that irrigation water use efficiency of maize can be improved up to 49 % greater using two row planting and 35% deficit irrigation than the other methods of planting pattern and depth of water without significantly affecting the grain yield components. The highest grain yield (40.43 qt/ha), biomass yield (206.91qt/ha) and IWUE (1.03 kg/m^3) was obtained from alternate two row planting and full CWR application, one row planting and full CWR application and alternate two row planting and 35% deficit irrigation respectively. It can be concluded that alternate two row method of planting and 35% deficit irrigation was found to be more appropriate in improving IWUE without significantly affecting yields of maize under conditions where shortage of irrigation water is a limiting factor for maize production. But at the same time not much generalizations can be made from the results of this one-year field experiment study especially for solving practical field irrigation problems. Hence it needs to be conducted the experiment for additional one year.

References

Ali, MH., Mohammad, AE., Simon, B., 2008. The effects of irrigation methods with effluent and irrigation scheduling on water use efficiency and corn yields in an arid region. Agricultural water management. 96(2009) 93-99

Dagdelen N., Basal H., Yılmaz E., Gurbuz T., Akcay S., 2008. Different drip irrigation regimes affect cotton yield, water use efficiency and fiber quality in western Turkey. Agric. Water Manage. 96 (2009), 111–120.

FAO (2002) Deficit irrigation practice. Water reports no. 22, Food and Agriculture Organization of the United Nations, Rome. 100 pp

Farré, I., Faci, J.M., 2009. Deficit irrigation in maize for reducing agricultural wateruse in a Mediterranean environment. Agric. Water Manage. 96, 383–394.

Henry EI., Baanda AS., Andrew KP, Tarimo., Henry F.M., 2008. Effects of deficit irrigation scheduling on yields and soil water balance of irrigated maize. IrrigSci (2008) 27:11–23. DOI 10.1007/s00271-008-0117-0

Irena R., and Clarence J., 2001 Understanding maize weed competition: resource competition light quality and the whole plant. Journal of field crops research 71 (2001) 139-150

Jalota SK, Sood A, Chahal GBS, Choudhary BU (2006) Crop water productivity of cottons (Gossypiumhirsutum L.) and wheat (Triticumaestivum L.) system as influenced by deficit irrigation, soil texture, and precipitation. Agric Water Manage 84:137–146

Kidane W., and Hints L., 2016. Effect of different furrow and plant spacing on yield and water use efficiency of maize. Agricultural Water Management 177 (2016) 215–220

Longo FD, Spears TD. 2003. Water Scarcity and Modern Irrigation, Valmont Water Management Group, Valmont Industries, Inc.: Valley, Nebraska, USA.

Mohammad K., and Afshin G., 2011 yield and water use efficiency of corn planted in one or two rows and applying furrow or drip tape irrigation systems in Ghazvin province, Iran. Irrig. and Drain. 60: 35–41 (2010)

Oktem, A., 2008. Effect of water shortage on yield, and protein and mineral compositions of drip-irrigated sweet corn in sustainable agricultural systems. Agricultural water management 95(2008)1 003–1010

Panda, R.K., Behera, S.K., Kashyap, P.S., 2004. Effective management of irrigation water for maize under stressed conditions. Agric. Water Manage. 66 (3), 181–203.

Prichard T, Hanson B, Schwankl L, Verdegaal P, Smith R (2004) Deficit irrigation of quality wine grapes using micro-irrigation techniques. Publications of University of California Co-operative Extension, Department of Land, Air and Water Resources, University of California, Davis, 5pp

R Core Team (2016) R: A language and environment for statistical computing. R Foundation for Statistical Computing, Vienna, Austria. URL https://www.R-project.org/.

Salah E.E.,,Essam A., Mohamed S.A., Urs S., 2008. Irrigation rate and plant density effects on yield and water use efficiency of drip-irrigated corn. Agricultural water management 95(2008) 836-844

Stanhill G, (1986) Water use efficiency. Adv. Agron. 39, 53–85.

Stone PJ, Wilson DR, Beid JB, Gillespie RN (2001) Water deficit effects on sweet corn I. water use, radiation use efficiency, growth, and yield. J Agric Res 52:103–113

Széles, A.V., Megyes, A., Nagy, J., 2012. Irrigation and nitrogen effects on the leafchlorophyll content and grain yield of maize in different crop years. Agric.Water Manage. 107, 133– 144.

Traore, S.B., Carlson, R.E., Pilcher, C.D., Rice, M.E., 2000. B t and NON BTmaize growth and development as affected by temperature and drought stress. Agron. J., 92(5): 1027- 1035.

Wang HX, Zhang L, Dawes WR, Liu CM (2001) Improving water use efficiency of irrigated crops in the North China Plain measurements and modelling. Agric Water Manage 48:151–167

Zhang X, You M, Wang X (2004) Effects of water deficits on winter wheat yield during its different development stages. ActaAgricBoreali-Sin 14:79–83